Rare earth elements (REEs) in shallow and deep water articulated brachiopods: sensitive tracers of paleo-oceanography

by

© Amir Halim Zaky Bakhit

A thesis submitted to the

School of Graduate Studies

in partial fulfillment of the requirements for the degree of

Doctor of Philosophy

Department of Earth Sciences

Memorial University of Newfoundland

July 2016

St. John's Newfoundland

ABSTRACT

Through time, oceans have experienced physicochemical variations in a response to the evolution of the earth and its atmosphere. Geochemical proxies are employed to define these variations, evaluate their magnitudes and identify the responsible factors. Because of the unique behavior of the rare earth elements (REEs) within the oceanic system, they have been proven to be a leading proxy for tracing changes in the marine geochemical cycle (Elderfield et al., 1988; Holser, 1997). However, obtaining a reliable rare earth element (REE) proxy seems to be very difficult. Several archives were investigated for their REE proxy potential but with limited success. The biggest difficulty which complicates our understanding is perhaps the ambiguous REE compositions acquired from both modern and fossil archives.

REEs are incorporated into the crystal lattice of the marine components in very small fractions. Investigating their REE contents and fractionations in the different modern and ancient archive requires complete elimination of the internal and the external contaminants. Without their removal, inputs from the bound oxides, detritus and/or organic matter overprint the archives' REE compositions. Despite the importance of the cleaning procedures, reviewing the literature reveals the lack of a rigorous methods or steps that should be followed to acquire uncontaminated REE signals. Therefore, the establishment of a reliable sample processing protocol that satisfies the most stringent demands for procuring reliable and robust REEs from marine materials is among the objectives of the thesis. To achieve this goal, five different cleaning procedures (P) were applied on *Liothyrella neozelanica* valves dredged from the deep water of the South Pacific Ocean

(north of New Zealand). P-1 consisted only of rinsing the specimens extensively with distilled water. P-2 was the immersion of the specimens in hydrogen peroxide for 3 continuous days. Physically cleaning the shells under binocular microscope using a sharp stainless-steel blade comprised the P-3 procedure. In P-4 the specimens were physically cleaned, then leached with 10% hydrochloric acid until they deemed white. In P-5 the specimens were processed using all above cleaning procedures (water washing, physical cleaning, H_2O_2 treatment, and HCl leaching).

The P-1 specimens yielded high concentrations of Mn, Fe, U and ∑REEs particularly Ce resulting from the primary layer, periostracum and the adsorptive particulates and detritus. P-2 specimens yielded similar trend as P-1, but with partial depletion in the Ce/Ce* anomalies. Specimens of P-3 (physical cleaning only) yielded depleted ∑REEs and lower Mn, Fe, and U concentrations with slightly negative Ce anomaly. P-4 and P-5 fragments yielded remarkable reductions if the ∑REE, Mn, Fe, U concentrations and 'normal' Ce anomaly, however, the P-4 fragments are slightly enriched in their ∑REE contents. The P-5 seems to be the ultimate protocol for modern shells but P4 should be applied to fossil shells due to the absence of the organic remnants adhering to the outermost shell.

The reproducibility of the clearing protocol on individuals of different water masses was evaluated by applying the P-3 and P-5 procedures on deep water shells recovered from the abyssal depths of the Caribbean Sea. Its validity for archives of different settings, on the other hand, was assessed by applying the P-1, P-2, P-3 and P-5 on shallow water shells from the Irminger Sea, west of Iceland. The results were uniform and consistent supporting

the reliability and robustness of the proposed protocol. However, it is infallible and its completion must be verified in the light of the archives' elemental composition.

The P-4 was applied to Ordovician, Silurian, Pennsylvanian and Permian brachiopods and near-micritc whole rock to test the efficiency of the suggested protocols on the ancient archives. The fossils yielded ∑REE, Mn, Fe, U concentrations and Ce anomalies comparable to their modern counterparts, while the whole rock are slightly to extensively enriched. Those with higher Fe and Mn contents than 300 and 100 ppm, respectively, their Ce/Ce* values should be adjusted by −13% to be considered for the paleoredox investigations.

One of the thesis main objectives is to evaluate the REE proxy potential of the brachiopods archive for paleooceanographic and paleoenvironmental investigations. This evaluation required minimizing the impact of variations in the environmental conditions on seawater REE compositions. It was, consequently, conducted by assessing the REE uptake of the deep water shells (>500 m) of the orders *Rhynchonellids* and *Terebratulids* obtained from the Caribbean Sea, North Atlantic, South Pacific and Southern Oceans. The shells display gradual enrichment REE_{SN} patterns with increasing atomic numbers that are punctuated consistently with the negative Ce_{SN} excursions. The REE contents of their secondary fibrous calcite layers are elevated relative to the ambient water masses by an average factor of 0.81×10^5. The REE distribution coefficients between the shells' crystal lattice and the ambient seawater vary consistently within the series in response to changes in ionic radii relative to that of the Ca^{2+} cation. The calculated log K_D values for the shells of two orders are remarkably similar and consistent with those of foraminiferal calcite.

The deep water shells yielded L:H and L:M ratios similar to those of their water masses, while their M:H ratios are notably different, defining a secondary trend that is directly proportional to the shells' depths. Although their Ce/Ce* anomalies are consistently negative, they vary significantly but in a manner reflecting the variations in the prevalent oceanographic conditions. The open water shells display a vertical Ce/Ce* profile relatively similar to the Ce vertical curve in seawater.

To assess the REE incorporation into different parts/layers of the brachiopod shell structure, and the impacts of changes in the seawater physicochemical parameters on the REE fractionations and distributions of the brachiopod archives, articulated shells of the orders Terebratulida and Thecideidina were obtained from the shallow waters (<500 m) of the Norwegian, the Irminger and the Ross Seas, the Denmark Strait, Bonne Bay and Bay of Fundy and Friday Harbor. Their REE compositions were correlated to those of the deep water settings. The umbo region is secreted with either selective REE uptake or species dependency during the growth of the juvenile stage, whereas the primary layer's REE incorporation is variable and incidental. Precipitation of the pedicle and brachial valves' secondary layers occur with a small range of differences that falls within the natural variation of the brachiopod's lattice. The Thecideidinid shells yielded remarkable variations in their elemental, REE compositions and the REE_{SN} patterns due to the domination of the primary layers over their structures. Seawater parameters of temperature, salinity and depth seem to have controls on the shells' REE composition. Depth plays a major rule on the shell REE fractionations, while temperature and salinity have moderate to minor impacts on the REE contents.

The shallow water shells have been divided into six depth intervals, and their L:H ratios were utilized to estimate the paleobathymetry of several Paleozoic formations. The evaluation was successful in placing the Permian Gyanyima, the Pennsylvanian Naco, Boggy and the Silurian Chicotte, Becscie and Jupiter Formations in shallow depths (<15-50 m).

ACKNOWLEDGMENTS

I would like to thank my supervisors Prof. Karem Azmy and Prof. Uwe Brand for their guidance, support and the chance to pursue research on such a timely and interesting topic. Without the treasured assistance they accorded me, this research project would never be completed.

I wish to express my deepest gratitude to my wife and parents for their unwavering support during the duration of my study. I would like to extend my gratitude to the National Institute of Water and Atmospheric research of New Zealand (NIWA) represented by Dr. Kareen Schnabel and Dr. Jeffrey Robinson for providing me with many samples, PEEP (Petroleum Exploration Enhancement Program) for the financial support to Karem Azmy, and NSERC (7961-09) for financial support to Uwe Brand.

I'm also grateful to MITACS-Accelerate internship program in partnership with Husky Oil for funding in part the last project of the thesis (Chapter 4).

TABLE OF CONTENTS

LIST OF TABLES

LIST OF FIGURESS

LIST OF APPENDIXES

Co-authorship Statement

The thesis is constructed in manuscript format and consisted of 5 chapters. Chapter 1 reviews the background literature, defines the critical imputes and outlines the main objectives of the study. Each of chapters 2 through 4 represents a research paper, and includes an introduction, sample localities, analytical methods, results, discussion and conclusion sections. The final chapter (chapter 5) summarizes the overall findings of the study and outlines the study significances.

The mainframe of the three research studies (chapters 2 to 4) of the thesis were designed primarily by Profs. Karem Azmy and Uwe Brand. As the primary author, I was responsible for all aspects of the three research projects (chapters 2 to 4), of reviewing the literature, formulating the research questions, performing the laboratory work, analyzing and interpreting the data preparing the manuscripts. Meanwhile, the co-authors (Prof. Profs. Karem Azmy and Uwe Brand) guided the research progress, gave the main advices for analysing and interpreting the data and corrected the written manuscript before submission.

Chapter 2 entitled "A new sample processing protocol for procuring seawater REE signatures in biogenic and abiogenic carbonates" has been published in the Chemical Geology Journal (2015), volume 416, pages 36-50. **Chapter 3** entitled "Rare earth elements in deep-water articulated brachiopods: Evaluation of seawater masses" has been published in the Chemical Geology Journal (2016), volume 435, pages 22-34., while **Chapter 4** entitled "Rare Earth Elements of shallow-water articulated brachiopods: a bathymetric sensor" has been accepted with moderate revision in *Palaeogeography, Palaeoclimatology, Palaeoecology* Journal.

With the exception of the Colville Arc brachiopods, specimens from around New Zealand (Lau Arc, Kermadec Ridge, Havre Trough and Northland Plateau) and Antarctica (Ross Sea) were provided by the New Zealand National Institute of Water and Atmospheric research (NIWA). Those from around Iceland (Denmark Strait, and Irminger, Iceland and Norwegian Seas) were dredged during the Meteor M85/3 expedition cruise of the IceAge project and were provided by Prof. Jörundur Svavarsson of University of Iceland. Bonne Bay shells were collected by scuba divers of the Ocean Sciences Centre of Memorial University of Newfoundland. Shells of Bay of Fundy, Friday Harbor, Caribbean Sea (Venezuela and Virgin Islands Basins) and Colville Arc were provided by Prof. Uwe Brand of Brock University. The Silurian brachiopod fossil and whole rock samples were provided by Prof. Karem Azmy and those of the Permian and Pennsylvanian by Prof. Uwe Brand.

CHAPTER 1

INTRODUCTION AND OVERVIEW

Modern oceanic investigations are essential for comprehending atmosphere and hydrosphere evolutions, reconstructing paleoenvironmental settings and interpreting mass extinction events (cf. Lécuyer et al., 1998, 2003, 2004; Trueman et al., 2006; Anderson et al., 2007; Garbelli et al., 2015). Variations in the physicochemical characteristics of seawater result in corresponding differences in the seawater rare earth element (REE) distribution (Bertram and Elderfield, 1993; Holser, 1997). Because of such properties as well as the unique chemical characteristics of the REEs in the seawater, the group has been considered as one of the most powerful probes for detecting changes in the marine geochemical parameters (German and Elderfield, 1990).

1.1. Seawater REEs

The fifteen lanthanides constituting the extremely coherent series of the REEs commonly occur in trivalent states in the low-temperature systems (de Baar et al., 1988; Bright et al., 2009). Promethium (Pm) is an exception as it has no stable or long-lived isotopes and exists in very minute quantities in the natural materials (Holser, 1997). In highly oxygenated surface water, the oxidation reaction of Ce^{3+} to Ce^{4+} takes place through bacterial mediation (Nozaki, 2001). The produced CeO_2 is highly insoluble and rapidly removed by scavenging causing depletion in soluble Ce^{3+} relative to other lanthanides

(Sholkovitz and Schneider, 1991; Piepgras and Jacobsen, 1992; Byrne and Sholkovitz, 1996). On other hand, reduction of Eu^{3+} to the less soluble Eu^{2+} state does not normally take place within oceanic water; it is mostly restricted to magmatic processes and/or high-temperature systems (Dubinin, 2004). Therefore, dissolved Eu concentrations in modern oceans are normal relative to the other elements except in areas of hydrothermal and mid-oceanic ridge activity, where Eu enrichment has been reported in deposited materials (Bau and Möller, 1992; Bau and Dulski, 1999; Bau et al., 2010; Craddock et al., 2010; Schmidt et al., 2010).

Weathering of the continental crust is the ultimate source of REEs, whereas the riverine discharge and atmospheric flux are their preliminary carriers into oceans (Goldstein and Hemming, 2003; Ryu et al., 2007; Chung et al., 2009; Hagedorn et al., 2011). REE distributions in the seawater are principally governed by the type of the terrigenous source and the mechanism of transportation (Alibo and Nozaki, 2004). In fluvial water, the REE concentrations are controlled primarily by the amount of the colloidal particulates (Lawrence and Kamber, 2006; Hannigan et al., 2010). The dissolved organic carbon and water discharge partly impact the fluvial REE composition; enrichments in the REE concentrations in general and the light elements in particular have been reported from the high water discharge and carbon rich rivers (Ingri et al., 2000; Deberdt et al., 2002; Gaillardet et al., 2003). Meanwhile, riverine pH fractionates, to some degree, the fluvial load of REEs (Gaillardet et al., 2003). Higher REE concentrations are observed in the low pH rivers, while heavy REE (HREE) enrichments accompanied with relative depletion in the total concentrations, are noticed in the more alkaline streams (Gaillardet et al., 1997). In general, REE concentrations in the fluvial water are notably

higher than their counterparts in seawater and differ extensively from one place to another (Nozaki et al., 2000a; Alibo and Nozaki, 2004). However, the extensive removal of REEs, especially the light REEs (LREEs), in the estuarine mixing zone controls the riverine REE input to the seawater (Nozaki et al., 2000b; Sholkovitz and Szymczak, 2000).

The direct fallout of terrestrial dust from atmosphere is the second main carrier of weathered REEs into seawater, predominantly to open ocean (e.g. Greaves et al., 1994, 1999; Nozaki, 2001). Unlike the riverine flux that enters oceans through the land–sea interface, the prevailing winds are capable of transporting dust and aerosols for relatively long distances from sources (Greaves et al., 1999). Aeolian input remarkably impacts surface water REE composition (Hongo et al., 2006). Thus, the geographical distribution of REEs in surface water is relatively important in tracing continental sources (Nozaki and Alibo, 2003a; Alibo and Nozaki, 2004). However, the influence decreases dramatically within the first few meters to reaching a negligibly low level in bottom water (Zhang and Nozaki, 1998; Nozaki and Alibo, 2003b).

Basalt alterations at spreading centers as well as the high temperature submarine fluids venting from hot springs constitute the hydrothermal flux of REEs into seawater that is of non-terrestrial origin (Michard et al., 1983; Sholkovitz et al., 1994; Bau and Dulski, 1999; Bau et al., 2010). The expelled fluids are significantly enriched in their REE concentrations (in particular, Eu and LREEs) comparing to the seawater (e.g. Craddock et al., 2010; Schmidt et al., 2010). However, ambient seawater to basaltic ridges and hydrothermal vents does not hold the REE signature of the hydrothermal fluids (cf. Elderfield and Greaves, 1982). Such compositional dissimilarity suggests that the

hydrothermal discharge of REEs into seawater is not enough to noticeably influence the oceanic pool of REEs (e.g. Hongo and Nozaki, 2001).

Several other less important sources have been suggested to impact the oceanic budget of REEs including; erosion of volcanic islands (Amakawa et al., 2000, 2004a,b; Sholkovitz and Szymczak, 2000), remineralization of the bottom sediments (Alibo and Nozaki, 2004), hydrothermal fluids seeped from the vent areas (Klinkhammer et al., 1994; Craddock et al., 2010; Schmidt et al., 2010), on shelf remineralization of river-transported sediments (Nozaki, 2001), submarine groundwater discharge near the coastal areas (Duncan and Shaw, 2003; Johannesson and Burdige, 2007; Johannesson et al., 2011) and the dissolution of aeolian dust and aerosols into the precipitated rainwater (Greaves et al., 1994; Nozaki et al., 1999). Although the impact of these local sources on the seawater REE composition is not evaluated yet, it has been suggested to explain the middle REE (MREE) enrichments in the western Pacific Ocean front of Papua New Guinea (Sholkovitz et al., 1999) and the strong depletion in LREEs and Gd in the southeastern Indian Ocean (Alibo and Nozaki, 2004).

The subsequent removal of the REEs by settling particulate matter controls their fractionation in the seawater (German et al., 1995). Scavenging particulates adsorb and transport REEs from near-surface water to bottom sediments during their settling down to the substrate (Nozaki, 2001; Picard et al., 2002). Such REE carriers include both organic (e.g. fecal and zooplankton) and detrital (e.g. silica, carbonates, inorganic oxides, terrestrial detritus coated with organic matter and/or oxides of manganese and iron) particles and Fe-Mn oxide nodules (Boyle et al., 1977; Goldstein and Jacobsen, 1988; Alibo and Nozaki, 1999, 2000). During their immersion trip, those carriers are exchanged through aggregation

and disaggregation which allows an efficient swap between dissolved and particulates REEs (Nozaki, 2001; Dubinin, 2004).

The gradual diminution of REE radii with increasing atomic number, lanthanide contraction, is the result of the progressive filling of their shielded 4f-orbital (de Baar et al., 1985a; Kim et al., 2012). It causes a gradual increase in the stability constant of free ion in solution across the series from La to Lu (Turner et al., 1981; Bright et al., 2009). The consequent very slight but systematic variations in their chemical properties lead to small fractionation in marine water driven by the preferential scavenging of the LREEs from the water column by sinking particulates relative to the HREEs (de Baar et al., 1985b; German and Elderfield, 1990; Bright et al., 2009). The La, Gd and Lu elements which own empty-, half- and completely-filled 4f electron shell respectively, are particularly more stable, and thus, have less tendency to complex with sinking particulates than the other REEs (de Baar et al., 1985a).

Measured REE concentrations are commonly normalized to eliminate the distinctive and odd variation in natural abundance (the Oddo-Harkins effect) and visualize their fractionation relative to the chief source, the upper continental crust (Kuss et al., 2001; Lacan and Jeandel, 2004; Censi et al., 2007a,b; Zhang et al., 2008). Because the natural abundances of REEs in shale and upper continental crust are closely approximated, several shale composites have been employed to normalize the REE concentrations (Taylor, 1964; Taylor and McLennan, 1985; Elderfield et al., 1988). Among those, Post-Archean Australian Shale (PAAS) and North American Shale Composite (NASC) first introduced by Nance and Taylor (1976) and Haskin et al. (1968) then improved by McLennan (1989) and Gromet et al. (1984), respectively, are the most preferable reference shale materials

(Dubinin, 2004). On the other hand, the REE composition of the magmatic rocks and hydrothermal fluids are often normalized not to the values in shales but chondorites, which assumed to represent the primordial abundances of the solar system (Klinkhammer et al., 1994).

The common shale normalized (SN) REE distribution patterns of modern oxygenated seawater resulted from the combination of these processes characterize by 1) gradual enrichment of the heavier REEs, 2) negative Ce excursion relative to the neighboring La and Pr and 3) occasionally occurring small positive La, Gd and Lu excursions (Bau et al., 1996, 2010; Shields and Webb, 2004; Bright et al., 2009). The only deviation of that trend are; positive anomalies of Ce_{SN} and Eu_{SN} reported from anoxic seawaters and hydrothermal vent sites, respectively (German and Elderfield, 1989; Hongo and Nozaki, 2001; Craddock et al., 2010; Schmidt et al., 2010).

REE concentrations (except Ce) in modern oceans exhibit "nutrient-like" gradual increase with depth curve, due to the progressive breaking down of suspended particulates (de Baar et al., 1985a; Nozaki, 2001). The released REE flux from the remineralization process is enriched in LREE relative to HREEs (Alibo and Nozaki, 1999). However, the deep oceanic water is enriched in the HREEs as a result of the high solubility of their complexes and the re-association of the LREE complexes to suspended particulates (Goldberg et al., 1963; Haley et al., 2004). On the contrary, Ce shows a unique "scavenged" vertical profile in seawater displaying a stepwise decrease from high values in surface water to nearly steady and low in deep water due to its rapid oxidization to highly insoluble discrete solid Ce-oxide grains (Nozaki, 2001; Haley et al., 2004). Consequently, the REE_{SN}

distribution pattern of bottom seawater displays 1) stronger Ce depletion and 2) heavy REE enrichments than the shallower water (Haley et al., 2004; Kim et al., 2012).

The insoluble Ce oxides adsorbed on particulates experience reductive dissolution under anoxic conditions, which enhances the Ce concentrations and subsequently shifts the Ce excursion of the corresponding seawater from negative to slightly positive (de Baar et al., 1988; German and Elderfield, 1989; German et al., 1991). The magnitude and direction of the Ce excursion is quantified by calculating the Ce_{SN} anomaly (Ce/Ce*), which represents the ratio of the Ce_{SN} concentrations versus the neighboring elements La_{SN}, Pr_{SN}, Nd_{SN} or Sm_{SN} (cf. de Baar et al., 1985a; Bau and Dulski, 1999). The corresponding values of Ce_{SN} anomaly are one (no anomaly) or more (positive) in anoxic seawater and less than 1 (negative) when oxygen exists (de Baar et al., 1988). In open ocean, the Ce_{SN} anomaly gets more pronounced (depleted) with depth because the decrease in the amount of dissolved Ce coincides with increases in La, Pr, Nd or Sm concentrations (de Baar et al., 1985a, 1988; German and Elderfield, 1990).

1.2. Modern brachiopods

Brachiopods have an extended geological record and are abundant in most Phanerozoic rocks (Brand et al., 2003, 2011). The first occurrence of fossil brachiopods in the Lower Cambrian strata coincides with the widespread appearance of mineralized skeletal organisms (Rudwick, 1970; Moore, 1997). Brachiopods were more diverse and numerous during the Paleozoic era, but with the Permo-Triassic mass extinction their diversity was drastically reduced and since then brachiopods have never retained their old levels (Gould and Calloway, 1980). Only 260 living brachiopod species have been

identified in the literature representing less than 1% of all brachiopods through geologic time (Tasch, 1980; Brand et al., 2003).

Meanwhile, the brachiopods fall into twenty-six orders within eight classes in three subphyla and are divided into two main categories, articulated and inarticulated (James et al., 1992). A toothed hinge-shell with simple opening and closing muscles characterize the articulated brachiopods, while the untoothed hinge-shell with a complex muscle system to keep the two halves aligned distinguish inarticulated brachiopods (Ruppert and Fox, 2004). Species of *Lingulata* and *Paterinata* class of *Linguliformae* subphylum, and *Craniiforma* class of the *Craniiformae* subphylum secrete inarticulated calcium phosphate and carbonate shells, respectively, whereas those of *Chileata*, *Obolellata*, *Kutorginata*, *Strophomenata* and *Rhynchonellata* classes of *Rhychonelliformea* subphylum secrete predominantly articulated calcium carbonate shells (Rudwick, 1970; Brand et al, 2003). With exception of *lingulids*, which have adopted infaunal habitats in soft sediments, brachiopods are generally sessile benthic marine invertebrates and mostly epifaunal (James et al., 1992).

Modern brachiopods inhabit all seas and oceans in all latitudes, depths and salinities from Arctic to Southern oceans, from the intertidal zone to abyssal plain and from high salinity to brackish-water (Ruppert and Fox, 2004; Logan, 2007; Zezina, 2008). However, only 30% of the species populate below the neritic zone (Brand et al., 2003). In general, brachiopods tend to avoid locations with strong currents and waves and preferably dwell in low-light habitats with well-oxygenated, normal salinity water (Rudwick, 1965; Thompson and Newton, 1987; Ruppert and Fox, 2004). Their growth rate is generally slow and differ seasonally (Peck et al., 1986). It is slower during the nutrient-rich summer season as brachiopods store food in their caeca for relative faster growth in winter (Peck et al., 1987).

The low metabolic rate and ability to consume stored proteins to fuel metabolism enable brachiopods to survive oligotrophic conditions (Peck et al., 1986, 1987; Rhodes and Thayer, 1991). Some articulated species are capable of anaerobic metabolism through adaptation of their metabolic enzymes and are hence able to survive periods of oxygen deprivation (James et al., 1992). In anoxic water, they dwell near to the oxycline boundary where suboxia to anoxia dominates seasonally (Brand et al., 2003).

The articulated brachiopods secrete multi-layers low-Mg calcite shells consist of proteinaceous periostracum membrane covers prominently outer primary and inner secondary layers and occasionally a tertiary layer in some species (Azmy et al., 1998, 2011, 2012; Auclair et al., 2003; Brand et al., 2003). The periostracum decomposes rapidly after death and therefore is absent in fossil shells (Emig, 1990; Brand et al., 2003). The primary, secondary and tertiary (if present) layers consist mostly of micrometer-sized granular, fibres and stacked prismatic calcite, respectively (Brand et al., 2003; Azmy et al., 2012). The thin primary layer is secreted with vital effect and, thus, in disequilibrium with the ambient seawater (Carpenter and Lohmann, 1995; Brand et al., 2003, 2013; Parkinson et al., 2005). In contrast, secondary and tertiary layers are secreted in isotopic equilibrium with no sign of biological fractionation (Veizer et al., 1999; Brand et al., 2003, 2011, 2013; Brand, 2004; Parkinson et al., 2005).

Due to the high resistance to aggressive diagenetic alteration and the equilibrium secretion, the low-Mg calcite of secondary and tertiary layers is considered an important proxy in identifying the original seawater chemistry (e.g. Brand and Veizer, 1980; Al-Aasm and Veizer, 1982; Brand, 1991; Bates and Brand, 1991; Veizer et al., 1999; Brand et al., 2012, 2013). It has been used successfully to assess the fluctuation in the $^{87}Sr/^{86}Sr$ values

of the ancient oceans (cf. Veizer et al., 1999; Korte et al., 2003, 2006) and determine the variation in the carbon and oxygen isotopic compositions and water temperatures of the Phanerozoic seawater (e.g. Azmy et al., 1998; Veizer et al., 1999; Korte et al., 2005a,b, 2008; Brand et al., 2013). Thus, several paleo-oceanographic, environmental and climatologic parameters (e.g. waxing and waning of the continental glaciers, continental and hydrothermal fluxes into seawater, tectonic activity, burial and re-oxidation of organic matter, bioproductivity and changing of the oceanic circulation patterns) are interpreted accurately based on it (Morrison and Brand, 1986; Veizer et al., 1999; Brand and Brenckle, 2001; Brand et al., 2013).

1.3. REE proxy evaluation

Different proxies have been investigated for their reliability in evaluating REE compositions and trends of ancient oceans. Among those, biogenic apatite has received the highest attention of several authors in the last three decades (e.g. Grandjean and Albarede, 1989; Bertram et al., 1992; Jarvis et al., 1994; Girard and Lécuyer, 2002; Chen et al., 2012; Song et al., 2012; Zhao et al., 2013). Modern marine phosphatic brachiopods and ichthyoliths have ∑REE contents of less than1 ppm and display seawater-like REE_{SN} patterns including the negative Ce anomalies (Wright et al., 1984, 1987; Elderfield and Pagett, 1986; Toyoda and Tokonami, 1990; Trueman and Tuross, 2003; Bright et al., 2009; Kocsis et al., 2010). On the contrary, the revealed REE concentrations and patterns of fossil marine phosphorites from shore-face to offshore sediments are significantly different from those of modern seas and oceans exhibiting extremely high ∑REE concentrations, MREE

bulge (bell shape) and/or HREE depletions (hat shape; e.g. Wright, 1985; Armstrong et al., 2001; Kemp and Trueman, 2003).

In order to explain the enigmatic REE compositions of biogenic apatite, two main hypotheses have been suggested. First, the composition of the primary carriers, which are responsible for the REE removal process from the water column, has changed (e.g. Roth, 1986; Grandjean-Lécuyer et al., 1993). Second, the REE compositions of the paleo-oceans were different (McArthur and Walsh, 1984; Grandjean et al., 1987, 1988; Ilyin, 1998a,b, 2004). On the contrary, several authors argued that recrystallization during fossilization of the original components is fundamental cause of such enigmatic REE composition and trends of the ancient biogenic apatites (Trueman and Tuross, 2003; Kohn, 2008; Kocsis et al., 2010). *In vivo* bones are composed of extremely small size but with very large surface area nonstoichiometric carbonate-hydroxyapatite crystallites and intimately associated with the collagenous matrix (Weiner and Price, 1986; Moradian-Oldak et al., 1991; Elliott, 2002; Rubin et al., 2003). Fossil bones, in contrast, are made of large size apatite crystals and display no porosity in the regions where collagen existed (Trueman et al., 2002, 2008a,b). When organism dies, the thermodynamically metastable carbonate-hydroxyapatite recrystallizes rapidly upon exposure to pore water (Trueman and Tuross, 2003, Trueman et al., 2003). New apatite crystals grow to replace the highly adsorptive crystallites completely and continue to fill the porosity that was originally occupied by collagen (Nielsen-Marsh and Hedges, 2000; Roberts et al., 2002; Smith et al., 2005). Due to the high cation exchange capacity of the bone crystallites, many REEs are diffused or adsorbed during the recrystallization process (Tuross et al., 1989; Koeppenkastrop and DeCarlo, 1992; Kolodny et al., 1996; Reynard et al., 1999; Trueman et al., 2003, 2004). In

the early diagenetic uptake, the REEs released from several labile phases accompanied to the change in pore water redox conditions are scavenged into the biogenic apatite (Trueman and Tuross, 2003; Trueman et al., 2006). The pore water composition, the recrystallization rate and the fossil thickness potentially influence the incorporation process and the REE ratios within the biogenic apatite (Trueman et al., 2011). Thereafter, the biogenic apatite remains essentially closed for any further addition or exchange of REEs (Lécuyer et al., 2004; Martin and Scher, 2004). The bell-shape, absence of negative Ce_{SN} anomalies and extreme high ∑REE concentrations of fossil biogenic apatite are, thus, representing the *post-mortem* early uptake of elements during the active interaction with pore-water (Trueman and Tuross, 2002; Bright et al., 2009). Meanwhile, it has been also argued that the late phase of diagenesis enhances to some degree the REE concentrations in biogenic apatite for up to 50% of the total content depending on the initial REE uptake conditions (Kocsis et al., 2010). The assurance of such exchanges with the host sediments has eliminated the biogenic apatite from reconstructing the ancient seawater REE chemistry (German and Elderfield, 1990). Consequently, the REE content preserved in fossil apatite has been used recently to assess the early diagenetic condition of burial environment rather than the geochemical composition of ancient seawater (cf. Murthy et al., 2004; Pucéat et al., 2004; Labs-Hochstein and MacFadden, 2006; Jiménez-Berrocoso et al., 2006; Trotter and Eggins, 2006; Kocsis et al., 2007, 2009, 2010, 2012, 2013; Ounis et al., 2008; Grandstaff and Terry Jr., 2009; Joachimski et al., 2009; MacFadden et al., 2010; Martin et al., 2010; Suarez et al., 2010; Tütken et al., 2011; Matton et al., 2012; Herwartz et al., 2013).

Timidly, few other biogenic proxies such as foraminifers, corals, reefal microbialites and bivalves have been assessed for their REE incorporation (e.g. Palmer, 1985; Sholkovitz and Shen, 1995; Webb and Kamber, 2000; Nothdurft et al., 2004; Olivier and Boyet, 2006; Loope et al., 2013; Johannesson et al., 2014). Sholkovitz and Shen (1995) argued that modern corals do not significantly fractionate REEs during uptake, however, the measurements of Akagi et al. (2004) show substantial REE distribution coefficient differences among different coral species suggesting species-dependent uptake. Although the REEs are not required for healthy metabolism, modern foraminiferal tests are relatively enriched in their REE contents with depleted HREE patterns relative to ambient seawater, suggesting a biological (vital) effect controls their REE uptake (Palmer, 1985). Moreover, their REE compositions increase by up to 10-fold at the sediment-water interface due to the interaction with pore-water (Roberts et al., 2012). Fossils of reefal microbalites exhibit REE_{SN} trend similar to the modern oxygenated seawater with negative Ce, positive La and Gd anomalies and uniform HREE enrichment but with notably higher REE concentrations than the other biogeochemical precipitates (Webb and Kamber, 2000; Nothdurft et al., 2004). Moreover, recent investigations on modern reefal microbialites and stromatolites suggested REE fractionations by organic ligands, bacterial cell walls, microbialite biofilms and/or exopolymeric substances during the precipitation associated with preferential incorporations of extremely high HREE concentrations (Johannesson et al., 2014). Very recently, Merschel and Bau (2015) and Ponnurangam et al. (2015) evaluated the REE composition of the modern *Mytelus* and suggested a biological control on their REE uptake.

1.4. Objectives

The REE signals revealed from most of the biogenic proxies are, thus, reflecting several other parameters (e.g. biological "vital" effect, pore water composition, post-depositional conditions... etc), not only the composition of ancient seawater. Obtaining a reliable palaeochemical indicator is one of the difficulties in this field (Elderfield and Pagett, 1986). Even more, the pilot study of Azmy et al. (2011) although it had encouraging outcomes, showed that the modern warm- and cold-water brachiopods "mainstream shells" exhibit typical LREE enrichments accompanied by slightly positive to negative Ce excursions followed by an otherwise invariant series. In addition, shells from localities of unusual productivity (such as upwelling currents, fluvial input and aerosol dust deposition) and those of the deep water settings are characterized by enrichment in their ∑REE concentrations and depletion in their HREEs relative to mainstream counterparts, as well as by complexity in their REE_{SN} trends. These observations of significant variations imply either 1) an overprinting of the brachiopods' REE compositions by internal (primary layer and proteinous periostracum membrane) and/or external (e.g. adsorptive nano-particulates, encrusting organisms, organic materials, and enclosed sediments to the shells punctuated structure) contamination, or 2) disequilibrium REE incorporations.

Despite the importance of the cleaning for preparing archives for geochemical analysis in general and REEs in particular, reviewing the literature reveals the lack of a rigorous sample processing protocol for cleansing the archives of the internal and external contaminants. There are several cleaning methods that are presented in the literatures include: 1) rinsing with water, ethanol, methanol or ammonium chloride, 2) physical processing consisting mainly of mechanical abrasion and/or ultrasonication, 3) chemical

treatment with hydrochloric, nitric, acetic acids or hydrogen peroxide, and 4) some combination of physical and chemical methods. However, the importance of each of these methods, their target contaminants and their impact on the shells' REE composition have not been quantified yet. Also, the subsequent effects of each of the contaminants on the REE compositions of the articulated brachiopods have not been investigated. The major impetus of the first study in the thesis (Chapter 2) is to introduce a definitive cleaning protocol consisting of a combination of physical and chemical procedures for preparing different archives to acquire primary REE signals. The second task consists of testing the protocols with modern and fossil counterparts as to their veracity in producing robust and reliable seawater REE signatures. In addition, the chapter assesses the contamination effects on the REE compositions and Ce/Ce* anomalies of fossil brachiopods and the enclosing near micritic carbonates, and correlate their compositions and patterns to those of fossil apatite counterparts in order to evaluate their validity for paleoredox studies.

The main aspect of the second study of the thesis (Chapter 3) is to evaluate the REE proxy potential of the uncontaminated modern articulated brachiopods for paleo-oceanic studies. This, in turn, requires, 1) determining whether their REE compositions reflect, in a predictable way, the characteristics of ambient water masses (e.g., dissolved oxygen and depth), 2) defining the tendency of reproducible analytical results among different marine organisms from similar oceanographic conditions, and 3) assessing differences, if present, based on physiochemical properties of the REEs and mineralogy. However, the oceanic budget of REEs is controlled primarily by riverine discharge, atmospheric deposition of dust and aerosols, and hydrothermal/magmatic flux (Elderfield et al., 1988; Nozaki, 2001; Bright et al., 2009). The first two sources influence mainly the shallow depths, while the

third impacts only the ambient water (Klinkhammer et al., 1983; Hongo and Nozaki, 2001). Therefore, to accurately evaluate the reliability of the brachiopod shells as paleo-oceanic REE indicators, it is necessary to minimize the effects of the external factors on the seawater REE compositions. Consequently, this chapter included only brachiopod shells from depths below the neritic environment (>500 m; Logan, 2007), where the impacts of the variation in the environmental parameters on the oceanic budget of the REEs are relatively small. The chapter also aims to 1) estimate the enrichments or the depletions in the REE uptake of modern brachiopods relative to their ambient water masses, 2) calculate the shells' distribution coefficients (log K_D) and correlate the values to those of the other archives, 3) investigate the Ce/Ce* profile of modern brachiopods, and 4) correlate the REE_{SN} patterns of the deep-water articulated brachiopods to the other archives which adopt similar life style.

A remarkable percentage of the fossil archive have adopted shallow water habitats in epeiric sea settings. Those epeiric seas were dominated by wide range of salinities, temperatures and depths (cf. Holmden et al., 1998). The accurate interpretation of their paleoenvironmental and paleodepositional settings, thus, requires understanding the impact of the prevalent oceanographic conditions on modern archive of relatively analogue settings. The third study in the thesis (Chapter 4) intends to 1) asses the REE contents of the shallow water (<500 m) articulated brachiopods from different seas and oceans, and 2) investigate the variations in the physicochemical parameter effects on the REE fractionations and distributions of the shallow (<500 m) and deep-water (>500 m) brachiopods. The results are aimed to be applied on Paleozoic fossil brachiopods and whole rock samples in an attempt to interpret their paleo-bathymetric settings based on the REE

contents. In supplementary aspects the study 1) evaluates the REE incorporations of the shell's structures (i.e. umbo region, primary layer, and secondary layer of the pedicel and brachial valves), and 2) assesses the species variation impacts on the shells' REE composition.

References

Akagi, T., Hashimoto, Y., Fu, F.F., Tsuno, H., Tao, H., and Nakano, Y. (2004). Variation of the distribution coefficients of rare earth elements in modern coral–lattices: species and site dependencies. *Geochimica et Cosmochimica Acta*, *68*(10), 2265–2273.

Al-Aasm, I., and Veizer, J. (1982). Chemical stabilization of low–Mg calcite: an example of brachiopods. *Journal of Sedimentary Petrology*, *52*, 1101–1109.

Alibo, D.S., and Nozaki, Y. (1999). Rare earth elements in seawater: particle association, shale normalization, and Ce oxidation. *Geochimica et Cosmochimica Acta,* 63, 363–372.

Alibo, D.S., and Nozaki, Y. (2000). Dissolved rare earth elements in the South China Sea: Geochemical characterization of the water masses. *Journal of Geophysical Research: Oceans (1978–2012), 105*(C12), 28771–28783.

Alibo, D.S., and Nozaki, Y. (2004). Dissolved rare earth elements in the eastern Indian Ocean: chemical tracers of the water masses. *Deep–Sea Research I*, *51*, 559–576.

Amakawa, H., Alibo, D.S., and Nozaki, Y. (2000). Nd isotopic composition and REE pattern in the surface waters of the eastern Indian Ocean and its adjacent seas. *Geochimica et Cosmochimica Acta, 64*, 1715–1727.

Amakawa, H., Alibo, D.S., and Nozaki, Y. (2000). Nd isotopic composition and REE pattern in the surface waters of the eastern Indian Ocean and its adjacent seas. *Geochimica et Cosmochimica Acta*, *64*(10), 1715–1727.

Amakawa, H., Alibo, D.S., and Nozaki, Y. (2004a). Nd concentration and isotopic composition distributions in surface waters of Northwest Pacific Ocean and its adjacent seas. *Geochemical Journal*, *38*(6), 493–504.

Amakawa, H., Nozaki, Y., Alibo, D.S., Zhang, J., Fukukawa K., and Nagai H. (2004b). Neodymium isotopic variations in Northwest Pacific waters. *Geochimica et Cosmochimica Acta*, *68*, 715–727.

Anderson, P.E., Benton, M.J., Trueman, C.N., Paterson, B.A., and Cuny, G. (2007). Palaeoenvironments of vertebrates on the southern shore of Tethys: the nonmarine Early Cretaceous of Tunisia. *Palaeogeography, Palaeoclimatology, Palaeoecology*, *243*(1), 118–131.

Armstrong, H.A., Pearson, D.G., and Griselin, M. (2001). Thermal effects on rare earth and strontium isotope chemistry in single conodont element. *Geochimica et Cosmochimica Acta, 65*, 435–441.

Auclair, C., Joachimski, M.M., and Lecuyer C. (2003). Deciphering kinetic, metabolic and environmental controls on stable isotope fractionations between seawater and the shell of *Terebratalia transversa* (Brachiopoda). *Chemical Geology, 202*, 59–78.

Azmy, K., Veizer, J., Bassett, M.G., and Copper, P. (1998). Oxygen and carbon isotopic composition of Silurian brachiopods: implications for coeval seawater and glaciations. *Geological Society of America Bulletin*, *110*, 1499–1512.

Azmy, K., Brand, U., Sylvester, P., Gleeson, S., Logan, A., and Bitner, M.A. (2011). Biogenic low–Mg calcite (brachiopods): proxy of seawater–REE composition, natural processes and diagenetic alteration. *Chemical Geology*, *280*, 180–190.

Azmy, K., Poty, E., and Mottequin, B. (2012). Biochemostratigraphy of the Upper Frasnian in the Namur–Dinant Basin, Belgium: Implications for a global Frasnian–Famennian pre–event, *Palaeogeography, Palaeoclimatology, Palaeoecology, 313–314*, 93–106.

Bates, N.R., and Brand, U. (1991). Environmental and physiological influences on isotopic and elemental composition of brachiopod shell calcite: implications for the isotopic evolution of Palaeozoic oceans. *Chemical Geology*, *94*, 67–78.

Bau, M., and Dulski, P. (1999). Comparing yttrium and rare earths in hydrothermal fluids from the Mid-Atlantic Ridge: implications for Y and REE behaviour during near-vent mixing and for the Y/Ho ratio of Proterozoic seawater. *Chemical Geology, 155*(1), 77–90.

Bau, M., and Möller, P. (1992). Rare earth element fractionation in metamorphogenic hydrothermal calcite, magnesite and siderite. *Mineralogy and Petrology*, *45*(3–4), 231–246.

Bau, M., Koschinsky, A., Dulski, P., and Hein, J.R. (1996). Comparison of the partitioning behaviours of yttrium, rare earth elements, and titanium between hydrogenetic marine ferromanganese crusts and seawater. *Geochimica et Cosmochimica Acta*, *60*(10), 1709–1725.

Bau, M., Balan, S., Schmidt, K., and Koschinsky, A. (2010). Rare earth elements in mussel shells of the Mytilidae family as tracers for hidden and fossil high–temperature hydrothermal systems. *Earth and Planetary Science Letters*, *299*(3), 310–316.

Bertram, C.J., and Elderfield, H. (1993). The geochemical balance of the rare earth elements and neodymium isotopes in the oceans. *Geochimica et Cosmochimica Acta*, *57*, 1957–1986.

Bertram, C.J., Elderfield, H., Aldridge, R.J., and Conway Morris, S. (1992). $^{87}Sr/^{86}Sr$, $^{143}Nd/^{144}Nd$ and REEs in Silurian phosphatic fossils. *Earth and Planetary Science Letters, 113*(1–2), 239–249.

Boyle, E.A., Edmond, J.M., and Sholkovitz, E.R. (1977). The mechanism of iron removal in estuaries. *Geochimica et Cosmochimica Acta, 41*, 1313– 1324.

Brand, U. (1991). Strontium isotope diagenesis of biogenic aragonite and low–Mg calcite. *Geochimica et Cosmochimica Acta*, *55*(2), 505–513.

Brand, U. (2004). Carbon, oxygen and strontium isotopes in Paleozoic carbonate components: an evaluation of original seawater–chemistry proxies. *Chemical Geology*, *204*(1), 23–44.

Brand, U., and Brenckle, P. (2001). Chemostratigraphy of the mid-Carboniferous boundary global stratotype section and point (GSSP), Bird Spring Formation, Arrow Canyon, Nevada, USA. *Palaeogeography, Palaeoclimatology, Palaeoecology*, 165(3), 321-347.

Brand, U., and Veizer, J. (1980). Chemical diagenesis of a multicomponent carbonate system–1: Trace elements. *Journal of Sedimentary Research*, 50(4), 1219–1236.

Brand, U., Logan, A., Hiller, N., and Richardson, J. (2003). Geochemistry of modern brachiopods: applications and implications for oceanography and paleoceanography. *Chemical Geology, 198*, 305–334.

Brand, U., Logan, A., Bitner, M.A., Ggriesshsaber, E., Azmy, K., and Buhl, D. (2011). What is the Ideal Proxy of Palaeozoic Seawater chemistry? *Memoirs of the Association of Australasian Palaeontologists*, *41*, 9–24.

Brand, U., Posenato, R., Came, R., Affek, H., Angiolini, L., Azmy, K., and Farabegoli, E. (2012). The end–Permian mass extinction: a rapid volcanic CO_2 and CH_4–climatic catastrophe. *Chemical Geology*, *322–323*, 121–144.

Brand, U., Azmy, K., Bitner, M.A., Logan, A., Zuschin, M., Came, R., and Ruggiero, E. (2013). Oxygen isotopes and $MgCO_3$ in brachiopod calcite and a new paleotemperature equation. *Chemical Geology, 359*, 23–31.

Bright, C.A., Cruse, A.M., Lyons, T.W., MacLeod, K.G., Glascock, M.D., and Ethington, R.L. (2009). Seawater rare–earth element patterns preserved in apatite of Pennsylvanian conodonts?, *Geochimica et Cosmochimica Acta*, *73*, 1609–1624.

Byrne, R.H., and Sholkovitz, E.R. (1996). Marine chemistry and geochemistry of the lanthanides. *Handbook on the physics and chemistry of rare earths*, *23*, 497–593.

Carpenter, S.J., and Lohmann, K.C. (1995). $\delta^{18}O$ and $\delta^{13}C$ values of modern brachiopods. *Geochimica et Cosmochimica Acta*, *59*: 3749–3764.

Censi, P., Larocca, D., Saiano, F., Placenti, F., and Bonanno, A. (2007a). Recognition of water masses according to geochemical signatures in the Central Mediterranean Sea: Y/Ho ratio and REE behaviour. *Journal of Chemical Ecology*. *23*, 139–155.

Censi, P., Sprovieri, M., Larocca, D., Arico, P., Saiano, F., Mazzola S., and Ferla P. (2007b). Alteration effects of volcanic ash in seawater: Anomalous Y/Ho ratios in coastal waters of the Central Mediterranean Sea. *Geochimica et Cosmochimica Acta*, *71*, 5405–5422.

Chen, X., Zhou, L., Wei, K., Wang, J., and Li, Z. (2012). The environmental index of the rare earth elements in conodonts: Evidence from the Ordovician conodonts of the Huanghuachang Section, Yichang area. *Chinese Science Bulletin*, *57*, 349–359.

Chung, C., You, C., and Chu, H. (2009). Weathering sources in the Gaoping (Kaoping) river catchments, southwestern Taiwan: Insights from major elements, Sr isotopes, and rare earth elements. *Journal of Marine Systems, 76*(4), 433–443.

Craddock, P.R., Bach, W., Seewald, J.S., Rouxel, O.J., Reeves, E., and Tivey, M.K. (2010). Rare earth element abundances in hydrothermal fluids from the Manus Basin, Papua New Guinea: Indicators of sub–seafloor hydrothermal processes in back–arc basins. *Geochimica et Cosmochimica Acta*, *74*(19), 5494–5513.

de Baar, H.J., Bacon, M.P., Brewer, P.G., and Bruland, K.W. (1985a). Rare earth elements in the Pacific and Atlantic Oceans. *Geochimica et Cosmochimica Acta*, *49*(9), 1943–1959.

de Baar, H.J., Brewer, P.G., and Bacon, M.P. (1985b). Anomalies in rare earth distributions in seawater: Gd and Tb. *Geochimica et Cosmochimica Acta*, *49*(9), 1961–1969.

de Baar, H.J., German, C.R., Elderfield, H., and Van Gaans, P. (1988). Rare earth element distributions in anoxic waters of the Cariaco Trench. G *Geochimica et Cosmochimica Acta*, *52*(5), 1203–1219.

Deberdt, S., Viers, J., and Dupré, B. (2002). New insights about the rare earth elements (REE) mobility in river waters. *Bulletin de la Société Géologique de France*, *173*(2), 147–160.

Dubinin A.V. (2004). Geochemistry of Rare Earth Elements in the Ocean. *Lithology and Mineral Resources*, *39*(4), 289–307. Translated from *Litologiya i Poleznye Iskopaemye*, *4*, 339–358.

Duncan, T., and Shaw, T.J. (2003). The mobility of rare earth elements and redox sensitive elements in the groundwater/seawater mixing zone of a shallow coastal aquifer. *Aquatic geochemistry*, *9*(3), 233–255.

Elderfield, H., and Greaves, M.J. (1982). The rare earth elements in seawater. *Nature, 296*, 214–219.

Elderfield, H., and Pagett, R. (1986). Rare earth elements in ichthyoliths: variations with redox conditions and depositional environment. *Science of the Total Environment*, *49*, 175–197.

Elderfield, H., Whitfield, M., Burton, J.D., Bacon, M.P., and Liss, P.S. (1988). The oceanic chemistry of the rare–earth elements [and discussion]. *Philosophical Transactions of the Royal Society of London A: Mathematical, Physical and Engineering Sciences*, *325*(1583), 105–126.

Elliott, J.C. (2002). Calcium phosphate biominerals. *Reviews in Mineralogy and Geochemistry, 48*(1), 427–453.

Emig, C.C. (1990). Examples of post–mortality alteration in recent brachiopod shells and (paleo) ecological consequences. *Marine Biology*, *104*, 233 238.

Gaillardet, J., Dupre, B., Allegre, C.J., and Négrel, P. (1997). Chemical and physical denudation in the Amazon River Basin. *Chemical geology*, *142*(3), 141–173.

Gaillardet, J., Viers, J., and Dupré, B. (2003). Trace elements in river waters. *Treatise on geochemistry*, *5*, 225–272.

Garbelli, C., Angiolini, L., Brand, U., Shen, S.Z., Jadoul, F., Posenato, R., Azmy, K., and Cao, C.Q. (2015). Neotethys seawater chemistry and temperature at the dawn of the end Permian mass extinction. *Gondwana Research*. In press.

German, C.R., and Elderfield, H. (1989). Rare earth elements in Saanich Inlet, British Columbia, a seasonally anoxic basin. Geochimica et Cosmochimica Acta, *53*(10), 2561–2571.

German, C.R., and Elderfield, H. (1990). Application of the cerium anomaly as a paleoredox indicator: the ground rules. *Paleoceanography*, *5*, 823–833.

German, C.R., Holliday, B.P., and Elderfield, H. (1991). Redox cycling of rare earth elements in the suboxic zone of the Black Sea. *Geochimica et Cosmochimica Acta*, *55*(12), 3553–3558.

German, C.R., Masuzawa, T., Greaves, M.J., Elderfield, H., and Edmond, J.M. (1995). Dissolved rare earth elements in the Southern Ocean: Cerium oxidation and the influence of hydrography. *Geochimica et Cosmochimica Acta*, *59*(8), 1551–1558.

Girard, C., and Lécuyer, C. (2002). Variations in Ce anomalies of conodonts through the Frasnian/Famennian boundary of Poland (Kowala–Holy Cross Mountains): implications for the redox state of seawater and biodiversity. *Palaeogeography, Palaeoclimatology, Palaeoecology, 181*, 299–311.

Goldberg, E.D., Koide, M., Schmitt, R.A., and Smith, R.H. (1963). Rare-Earth distributions in the marine environment. *Journal of Geophysical Research*, *68*(14), 4209–4217.

Goldstein, S.L., and Hemming, S.R. (2003). Long–lived isotopic tracers in oceanography, paleoceanography and ice sheet dynamics, in: H. Elderfield (Ed.), *Treatise on Geochemistry*, V.6, Elsevier, Oxford, 453–489.

Goldstein, J., and Jacobsen, B. (1988). Rare earth elements in river waters. *Earth and Planetary Science Letters, 89*, 35–47.

Gould, S.J., and Calloway, C.B. (1980). Clams and brachiopods–ships that pass in the night. *Paleobiology*, 383–396.

Grandjean, P., Cappetta, H., Michard, A., and Albaréde, F. (1987). The assessment of REE patterns and $^{143}Nd/^{144}Nd$ ratios in fish remains. *Earth and Planetary Science Letters, 84*, 181–196.

Grandjean, P., Cappetta H., and Albaréde F. (1988). The REE and εNd of 40–70 Ma old fish debris from the west–African platform. *Geophysical Research Letters,* 15, 389–392.

Grandjean-Lécuyer, P., Feist, R., and Albaréde, F. (1993). Rare earth elements in old biogenic apatites. *Geochimica et Cosmochimica Acta*, *57*, 2507–2514.

Grandjean-Lécuyer, P., and Albaréde, F. (1989). Ion probe measurement of rare–earth elements in biogenic phosphates. *Geochimica et Cosmochimica Acta, 53*, 3179–3183.

Grandstaff, D.E., and Terry, D.O. (2009). Rare earth element composition of Paleogene vertebrate fossils from Toadstool Geologic Park, Nebraska, USA. *Applied Geochemistry*, *24*(4), 733–745.

Greaves, M.J., Statham, P.J., and Elderfield, H. (1994). Rare Earth Element Mobilization from Marine Atmospheric Dust into Seawater, *Marine Chemistry*, *46*, 255–260.

Greaves, M.J., Elderfield, H., and Sholkovitz, E.R. (1999). Aeolian sources of rare earth elements to the Western Pacific Ocean. *Marine Chemistry*, *68*(1), 31–38.

Gromet, L.P., Haskin, L.A., Korotev, R.L., and Dymek, R.F. (1984). The "North American shale composite": its compilation, major and trace element characteristics. *Geochimica et Cosmochimica Acta*, *48*(12), 2469–2482.

Hagedorn, B., Cartwright, I., Raveggi, M., and Maas, R. (2011). Rare earth element and strontium geochemistry of the Australian Victorian Alps drainage system: Evaluating the dominance of carbonate vs. aluminosilicate weathering under varying runoff. *Chemical Geology*, *284*, 105–126.

Haley, B.A., Klinkhammer, G.P., and McManus, J. (2004). Rare earth elements in pore waters of marine sediments. *Geochimica et Cosmochimica Acta*, *68*(6), 1265–1279.

Hannigan, R., Dorval, E., and Jones, C. (2010). The rare earth element chemistry of estuarine surface sediments in the Chesapeake Bay. *Chemical Geology*, *272*(1), 20–30.

Haskin, L.A., and Haskin, M.A. (1968). Rare–earth elements in the Skaergaard intrusion. *Geochimica et Cosmochimica Acta*, *32*(4), 433–447.

Herwartz, D., Tütken, T., Jochum, K.P., and Sander, P.M. (2013). Rare earth element systematics of fossil bone revealed by LA-ICPMS analysis. *Geochimica et Cosmochimica Acta*, *103*, 161–183.

Holmden, C., Creaser, R.A., Muehlenbachs, K.L.S.A., Leslie, S.A., and Bergström, S.M. (1998). Isotopic evidence for geochemical decoupling between ancient epeiric seas and bordering oceans: implications for secular curves. *Geology*, *26*(6), 567–570.

Holser, W.T. (1997). Evaluation of the application of rare–earth elements to paleoceanography. *Palaeogeography, Palaeoclimatology, Palaeoecology*, *132*(1), 309–323.

Hongo, Y., and Nozaki, Y. (2001). Rare earth element geochemistry of hydrothermal deposits and *Calyptogena* shell from the Iheya Ridge vent field, Okinawa Trough. *Geochemical Journal*, *35*, 347–354.

Hongo, Y., Obata, H., Alibo, D., and Nozaki, Y. (2006). Spatial Variations of Rare Earth Elements in North Pacific Surface Water. *Journal of Oceanography*, 62, 441–455.

Ilyin, A.V. (1998a). Rare–earth element geochemistry of the Mesozoic phosphorites of the East European Platform, with applications to some problems of phosphogenesis. *Geochemistry international*, *36*(6), 489–495.

Ilyin, A.V. (1998b). Rare–Earths Geochemistry of "Old" Phosphorites and Probability of Direct Synsedimentational Precipitation and Accumulation of Phosphate, *Chemical Geology*, *144*, 243–256.

Ilyin, A.V. (2004). The Khubsugul phosphate–bearing basin: new data and concepts. *Lithology and Mineral Resources*, *39*(5), 454–467.

Ingri, J., Widerlund, A., Land, M., Gustafsson, Ö., Andersson, P., and Öhlander, B. (2000). Temporal variations in the fractionation of the rare earth elements in a boreal river; the role of colloidal particles. *Chemical Geology*, *166*(1), 23–45.

James, M.A., Ansell, A.D., Collins, M.J., Curry, G.B., Peck, L.S., and Rhodes, M.C. (1992). Biology of living brachiopods. *Advances in Marine Biology*, *28*, 175–387.

Jarvis, I., Burnett, W., Nathan, Y., Almbaydin, F.S.M., Attia, A.K.M., Castro, L.N., Flicoteaux, R., Hilmy, M.E., Husain, V., Qutawnah, A.A., Serjani, A., and Zanin, Y.N. (1994). Phosphorite geochemistry: state–of–the–art and environmental concerns. *Eclogae Geologicae Helvetiae, 87*, 643–700.

Jiménez-Berrocoso, Á., Olivero, E.B., and Elorza, J. (2006). New petrographic and geochemical insights on diagenesis and palaeoenvironmental stress in Late Cretaceous inoceramid shells from the James Ross Basin, Antarctica. *Antarctic Science*, *18*(03), 357–376.

Joachimski, M.M., Breisig, S., Buggisch, W., Talent, J.A., Mawson, R., Gereke, M., Morrow, J.R., Day, J., and Weddige, K. (2009). Devonian climate and reef evolution:

insights from oxygen isotopes in apatite. *Earth and Planetary Science Letters, 284*, 599–609.

Johannesson, K.H., and Burdige, D.J. (2007). Balancing the global oceanic neodymium budget: Evaluating the role of groundwater. *Earth and Planetary Science Letters*, *253*(1), 129–142.

Johannesson, K.H., Chevis, D.A., Burdige, D.J., Cable, JE., Martin, J. B., and Roy, M. (2011). Submarine groundwater discharge is an important net source of light and middle REEs to coastal waters of the Indian River Lagoon, Florida, USA. *Geochimica et Cosmochimica Acta*, *75*(3), 825–843.

Johannesson, K.H., Telfeyan, K., Chevis, D.A., Rosenheim, B.E., and Leybourne, M.I. (2014). Rare earth elements in stromatolites–1. Evidence that modern terrestrial stromatolites fractionate rare earth elements during incorporation from ambient waters. In *Evolution of Archean Crust and Early Life,* Springer Netherlands, 385–411.

Kemp, R.A., and Trueman, C. (2003). Rare earth elements in Solnhofen biogenic apatite: geochemical clues to the paleoenvironment. *Sedimentary Geology*, *155*, 109–127.

Kim, J.H., Torres, M.E., Haley, B.A., Kastner, M., Pohlman, J.W., Riedel, M., and Lee, Y.J. (2012). The effect of diagenesis and fluid migration on rare earth element distribution in pore fluids of the northern Cascadia accretionary margin. *Chemical Geology*, *291*, 152–165.

Klinkhammer, G., Elderfield, H., and Hudson, A. (1983). Rare earth elements in seawater near hydrothermal vents. *Nature*, *305*, 185–188.

Klinkhammer, G., German, C.R., Elderfield, H., Greaves, M.J., and Mitra, A. (1994). Rare earth elements in hydrothermal fluids and plume particulates by inductively coupled plasma mass spectrometry. *Marine Chemistry*, *45*(3), 179–186.

Kocsis, L., Vennemann, T.W., and Fontignie, D. (2007). Migration of sharks into freshwater systems during the Miocene and implications for Alpine paleoelevation. *Geology*, *35*(5), 451–454.

Kocsis, L., Vennemann, T.W., Hegner, E., Fontignie, D., and Tütken, T. (2009). Constraints on Miocene oceanography and climate in the Western and Central Paratethys: O–, Sr–, and Nd–isotope compositions of marine fish and mammal remains. *Palaeogeography, Palaeoclimatology, Palaeoecology*, *271*(1), 117–129.

Kocsis, L., Trueman, C.N., and Palmer, M.R. (2010). Protracted diagenetic alteration of REE contents in fossil bioapatites: direct evidence from Lu–Hf isotope systematics. *Geochimica et Cosmochimica Acta*, *74*(21), 6077–6092.

Kocsis, L., Dulai, A., Bitner, M. A., Vennemann, T., and Cooper, M. (2012). Geochemical compositions of Neogene phosphatic brachiopods: Implications for ancient environmental and marine conditions. *Palaeogeography, Palaeoclimatology, Palaeoecology*, *326*, 66–77.

Kocsis, L., Ounis, A., Chaabani, F., and Salah, N.M. (2013). Paleoenvironmental conditions and strontium isotope stratigraphy in the Paleogene Gafsa Basin (Tunisia) deduced from geochemical analyses of phosphatic fossils. *International Journal of Earth Sciences*, *102*(4), 1111–1129.

Koeppenkastrop, D., and De Carlo, E.H. (1992). Sorption of rare earth elements from seawater onto synthetic mineral particles: an experimental approach. *Chemical Geology*, *95*, 251– 263.

Kohn, M.J. (2008). Models of diffusion–limited uptake of trace elements in fossils and rates of fossilization. *Geochimica et Cosmochimica Acta*, *72*(15), 3758–3770.

Kolodny, Y., Luz, B., Sander, M., and Clemens, W.A. (1996). Dinosaur bones: fossils or pseudomorphs? The pitfalls of physiology reconstruction from apatitic fossils. *Palaeogeography, Palaeoclimatology, Palaeoecology*, *126*(1), 161–171.

Korte, C., Kozur, H.W., Bruckschen, P., and Veizer, J. (2003). Strontium isotope evolution of Late Permian and Triassic seawater. *Geochimica et Cosmochimica Acta*, *67*(1), 47–62.

Korte, C., Jasper, T., Kozur, H.W., and Veizer, J. (2005a). $\delta^{18}O$ and $\delta^{13}C$ of Permian brachiopods: a record of seawater evolution and continental glaciation. *Palaeogeography, Palaeoclimatology, Palaeoecology*, *224*(4), 333–351.

Korte, C., Kozur, H.W., and Veizer, J. (2005b). $\delta^{18}O$ and $\delta^{13}C$ values of Triassic brachiopods and carbonate rocks as proxies for coeval seawater and palaeotemperature. *Palaeogeography, Palaeoclimatology, Palaeoecology*, *226*(3), 287–306.

Korte, C., Jasper, T., Kozur, H.W., and Veizer, J. (2006). $^{87}Sr/^{86}Sr$ record of Permian seawater. *Palaeogeography, Palaeoclimatology, Palaeoecology*, *240*(1), 89–107.

Korte, C., Jones, P.J., Brand, U., Mertmann, D., and Veizer, J. (2008). Oxygen isotope values from high–latitudes: clues for Permian sea–surface temperature gradients and Late Palaeozoic deglaciation. *Palaeogeography, Palaeoclimatology, Palaeoecology*, *269*(1), 1–16.

Kuss, J., Garbe-Schonberg, C.D., and Kremling, K. (2001). Rare earth elements in suspended particulate material of North Atlantic surface waters. *Geochimica et Cosmochimica Acta*, *65*, 187–199.

Labs-Hochstein, J., and MacFadden, B.J. (2006). Quantification of diagenesis in Cenozoic sharks: elemental and mineralogical changes. *Geochimica et Cosmochimica Acta*, *70*(19), 4921–4932.

Lacan, F., and Jeandel, C. (2004). Neodymium isotopic composition and rare earth element concentrations in the deep and intermediate Nordic Seas: Constraints on the Iceland Scotland Overflow Water signature. *Geochemistry, Geophysics, Geosystems*, *5*(11), 1–10.

Lawrence, M.G., and Kamber, B.S. (2006). The behaviour of the rare earth elements during estuarine mixing—revisited. *Marine Chemistry*, *100*(1), 147–161.

Lawrence, M.G., Greig, A., Collerson, K.D., and Kamber, B. S. (2006). Rare earth element and yttrium variability in South East Queensland waterways. *Aquatic Geochemistry*, *12*(1), 39–72.

Lécuyer, C., Grandjean, P., Barrat, J.A., Emig, C.C., Nolvak, J., Paris, F., and Robardet, M. (1998). $\delta^{18}O$ and REE contents of phosphatic brachiopods: a comparison between modern and lower Paleozoic populations. *Geochimica et Cosmochimica Acta, 62*, 2429–2436.

Lécuyer, C., Bogey, C., Garcia, J.P., Grandjean, P., Barrat, J.A., Bardet, N., and Pereda-Superbiola, X. (2003). Stable isotope composition and rare earth element content of vertebrate remains from the late Cretaceous of northern Spain (Lano): did the environmental record survive?, *Palaeogeography, Palaeoclimatology, Palaeoecology*, *193*, 457–471.

Lécuyer, C., Reynard, B., and Grandjean, P. (2004). Rare earth element evolution of Phanerozoic seawater recorded in biogenic apatites. *Chemical Geology,* 204, 63–102.

Logan, A. (2007). Geographic distribution of extant articulated brachiopods. In: Selden, P. A. (ed.): Treatise on Invertebrate Paleontology, Part H (Revised), Brachiopoda, 6 (supplement), 3082–3115. The Geological Society of America and the University of Kansas, Boulder, Colorado and Lawrence, Kansas.

Loope, G.R., Kump, L.R., and Arthur, M.A. (2013). Shallow water redox conditions from the Permian–Triassic boundary microbialite: The rare earth element and iodine geochemistry of carbonates from Turkey and South China. *Chemical Geology*, *351*, 195–208.

MacFadden, B.J., DeSantis, L.R., Hochstein, J.L., and Kamenov, G.D. (2010). Physical properties, geochemistry, and diagenesis of xenarthran teeth: prospects for interpreting the paleoecology of extinct species. *Palaeogeography, Palaeoclimatology, Palaeoecology*, *291*(3), 180–189.

Martin, E.E., and Scher, H.D. (2004). Preservation of seawater Sr and Nd isotopes in fossil fish teeth: bad news and good news. *Earth and Planetary Science Letters*, *220*(1), 25–39.

Martin, E.E., Blair, S.W., Kamenov, G.D., Scher, H.D., Bourbon, E., Basak, C., and Newkirk, D.N. (2010). Extraction of Nd isotopes from bulk deep sea sediments for paleoceanographic studies on Cenozoic time scales. *Chemical Geology*, *269*(3), 414–431.

Matton, O., Cloutier, R., and Stevenson, R. (2012). Apatite for destruction: Isotopic and geochemical analyses of bioapatites and sediments from the Upper Devonian Escuminac Formation (Miguasha, Québec). *Palaeogeography, Palaeoclimatology, Palaeoecology, 361*, 73–83.

McArthur, J.M., and Walsh, J.N. (1984). Rare–earth geochemistry of phosphorites. *Chemical Geology, 47*, 91–220.

McLennan, S.M. (1989). Rare earth elements in sedimentary rocks: influence of provenance and sedimentary processes. In: Lipin, B.R., McKay, G.A. (Eds.), Geochemistry and Mineralogy of Rare Earth Elements, *Mineralogical Society of America Review Mineralogy*, *21*, 169–200.

Merschel, G., and Bau, M. (2015). Rare earth elements in the aragonitic shell of freshwater mussel Corbicula fluminea and the bioavailability of anthropogenic lanthanum, samarium and gadolinium in river water. *Science of The Total Environment*, *533*, 91–101.

Michard, A., Albarede, F., Michard, G., Minster, J.F., and Charlou, J.L. (1983). Rare–earth elements and uranium in high–temperature solutions from East Pacific Rise hydrothermal vent field (13 N). *Nature*, *303*, 795–797.

Moore, R.C. (1997). Treatise on invertebrate paleontology, Geological society of America.

Moradian-Oldak, J., Weiner, S., Addadi, L., Landis, W.J., and Traub, W. (1991). Electron imaging and diffraction study of individual crystals of bone, mineralized tendon and synthetic carbonate apatite. *Connective tissue research*, *25*(3–4), 219–228.

Morrison, J.O., and Brand, U. (1986). Paleoscene# 5. Geochemistry of recent marine invertebrates. *Geoscience Canada*, *13*(4), 237–254.

Murthy, R., Kidder, D., Mapes, R., and Hannigan, R. (2004). Rare–earth element chemistry of Mississippianage phosphate nodules in the Fayetteville Shale of Oklahoma and Arkansas. *Environmental Geosciences*, *11*(2), 99–111.

Nance, W.B., and Taylor, S.R. (1976). Rare earth element patterns and crustal evolution–I. Australian post–Archean sedimentary rocks. *Geochimica et Cosmochimica Acta*, *40*(12), 1539–1551.

Nielsen-Marsh, C.M., and Hedges, R.E. (2000). Patterns of diagenesis in bone I: the effects of site environments. *Journal of Archaeological Science*,*27*(12), 1139–1150.

Nothdurft, L.D., Webb, G.E., and Kamber, B.S. (2004). Rare earth element geochemistry of Late Devonian reefal carbonates, Canning Basin, Western Australia: confirmation of a seawater REE proxy in ancient limestones. *Geochimica et Cosmochimica Acta*, *68*(2), 263–283.

Nozaki, Y. (2001). Rare Earth Elements and their Isotopes in the Ocean. Encyclopedia of Ocean Sciences, *4*, 2354–2366.

Nozaki, Y., and Alibo, D. (2003a). Dissolved rare earth elements in the Southern Ocean, southwest of Australia: Unique patterns compared to the South Atlantic data. *Geochemical Journal*, *37*, 47–62.

Nozaki, Y., and Alibo, D. (2003b). Importance of vertical geochemical processes in controlling the oceanic profiles of dissolved rare earth elements in the northeastern Indian Ocean. *Earth and Planetary Science Letters, 205*, 155–172.

Nozaki, Y., Alibo, D., Amakawa, H., Gamo, T., and Hasumoto, H. (1999). Dissolved rare earth elements and hydrography in the Sulu Sea, *Geochimica et Cosmochimica Acta*, *63*(15), 2171–2181.

Nozaki, Y., Lerche, D., Alibo, D.S., and Tsutsumi, M. (2000a). Dissolved indium and rare earth elements in three Japanese rivers and Tokyo Bay: evidence for anthropogenic Gd and In. *Geochimica et Cosmochimica Acta*, *64*(23), 3975–3982.

Nozaki, Y., Lerche, D., Alibo, D.S., and Snidvongs, A. (2000b). The estuarine geochemistry of rare earth elements and indium in the Chao Phraya River, Thailand. *Geochimica et Cosmochimica Acta*, *64*(23), 3983–3994.

Olivier, N., and Boyet, M. (2006). Rare earth and trace elements of microbialites in Upper Jurassic coral–and sponge–microbialite reefs. *Chemical Geology*, *230*(1), 105–123.

Ounis, A., Kocsis, L., Chaabani, F., and Pfeifer, H.R. (2008). Rare earth elements and stable isotope geochemistry ($\delta^{13}C$ and $\delta^{18}O$) of phosphorite deposits in the Gafsa Basin, Tunisia. *Palaeogeography, Palaeoclimatology, Palaeoecology*, *268*(1), 1–18.

Palmer, M.R. (1985). Rare earth elements in foraminifera tests. *Earth and Planetary Science Letters, 73*, 285–298.

Parkinson, D., Curry, G.B., Cusack, M., Fallick A.E. (2005). Shell structure, patterns and trends of oxygen and carbon stable isotopes in modern brachiopod shells. *Chemical Geology*, *219*, 193–235.

Peck, L., Morris, D., and Clarke, A. (1986). The caeca of punctate brachiopods: a respiring tissue not a respiratory organ. *Lethaia*, *19*(3), 232–232.

Peck, L.S., Clarke, A., and Holmes, L.J. (1987). Summer metabolism and seasonal changes in biochemical composition of the Antarctic brachiopod *Liothyrella uva* (Broderip, 1833). *Journal of experimental marine biology and ecology*, *114*(1), 85–97.

Picard, S., Lécuyer, C., Barrat, J.A., Garcia, J.P., Dromart, G., and Sheppard, S.M.F. (2002). Rare earth element contents of Jurassic fish and reptile teeth and their potential relation to seawater composition (Anglo–Paris Basin, France and England). *Chemical Geology*, *186*, 1–16.

Piepgras, D., and Jacobsen, S. (1992). The behavior of rare earth elements in seawater: Precise determination of variations in the North Pacific water column. *Geochimica et Cosmochimica Acta*, *56*, 1851–1862.

Ponnurangam, A., Bau, M., Brenner, M., and Koschinsky, A. (2015). Mussel shells of *Mytilus edulis* as bioarchives of the rare earth elements and yttrium distribution in seawater and the potential impact of pH and temperature on the partitioning behaviour. *Biogeosciences Discussions*, *12*(17).

Pucéat, E., Reynard, B., and Lécuyer, C. (2004). Can crystallinity be used to determine the degree of chemical alteration of biogenic apatites?. *Chemical Geology*, *205* (1), 83–97.

Reynard, B., Lécuyer, C., and Grandjean, P. (1999). Crystal–chemical controls on rare–earth element concentrations in fossil biogenic apatites and implications for paleoenvironmental reconstructions. *Chemical Geology, 155*, 233–241.

Rhodes, M.C., and Thayer, C.W. (1991). Mass extinctions: ecological selectivity and primary production. *Geology*, *19*(9), 877–880.

Roberts, S.J., Smith, C.I., Millard, A., and Collins, M.J. (2002). The taphonomy of cooked bone: characterizing boiling and its physico–chemical effects. *Archaeometry*, *44*(3), 485–494.

Roth, P.H. (1986). Mesozoic palaeoceanography of the North Atlantic and Tethys oceans. *Geological Society, London, Special Publications*, *21*(1), 299–320.

Rubin, M.A., Jasiuk, I., Taylor, J., Rubin, J., Ganey, T., and Apkarian, R.P. (2003). TEM analysis of the nanostructure of normal and osteoporotic human trabecular bone. *Bone*, *33*(3), 270–282.

Rudwick, M.J.S. (1965). Ecology and paleoecology: in Treatise on Invertebrate Paleontology, Part H, Brachiopod. Boulder F., *Geological Society of America, 1*, H199–H214.

Rudwick, M.J.S. (1970). Living and Fossil Brachiopods, *Hutchinson University Library*, London, 199p.

Ruppert, E.E., and Fox, R.S. (2004). Invertebrate zoology: a functional evolutionary approach, in Barnes R.D., *Invertebrate Zoology*, Brooks/Cole, Belmont, CA.

Ryu, J.S., Lee, K.S., Lee, S.G., Lee, D., and Changd H.W. (2007). Seasonal and spatial variations of rare earth elements in rain waters, river waters and total suspended particles in air in South Korea. *Journal of Alloys and Compounds, 437*, 344–350.

Schmidt, K., Garbe–Schönberg, D., Bau, M., and Koschinsky, A. (2010). Rare earth element distribution in> 400 C hot hydrothermal fluids from 5S, MAR: The role of anhydrite in controlling highly variable distribution patterns. *Geochimica et Cosmochimica Acta*, *74*(14), 4058–4077.

Shields, G., and Webb, G.E. (2004). Has the REE composition of seawater changed over geological time?. *Chemical Geology*, *204*(1–2): 103–107.

Sholkovitz, E.R., and Schneider, D. L. (1991). Cerium redox cycles and rare earth elements in the Sargasso Sea. *Geochimica et Cosmochimica Acta*, *55*(10), 2737–2743.

Sholkovitz, E.R., and Shen, G.T. (1995). The incorporation of rare–earth elements in modern coral. *Geochimica et Cosmochimica Acta*, *59*, 2749–2756.

Sholkovitz, E.R, and Szymczak, R. (2000). The estuarine chemistry of rare earth elements: comparison of the Amazon, Fly, Sepik and the Gulf of Papua systems. *Earth and Planetary Science Letters*, *179*(2), 299–309.

Sholkovitz, E.R., Landing, W.M., and Lewis, B.L. (1994). Ocean particle chemistry: the fractionation of rare earth elements between suspended particles and seawater. *Geochimica et Cosmochimica Acta*, *58*(6), 1567–1579.

Sholkovitz, E.R., Elderfield, H., Szymczak, R., and Casey, K. (1999). Island weathering: River sources of rare earth elements to the Western Pacific Ocean. *Marine Chemistry*, *68*(1–2), 39–57.

Smith, C.I., Craig, O.E., Prigodich, R.V., Nielsen-Marsh, C.M., Jans, M.M.E., Vermeer, C., and Collins, M.J. (2005). Diagenesis and survival of osteocalcin in archaeological bone. *Journal of Archaeological Science*, *32*(1), 105–113.

Song, H., Wignall, P.B., Tong, J., Bond, D.P., Song, H., Lai, X., and Chen, Y. (2012). Geochemical evidence from bio–apatite for multiple oceanic anoxic events during Permian–Triassic transition and the link with end–Permian extinction and recovery. *Earth and Planetary Science Letters*, *353*, 12–21.

Suarez, C.A., Macpherson, G.L., González, L.A., and Grandstaff, D.E. (2010). Heterogeneous rare earth element (REE) patterns and concentrations in a fossil bone: implications for the use of REE in vertebrate taphonomy and fossilization history. *Geochimica et Cosmochimica Acta*, *74*(10), 2970–2988.

Tasch, P. (1980). Paleobiology of the Invertebrates. Wiley, New York, 251– 311.

Taylor, S.R. (1964). Trace element abundances and the chondritic earth model. *Geochimica et Cosmochimica Acta*, *28*(12), 1989–1998.

Taylor, S.R., and McLennan, S.M. (1985). The continental crust: its composition and evolution. Blackwell Scientific Publication, Palo Alto, CA.

Thompson, J.B., and Newton, C.R. (1987). Ecological reinterpretation of dysaerobic Leiorhynchus fauna: Geneseo black shale, central New York. *Palaios*, *2*, 274–281.

Toyoda, K., and Tokonami, M. (1990). Diffusion of rare–earth elements in fish teeth from deep–sea sediments. *Nature, 345*, 607–609.

Trotter, J.A., and Eggins, S.M. (2006). Chemical systematics of conodont apatite determined by laser ablation ICPMS. *Chemical Geology*, *233*(3), 196–216.

Trueman, C.N., and Tuross, N. (2002). Trace elements in recent and fossil bone apatite. *Reviews in mineralogy and geochemistry*, *48*(1), 489–521.

Trueman, C.N., Benton, M. J., and Palmer, M.R. (2003). Geochemical taphonomy of shallow marine vertebrate assemblages. *Palaeogeography, Palaeoclimatology, Palaeoecology, 197*(3), 151–169.

Trueman, C.N., Behrensmeyer, A.K., Tuross, N., and Weiner, S. (2004). Mineralogical and compositional changes in bones exposed on soil surfaces in Amboseli National Park, Kenya: diagenetic mechanisms and the role of sediment pore fluids. *Journal of Archaeological Science*, *31*(6), 721–739.

Trueman, C.N., Behrensmeyer, A.K., Potts, R., and Tuross, N. (2006). High–resolution records of location and stratigraphic provenance from the rare earth element composition of fossil bones. *Geochimica et Cosmochimica Acta*, *70*(17), 4343–4355.

Trueman, C.N., Palmer, M.R., Field, J., Privat, K., Ludgate, N., Chavagnac, V., Eberth D.A., Cifelli R., and Rogers, R.R. (2008a). Comparing rates of recrystallisation and the potential for preservation of biomolecules from the distribution of trace elements in fossil bones. *Comptes Rendus Palevol*, *7*(2), 145–158.

Trueman, C.N., Privat, K., and Field, J. (2008b). Why do crystallinity values fail to predict the extent of diagenetic alteration of bone mineral?. *Palaeogeography, Palaeoclimatology, Palaeoecology*, *266*(3), 160–167.

Trueman, C.N., Kocsis, L., Palmer, M.R., and Dewdney, C. (2011). Fractionation of rare earth elements within bone mineral: a natural cation exchange system. *Palaeogeography, Palaeoclimatology, Palaeoecology*, *310*(1), 124–132.

Turner, D.R., Whitfield, M., and Dickson, A.G. (1981). The equilibrium speciation of dissolved components in freshwater and sea water at 25C and 1 atm pressure. *Geochimica et Cosmochimica Acta*, *45*(6), 855–881.

Tuross, N., Behrensmeyer, A.K., Eanes, E.D., Fisher, L.W., and Hare, P.E. (1989). Molecular preservation and crystallographic alterations in a weathering sequence of wildebeest bones. *Applied Geochemistry*, *4*(3), 261–270.

Tütken, T., Vennemann, T.W., and Pfretzschner, H.U. (2011). Nd and Sr isotope compositions in modern and fossil bones–Proxies for vertebrate provenance and taphonomy. *Geochimica et Cosmochimica Acta*, *75*(20), 5951–5970.

Veizer, J., Ala, D., Azmy, K., Bruckschen, P., Bruhn, F., Buhl, D., Carden, G., Diener, A., Ebneth, S., Goddris, Y., Jasper, T., Korte, C., Pawellek, F., Podlaha, O., Strauss, H.

(1999). $^{87}Sr/^{86}Sr$, $\delta^{13}C$ and $\delta^{18}O$ evolution of Phanerozoic seawater. *Chemical Geology*, *161*, 59–88.

Webb, G.E., and Kamber, B.S. (2000). Rare earth elements in Holocene reefal microbialites: a new shallow seawater proxy. *Geochimica et Cosmochimica Acta, 64*, 1557–1565.

Weiner, S., and Price, P.A. (1986). Disaggregation of bone into crystals. *Calcified Tissue International*, *39*(6), 365–375.

Wright, J. (1985). Rare earth element distributions in Recent and fossil apatite: implications for paleoceanography and stratigraphy. Ph.D. dissertation. University of Oregon, Eugene. 259p.

Wright, J., Seymour, R.S., and Shaw, H.F. (1984). REE and Nd isotopes in conodont apatite: variations with geological age and depositional environment. *Geological Society of America Special Papers*, *196*, 325–340.

Wright, J., Schrader, H., and Holser, W.T. (1987). Paleoredox variations in ancient oceans recorded by rare earth elements in fossil apatite. *Geochimica et Cosmochimica Acta*, *51*(3), 631–644.

Zezina, O.N. (2008). Biogeography of the recent brachiopods. *Paleontological Journal*, *42*(8), 830–858.

Zhang, J., and Nozaki, Y. (1998). Behavior of rare earth elements in seawater at the ocean margin: A study along the slopes of the Sagami and Nankai troughs near Japan. *Geochimica et Cosmochimica Acta, 62*(8), 1307–1317.

Zhang, Y., Lacan, F., and Jeandel, C. (2008). Dissolved rare earth elements tracing lithogenic inputs over the Kerguelen Plateau (Southern Ocean). *Deep–Sea Research II*, *55*, 638–652.

Zhao, L., Chen, Z.Q., Algeo, T.J., Chen, J., Chen, Y., Tong, J., Gao S., Zhou l., Hu Z., and Liu, Y. (2013). Rare–earth element patterns in conodont albid crowns: Evidence for massive inputs of volcanic ash during the latest Permian biocrisis?. *Global and Planetary Change*, *105*, 135–151.

CHAPTER 2

A NEW SAMPLE PROCESSING PROTOCOL FOR PROCURING SEAWATER REE SIGNATURES IN BIOGENIC AND ABIOGENIC CARBONATES

(Published in *Chemical Geology* (2015), V. 416, pp. 36-50)

Amir H. Zaky[a], Uwe Brand[b], and Karem Azmy[a]

[a] Department of Earth Sciences, Memorial University of Newfoundland, St. John's, NL, A1B 3X5 Canada.
[b] Department of Earth Sciences, Brock University, St. Catharines, ON, L2S 3A1 Canada.

ABSTRACT

Rare Earth Elements are important proxies for tracing the evolution and redox history of the Earth's hydrosphere. Many biogenic and abiogenic archives have been analyzed for their REE contents with qualified success, which may be due to depositional and post-depositional alteration effects. Review of the database reveals a lack of a rigorous sample processing protocol and probably the leading cause for the spurious REE results reported in the literature.

We propose a 'sample cleaning protocol' that should satisfy the most stringent demands for procuring reliable and robust REEs from marine materials. Without cleaning, the results may represent REE compositions not only of the shell's structure but also of lattice-bound oxides, detritus, particulates and organic remnants. Thus, cleaning of material is a fundamental step that should be conducted with care and attention to detail prior to analyzing their REE contents. To achieve this goal, valves from recently dead *Liothyrella neozelanica* recovered from deep water of the South Pacific Ocean (north of New Zealand)

were subjected to five different cleaning procedures. In Procedure – 1 (P-1) valve fragments were only washed and rinsed with distilled water. In Procedure – 2 (P-2) a set of fragments was immersed in 2.5 % hydrogen peroxide (H_2O_2) for three continuous days and then water washed. In Procedure – 3 (P-3) valve fragments were physically cleaned using a sharp stainless-steel blade and then water washed. In Procedure – 4 (P-4) a set of fragments was physically cleaned then immersed briefly in 10 % hydrochloric acid (HCl) until they were deemed clean, and then water washed. In Procedure – 5 (P-5) the last set of fragments was processed using all cleaning protocols such as physical scraping, H_2O_2, HCl leaches and water washing.

Detritus and nano-particulates adsorbed on the calcitic structure of brachiopod shells including the proteinaceous periostracum may lead to elevated ∑REE content, anomalous Ce/Ce* and elevated Mn, Fe and U concentrations as documented by the P-1 protocol results. Hydrogen peroxide immersion (P-2) eliminates primarily the organic tissue, which leads to an invariant Ce/Ce* anomaly. Physical cleaning (P-3) removes adsorptive nano-particulates and the periostracum, and leads to depleted ∑REE and lower Mn, Fe, and U concentrations with a slight Ce/Ce* anomaly. Physical cleaning followed by chemical cleaning (P-4 and P-5) removes adsorptive particulates, organic remnants, the periostracum and the primary layer. These last two procedures produce drastic reductions in ∑REE, Mn, Fe, and U concentrations and normal Ce/Ce* anomalies with typical seawater REE signatures in brachiopod calcite.

Procedure P-4 was tested on Silurian, Pennsylvanian and Permian brachiopods and enclosing whole rock as well as conodonts and fish debris to assess the reliability of REE contents in Deep-Time fossils and carbonates. The brachiopod shells contain ∑REEs, Mn,

Fe, and U concentrations and Ce/Ce* values comparable to their modern counterparts, while in the coeval micritic whole rock they are slightly to significantly enriched. Those with elevated Fe and Mn (by more than 300 and 100 ppm, respectively) their Ce/Ce* values should be adjusted by -13% if they are to be considered in paleoredox investigations. In contrast, REE contents of conodonts give the typical 'bell shape' trend for the lanthanides indicative of post-depositional alteration coupled with extraneous Ce/Ce* anomaly values. Strict adherence to the proposed sample processing protocol is critical if we want reliable and robust 'seawater' REE signatures from brachiopods and whole rocks, and potentially other archives.

2.1. Introduction

Rare earth elements (REEs) are powerful tools for modeling the hydrosphere, reconstructing paleoenvironmental settings and investigating mass extinction events (cf. Wright et al., 1984, 1987; Lécuyer et al., 1998, 2003, 2004; Reynard et al., 1999; Webb and Kamber, 2000; Kemp and Trueman, 2003; Trueman et al., 2006; Anderson et al., 2007; Garbelli et al. 2015). The naturally occurring fourteen lanthanides, constituting the REE group, occur in the trivalent state in seawater. However, redox changes the oxidation state of certain elements to either tetravalent or divalent. In highly oxygenated seawater, oxidation reaction of Ce^{3+} to Ce^{4+} takes place through bacterial mediation. The CeO_2 product of this reaction is highly insoluble and rapidly removed due to scavenging by sinking organic particulates and ferromanganese nodules causing Ce depletion in the corresponding dissolved concentrations (Elderfield and Greaves, 1982; Sholkovitz and Schneider, 1991; Piepgras and Jacobsen, 1992; German et al., 1995; Byrne and Sholkovitz,

1996, Nozaki, 2001). Therefore, well oxygenated seas and open-oceans are depleted in Ce whereas anoxic water is enriched in it (Elderfield and Sholkovitz, 1987; de Baar et al., 1988; Sholkovitz et al., 1989, 1992; German et al., 1991; Haley et al., 2004). On the other hand, reduction of Eu^{3+} to Eu^{2+} is mostly restricted to magmatic processes and high-temperature systems (Dubinin, 2004). Thus, Eu concentrations do not vary significantly in seawater except in areas of hydrothermal and mid-oceanic ridge activity, where Eu enrichment has been reported in deposited material (Michard et al., 1983; Sverjensky, 1989; Bau, 1991; Bau and Möller, 1992; Bau and Dulski, 1999; Nozaki, 2001; Bau et al., 2010).

The gradual diminution of the REE radii with increasing atomic number, the lanthanide contraction, is the result of the progressive filling of their shielded 4f-orbital (de Baar et al., 1985a; Nozaki, 2001; Kim et al., 2012). It causes a gradual increase in the stability constant of the free ion in solution across the series from La to Lu (Turner et al., 1981; Bright et al., 2009). The consequently small, but systematic change in their chemical properties leads to slight fractionation in marine water driven by the preferential scavenging of the light elements from the water by sinking particulates relative to the heavy ones (de Baar et al., 1985a; German and Elderfield, 1989; German et al., 1991; Bright et al., 2009). Lanthanum, Gd and Lu, with empty-, half- and completely-filled 4f electron shells, respectively, are particularly stable, and thus, have lower tendencies to complex with sinking particulates than the other rare earth elements (de Baar et al., 1985a). The common shale normalized (SN) REE distribution pattern of modern oxygenated seawater results from the gradual enrichment with increasing atomic number punctuated by a negative Ce excursion relative to adjacent La and Pr, with occasionally small positive La, Gd and Lu excursions (de Baar et al., 1985a, 1985b; Elderfield et al., 1988; Bau et al., 1996, 2010;

Nozaki, 2001; Shields and Webb 2004; Bright et al., 2009). In a deviation from that trend, slightly to extensively positive Ce_{SN} and Eu_{SN} anomalies have been reported from anoxic seawater and hydrothermal vent sites, respectively (de Baar et al., 1988; German and Elderfielld, 1989; de Baar, 1991; German et al., 1991; Hongo and Nozaki, 2001; Craddock et al., 2010; Schmidt et al., 2010).

Under anoxic conditions, insoluble cerium oxide, adsorbed on sinking particulates experiences reductive dissolution (de Baar et al., 1988). Such dissolution restores the Ce concentration to its original value and subsequently shifts the Ce excursion of the corresponding seawater REE_{SN} pattern from negative to near unity (German and Elderfield, 1989; German et al., 1991). The magnitude and direction of the Ce excursion is quantified by calculating the Ce_{SN} anomaly (Ce/Ce*), which represents the ratio of the shale-normalized concentration of Ce versus that of neighboring elements La, Pr, Nd or Sm (e.g., de Baar et al., 1985b; Bau and Dulski, 1996). The corresponding value of the Ce_{SN} anomaly is 1 (no anomaly) or more (positive) in anoxic seawater, and less than 1 (negative) when oxygen exists (de Baar et al., 1985a). In open seawater, the Ce/Ce* anomaly gets more pronounced with depth due to a decrease in the amount of dissolved Ce with concomitant enrichments in La, Pr, Nd or Sm (de Baar et al., 1985b, 1988; German and Elderfield, 1989)

REE concentrations, behavior, distribution and redox cycling in modern seas and oceans have been investigated in the last few decades, but its composition in Phanerozoic oceans is still unresolved (Azmy et al., 2011). The biggest difficulty complicating our understanding is the sparse information about the REE signal acquired by modern and fossil carbonate and apatite archives. Biogenic apatite deemed to be the most reliable material for REE studies has been investigated thoroughly in the last few decades (e.g., McArthur and

Walsh, 1984; Wright et al., 1984, 1987; Elderfield and Pagett, 1986; Lécuyer et al., 1998, 2003, 2004; Girard and Lécuyer 2002; Picard et al., 2002; Kemp and Trueman, 2003). It has been noted, that modern marine phosphatic brachiopods and ichthyoliths have ∑REE contents of less than 1 ppm and display seawater-like REE_{SN} patterns including negative Ce anomalies (Zhang and Nozaki, 1996; Wright, 1985, Elderfield and Pagett, 1986; Grandjean et al., 1987; Toyoda and Tokonami, 1990; Lécuyer et al., 1998, 2004). In contrast, REE signals from fossil marine phosphorites exhibit elevated ∑REE contents, middle REE enrichment (bell shape) and/or heavy REE depletion (e.g., Elderfield and Pagett, 1986; Trueman and Palmer, 1997; Reynard et al., 1999; Trueman and Tuross, 2002; Martin and Scher, 2004; Bright et al., 2009; Kocsis et al., 2010). In order to explain the enigmatic REE signals, two main hypotheses have been suggested in the literature. First, the composition of the primary carrier responsible for REE removal from the water column has changed (e.g., Roth, 1986; Grandjean - Lécuyer et al., 1993), and second, the REE composition of paleo-seawater has evolved with geologic time (McArthur and Walsh, 1984; Grandjean et al., 1987, 1988; Ilyin, 1998; Picard et al., 2002).

Recrystallization occurs spontaneously during fossilization of biogenic apatite (Trueman and Tuross, 2002; Kohn, 2008; Kocsis et al., 2010). Modern bones are composed of extremely small nonstoichiometric carbonate-hydroxyapatite crystallites and are intimately associated with the collagenous matrix (Weiner and Price, 1986; Moradian-Oldak et al., 1991; Elliott, 2002; Rubin et al., 2003). Fossil phosphorite, on the other hand, is made up of large-sized apatite crystals and is nonporous in the region of the collagen (Trueman et al., 2002, 2008a, b). It has been argued that soon after death and upon exposure of the apatite to pore-water, new apatite crystals grow to replace the highly adsorptive

metastable carbonate-hydroxyapatite and continue to fill the porosity that was originally occupied by the collagen (Tuross et al., 1989; Reynard et al., 1999; Roberts et al., 2012; Smith et al., 2005). In addition to that, REEs released from labile phases due to changes in pore-water redox conditions in the diagenetic environment may be incorporated into the biogenic apatite crystal lattice (Trueman and Tuross, 2002; Trueman et al., 2006). Because of that and the mineralogical dissimilarities between the initial and the final apatite products of the recrystallization process, several authors characterize the bell-shape, absence of negative Ce anomalies and the extremely elevated ∑REE concentrations of phosphatic archives synonymous to diagenetic alteration (McArthur and Walsh, 1984; Elderfield and Pagett, 1986; Trueman and Tuross, 2002; Trueman et al., 2002, 2004, 2006, 2008a,b; Bright et al., 2009; Kocsis et al., 2010). Late phase diagenesis may also enhance the REE concentrations of biogenic apatite by up to 50 % of the total content depending on REE-uptake conditions (Kocsis et al., 2010).

The REE contents of archives such as foraminifers, corals and reefal microbialites have received some attention (e.g., Palmer, 1985; Sholkovitz and Shen, 1995; Webb and Kamber, 2000; Kamber and Webb, 2001; Nothdurft et al., 2004; Olivier and Boyet, 2006; Roberts et al., 2012; Loope et al., 2013; Johannesson et al., 2014). Sholkovitz and Shen (1995) argued that modern corals do not fractionate REEs significantly during uptake. However, the measurements of Akagi et al. (2004) show substantial REE differences in distribution coefficient among different coral species suggesting a species-dependent uptake. Although REEs are not involved in the metabolic process, modern foraminiferal tests are enriched in REEs and display a depleted heavy REE_{SN} pattern relative to the ambient seawater that suggests a biological (vital) effect controlling their uptake (Palmer,

1985). In addition to that, their REE compositions increase by up to 1 order of magnitude at the sediment-water interface due to the interaction with pore-water (Roberts et al., 2012). Fossils of reefal microbialites exhibit REE_{SN} similar to modern oxygenated seawater with negative Ce/Ce*, positive La and Gd anomalies but with notably elevated ∑REE concentrations than other biogeochemical precipitates (Webb and Kamber, 2000; Kamber and Webb, 2001; Nothdurft et al., 2004). Recent investigations of modern reefal microbialites and stromatolites suggest REE fractionation by organic ligands, bacterial cell walls, microbialite biofilms and/or exo-polymeric substances during precipitation expressed by preferential incorporation of the heavy REEs (Johannesson et al., 2014).

Brachiopods are divided into two, the articulated and inarticulated, groups (James et al., 1992). The toothed hinge and simple opening and closing muscle-system shells belong to the former, while the untoothed hinge and complex muscle-system shells are members of the latter group (Ruppert and Fox, 2004). With exception of the lingulids, which have adopted infaunal habitats in soft sediments, brachiopods are generally sessile benthic marine invertebrates and mostly epifaunal (James et al., 1992). Modern ones inhabit all seas and oceans of all latitudes, depths and salinities (Ruppert and Fox, 2004; Logan, 2007; Zezina, 2008; Brand et al., 2013). Generally, they tend to avoid locations with strong currents and waves and preferably dwell in low-light spaces of well-oxygenated normal salinity environments (Rudwick, 1965; Fürsich and Hurst, 1974; Emig, 1990; Kowalewski et al., 2002).

Articulated brachiopods precipitate multi-layer calcite shells consisting of a few micrometer thick granular primary layer underlain by a fibrous secondary layer that occasionally overlies a prismatic and/or fibrous tertiary layer in some species (Brand and

Veizer, 1980; Al-Aasm and Veizer, 1982; Azmy et al., 1998, 2011; Brand et al., 2003, 2011, 2012, 2013; Parkinson et al., 2005). The brachiopod shell is covered on the outside by the proteinaceous periostracum that allows ions required for crystallization to accumulate (James et al., 1992; Moore, 1997). Their inner layers (secondary and tertiary) are proven to retain primary geochemical signatures in equilibrium with the ambient seawater, while the primary layer does not (e.g., Lowenstam, 1961; Carpenter and Lohmann, 1995; Parkinson et al., 2005; Brand et al., 2013, 2015).

The widespread occurrence in Phanerozoic rocks, the high resistivity of their calcitic phase to diagenetic alteration and the isotope equilibrium secretion of their shells make articulated brachiopods an important archival candidate for REE investigations. In preliminary studies, Azmy et al. (2011, 2012) evaluated their REE contents. Although the results of these two studies were encouraging, REE values of some shells from extreme environments and deep water were less convincing suggesting a confounding factor. They probably represent inputs of the primary layer, proteinous periostracum, adsorptive nano-particulates, encrusting organisms, organic materials, and enclosed sediments to the shells punctuated structure. This in turn suggests the necessity of further investigations to evaluate the impacts of each of these contaminants on the REE compositions of articulated brachiopods. It also emphasizes the need for appropriate procedures for cleaning not only brachiopod shells but other archives as well if we want to acquire primary seawater REE signals. This is the major impetus of the current study, to introduce a definitive cleaning protocol consisting of a combination of physical and chemical procedures for preparing different archives for REE investigations. The second task consists of testing the protocols

with modern and fossil counterparts as to their veracity in producing robust and reliable seawater REE signatures.

2.2. Sample material

The study involves modern and well-preserved Paleozoic articulated brachiopods (Fig. 2-1; Table 2-1) and their enclosing whole rock (Appendix 2-1). Meanwhile for comparison purpose, we compiled from the literature the REE compositions of some coeval conodonts and phosphatic fish debris (Wright, 1985; Bright et al., 2009; Zhao et al., 2013).

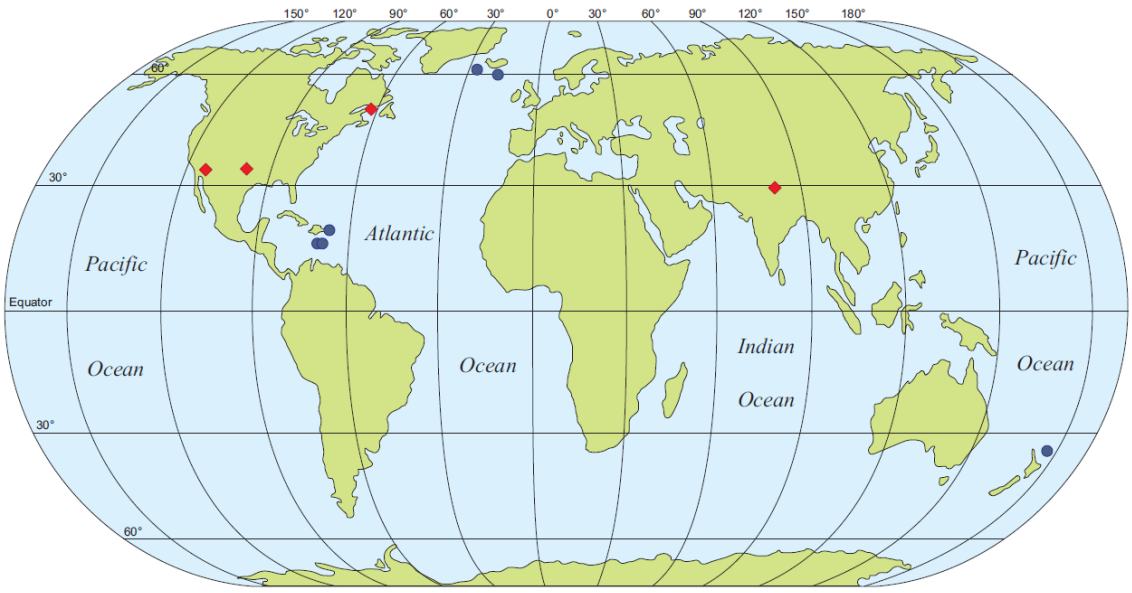

Figure 2-1. Locality diagram of modern (blue circles), and fossil brachiopod and whole rock (red diamonds) samples (data in Table 2-1 and Appendix 2-1).

2.2.1. Modern shells

Five *Liothyrella neozelanica* valves from an unnamed seamount located west of volcano L (Station TAN0205/102; 34.7097664°S, 178.5747528°E) in the South Pacific,

North of New Zealand, are investigated in this study. They were dredged on April, 28th 2002 from water depths of between 1115 to 1172 m by the *RV Tangaroa* during the TAN0205 expedition voyage. Also included in this study are, (1) one *Chlidonophora incerta* shell (two REE analyses) from deep water (3940 m) of the Caribbean Sea, south of the U.S. Virgin Islands, previously evaluated by Azmy et al. (2011) and re-evaluated by Zaky et al. (2015), (2) six *C. incerta* shells (six REE analyses) recovered from water depths between 3986 and 3998 m in the Caribbean Sea, north of Venezuela (from Zaky et al., 2015), and (3) fifteen *Macandrevia cranium* shells from the North Atlantic Ocean, west of Iceland; two of them dredged from ~2560 m depth of the Iceland Basin (three REE analyses) and the rest (six REE analyses) dredged from ~2530 m depth of the Irminger Basin (from Zaky et al. 2015).

2.2.2. Fossil shells and whole rock

The whole rock database includes eleven samples from the Gyanyima, two from the Naco, one from the Boggy, another one from the Chicotte, four from the Jupiter (two of them published in Azmy et al., 2011) and one from the Becscie Formations. They were acquired from the same horizons as the fossil shells to ensure similarity in paleoenvironmental condition. The diagenetic state of the fossil brachiopods and their whole rocks were screened and assessed by Brand (1987; 1989 a, b; 1990; 1991), Smith et al. (1994), Azmy et al. (1998; 2011) and Garbelli et al. (2015).

Table 2-1. Species, sample numbers, depth/formation and location of the modern and Paleozoic fossil brachiopod shells.

Species	*N*	Depth (m) / Formation	Location	Co-ordinates
Modern				
Liothyrella neozelanica	26*	1115-1172	South Pacific Ocean	34.7080°S, 178.5748°E
Chlidonophora incerta	2*,a	3940	Virgin Islands Basin, Caribbean Sea	17.9167°N, 64.7833°W
"	6b	3986-3998	Venezuela Basin, Caribbean Sea	15.6571°N, 69.1943°W & 15.7370°N, 69.8180°W
Macandrevia cranium	6*	2504.7-2531.8	Irminger Basin, North Atlantic.	61.6417°N, 31.3562°W
"	3b	2567.7-2568.5	Iceland Basin, North Atlantic	60.3573°N, 18.1357°W
Fossil				
Latest Lopingian (Late Permian)				
Costiferina indica	2c	Gyanyima	Tibet, China	30.71067°N, 80.6951°E
C. spiralis	1c	"	"	"
Dielasma sp.	1c	"	"	"
Marginalosa sp.	1c	"	"	"
Martinia sp.	1c	"	"	"
Neospirifer sp.	1c	"	"	"
Permophricodothyris sp.	2c	"	"	"
Richthofenia lawrenciana	1c	"	"	"
Late Desmoinsian (Middle Pennsylvanian)				
Composita subtilita	3*	Naco	Arizona, USA	34.3261°N, 111.1140°W
Mid Desmoinesian (Middle Pennsylvanian)				
Marginifera muricatina	3*	Boggy	Oklahoma, USA	34.4456°N, 96.9614°W
Llandovery (Early Silurian)				
Gotatrypa gibbosa	2a	Chicotte	Quebec, Canada	49.3631°N, 62.8344°W
Gotatrypa sp.	6a 5*	Jupiter	"	49.3128°N, 62.8750°W & 49.3631°N, 62.8344°W
Virgiana barrandii	1*	Becscie	"	49.3631°N, 62.8344°W

Note: (N) number of samples.
* New data in this study.
a From Azmy et al. (2011).
b From Zaky et al. (2015).
c From Garbelli et al. (2015).

2.3. Traditional Protocols

Although cleaning is a fundamental step for preparing archives for geochemical analysis in general and REEs in particular, it does not receive much attention in the literature. We reviewed 53 articles (Appendix 2-2) that dealt with different REE archives like conodonts, fish teeth and debris, vertebrate remains, phosphorites, foraminifera, corals, microbialites, inarticulated and articulated brachiopods and micritic limestone. We noticed that in nearly half of the articles (Table 2-2) the authors did not mention the cleaning steps or just visually examined the specimens for contaminants.

Cleaning procedures conducted on the different REE archives and mentioned in the reviewed articles include: 1) rinsing with water, ethanol, methanol or ammonium chloride, 2) physical processing consisting mainly of mechanical abrasion and/or ultrasonication, 3) chemical treatment with hydrochloric, nitric, acetic acids or hydrogen peroxide, and 4) a combination of physical and chemical methods (Table 2-2). However, it is clear from the review that there is no standard cleaning protocol that researchers follow for acquiring robust REE signals from marine archives.

Table 2-2. Traditional cleaning procedures of the different biogenic and abiogenic REE archives compiled from 53 published articles (more details in Appendix 2-2).

Cleaning procedures	***N***
Not mentioned	23
Visually examined	2
Water washed	3
Physically cleaned	8
Washed (water, ethanol, methanol or ammonium chloride) and physically cleaned	10
Water washed, physically cleaned and HNO_3	1
Physically cleaned and HCL	3
Water washed and HNO_3	1
Water washed and H_2O_2	1
Chemically cleaned by sodium hypochlorite; acetic acid-acetate buffer	1
Total	53

2.4. New Protocol

Establishing an effective protocol for cleaning the different archives requires first examining the impacts and the consequences of each proposed procedure (washing, mechanical abrasion, acid leaching or the physical and chemical combination method) on the REE signals of the evaluated archives. To accomplish this objective, five recently dead *Liothyrella neozelanica* valves (black outside and grayish brown inside; Fig. 2-2A) were

obtained for this task from deep water of the southwest Pacific (north of New Zealand, Table 2-1). We avoided the umbo area including muscle attachment area of the brachial (dorsal) and pedicle (ventral) valves because they give extraneous elemental and isotope results (cf. Carpenter and Lohmann, 1995; Brand et al., 2003; Parkinson et al. 2005).

Twenty-six segments were obtained from the five valves; five segments of them received no cleaning except a distilled water rinse (Procedure-1). Four segments were immersed in 2.5 % hydrogen peroxide (H_2O_2) for three continuous days (Procedure-2). Four segments were cleaned physically by abrasion under binocular microscope using a sharp stainless-steel blade (Procedure-3). Another four segments were physically cleaned and then leached with 10 % hydrochloric acid (HCl) until they turned white (Procedure-4). The last nine segments were processed following all previously mentioned steps (water washing, H_2O_2 treatment, physical abrasion and HCl leaching; Procedure-5).

2.4.1. Analytical Methodology

About 10 mg of each sample (weighed to four decimal places) was spiked with a drop of 8N HNO_3 and then digested for about a week in 10 mL 0.2N distilled HNO_3. After that, exactly 2 mL of each sample solution was diluted with 3 mL 0.2N HNO_3 and analyzed for Ca, Mg, Mn, Fe, U and REE contents at the CREAIT facility of Memorial University of Newfoundland using a Perkin Elmer Sciex inductively coupled plasma mass spectrometer (ICP-MS) that is equipped with a Seaspray U-series nebulizer, standard nickel sampling/skimmer cones and cyclonic spray chamber, and operated in the standard mode. Relative uncertainties of measurements compared to the standard reference materials DLS 88a and CCH-1 are better than 5% (cf. Azmy et al., 2009, 2011). The samples were

analyzed in eight different runs between 2014 and 2015; the measurements of blanks, the standards and the detection limit of each element of the different runs are reported in Appendix 2-1.

The REE concentrations of all investigated parts, modern and fossil brachiopods and whole rock, were shale normalized (SN) to the Post-Archean Australian Shale values of McLennan (1989; PAAS). Ce anomalies (Ce/Ce*) were calculated with the de Baar et al. (1988) equation: $Ce/Ce^* = [3(Ce_{Sample}/Ce_{Shale})]/[2(La_{Sample}/La_{Shale})+(Nd_{Sample}/Nd_{Shale})]$. Trace elements were calculated to a 100 % carbonate basis (cf. Brand and Veizer, 1980), and all geochemical results are presented in Appendix 2-1.

2.5. REE Results

2.5.1. Procedure-1

For procedure 1, we opted to rinse brachiopod shells and fragments with copious amounts of distilled water followed by air-drying prior to powdering and digesting for analytical analysis. The shell fragments of Procedure-1 (P-1) subjected to no more than washing/rinsing with distilled water, disclose gradually enriched REE_{SN} trends with increasing atomic number (Fig. 2-2A). However, the brachiopod REE trends are different from that of nearby South Pacific deep-water (Station SA12; ~900 km northwest of Volcano L) from corresponding depths (991-1485 m) depicted by the shaded pattern in Figure 2-2A (Zhang and Nozaki 1996). The REE enrichment of the brachiopods is less pronounced displaying nearly flat patterns due to partial enrichments in the light REEs, and Ce excursions deflected in the opposite direction (positive excursion). Their Ce/Ce* values are positive varying between 1 and 1.35 with an average of 1.13, whereas sample WW-2 is

an exception with a slightly negative anomaly of about 0.78. These brachiopod Ce/Ce* results are in stark contrast to the Ce anomalies of the nearby deep seawater that are negative with Ce/Ce* values of around 0.07 (Fig. 2-3; Table 2-3). In addition, the P-1 brachiopod shell fragments have Mn and Fe contents much higher compared to those normally observed in other modern counterparts (Fig. 2-4; Table 2-3; cf. Morrison and Brand, 1986; Brand et al., 2003). The high REE and Ce/Ce* results (Table 2-3) suggest either anoxic water conditions prevailed in the area during shell precipitation, which is not supported by the REE contents and Ce/Ce* values of the ambient seawater, or disequilibrium incorporation of REEs into the brachiopod shells. Alternatively, our favored conclusion, that this cleaning step was insufficient and the measured REE contents do not represent calcite-bound REEs nor a seawater signature.

2.5.2. Procedure-2

For procedure 2, we opted to immerse the brachiopod shell fragments in hydrogen peroxide for three days (a common procedure for removing organic tissue from modern biogenic material) followed by rinsing with distilled water and air-drying before analysis. Although the REE_{SN} patterns of the hydrogen peroxide treated fragments of P-2 are quite similar to those of the P-1 process, their Ce excursions are different; they diverge in direction corresponding to none or slight negative excursions (Fig. 2-2B). The Mn, Fe, and U concentrations of the P-2 shell fragments are slightly lower relative to those of the P-1 fragments, but still much higher than those of modern counterparts (Fig. 2-4; Table 2-3; Brand et al., 2003). Their Ce anomalies with an average value of about 0.72, except for one sample, are more negative than those of the P-1 cleaned fragments (Fig. 2-3; Table 2-3). These geochemical results prove that the hydrogen peroxide treatment only partly

resolves the original Ce concentrations while it is insufficient in resolving trace chemistry in shell calcite in any way related to that of the ambient seawater. These results challenge the veracity of hydrogen peroxide for cleaning biogenic carbonates for their REE and trace chemistry.

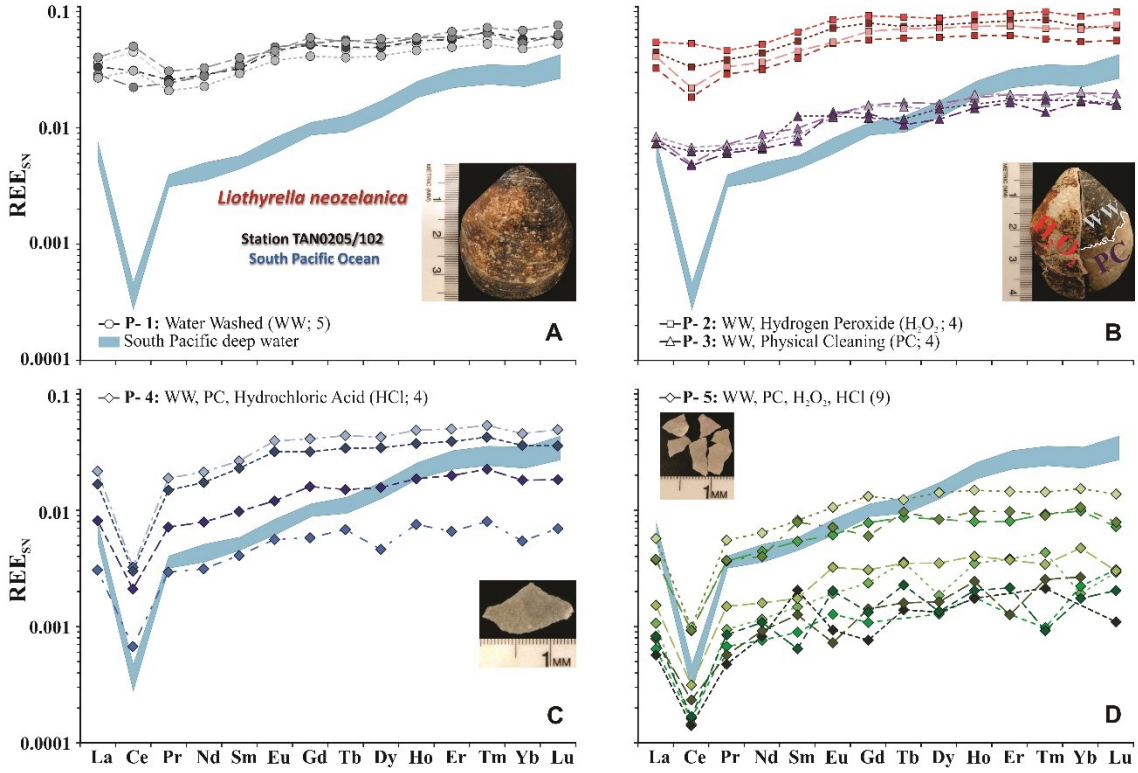

Figure 2-2. REE_{SN} patterns of *Liothyrella neozelanica* with cleaning consisting of five procedures. The blue shaded pattern in panel A is the ambient seawater REE content at station SA-12 (991-1485 m; $N = 3$) in the southwest Pacific Ocean (Zhang and Nozaki, 1996) normalized to PAAS and multiplied by 10^5. (A) REE results of five water-washed brachiopod fragments; cleaning Procedure -1 (P-1, WW; 5), (B) REE results of four brachiopod fragments washed with hydrogen peroxide and water ; cleaning Procedure -2 (P-2, H_2O_2, WW; 4) and REE results of four brachiopod fragments physically cleaned and water washed; cleaning Procedure -3 (P-3, PC, WW; 4), (C) REE results of four brachiopod fragments physically and chemically cleaned and water washed; Procedure-4 (P-4, HCl, WW; 4, and (D) REE results of nine brachiopod fragments physically- and chemically-cleaned and water-washed; cleaning Procedure -5 (P-5, PC, H_2O_2, HCl, WW; 9). Panel insets are photos of shells and fragments prepared in the appropriate cleaning procedure from *Liothyrella neozelanica* from the South Pacific Ocean.

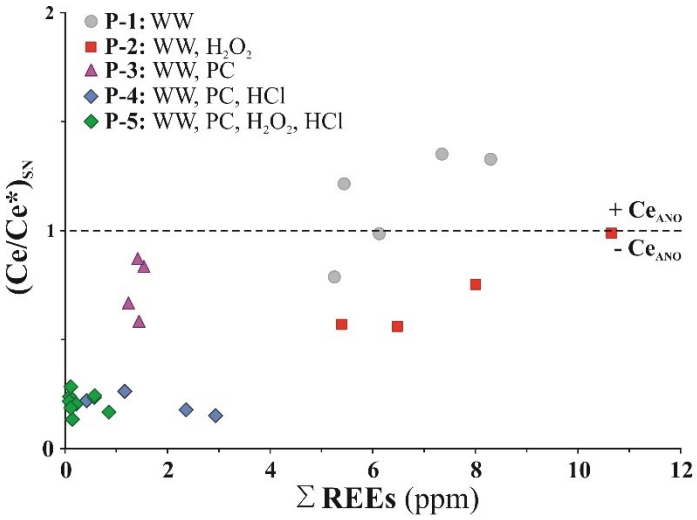

Figure 2-3. Ce/Ce* and REE_{SN} distributions of the five different cleaning procedures of the new protocol. The Ce/Ce* values were calculated with the equation of de Baar et al. (1988), and $+Ce_{ano}$ and $-Ce_{ano}$ interpretations are according to German and Elderfield (1989).

Table 2-3. Average Mn, Fe, U and ∑REE concentrations (in ppm), Ce anomalies (Ce/Ce*) and $(La/Yb)_{SN}$ values using the new cleaning protocol in modern brachiopods (P-1 to P-5, this study) and those of Brand et al. (2003, 2013).

	N	Mn	Fe	U	∑REE	Ce/Ce*	$(La/Yb)_{SN}$
P-1: WW	5	1184	1976	0.205	6.5	1.13	0.58
P-2: WW, H_2O_2	4	850	1046	0.122	7.6	0.72	0.42
P-3: WW, PC	4	142	564	0.024	1.4	0.74	0.59
P-4: WW, PC, HCl	4	51	105	0.013	1.7	0.20	0.47
P-5: WW, PC, H_2O_2, HCl	9	10	107	0.006	0.3	0.21	0.34
P-4 (Brand et al., 2003)	259	40	102		0.2[a]	0.07[b]	0.23[b]
P-4 (Brand et al., 2013)	368	16	46				

Note: (WW) Water Washed, (H_2O_2) Hydrogen Peroxide, (PC) Physical Cleaning, (HCl) Hydrochloric Acid and (*N*) number of samples.
Brand et al. results generated by AAS.
[a]: from Azmy et al. (2011).
[b]: average Ce/Ce* and $(La/Yb)_{SN}$ values of the seawater (991-1485 m; $N = 3$) of station SA-12 in the Southwest Pacific Ocean (Zhang and Nozaki, 1996).

2.5.3. Procedure-3

For procedure 3, we opted to physically clean the shells and fragments until there was no visible sign of external or organic contaminants remaining, even after examination under binocular microscope, prior to rinsing with distilled water and following with air-drying before REE analysis. The physically cleaned fragments of P-3 display notably

different REE_{SN} patterns from those cleaned in P-1 and P-2 procedures (Fig. 2-2B). The progressive enrichment is more pronounced and the overall REE concentrations are more depleted (especially the light REEs) by an order of magnitude. On the other hand, the Ce excursions differ insignificantly from those which have undergone procedure P-2 but notably to those of procedure P-1; they tend to coincide with the excursion direction of the ambient seawater but contradict it in amplitude (Fig. 2-2B). Although, the P-3 fragments are four to eight times less enriched in Mn, Fe, U and ∑REE contents relative to the tested fragments of P-1 and P-2 (Fig. 2-4), they are still higher than those of other modern counterparts (Table 2-3; Brand et al., 2003; 2013). Their slightly negative Ce/Ce* values (average= 0.74) are remarkably high and inconsistent with those of the ambient seawater (average=0.07; Fig. 2-3; Table 2-3). The difference in REE contents between P-1 and P-2 results, but lower values with that of the P-3 fragments accompanied by relatively more distinct enrichment patterns, suggests better success of the latter cleaning procedure. Despite the qualified success in acquiring better REE_{SN} patterns, the high Mn, Fe contents and REE enrichment and the less depleted Ce excursions and anomalies of the P-3 fragments relative to that of the nearby seawater limit the capability and effectiveness of the physical abrasion process. It is insufficient in obtaining seawater REE compositions and signatures from brachiopod-calcite archives.

2.5.4. Procedure-4

For procedure 4, we opted to physically and chemically clean the shell fragments followed by water rinsing and air-drying. Chemical treatment consisted of leaching shells or fragments with 10 % hydrogen chloride acid until the calcite looked clean and dousing

in distilled water to stop the process. The physically cleaned and acid leached fragments of P-4 display REE_{SN} patterns somewhat similar to those of process P-3 but with more prominent negative Ce excursions and better refined enrichment trends (Fig. 2-2C). The U and ∑REE concentrations are not significantly different from those of the P-2 fragments, however the Mn and Fe concentrations are 3 to 5 times more depleted (Fig. 2-4; Table 2-3). Likewise, the Ce/Ce* anomaly is significantly depleted compared to those of the previous procedures (P-1, P-2 and P-3), and with an average value of 0.20 comparable to that of the nearby seawater (0.07; Fig. 2-3; Table 2-3). Thus, the strong similarities between REE_{SN} patterns and Ce/Ce* anomalies of the P-4 fragments and its nearby seawater suggest a high degree of efficiency of this procedure in the cleaning of biogenic calcite archives. Thus, we conclude that biogenic calcite and other archives should be cleaned using at least this protocol prior to REE and trace element analyses.

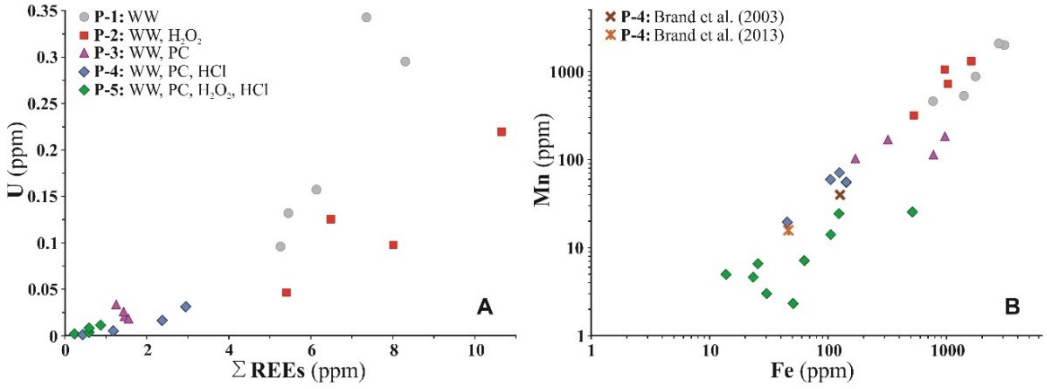

Figure 2-4. Scatter diagrams of ∑REEs, U, Mn and Fe contents retrieved from treatment by the five cleaning protocols (P-1 to P-5, Figure 2-2) and average values of modern counterparts (Brand et al., 2003, 2013). (A) ∑REEs and U distribution, and (B) Mn and Fe distribution of the total database (Appendix 2-1).

2.5.5. Procedure-5

For procedure 5, we opted to use all cleaning steps proposed in procedures 1 through 4. The REE_{SN} patterns of the physically cleaned, hydrogen peroxide treated and acid-

leached shell fragments of P-5 are similar to those of P-4, however they are slightly depleted in total REE magnitude by nearly a half (Fig. 2-2D). The magnitude of the Ce excursion, on the other hand, does not vary significantly from those following the P-4 procedure and that of the nearby seawater. In contrast, the P-5 treated fragments yielded slightly lower Mn, U and ∑REE concentrations relative to those of P-4 but comparable Fe concentrations (Fig. 2-4; Table 2-3). The average Ce anomalies of P-5 fragments of about 0.21 is similar to the same average value of the P-4 fragments (Fig. 2-3; Table 2-3). The small differences in chemical results between cleaning procedures P-4 and P-5 suggest that these two procedures are optimal in obtaining seawater REE signatures from biogenic archives, and we strongly recommend that biogenic archives be cleaned with these two protocols.

2.5.6. Summary

Sinking manganese, iron and uranium oxide particulates scavenge dissolved REEs with preference for the light and middle ones from seawater (de Baar et al., 1988; German and Elderfield, 1989; Bau and Koschinsky, 2009). Dissolved Ce, on other hand, is scavenged primarily from seawater by sinking organically-coated particulates (Haley et al., 2004), while insoluble cerium dioxide nano-particles are adsorbed by organic matter like algae (Quik et al., 2010). In the absence of proper cleaning procedures, as in P-1, cross-contamination of bottom sediments associated with manganese, iron and uranium particulates on shell surfaces may elevate the light REE and ∑REE concentrations of archives, while encrusting organisms and organic remnants may enhance the Ce composition (Fig. 2-5). In summary, physical cleaning removes mostly adhering particulates and a notable percentage of the periostracum, which in turn restores shell's

REE concentrations to near normal values; except for Ce that is only slightly depleted. In contrast, cleaning samples with just hydrogen peroxide may eliminate encrusting organisms, organic remnants and the periostracum, but it does not retrieve genuine seawater REE and Ce/Ce* signatures (Fig. 2-5). Immersing shells in HCl, on the other hand, not only dissolves the primary layer but also removes any surface-attached contaminants. Therefore, retrieving an original REE signal retained in articulated brachiopods requires physical cleaning followed by chemical procedures to fully remove any organic tissue, the primary layer (if present) and surface-attached contaminants (Fig. 2-5). Thus, we propose that Procedure-5 is the best protocol to follow for cleaning modern biogenic marine materials, whereas Procedure-4 may be used on fossil marine material due to the lack of organic matter on or within the shell.

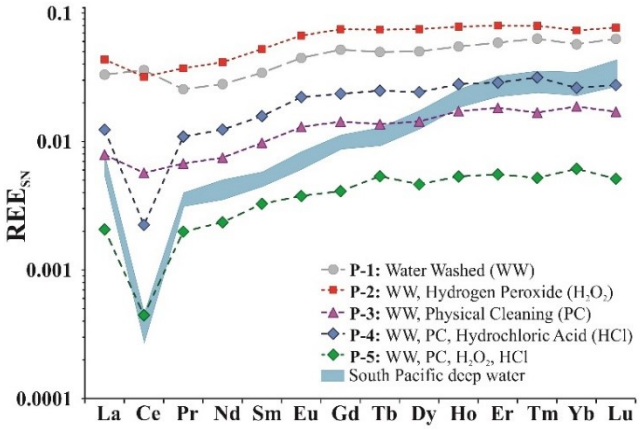

Figure 2-5. Average REE_{SN} patterns retrieved by the five procedures (P-1 to P-5) used in the proposed cleaning protocol; blue shaded pattern represents the seawater REE content at station SA-12 (991-1485 m; $N = 3$) in the southwest Pacific Ocean (Zhang and Nozaki, 1996) normalized to PAAS and multiplied by 10^5.

2.6. Evaluation - Case studies

In order to evaluate the effectiveness of the proposed cleaning protocol, modern brachiopods from different water masses as well as several well-preserved fossil counterparts with their enclosing whole rock and biogenic apatite were tested for the

robustness of their REE and Ce/Ce* signatures. Brachiopods presented in this section were extensively screened for preservation of 'primary' trace chemistry and isotope compositions (Brand, 1989b; Azmy et al. 2011; Garbelli et al., 2015).

2.6.1. Case Study 1 – Caribbean Sea brachiopods

This case study was designed to evaluate the efficacy of the proposed protocol on individuals from different water masses. In it, we compared the REE contents of two deep-water brachiopods from two basins of the Caribbean Sea that were cleaned using different procedures (e.g., Azmy et al., 2011). Six specimens of *Chlidonophora incerta* from deep-water of the Venezuela Basin (3986-3998 m) in the middle of the Caribbean Sea were cleaned using Procedure-5. Another, three samples of the same species from similar depth (3940 m) in the Virgin Islands Basin, northeast Caribbean Sea were cleaned using Procedure-3 (Azmy et al., 2011).

The deep waters of the two basins have the same origin (North Atlantic Deep Water; Fratantoni et al., 1997). However, the dissolved oxygen content in the deep water of the Virgin Islands Basin (>6 mL/L; Metcalf, 1976) is slightly higher than that in the Venezuela Basin (~5.1 mL/L; Williams et al., 1986; Briggs et al., 1996) because the deep water inflow into the Caribbean eastern basins takes place through the Anegada-Jungfern Passages in the northeast (Borenas and Nikolopoulos, 2000). The average REE_{SN} pattern of the Caribbean Sea deep water below 3500 m (station 220-1&2, ~100 Km east of Venezuelan Basin stations) displays the main features of the open seawater of a progressive enrichment with increasing atomic number, which is punctuated with large negative Ce excursion with average Ce/Ce* value of 0.14 (Fig. 2-6A; Table 2-4; Osborne et al., 2015).

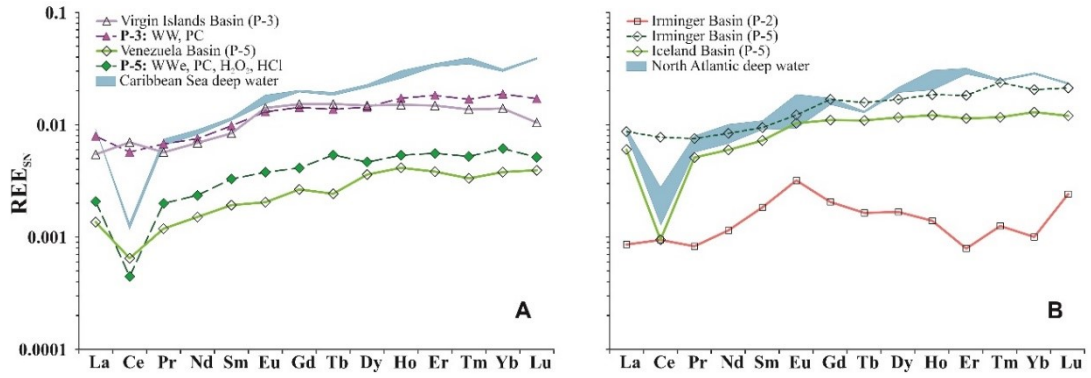

Figure 2-6. Evaluation of different cleaning protocols on modern brachiopods from different water masses. (A) Average REE_{SN} patterns of only physically cleaned *Chlidonophora incerta* shells from the Virgin Islands Basin, eastern Caribbean Sea (P-3), and physically and chemically cleaned samples of the same species from the Venezuela Basin, central Caribbean Sea (P-5), compared to average REE_{SN} patterns of the South Pacific P-3 and -5 materials, and Caribbean seawater (blue shaded pattern). (B) Average REE_{SN} patterns of hydrogen peroxide (P-2) and physically and chemically (P-5) cleaned *Macandrevia cranium* shells from the Irminger Basin (North Atlantic) and physically and chemically cleaned counterparts from the Iceland Basin (P-5), and average REE signatures of North Atlantic seawater (blue shaded pattern). The REE contents of the Caribbean seawater are from station 220-1&2 (3487 - 4482 m; $N = 2$) of Osborne et al. (2015), while those of the North Atlantic seawater are from Lacan and Jeandel (2005) representing station 9 in the Irminger Basin (2100 m; $N = 1$) and station 12 in the Iceland Basin (2020 m; $N = 1$); values of the two water masses are normalized to PAAS and multiplied by 10^5.

The mean REE_{SN} patterns of the Virgin Islands (n=2) and Venezuela Basins (n=6) brachiopods display gradual REE enrichment trends (Fig. 2-6A). However, the REE_{SN} pattern of Virgin Islands Basin specimens is nearly one order of magnitude higher than that of the Venezuela Basin specimens and is accompanied by a positive Ce excursion. The Venezuela Basin REE_{SN} trend, on the other hand, is similar to that of the nearby seawater displaying a large negative Ce excursion and more pronounced enrichments. Indeed, the REE_{SN} pattern of the Virgin Islands Basin brachiopods is similar to that of South Pacific brachiopods processed with just the P-3 cleaning procedure, whereas the REE_{SN} pattern of Venezuela Basin brachiopods is similar to South Pacific brachiopods cleaned with procedure P-5 (Fig. 2-6A).

Table 2-4. Average Mn, Fe, U and ∑REE concentrations (in ppm), Ce anomalies (Ce/Ce*) and $(La/Yb)_{SN}$ values of modern Caribbean Sea and North Atlantic Ocean brachiopods and fossil (Permian, Pennsylvanian and Silurian) brachiopods, whole rock, conodonts and biogenic apatite.

	N	Mn	Fe	U	∑REE	Ce/Ce*	$(La/Yb)_{SN}$
Case study – modern							
Caribbean Sea							
Virgin Islands Basin (P-3)	2	38	540	0.032	1.4	1.18	0.40
Venezuela Basin (P-5)	6	16	164	0.020	0.2	0.49	0.36
Seawater						0.14[e]	0.30[e]
North Atlantic Ocean							
Irminger Basin (P-2)	2	21	27	0.009	0.2	0.99	0.88
Irminger Basin (P-5)	4	205	352	0.021	1.7	0.90	0.43
Iceland Basin (P-5)	3	28	75	0.006	0.8	0.17	0.46
Seawater						0.23[f]	0.31[f]
Case study – fossil							
Late Permian							
Brachiopods	10	36	460	0.089	7.8	0.36	1.15
Whole rock	11	59	278	0.832	33.5	0.33	1.28
Conodonts[a]	4				52.9	0.74	2.72
Biogenic apatite[b]	4				897.2	0.62	1.73
Mid Pennsylvanian							
Brachiopods[1]	3	60	676	0.267	13.3	0.64	1.39
Whole rock[1]	2	156	1462	1.070	25.3	0.74	1.50
Brachiopods[2]	3	64	463	0.285	2.3	0.66	1.07
Whole rock[2]	1	256	1682	0.925	21.0	0.79	1.38
Conodonts[b,c]	28				482.2	1.06	1.26
Biogenic apatite[b]	2				1908.6	0.23	1.65
Silurian							
Brachiopods	14	33	591	0.036	2.4	0.68	1.22
Whole rock	6	267	6070	0.222	27.2	0.82	1.21
Conodonts[b]	3				1938.7	0.87	1.40
Biogenic apatite[b]	1				8292.4	0.91	1.50

Note: (*N*) number of samples; (P) procedure number of the new protocol
[1]: Late Desmoinsian.
[2]: Mid Desmoinsian.
[a]: Zhao et al. (2013)
[b]: Wright (1985)
[c]: Bright et al. (2009)
[e]: average Ce/Ce* and $(La/Yb)_{SN}$ values of seawater (3487 - 4482 m; $N = 2$) of station 220-1&2 in the Caribbean Sea (Osborne et al., 2015)
[f]: average Ce/Ce* and $(La/Yb)_{SN}$ values of seawater at station 9 in the Irminger Basin (2100 m; $N = 1$) and at station 12 in the Iceland Basin (2020 m; $N = 1$) in the North Atlantic Ocean (Lacan and Jeandel, 2005)

The Mn content in the Virgin Islands Basin P-3 (38 ppm) is greater than in the Venezuela Basin P-5 (16 ppm; Table 2-4), but the two values are insignificantly different from those of modern counterparts (16-40 ppm; Brand et al., 2003, 2013; Table 2-3). The U is also enriched but slightly in the Virgin Island Basin P-3 materials (0.032 ppm) relative to those of the Venezuela Basin P-5 (0.020 ppm). In contrast, the Fe compositions of the brachiopods from the two basins are elevated compared to average values of modern counterparts (46 - 102 ppm; Brand et al., 2003, 2013; Table 2-3). However, Fe

concentrations in P-5s from the Venezuela Basin are within the natural variation of Fe observed in modern brachiopods from the North Atlantic (1.1 - 401 ppm; Brand et al., 2003), whereas Fe in P-3s from the Virgin Island Basin (540 ppm; Table 2-4) is much higher (Table 2-3).

The deep-water of the Virgin Islands Basin is well oxygenated, the brachiopod samples depict positive Ce/Ce* anomalies with an average of 1.18 suggesting anoxic seawater conditions (Table 2-4). In contrast, specimens from the Venezuela Basin display negative Ce/Ce* values (average=0.49) suggesting oxic bottom seawater (Table 2-4). The high Ce/Ce* values of the Virgin Island samples coupled with the oxygenated ambient seawater as well as their elevated Fe concentrations are probably related to insufficient cleaning by procedure P-3. But, the agreement of Ce/Ce* anomalies of those from the Venezuela Basin with oxygenated seawater conditions and their REE pattern strongly support the suitability of procedure P-5 (Fig. 2-6A) in obtaining seawater REE signatures. The similarity in REE trends of the Venezuela and Virgin Islands Basins materials with those of the test material from the South Pacific (Procedures 5 and 3, respectively) confirms the reliability of our proposed cleaning protocol for modern brachiopod shells and realizes their potential as seawater REE archives. Overall, the P-5 - treated material retrieves the most representative REE signatures, and it allows for tracing the oxic environment independent of geographic location.

2.6.2. Case Study 2 – North Atlantic brachiopods

The rationale for conducting this case study are, 1) to shed light on the importance of the archive's elemental composition in assessing the completion of the cleaning

procedures, and 2) to evaluate the impact of not removing the primary layer on the REE contents and patterns of the archive. Brachiopods for this case study were obtained from the Irminger and Iceland Basins of the North Atlantic, and shells of *Macandrevia cranium* were subjected to two different cleaning procedures. Large (1-2 cm) specimens recovered from the Iceland Basin, were cleaned using Procedure-5, whereas small (< 0.2 cm) and med-size (0.5-0.8 cm) specimens from the Irminger Basin were cleaned using Procedures-2 and 5, respectively.

The Mn, Fe and U contents of Irminger Basin P-2 and Iceland Basin P-5 treated samples (Table 2-4) are similar to those of other modern counterparts (Mn= 16-40 ppm and Fe= 46-102 ppm; Table 2-3; Brand et al., 2003, 2013), whereas the P-5 treated-samples from the Irminger Basin are significantly enriched (Table 2-4). The Irminger Basin P-2 specimens yield an average ∑REEs concentration of ~0.2 ppm (Table 2-4), and their mean REE_{SN} trend exhibits remarkable enrichment of the middle REEs relative to the heavier ones (Fig. 2-6B). On the other hand, the P-5 cleaned specimens of the Iceland and Irminger Basins yield mean ∑REE concentrations 0.8 and 1.7 ppm, respectively (Table 2-4). Their mean REE_{SN} patterns are significantly different from that of the Irminger Basin P-2 samples displaying trends similar to those of the ambient seawater (Fig. 2-6B). However, the mean REE pattern of Iceland Basin P-5 shells is punctuated by a negative Ce excursion, while that of the Irminger Basin P-5 is not. Nevertheless, Irminger Basin P-2 and P-5 cleaned materials depict Ce anomalies with mean values of 0.99 and 0.90, respectively (Table 2-4). In contrast, the Ce anomalies of those from the Iceland Basin P-5 are significantly depleted with an average value of 0.17 (Table 2-4).

The deep waters of the Irminger and Iceland Basins are well oxygenated with dissolved oxygen levels of ~6.5 mL/L below 2500 m in the former (Falina et al., 2007) and 6.4 mL/L below 1750 m in the latter (Inall and Sherwin, 2006). Moreover, the two basins are oceanographically linked to North Atlantic water circulation, and the Iceland-Scotland Overflow Current transports cold polar Norwegian Sea Deep Water first into the Iceland Basin then into the Irminger Basin (Stransky and Brandt, 2010; Våge et al., 2011). Meanwhile, Labrador Sea water comprises the deep intermediate water of the Irminger Basin and spreads through fracture zones across the Mid-Atlantic Ridge into the Iceland Basin (Malmberg, 2004). The REE_{SN} trends of the deep waters of the two basins are insignificantly different from that of open ocean exhibiting large negative Ce excursions with an average Ce/Ce* of 0.23 (Lacan and Jeandel, 2005).

Although the Irminger Basin and Iceland Basin specimens are from well oxygenated seawater (Inall and Sherwin, 2006; Falina et al., 2007), only the Ce anomaly from the latter basin is in agreement with that of the ambient seawater. In contrast, the Ce anomaly of the former basin indicates suboxic to anoxic deep water. The insignificant differences between the elemental compositions of the Iceland Basin P-5 (Table 2-3) and the modern counterparts (Table 2-3) reflect the success of the P-5 procedure in effectively cleaning these samples. The elevated Mn, Fe, U and ∑REE contents in the P-5 samples from the Irminger Basin relative to those of Iceland Basin (P-5, Table 2-4) and the modern counterparts (Table 2-3), on the other hand, imply that the P-5 procedure was inadequate in removing external contaminants such as ferromanganese oxides, which are known to scavenge REEs from seawater (de Baar et al., 1988). This suggests that our proposed

protocol is not infallible, and indeed its completion must be verified by a secondary screening test and the archive's elemental content (Mn, Fe and U) serves the purpose.

For small samples the full cleaning process may not be done for fear of losing material during the acid leaching step. It results in processing shells without removing their primary layers that are precipitated in isotopic disequilibrium with ambient seawater (Lowenstam, 1961; Carpenter and Lohmann, 1995; Parkinson et al., 2005) as in the case of Irminger Basin P-2 material. The similarity between the Mn, Fe, U and even the ∑REE contents (Table 2-4) of Iceland Basin P-5 (primary layer removed) and Irminger Basin P-2 (primary layer present) samples, and at the same time their insignificant difference from those of the modern counterparts (Table 2-3) suggest that the non-removal of the primary layer has no effect on the elemental and ∑REE concentration of the brachiopod archive. In contrast, its presence appears to have a direct influence on the REE distributions within the sample proposing selective incorporation of certain REEs (in this case: Ce and middle REEs). This part of the case study implies that removing unwanted layers (internal contaminants) is of the same importance as cleaning the archive of external contaminants, and omitting a step of the proposed protocol may significantly influence the acquired REE signals.

2.6.3. Case Study 3 - Fossil brachiopods and whole rock

Procedure-4 of the new protocol scheme was used on thirty well-preserved Paleozoic brachiopod shells from the, 1) the Uppermost Lopingian (Upper Permian) Gyanyima Formation of Tibet, 2) the Upper and Middle Desmoinsian (Middle Pennsylvanian) Naco and Boggy Formations of central Arizona and southern Oklahoma,

respectively, and 3) the Llandovery (Lower Silurian) Chicotte, Jupiter and Becscie Formations of Anticosti Island (Table 2-1). In addition to that, it was applied to eighteen coeval whole- rock samples (Appendix 2-1) to compare results and consequently to assess the applicability, impact and efficiency of the new protocol to non-biogenic (abiogenic) REE archives as well. Physical abrasion is not appropriate to whole rock material instead the physical cleaning step was modified by cutting (removing) the weathered surface to get at the fresh interior carbonate for REE analysis.

Preservation of near primary geochemical signatures in the investigated Paleozoic fossils is well documented in Table 2-1 and previously mentioned studies (Brand, 1987, 1989a, b, 1990, 1991; Smith et al., 1994; Azmy et al., 1998, 2011; Garbelli et al., 2015). The Sr, Mn, Fe and U concentrations of the Paleozoic fossils, in general, fall within the range of their modern counterparts (Fig. 2-7A, B, C). The enrichment in Fe concentrations of some samples is perhaps from the input of bacterial pyrite embedded within the fabric of the secondary layers (cf. Brand and Morrison, 1987). In contrast, the Mn, Fe and U concentrations in the whole rocks are slightly to distinctly enriched relative to those of the coeval brachiopods, while their Sr concentrations are depleted (Fig. 2-7A, B, C; Table 2-4). Differences in Mn concentrations between whole rock and fossil shells (ΔMn) vary from -0.3 ppm in the Permian 3 horizon to 610.7 ppm in the Silurian 3-1 horizon with an average of 161.1 ppm (Table 2-5). The Fe differences (ΔFe) are more pronounced (average= 424.3 ppm), they differ between -0.8 ppm in Permian 2 horizon to 2564 ppm in Silurian 4 horizon (Table 2-5). In contrast, U concentrations display less variation (average= 0.410) in delta values (ΔU), they vary between 0.004 ppm (Per. 4 horizon) to 2.352 (Per. 9; Table 2-5).

The minus values imply that the whole rock has lower concentration compared to the coeval fossil shell.

Late Permian brachiopods of Tibet and Pennsylvanian ones of Arizona have enriched ∑REE contents compared to the South Pacific modern counterparts treated with the P-4 protocol (Tables 2-3, 2-4), whereas those from the Pennsylvanian of Oklahoma and the Silurian of Anticosti Island yielded comparable ∑REE results (Fig. 2-7C, D; Tables 2-3, 2-4). In contrast, the REE concentrations in the coeval whole rock samples of the Late Permian, the Late and Middle Desmoinsian of Arizona and Oklahoma, and the Early Silurian are slightly to significantly different (Table 2-4). Differences between ΔREEs range from a low of 0.36 ppm in Permian 9 horizon to a high of 88.7 ppm in Permian 10 horizon with an average value of 25.81 ppm (Table 2-5). The REE_{SN} patterns of the mean values of the Late Permian and Late Desmoinsian (Arizona) brachiopods are one order of magnitude higher than the mean trend of South Pacific Procedure-4 samples, while the mean REE_{SN} patterns of Middle Desmoinsian (Oklahoma) and Early Silurian brachiopods fall within the same range of the modern P-4 mean trend (Fig. 2-8). The coeval whole rocks display remarkably similar mean REE_{SN} patterns to those of the coeval brachiopod shells, but are enriched in contents by one to two orders of magnitude (Fig. 2-8).

The average Ce/Ce* of the fossil brachiopods vary between 0.36, 0.64, 0.66 and 0.68 in the shells of the L. Permian, L. and M. Desmoinsian, and E. Silurian, respectively (Table 2-4). Although the ∑REE contents are different between brachiopod and coeval whole rock, their Ce/Ce* values are not significantly different (Fig. 2-7D; Table 2-5). Meanwhile, the variations in the ΔCe/Ce* (Ce/Ce*[whole rock] – Ce/Ce*[brachiopods])

are independent (R^2= 0.0061) of the corresponding ΔREEs (Fig. 2-9A). At the maximum ΔREEs of 88.7 ppm between shell and whole rock (horizon Per. 10; Table 2-5), the corresponding ΔCe/Ce* value is only 0.043. The highest ΔCe/Ce* value of 0.21 (30.6 %) was recorded in Silurian horizon Sil. 4 at ΔREEs of only 14.3 ppm, whereas the lowest value of 0.1 % was recorded in materials from Permian horizon Per. 5 with ΔREE of 15.7 ppm (Table 2-5).

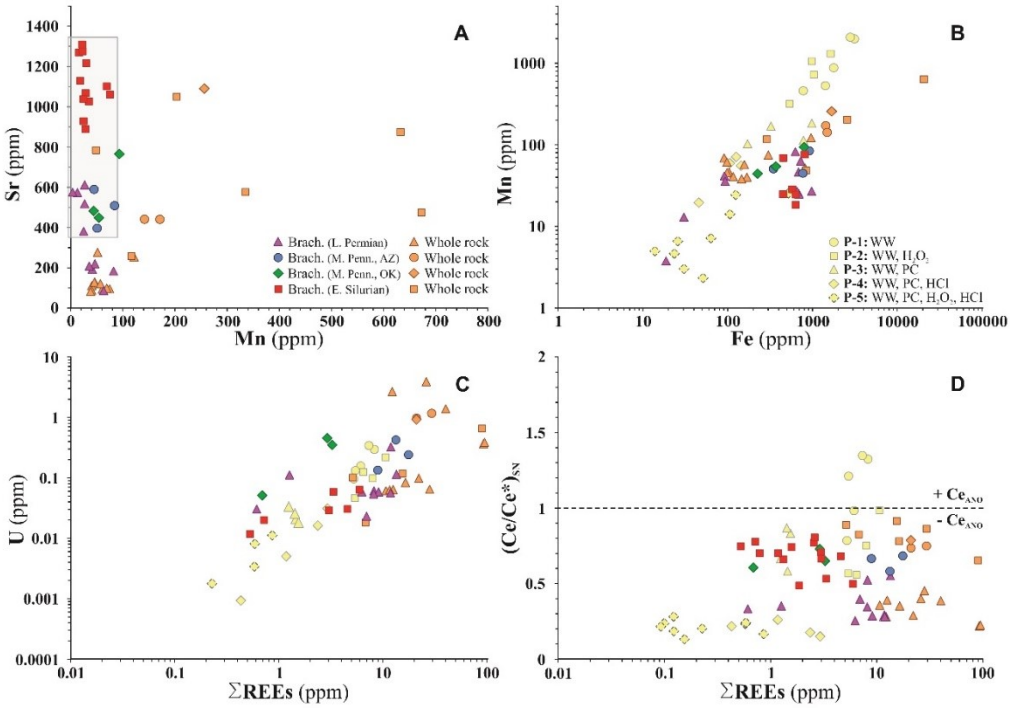

Figure 2-7. Scatter diagrams of Sr, Mn, Fe, U and ∑REE contents and Ce/Ce* values of fossil brachiopod and whole rock archives (A) Sr vs. Mn; shaded gray box represents the natural variation of well-preserved shells, (B) Mn vs. Fe and (C) U vs. ∑REEs and (D) Ce/Ce* vs. ∑REEs for Late Permian (Tibet), Pennsylvanian (Arizona and Oklahoma) and Early Silurian (Anticosti Island) well-preserved brachiopods and near micritic whole rock (yellow symbols represent values of the South Pacific brachiopods of the different five procedures of the new cleaning protocol).

Table 2-5. ΔMn, ΔFe, ΔU, ΔREEs and ΔCe/Ce* values of whole rock- fossil pairs from the Late Permian, Late Desmoinsian, Mid Desmoinsian, and Early Silurian.

Horizon	ΔMn	ΔFe	ΔU	ΔΣREEs	ΔCe/Ce*	
					value	%
Late Permian (Tibet)						
Per. 10-2	11.4	-513.2	0.326	88.7	-0.03	-11.8
Per. 10-1	13.4	-490.7	0.308	86.5	-0.03	-13.2
Per. 9	24.6	-157.6	2.352	0.36	0.00	-0.5
Per. 8	53.2	138.2	1.355	39.6	0.05	15.9
Per. 7	108.7	929.7	N/A	12.6	-0.15	-27.5
Per. 6	9.9	5.2	0.042	10.3	0.00	-1.6
Per. 5	15.7	-577.3	-0.028	15.2	0.00	0.1
Per. 4	-21.3	-529.8	0.040	4.7	-0.12	-29.1
Per. 3	-0.3	-579.3	0.007	2.5	0.01	3.5
Per. 2	27.7	-0.8	0.006	3.4	0.10	35.9
Per. 1	11.7	-424.7	0.004	20.0	-0.07	-13.7
Average	23.15	-200.02	0.44	25.81	-0.02	-3.8
Late Desmoinsian (Arizona)						
Penn. 3-2	86.9	521.0	0.927	11.8	0.07	9.5
Penn. 3-1	126.3	664.5	1.035	20.5	0.08	12.5
Penn. 2	90.9	1143.8	0.546	7.7	0.15	26.5
Average	101.4	776.4	0.836	13.4	0.10	16.2
Mid Desmoinsian (Oklahoma)						
Penn. 1-3	162.7	888.0	0.874	20.3	0.18	29.7
Penn. 1-2	212.0	1457.2	0.472	18.1	0.06	7.9
Penn. 1-1	202.1	1313.4	0.575	17.8	0.14	21.0
Average	192.3	1219.5	0.640	18.7	0.12	19.5
Early Silurian (Canada)						
Sil. 6	30.1	207.0	0.080	4.4	0.11	14.2
Sil. 5	N/A	N/A	N/A	28.7	0.16	23.1
Sil. 4-3	180.2	2564.0	0.118	13.9	0.17	23.3
Sil. 4-2	178.6	1932.7	0.106	15.0	0.17	22.5
Sil. 4-1	187.2	2564.0	0.118	14.3	0.21	30.6
Sil. 3-3	563.7	N/A	0.589	84.2	0.15	31.1
Sil. 3-2	557.0	N/A	0.594	86.8	0.12	22.8
Sil. 3-1	610.7	N/A	0.653	88.3	0.17	34.3
Sil. 2-4	306.5	-577.4	-0.029	13.2	0.12	17.3
Sil. 2-3	310.3	-449.8	-0.030	11.7	0.10	14.4
Sil. 2-2	306.0	N/A	N/A	13.3	0.07	10.1
Sil. 2-1	305.0	N/A	N/A	14.9	0.12	18.1
Sil. 1-2	81.6	289.3	0.018	4.2	0.02	2.4
Sil. 1-1	81.6	289.3	0.018	4.2	0.06	7.2
Average	284.5	852.4	0.2	28.4	0.1	19.4
Average*					**0.1**	**12.8**

Note: ΔMn = Mn(whole rock) – Mn(brachiopods), similar for Δ Fe, ΔU, ΔREE and ΔCe/Ce*.
Negative values mean the whole rock is enriched relative to the fossil shells and vice versa.
*: Mean values of the four time periods.

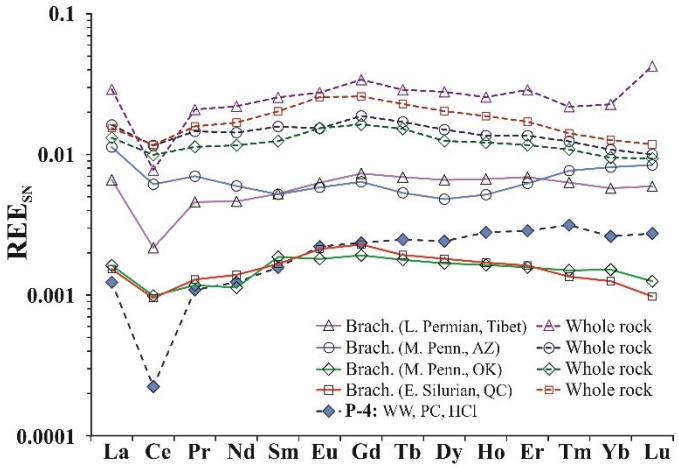

Figure 2-8. Average REE_{SN} patterns of well preserved Paleozoic brachiopods and coeval near micritic whole rock compared to average REE_{SN} results of P-4 cleaned modern brachiopod material.

Variations in ΔCe/Ce* seem to correspond to variations in the concentrations of some of the trace elements within samples. The highest ΔFe value of 2564 ppm coincides with the maximum ΔCe/Ce* value of 0.21 (30.6 %; Sil. 4-1 horizon; Table 2-5). The correlation plot of the ΔCe/Ce* and ΔFe values of the investigated Paleozoic horizons implies a moderate degree of dependency (R^2= 0.3755; Fig. 2-9B). The Mn seems to have the same impact but of slightly lesser strength (R^2= 0.311; Fig. 2-9C); although the highest ΔMn value of 610.7 ppm at Silurian 3 horizon accompanies to relatively less elevated ΔCe/Ce* of 0.17, this value represents the maximum percentage variation (34.3%; Table 2-5). In general, micritic whole rocks with Fe and Mn contents greater than 300 and 100 ppm, respectively, display positive variations in their ΔCe/Ce of about ~13% (rounded up total average, Table 2-5). We suggest that to get a most near-primary seawater Ce anomaly from whole rock (at least up to the Silurian) that their Ce/Ce* be adjusted down by about 13 %. Uranium content, on the contrary, is of less importance, because the variation in the ΔU (Fig. 2-9D) does not have a significant influence on coeval ΔCe/Ce (R^2= 0.0027).

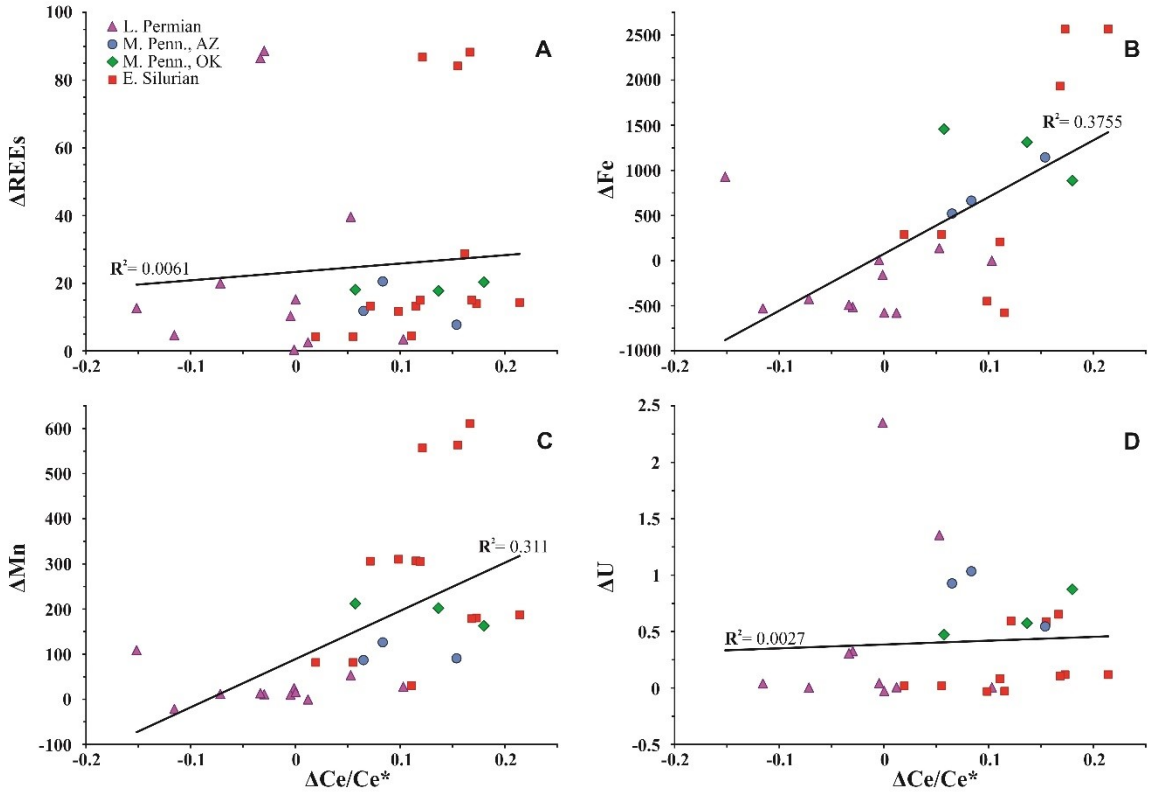

Figure 2-9. Scatter diagram of Δ variations in trace and REE chemistry. A) ΔREEs (REEs in whole rock minus REEs in brachiopods), B) ΔFe, C) ΔMn and D) ΔU of whole rock relative to coeval brachiopods versus their ΔCe/Ce* values (data in Table 5). Negative number means whole rock is relatively depleted to the fossil shell and vice versa.

Distribution coefficients of REEs are remarkably close to one another, so that the Ce anomaly and REE_{SN} pattern should not vary significantly at low water/rock interaction ratios (cf. Brand and Veizer, 1980). This explains the high preservation potential of the Ce anomaly in slightly altered fossil brachiopods and in near micrite samples that are only slightly enriched in their Fe (<300 ppm) and Mn (<100 ppm). The elevated elemental contents (Mn, Fe and U) in some of the whole rock samples suggests that, although the physical state of the whole rock is preserved, they were subjected to a certain degree of elemental alteration during their diagenetic stabilization process, and their mineralogy (aragonite or calcite) played a certain control on it (cf. Brand and Veizer, 1980; Brand,

2004; Brand et al., 2011, 2012). Thus, if the whole rock archive is sampled from fresh micrite, and its chemical evaluation proves it is insignificantly enriched in Mn and Fe it may be as good as that of fossil brachiopods in terms of a Ce/Ce* anomaly signature for paleoredox purposes. Although suitable, the elevated Fe and Mn contents of near micritic whole rock samples suggest that reduction is required for their Ce anomalies by 13% to be consistent with those of their coeval brachiopods. With the 'small' Ce* adjustment, whole rock is potentially a good archive for paleoredox investigations, especially for the recognition of ancient anoxia in the absence of the other indicators such as biogenic material.

2.6.4. Case Study 4 - Biogenic apatite and conodonts

In a final step to test the robustness of the new cleaning protocol, we compared our Paleozoic biogenic and abiogenic calcite results with the published apatite archive. Permian phosphorites are represented by conodonts from the Latest Lopingian (Bid 24E of Meishan section) and fish debris from the Late Guadalupian and Early Wolfcampian compiled from Zhao et al. (2013) and Wright (1985). Desmoinesian material consists of conodonts and fish debris from Bright et al. (2009) and Wright (1985), Llandoverian material consists of conodonts and a single fish bone from Wright (1985). Zhao et al. (2013) did not mention their cleaning procedure but they separated and analyzed only the albid crowns of the conodonts; the denser and the most resistant part to diagenetic alteration. On the other hand, Wright (1985) washed fish debris and conodonts in acetone, and then cleaned them in an ultrasonic bath of absolute ethanol. Similarly, for removing adhering particles, Bright et al. (2009) cleaned their conodonts in a de-ionized water ultrasonic bath.

The average ∑REE concentrations in the conodonts and fish debris of the Late Permian, Middle Pennsylvanian and Early Silurian are 26 to 3500 times higher than that of coeval brachiopods and 6 to 304 times higher than that of corresponding whole rock (Table 2-4). In addition, average Ce/Ce* anomalies of Permian, Pennsylvanian and Silurian conodonts and fish debris are enhanced relative to corresponding values of coeval brachiopods and whole rock (Table 2-4). Furthermore, the mean REE_{SN} patterns of the conodonts and fish debris are completely different from that of brachiopods and whole rocks, and by inference to that of seawater (Fig. 2-10). The conodonts display Middle REE enrichments and heavy REE depletions in their REE_{SN} trends without a Ce excursion in the Permian (Fig. 2-10A) and Silurian (Fig. 2-10C), and a positive Ce excursion in the Pennsylvanian samples (Fig. 2-10B). Fish remnants exhibit REE trends similar to that of the coeval conodonts but are an order of magnitude higher and accompanied by negative Ce excursions in the Permian (Fig. 2-10A) and Pennsylvanian (Fig. 2-10B) and with no excursion in the Silurian material (Fig. 2-10C).

The elevated ∑REE concentrations, the anomalous Ce anomalies and the ambiguous REE_{SN} patterns of the biogenic apatite may reflect either diagenetic alteration (as suggested by many authors such as Elderfield and Pagett (1986), Grandjean and Albarede (1989), Bertram et al. (1992), Murthy et al. (2004), Pucéat et al. (2004), Jiménez-Berrocoso et al. (2006), Trotter and Eggins (2006), Trueman et al. (2006, 2008 a,b, 2011), Anderson et al. (2007), Bright et al. (2009), MacFadden et al. (2010), Suarez et al. (2010), Brand et al. (2011), Tütken et al. (2011), and Herwartz et al. (2013), and/or the lack of an appropriate cleaning procedure. We consider the lack of proper cleaning a primary source

for anomalous REE values and signatures, however, more focused research is needed to verify the actual cause for the spurious apatite REE results observed in conodonts, which seriously limits this archive and its REE contents as a paleoredox proxy.

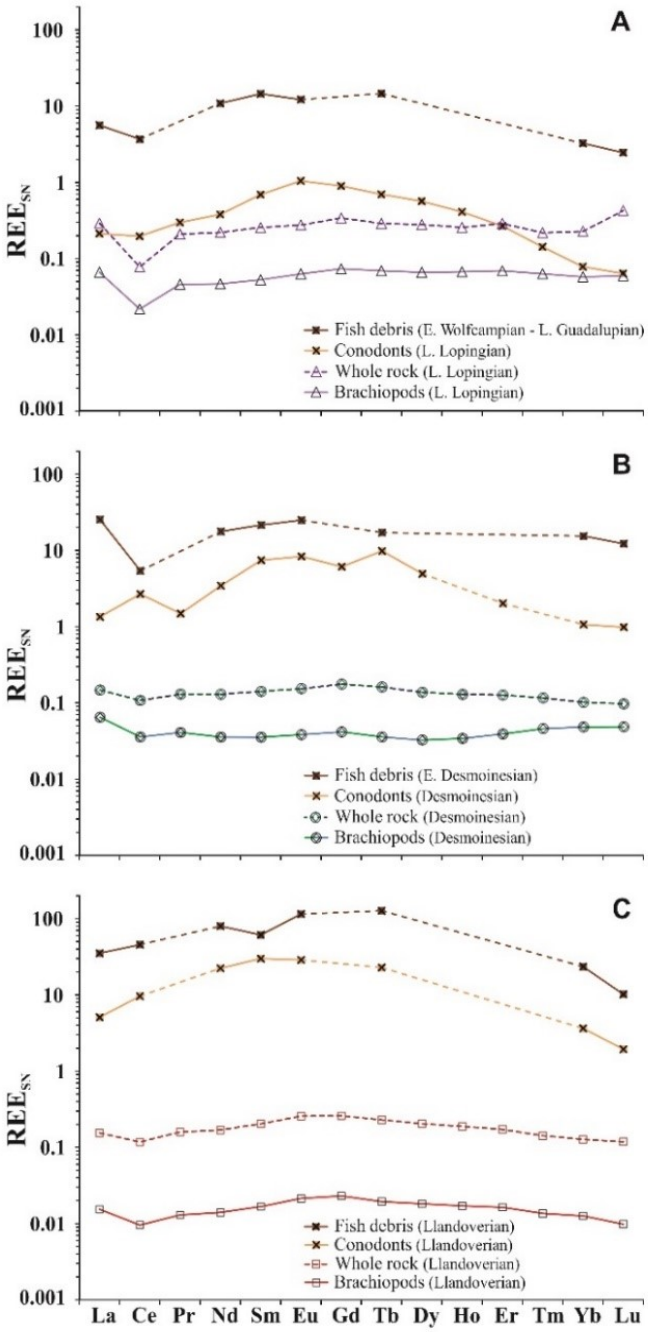

Figure 2-10. Average REE_{SN} patterns of well-preserved brachiopods, whole rock and biogenic apatite (conodonts and fish debris) from (A) the Early Wolfcampian-Late Guadalupian, and Latest Lopingian (Permian), (B) Desmoinsian (Pennsylvanian) and (C) Llandoverian (Silurian) compiled from Wright (1985), Bright et al. (2009) and Zhao et al. (2013).

2.7. Conclusions

A database of modern and fossil brachiopods was tested with different cleaning procedures for the robustness of their seawater REE signatures. Subsequently, ancient material of brachiopods, whole rock and conodonts and fish debris was evaluated for their robustness as archives of seawater REE signatures.

1- Our cleaning protocol consists of five different procedures (P-1 to P-5), with important outcomes for garnering seawater REE signatures from biogenic marine archives,

2- Procedure 1, consisted only of washing specimens with distilled water prior to REE analysis. The results are not consistent with REE contents stored in the calcite lattice but instead with contaminants (e.g., oxides) adhering to the outer shell surface,

   Procedure 2, consisted of cleaning by immersion in hydrogen peroxide with similar results to that of procedure 1,

   Procedure 3, consisted of the physical removal of the outer organic tissue (periostracum) and minor amounts of the primary layer with slightly improved REE results,

   Procedure 4, consisted of physical removal of the organic tissue and adhering surface contaminants followed by an acid leach with 10 % hydrochloric acid and final rinsing with distilled water, this procedure gave REE results consistent with seawater signatures,

Procedure 5, consisted of a combination of all cleaning steps from procedures 1-4, with REE results similar to that of procedure P-4 in giving seawater REE signatures including Ce anomalies,

3- To attain robust seawater REE signatures, we must adhere to the cleaning steps outlined in procedure P-5 for modern biogenic archives, and to those in procedure P-4 for fossil archives, including whole rock,

4- To assure greatest confidence of the REE results, all brachiopod materials should be carefully screened for anomalous Mn, Fe, U and ∑REE contents relative to modern and well-preserved fossil counterparts, and

5- Based on our case studies, only Ce/Ce* values of properly cleaned and screened brachiopods and micritic whole rock with slightly elevated Fe and Mn compositions should be considered reliable proxies of paleoredox.

6- When the Fe and Mn contents of micritic whole rock are greater than 300 and 100 ppm, respectively, we recommend that the Ce anomaly value be adjusted by −13%.

Acknowledgments

We thank the reviewers for their insightful comments, and the National Institute of Water and Atmospheric research (NIWA) and Dr. Jörundur Svavarsson for supplying us with brachiopod shells, and NSERC (7961-09) for financial support to Uwe Brand.

References

Akagi, T., Hashimoto, Y., Fu, F.F., Tsuno, H., Tao, H., and Nakano, Y. (2004). Variation of the distribution coefficients of rare earth elements in modern coral–lattices: species and site dependencies. *Geochimica et Cosmochimica Acta*, *68*(10), 2265–2273.

Al–Aasm, I., and Veizer, J. (1982). Chemical stabilization of low–Mg calcite: an example of brachiopods. *Journal of Sedimentary Petrology*, *52*, 1101–1109.

Anderson, P.E., Benton, M.J., Trueman, C.N., Paterson, B.A., and Cuny, G. (2007). Palaeoenvironments of vertebrates on the southern shore of Tethys: the nonmarine Early Cretaceous of Tunisia. *Palaeogeography, Palaeoclimatology, Palaeoecology*, *243*(1), 118–131.

Azmy, K., Veizer, J., Bassett, M.G., and Copper, P. (1998). Oxygen and carbon isotopic composition of Silurian brachiopods: implications for coeval seawater and glaciations. *Geological Society of America Bulletin*, *110*, 1499–1512.

Azmy, K., Poty, E., and Brand, U. (2009). High–resolution isotope stratigraphy of the Devonian–Carboniferous boundary in the Namur–Dinant Basin, Belgium. *Sedimentary Geology*, *216*(3), 117–124.

Azmy, K., Brand, U., Sylvester, P., Gleeson, S., Logan, A., and Bitner, M.A. (2011). Biogenic low–Mg calcite (brachiopods): proxy of seawater–REE composition, natural processes and diagenetic alteration. *Chemical Geology*, *280*, 180–190.

Azmy, K., Poty, E., and Mottequin, B. (2012). Biochemostratigraphy of the Upper Frasnian in the Namur–Dinant Basin, Belgium: Implications for a global Frasnian–Famennian pre–event, *Palaeogeography, Palaeoclimatology, Palaeoecology, 313–314*, 93–106.

Bau, M. (1991). Rare–earth element mobility during hydrothermal and metamorphic fluid–rock interaction and the significance of the oxidation state of europium. *Chemical Geology*, *93*(3), 219–230.

Bau, M., Koschinsky, A., Dulski, P., and Hein, J.R. (1996). Comparison of the partitioning behaviours of yttrium, rare earth elements, and titanium between hydrogenetic marine ferromanganese crusts and seawater. *Geochimica et Cosmochimica Acta*, *60*(10), 1709–1725.

Bau, M., and Dulski, P. (1999). Comparing yttrium and rare earths in hydrothermal fluids from the Mid–Atlantic Ridge: implications for Y and REE behaviour during near–vent mixing and for the Y/Ho ratio of Proterozoic seawater. *Chemical Geology, 155*(1), 77–90.

Bau, M., and Koschinsky, A. (2009). Oxidative scavenging of cerium on hydrous Fe oxide: evidence from the distribution of rare earth elements and yttrium between Fe oxides and Mn oxides in hydrogenetic ferromanganese crusts. *Geochemical Journal*, *43*(1), 37–47.

Bau, M., and Möller, P. (1992). Rare earth element fractionation in metamorphogenic hydrothermal calcite, magnesite and siderite. *Mineralogy and Petrology*, *45*(3–4), 231–246.

Bau, M., Koschinsky, A., Dulski, P., and Hein, J.R. (1996). Comparison of the partitioning behaviours of yttrium, rare earth elements, and titanium between hydrogenetic marine

ferromanganese crusts and seawater. *Geochimica et Cosmochimica Acta*, *60*(10), 1709–1725.

Bau, M., Balan, S., Schmidt, K., and Koschinsky, A. (2010). Rare earth elements in mussel shells of the Mytilidae family as tracers for hidden and fossil high–temperature hydrothermal systems. *Earth and Planetary Science Letters*, *299*(3), 310–316.

Bertram, C.J., Elderfield, H., Aldridge, R.J., and Morris, S.C. (1992). $^{87}Sr/^{86}Sr$, $^{143}Nd/^{144}Nd$ and REEs in Silurian phosphatic fossils. *Earth and Planetary Science Letters*, *113*(1), 239–249.

Borenäs, K., and Nikolopoulos, A. (2000). Theoretical calculations based on real topography of the maximum deep–water flow through the Jungfern Passage. *Journal of marine research*, *58*(5), 709–719.

Brand, U. (1987). Biogeochemistry of nautiloids and paleoenvironmental aspects of Buckhorn seawater (Pennsylvanian), southern Oklahoma. *Palaeogeography, Palaeoclimatology, Palaeoecology*, *61*, 255–264.

Brand, U. (1989a). Aragonite–calcite transformation based on Pennsylvanian molluscs. *Geological Society of America Bulletin*, *101*(3), 377–390.

Brand, U. (1989b). Biogeochemistry of Late Paleozoic North American brachiopods and secular variation of seawater composition. *Biogeochemistry*, *7*(3), 159–193.

Brand, U. (1990). Chemical diagenesis and dolomitization of Paleozoic high–Mg calcite crinoids. *Carbonates and Evaporites*, *5*(2), 179–196.

Brand, U. (1991). Strontium isotope diagenesis of biogenic aragonite and low–Mg calcite. *Geochimica et Cosmochimica Acta*, *55*(2), 505–513.

Brand, U. (2004). Carbon, oxygen and strontium isotopes in Paleozoic carbonate components: an evaluation of original seawater–chemistry proxies. *Chemical Geology*, *204*(1), 23–44.

Brand, U., and Morrison, J.O. (1987). Diagenesis and pyritization of crinoid ossicles. *Canadian Journal of Earth Sciences*, *24*(12), 2486–2498.

Brand, U., and Veizer, J. (1980). Chemical diagenesis of a multicomponent carbonate system–1: Trace elements. *Journal of Sedimentary Research*, 50(4), 1219–1236.

Brand, U., Logan, A., Hiller, N., and Richardson, J. (2003). Geochemistry of modern brachiopods: applications and implications for oceanography and paleoceanography. *Chemical Geology, 198*, 305–334.

Brand, U., Logan, A., Bitner, M.A., Ggriesshsaber, E., Azmy, K., and Buhl, D. (2011). What is the Ideal Proxy of Palaeozoic Seawater chemistry? *Memoirs of the Association of Australasian Palaeontologists*, *41*, 9–24.

Brand, U., Jiang, G., Azmy, K., Bishop, J., and Montañez, I.P. (2012). Diagenetic evaluation of a Pennsylvanian carbonate succession (Bird Spring Formation, Arrow Canyon, Nevada, USA)—1: Brachiopod and whole rock comparison. *Chemical Geology*, *308*, 26–39.

Brand, U., Azmy, K., Bitner, M.A., Logan, A., Zuschin, M., Came, R., and Ruggiero, E. (2013). Oxygen isotopes and $MgCO_3$ in brachiopod calcite and a new paleotemperature equation. *Chemical Geology, 359*, 23–31.

Brand, U., Azmy, K., Griesshaber, E., Bitner, M.A., Logan, A., Zuschin, M., Ruggiero, E., and Colin, P.L. (2015). Carbon isotope composition in modern brachiopod calcite: A case of equilibrium with seawater?. *Chemical Geology*, *411*, 81–96.

Briggs, K.B., Richardson, M.D., and Young, D.K. (1996). The classification and structure of megafaunal assemblages in the Venezuela Basin, Caribbean Sea. *Journal of marine research*, *54*(4), 705–730.

Bright, C.A., Cruse, A.M., Lyons, T.W., MacLeod, K.G., Glascock, M.D., and Ethington, R.L. (2009). Seawater rare–earth element patterns preserved in apatite of Pennsylvanian conodonts?, *Geochimica et Cosmochimica Acta*, *73*, 1609–1624.

Byrne, R.H., and Sholkovitz, E.R. (1996). Marine chemistry and geochemistry of the lanthanides. *Handbook on the physics and chemistry of rare earths*, *23*, 497–593.

Carpenter, S.J., and Lohmann, K.C. (1995). $\delta^{18}O$ and $\delta^{13}C$ values of modern brachiopods. *Geochimica et Cosmochimica Acta*, *59*: 3749–3764.

Craddock, P.R., Bach, W., Seewald, J.S., Rouxel, O.J., Reeves, E., and Tivey, M.K. (2010). Rare earth element abundances in hydrothermal fluids from the Manus Basin, Papua New Guinea: Indicators of sub–seafloor hydrothermal processes in back–arc basins. *Geochimica et Cosmochimica Acta*, *74*(19), 5494–5513.

de Baar, H.J. (1991). On cerium anomalies in the Sargasso Sea. *Geochimica et Cosmochimica Acta*, *55*(10), 2981–2983.

de Baar, H.J., Bacon, M.P., Brewer, P.G., and Bruland, K.W. (1985a). Rare earth elements in the Pacific and Atlantic Oceans. *Geochimica et Cosmochimica Acta*, *49*(9), 1943–1959.

de Baar, H.J., Brewer, P.G., and Bacon, M.P. (1985b). Anomalies in rare earth distributions in seawater: Gd and Tb. *Geochimica et Cosmochimica Acta*, *49*(9), 1961–1969.

de Baar, H.J., German, C.R., Elderfield, H., and Van Gaans, P. (1988). Rare earth element distributions in anoxic waters of the Cariaco Trench. G *Geochimica et Cosmochimica Acta*, *52*(5), 1203–1219.

Dubinin A.V. (2004). Geochemistry of Rare Earth Elements in the Ocean. *Lithology and Mineral Resources*, *39*(4), 289–307. Translated from *Litologiya i Poleznye Iskopaemye*, *4*, 339–358.

Elderfield, H., and Greaves, M.J. (1982). The rare earth elements in seawater. *Nature, 296*, 214–219.

Elderfield, H., and Pagett, R. (1986). Rare earth elements in ichthyoliths: variations with redox conditions and depositional environment. *Science of the Total Environment*, *49*, 175–197.

Elderfield, H., and Sholkovitz, E.T. (1987). Rare earth elements in the pore waters of reducing nearshore sediments. *Earth and Planetary Science Letters*, *82*(3), 280–288.

Elderfield, H., Whitfield, M., Burton, J.D., Bacon, M.P., and Liss, P.S. (1988). The oceanic chemistry of the rare–earth elements [and discussion]. *Philosophical Transactions of the Royal Society of London A: Mathematical, Physical and Engineering Sciences*, *325*(1583), 105–126.

Elderfield, H., Upstill–Goddard, R., and Sholkovitz, E.R. (1990). The rare earth elements in rivers, estuaries, and coastal seas and their significance to the composition of ocean waters. *Geochimica et Cosmochimica Acta*, *54*(4), 971–991.

Elliott, J.C. (2002). Calcium phosphate biominerals. *Reviews in Mineralogy and Geochemistry, 48*(1), 427–453.

Emig, C.C. (1990). Examples of post–mortality alteration in recent brachiopod shells and (paleo) ecological consequences. *Marine Biology*, *104*, 233 238.

Falina, A., Sarafanov, A., and Sokov, A. (2007). Variability and renewal of Labrador Sea Water in the Irminger Basin in 1991–2004. *Journal of Geophysical Research: Oceans (1978–2012)*, *112*(C1).

Fratantoni, D.M., Zantopp, R.J., Johns, W.E., and Miller, J. L. (1997). Updated bathymetry of the Anegada–Jungfern Passage complex and implications for Atlantic inflow to the abyssal Caribbean Sea. *Journal of Marine Research*, *55*(5), 847–860.

Fürsich, F.T., and Hurst, J.M. (1974). Environmental factors determining the distribution of brachiopods. *Palaeontology*, *17*(4), 879–900.

Garbelli, C., Angiolini, L., Brand, U., Shen, S.Z., Jadoul, F., Posenato, R., Azmy, K., and Cao, C.Q. (2015). Neotethys seawater chemistry and temperature at the dawn of the end Permian mass extinction. *Gondwana Research*. In press.

German, C.R., and Elderfield, H. (1989). Rare earth elements in Saanich Inlet, British Columbia, a seasonally anoxic basin. Geochimica et Cosmochimica Acta, *53*(10), 2561–2571.

German, C.R., Holliday, B.P., and Elderfield, H. (1991). Redox cycling of rare earth elements in the suboxic zone of the Black Sea. *Geochimica et Cosmochimica Acta*, *55*(12), 3553–3558.

German, C.R., Masuzawa, T., Greaves, M.J., Elderfield, H., and Edmond, J.M. (1995). Dissolved rare earth elements in the Southern Ocean: Cerium oxidation and the influence of hydrography. *Geochimica et Cosmochimica Acta*, *59*(8), 1551–1558.

Girard, C., and Lécuyer, C. (2002). Variations in Ce anomalies of conodonts through the Frasnian / Famennian boundary of Poland (Kowala – Holy Cross Mountains): implications for the redox state of seawater and biodiversity. *Palaeogeography, Palaeoclimatology, Palaeoecology, 181*, 299–311.

Grandjean, P., and Albarède, F. (1989). Ion probe measurement of rare earth elements in biogenic phosphates. *Geochimica et Cosmochimica Acta*, *53*(12), 3179–3183.

Grandjean, P., Cappetta, H., Michard, A., and Albarede, F. (1987). The assessment of REE patterns and $^{143}Nd/^{144}Nd$ ratios in fish remains. *Earth and Planetary Science Letters*, *84*(2), 181–196.

Grandjean, P., Cappetta, H., and Albarède, F. (1988). The REE and εNd of 40–70 Ma old fish debris from the west-African platform. *Geophysical Research Letters*, *15*(4), 389–392.

Grandjean–Lécuyer, P., Feist, R., and Albaréde, F. (1993). Rare earth elements in old biogenic apatites. *Geochimica et Cosmochimica Acta*, *57*, 2507–2514.

Greaves, M.J., Elderfield, H., and Sholkovitz, E.R. (1999). Aeolian sources of rare earth elements to the Western Pacific Ocean. *Marine Chemistry*, *68*(1), 31–38.

Haley, B.A., Klinkhammer, G.P., and McManus, J. (2004). Rare earth elements in pore waters of marine sediments. *Geochimica et Cosmochimica Acta*, *68*(6), 1265–1279.

Herwartz, D., Tütken, T., Jochum, K.P., and Sander, P.M. (2013). Rare earth element systematics of fossil bone revealed by LA–ICPMS analysis. *Geochimica et Cosmochimica Acta*, *103*, 161–183.

Hongo, Y., and Nozaki, Y. (2001). Rare earth element geochemistry of hydrothermal deposits and Calyptogena shell from the Iheya Ridge vent field, Okinawa Trough. *Geochemical Journal*, *35*, 347–354.

Ilyin, A.V. (1998). Rare–Earths Geochemistry of "Old" Phosphorites and Probability of Direct Synsedimentational Precipitation and Accumulation of Phosphate, *Chemical Geology*, *144*, 243–256.

Inall, M., and Sherwin, T. B. (2006). SEA7 Technical Report–Hydrography. *A report to the Department of Trade and Industry*, 76.

James, M.A., Ansell, A.D., Collins, M.J., Curry, G.B., Peck, L.S., and Rhodes, M.C. (1992). Biology of living brachiopods. *Advances in Marine Biology*, *28*, 175–387.

Jeandel, C., Delattre, H., Grenier, M., Pradoux, C., and Lacan, F. (2013). Rare earth element concentrations and Nd isotopes in the Southeast Pacific Ocean. *Geochemistry, Geophysics, Geosystems*, *14*(2), 328–341.

Jiménez–Berrocoso, Á., Olivero, E.B., and Elorza, J. (2006). New petrographic and geochemical insights on diagenesis and palaeoenvironmental stress in Late Cretaceous inoceramid shells from the James Ross Basin, Antarctica. *Antarctic Science*, *18*(03), 357–376.

Johannesson, K.H., Telfeyan, K., Chevis, D.A., Rosenheim, B.E., and Leybourne, M.I. (2014). Rare earth elements in stromatolites–1. Evidence that modern terrestrial stromatolites fractionate rare earth elements during incorporation from ambient waters. In *Evolution of Archean Crust and Early Life,* Springer Netherlands, 385–411.

Kamber, B.S., and Webb, G.E. (2001). The geochemistry of late Archaean microbial carbonate: implications for ocean chemistry and continental erosion history. *Geochimica et Cosmochimica Acta*, *65*(15), 2509–2525.

Kemp, R.A., and Trueman, C. (2003). Rare earth elements in Solnhofen biogenic apatite: geochemical clues to the paleoenvironment. *Sedimentary Geology*, *155*, 109–127.

Kim, J.H., Torres, M.E., Haley, B.A., Kastner, M., Pohlman, J.W., Riedel, M., and Lee, Y.J. (2012). The effect of diagenesis and fluid migration on rare earth element

distribution in pore fluids of the northern Cascadia accretionary margin. *Chemical Geology*, *291*, 152–165.

Kocsis, L., Trueman, C.N., and Palmer, M.R. (2010). Protracted diagenetic alteration of REE contents in fossil bioapatites: direct evidence from Lu–Hf isotope systematics. *Geochimica et Cosmochimica Acta*, *74*(21), 6077–6092.

Kohn, M.J. (2008). Models of diffusion–limited uptake of trace elements in fossils and rates of fossilization. *Geochimica et Cosmochimica Acta*, *72*(15), 3758–3770.

Kowalewski, M., Simões, M.G., Carroll, M., and Rodland, D.L. (2002). Abundant brachiopods on a tropical, upwelling–influenced shelf (Southeast Brazilian Bight, South Atlantic). *Palaios*, *17*(3), 277–286.

Lacan, F., and Jeandel, C. (2004). Neodymium isotopic composition and rare earth element concentrations in the deep and intermediate Nordic Seas: Constraints on the Iceland Scotland Overflow Water signature. *Geochemistry, Geophysics, Geosystems*, *5*(11), 1–10.

Lécuyer, C., Grandjean, P., Barrat, J.A., Emig, C.C., Nolvak, J., Paris, F., and Robardet, M. (1998). $\delta^{18}O$ and REE contents of phosphatic brachiopods: a comparison between modern and lower Paleozoic populations. *Geochimica et Cosmochimica Acta, 62*, 2429–2436.

Lécuyer, C., Bogey, C., Garcia, J.P., Grandjean, P., Barrat, J.A., Bardet, N., and Pereda–Superbiola, X. (2003). Stable isotope composition and rare earth element content of vertebrate remains from the late Cretaceous of northern Spain (Lano): did the environmental record survive?, *Palaeogeography, Palaeoclimatology, Palaeoecology*, *193*, 457–471.

Lécuyer, C., Reynard, B., and Grandjean, P. (2004). Rare earth element evolution of Phanerozoic seawater recorded in biogenic apatites. *Chemical Geology,* 204, 63–102.

Logan, A. (2007). Geographic distribution of extant articulated brachiopods. In: Selden, P. A. (ed.): Treatise on Invertebrate Paleontology, Part H (Revised), Brachiopoda, 6 (supplement), 3082–3115. The Geological Society of America and the University of Kansas, Boulder, Colorado and Lawrence, Kansas.

Loope, G.R., Kump, L.R., and Arthur, M.A. (2013). Shallow water redox conditions from the Permian–Triassic boundary microbialite: The rare earth element and iodine geochemistry of carbonates from Turkey and South China. *Chemical Geology*, *351*, 195–208.

Lowenstam, H.A. (1961). Mineralogy, O^{18}/O^{16} ratios, and strontium and magnesium contents of recent and fossil brachiopods and their bearing on the history of the oceans. *The Journal of Geology*, 241–260.

MacFadden, B.J., DeSantis, L.R., Hochstein, J.L., and Kamenov, G.D. (2010). Physical properties, geochemistry, and diagenesis of xenarthran teeth: prospects for interpreting the paleoecology of extinct species. *Palaeogeography, Palaeoclimatology, Palaeoecology*, *291*(3), 180–189.

Malmberg, S.A. (2004). The Iceland Basin: topography and oceanographic features. Marine Research Institute, *Reykjavik Report, 109*, 1–41.

Martin, E.E., and Scher, H.D. (2004). Preservation of seawater Sr and Nd isotopes in fossil fish teeth: bad news and good news. *Earth and Planetary Science Letters*, *220*(1), 25–39.

McArthur, J.M., and Walsh, J.N. (1984). Rare–earth geochemistry of phosphorites. *Chemical Geology, 47*, 91–220.

McLennan, S.M. (1989). Rare earth elements in sedimentary rocks: influence of provenance and sedimentary processes. In: Lipin, B.R., McKay, G.A. (Eds.), Geochemistry and Mineralogy of Rare Earth Elements, *Mineralogical Society of America Review Mineralogy*, *21*, 169–200.

Metcalf, W.G. (1976). Caribbean-Atlantic water exchange through the Anegada-Jungfern passage. *Journal of Geophysical Research*, *81*(36), 6401–6409.

Michard, A., Albarede, F., Michard, G., Minster, J.F., and Charlou, J.L. (1983). Rare–earth elements and uranium in high–temperature solutions from East Pacific Rise hydrothermal vent field (13 N). *Nature*, *303*, 795–797.

Moore, R.C. (1997). Treatise on invertebrate paleontology, Geological society of America.

Moradian–Oldak, J., Weiner, S., Addadi, L., Landis, W.J., and Traub, W. (1991). Electron imaging and diffraction study of individual crystals of bone, mineralized tendon and synthetic carbonate apatite. *Connective tissue research*, *25*(3–4), 219–228.

Morrison, J. O., & Brand, U. (1986). Paleoscene# 5. Geochemistry of recent marine invertebrates. *Geoscience Canada, 13*(4), 237–254.

Murthy, R., Kidder, D., Mapes, R., and Hannigan, R. (2004). Rare–earth element chemistry of Mississippianage phosphate nodules in the Fayetteville Shale of Oklahoma and Arkansas. *Environmental Geosciences*, *11*(2), 99–111.

Nothdurft, L.D., Webb, G.E., and Kamber, B.S. (2004). Rare earth element geochemistry of Late Devonian reefal carbonates, Canning Basin, Western Australia: confirmation of a seawater REE proxy in ancient limestones. *Geochimica et Cosmochimica Acta*, *68*(2), 263–283.

Nozaki, Y. (2001). Rare Earth Elements and their Isotopes in the Ocean. Encyclopedia of Ocean Sciences, *4*, 2354–2366.

Olivier, N., and Boyet, M. (2006). Rare earth and trace elements of microbialites in Upper Jurassic coral–and sponge–microbialite reefs. *Chemical Geology*, *230*(1), 105–123.

Osborne, A.H., Haley, B.A., Hathorne, E.C., Plancherel, Y., and Frank, M. (2015). Rare earth element distribution in Caribbean seawater: Continental inputs versus lateral transport of distinct REE compositions in subsurface water masses. *Marine Chemistry*. *177*, 172–183.

Palmer, M.R. (1985). Rare earth elements in foraminifera tests. *Earth and Planetary Science Letters*, *73*(2), 285–298.

Parkinson, D., Curry, G.B., Cusack, M., Fallick A.E. (2005). Shell structure, patterns and trends of oxygen and carbon stable isotopes in modern brachiopod shells. *Chemical Geology*, *219*, 193–235.

Picard, S., Lécuyer, C., Barrat, J.A., Garcia, J.P., Dromart, G., and Sheppard, S.M.F. (2002). Rare earth element contents of Jurassic fish and reptile teeth and their potential relation to seawater composition (Anglo–Paris Basin, France and England). *Chemical Geology*, *186*, 1–16.

Piepgras, D., and Jacobsen, S. (1992). The behavior of rare earth elements in seawater: Precise determination of variations in the North Pacific water column. *Geochimica et Cosmochimica Acta*, *56*, 1851–1862.

Pucéat, E., Reynard, B., and Lécuyer, C. (2004). Can crystallinity be used to determine the degree of chemical alteration of biogenic apatites?. *Chemical Geology*, *205* (1), 83–97.

Quik, J.T., Lynch, I., Van Hoecke, K., Miermans, C.J., De Schamphelaere, K.A., Janssen, C.R., Dawson, K.A., Cohen Stuart, M.A. and Van De Meent, D. (2010). Effect of natural organic matter on cerium dioxide nanoparticles settling in model fresh water. *Chemosphere*, *81*(6), 711–715.

Reynard, B., Lécuyer, C., and Grandjean, P. (1999). Crystal–chemical controls on rare–earth element concentrations in fossil biogenic apatites and implications for paleoenvironmental reconstructions. *Chemical Geology, 155*, 233–241.

Roberts, N.L., Piotrowski, A.M., Elderfield, H., Eglinton, T.I., and Lomas, M.W. (2012). Rare earth element association with foraminifera. *Geochimica et Cosmochimica Acta*, *94*, 57–71.

Roth, P.H. (1986). Mesozoic palaeoceanography of the North Atlantic and Tethys oceans. *Geological Society, London, Special Publications*, *21*(1), 299–320.

Rubin, M.A., Jasiuk, I., Taylor, J., Rubin, J., Ganey, T., and Apkarian, R.P. (2003). TEM analysis of the nanostructure of normal and osteoporotic human trabecular bone. *Bone*, *33*(3), 270–282.

Rudwick, M.J.S. (1965). Ecology and paleoecology: in Treatise on Invertebrate Paleontology, Part H, Brachiopod. Boulder F., *Geological Society of America, 1*, H199–H214.

Ruppert, E.E., and Fox, R.S. (2004). Invertebrate zoology: a functional evolutionary approach, in Barnes R.D., *Invertebrate Zoology*, Brooks/Cole, Belmont, CA.

Schmidt, K., Garbe–Schönberg, D., Bau, M., and Koschinsky, A. (2010). Rare earth element distribution in> 400 C hot hydrothermal fluids from 5S, MAR: The role of anhydrite in controlling highly variable distribution patterns. *Geochimica et Cosmochimica Acta*, *74*(14), 4058–4077.

Shields, G., and Webb, G.E. (2004). Has the REE composition of seawater changed over geological time?. *Chemical Geology*, *204*(1–2): 103–107.

Sholkovitz, E.R., and Schneider, D. L. (1991). Cerium redox cycles and rare earth elements in the Sargasso Sea. *Geochimica et Cosmochimica Acta*, *55*(10), 2737–2743.

Sholkovitz, E.R., and Shen, G.T. (1995). The incorporation of rare–earth elements in modern coral. *Geochimica et Cosmochimica Acta*, *59*, 2749–2756.

Sholkovitz, E R., Piepgras, D.J., and Jacobsen, S.B. (1989). The pore water chemistry of rare earth elements in Buzzards Bay sediments. *Geochimica et Cosmochimica Acta*, *53*(11), 2847–2856.

Sholkovitz, E.R., Shaw, T.J., and Schneider, D.L. (1992). The geochemistry of rare earth elements in the seasonally anoxic water column and porewaters of Chesapeake Bay. *Geochimica et Cosmochimica Acta*, *56*(9), 3389–3402.

Smith, P.E., Brand, U., and Farquhar, R.M. (1994). U–Pb systematics and alteration trends of Pennsylvanian–aged aragonite and calcite. *Geochimica et cosmochimica acta*, *58*(1), 313–322.

Smith, C.I., Craig, O.E., Prigodich, R.V., Nielsen–Marsh, C.M., Jans, M.M.E., Vermeer, C., and Collins, M.J. (2005). Diagenesis and survival of osteocalcin in archaeological bone. *Journal of Archaeological Science*, *32*(1), 105–113.

Stransky, B., and Brandt, A. (2010). Occurrence, diversity and community structures of peracarid crustaceans (Crustacea, Malacostraca) along the southern shelf of Greenland. *Polar biology*, *33*(6), 851–867.

Suarez, C.A., Macpherson, G.L., González, L.A., and Grandstaff, D.E. (2010). Heterogeneous rare earth element (REE) patterns and concentrations in a fossil bone: implications for the use of REE in vertebrate taphonomy and fossilization history. *Geochimica et Cosmochimica Acta*, *74*(10), 2970–2988.

Sverjensky, D.A. (1984). Europium redox equilibria in aqueous solution. *Earth and Planetary Science Letters*, *67*(1), 70–78.

Toyoda, K., and Tokonami, M. (1990). Diffusion of rare–earth elements in fish teeth from deep–sea sediments. *Nature, 345*, 607–609.

Trotter, J.A., and Eggins, S.M. (2006). Chemical systematics of conodont apatite determined by laser ablation ICPMS. *Chemical Geology*, *233*(3), 196–216.

Trueman, C.N., and Palmer, M.R. (1997). Diagenetic origin of REE in vertebrate apatite: a reconsideration of Samoilov and Benjamini, 1996. *Palaios*, 495–497.

Trueman, C.N., and Tuross, N. (2002). Trace elements in recent and fossil bone apatite. *Reviews in mineralogy and geochemistry*, *48*(1), 489–521.

Trueman, C.N., Behrensmeyer, K., Potts, R., and Tuross, N. (2002). Rapid diagenesis in bone mineral: mechanisms and applications. *Geochimica et Cosmochimica Acta*, *66*(15A), A786–A786.

Trueman, C.N., Behrensmeyer, A.K., Tuross, N., and Weiner, S. (2004). Mineralogical and compositional changes in bones exposed on soil surfaces in Amboseli National Park, Kenya: diagenetic mechanisms and the role of sediment pore fluids. *Journal of Archaeological Science*, *31*(6), 721–739.

Trueman, C.N., Behrensmeyer, A.K., Potts, R., and Tuross, N. (2006). High–resolution records of location and stratigraphic provenance from the rare earth element composition of fossil bones. *Geochimica et Cosmochimica Acta*, *70*(17), 4343–4355.

Trueman, C.N., Palmer, M.R., Field, J., Privat, K., Ludgate, N., Chavagnac, V., Eberth D.A., Cifelli R., and Rogers, R.R. (2008a). Comparing rates of recrystallisation and the

potential for preservation of biomolecules from the distribution of trace elements in fossil bones. *Comptes Rendus Palevol*, *7*(2), 145–158.

Trueman, C.N., Privat, K., and Field, J. (2008b). Why do crystallinity values fail to predict the extent of diagenetic alteration of bone mineral?. *Palaeogeography, Palaeoclimatology, Palaeoecology*, *266*(3), 160–167.

Trueman, C.N., Kocsis, L., Palmer, M.R., and Dewdney, C. (2011). Fractionation of rare earth elements within bone mineral: a natural cation exchange system. *Palaeogeography, Palaeoclimatology, Palaeoecology*, *310*(1), 124–132.

Turner, D.R., Whitfield, M., and Dickson, A.G. (1981). The equilibrium speciation of dissolved components in freshwater and sea water at 25C and 1 atm pressure. *Geochimica et Cosmochimica Acta*, *45*(6), 855–881.

Tuross, N., Behrensmeyer, A.K., Eanes, E.D., Fisher, L.W., and Hare, P.E. (1989). Molecular preservation and crystallographic alterations in a weathering sequence of wildebeest bones. *Applied Geochemistry*, *4*(3), 261–270.

Tütken, T., Vennemann, T.W., and Pfretzschner, H.U. (2011). Nd and Sr isotope compositions in modern and fossil bones–Proxies for vertebrate provenance and taphonomy. *Geochimica et Cosmochimica Acta*, *75*(20), 5951–5970.

Våge, K., Pickart, R.S., Sarafanov, A., Knutsen, Ø., Mercier, H., Lherminier, P., van Aken, H.M., Meincke, J., Quadfasel, D., and Bacon, S. (2011). The Irminger Gyre: Circulation, convection, and interannual variability. *Deep Sea Research Part I: Oceanographic Research Papers*, *58*(5), 590–614.

Webb, G.E., and Kamber, B.S. (2000). Rare earth elements in Holocene reefal microbialites: a new shallow seawater proxy. *Geochimica et Cosmochimica Acta, 64*, 1557–1565.

Weiner, S., and Price, P.A. (1986). Disaggregation of bone into crystals. *Calcified Tissue International*, *39*(6), 365–375.

Williams, R.T., Sarmiento, J.L., Rhines, P., Smethie, W.M., Rooth, C.G.H., Key, R.M., Takahashi, T., and Collins, C. (1986). Transient tracers in the ocean. Tropical Atlantic study, 1 December 1982–18 February 1983. Shipboard physical and chemical data report. *Scripps Institution of Oceanography Tech. Rep. Ref.*, (86–16), 310.

Wright, J. (1985). Rare earth element distributions in Recent and fossil apatite: implications for paleoceanography and stratigraphy. Ph.D. dissertation. University of Oregon, Eugene. 259p.

Wright, J., Seymour, R.S., and Shaw, H.F. (1984). REE and Nd isotopes in conodont apatite: variations with geological age and depositional environment. *Geological Society of America Special Papers*, *196*, 325–340.

Wright, J., Schrader, H., and Holser, W.T. (1987). Paleoredox variations in ancient oceans recorded by rare earth elements in fossil apatite. *Geochimica et Cosmochimica Acta*, *51*(3), 631–644.

Zaky, A., Brand, U., Azmy, K., Logan, A., and Svavarsson, J. (2015). Rare Earth Elements of modern shelf and deep–water articulated brachiopods: evaluation of seawater masses. *Permophiles*, *61*, 98–100.

Zezina, O.N. (2008). Biogeography of the recent brachiopods. *Paleontological Journal*, *42*(8), 830–858.

Zhang, J., and Nozaki, Y. (1996). Rare earth elements and yttrium in seawater: ICP–MS determinations in the East Caroline, Coral Sea, and South Fiji basins of the western South Pacific Ocean. *Geochimica et Cosmochimica Acta*, *60*(23), 4631–4644.

Zhao, L., Chen, Z.Q., Algeo, T.J., Chen, J., Chen, Y., Tong, J., Gao S., Zhou l., Hu Z., and Liu, Y. (2013). Rare–earth element patterns in conodont albid crowns: Evidence for massive inputs of volcanic ash during the latest Permian biocrisis?. *Global and Planetary Change*, *105*, 135–151.

CHAPTER 3

RARE EARTH ELEMENTS IN DEEP-WATER ARTICULATED BRACHIOPODS: EVALUATION OF SEAWATER MASSES

(Published in *Chemical Geology* (2016), V. 435, pp. 22-34)

Amir H. Zaky[a], Karem Azmy[a], Uwe Brand[b] and Jörundur Svavarsson[c]

[a] Department of Earth Sciences, Memorial University of Newfoundland, St. John's, NL, A1B 3X5 Canada.
[b] Department of Earth Sciences, Brock University, St. Catharines, ON, L2S 3A1 Canada.
[c] Institute of Biology, University of Iceland, Askja, Sturlugata 7, 101 Reykjavík, Iceland.

ABSTRACT

Modern articulated brachiopods of the orders *Rhynchonellids* and *Terebratulids* were obtained from below the neritic zone of the Caribbean Sea, North Atlantic, South Pacific and Southern Oceans to evaluate the proxy potential of their rare earth element (REE) contents. Shells of the two orders display similar REE distribution coefficients that vary consistently within the series in response to changes in ionic radii relative to that of the Ca^{2+} cation, which, in turn, excludes the possibility of a biological control on their REE incorporation. The calculated log K_D values for the brachiopods are similar to those documented in other investigations, and as a consequence, shell calcite is enriched in REE concentrations relative to ambient water masses by an average of $0.81x10^5$.

Brachiopods from the four areas yielded $LREE_{SN}$ and $MREE_{SN}$ characteristic of their ambient water mass, exhibiting gradual enrichments with increasing atomic number as well as negative Ce_{SN} excursions. Their $HREE_{SN}$ values, on the other hand, define a trend

that varies with water depth. Overall, the Ce/Ce* profile of open-water deep-sea brachiopods is coupled with that of the ambient seawater. Our study confirms the robustness of REEs in deep-water (>500 m) articulated brachiopods and supports their use as a proxy of paleo-oceanography, specifically water mass and redox.

3.1. Introduction

Seawater documents physical and chemical variations in response to the evolution of the Earth and atmosphere. Geochemical proxies help identify these variations, evaluate their magnitudes and define their principal factors (e.g., Veizer et al., 1999). Rare Earth Elements (REEs) have been utilized for reconstructing numerous paleoceanographic parameters including ocean stratification, redox status, hydrothermal fluxes and sedimentary provenance (e.g., Grandjean et al., 1987; Lécuyer et al., 2004; Kocsis et al., 2007).

The fourteen naturally-occurring lanthanides constituting the REE series commonly exist in the trivalent state and exhibit similar chemical properties in low-temperature systems. Redox reactions change the oxidation state of Ce, and thus, well oxygenated seas and open oceans are depleted in Ce whereas anoxic water is enriched in Ce (Elderfield and Sholkovitz, 1987; de Baar et al., 1988; Liu et al., 1988; German et al., 1991). On the other hand, the reduction of Eu^{3+} to Eu^{2+} is associated with magmatic processes and/or high-temperature systems (Dubinin, 2004). REE concentrations are normalized to eliminate the distinctive and odd variation in natural abundance (the Oddo-Harkins effect) and visualize their fractionation relative to the chief source, the upper continental crust (Kuss et al., 2001). The shale-normalized ($_{SN}$) REE distribution pattern of modern oxygenated seawater

is characterized by a progressive enrichment trend and negative Ce excursion (e.g., Elderfield and Greaves 1982; German et al., 1995). Small but systematic changes in the chemical properties of the group lead to slight fractionation in seawater driven by the preferential scavenging of the light elements by sinking particulates relative to heavy ones (de Baar et al., 1985a; German and Elderfield, 1990; German et al., 1991). All REEs (except Ce) in modern oceans exhibit a "nutrient-like" trend with increasing water depth, due to the progressive degradation of suspended particulates (de Baar et al., 1985a; Nozaki, 2001). The REE flux released during the remineralization process is enriched in light REEs (LREEs) relative to heavy REEs (HREEs; Alibo and Nozaki, 1999). Deep ocean water is enriched in HREEs as a result of the high solubility of their complexes in seawater and the re-association of LREE complexes to suspended particulates (Goldberg et al., 1963; Haley et al., 2004). Cerium shows a unique "scavenged" vertical profile in seawater displaying a stepwise decrease from high values in surface water to nearly steady and low values in deep water due to its rapid oxidization to highly insoluble Ce oxide (Moffett 1990; Nozaki, 2001; Haley et al., 2004; Christenson and Schijf, 2011). Consequently, the REE_{SN} distribution pattern of bottom seawater displays stronger Ce depletions and HREE enrichments than shallower water (de Baar et al., 1988; Haley et al., 2004; Kim et al., 2012).

The oceanic budget of REEs is controlled primarily by riverine discharge, atmospheric deposition of dust and aerosols, and hydrothermal/magmatic flux (Elderfield et al., 1988; Nozaki, 2001; Bright et al., 2009; Abbott et al., 2015; Rousseau et al., 2015). The Influence of the first two sources is relatively negligible at deep-water depths, while the third impacts only the ambient water in the immediate vicinity (Klinkhammer et al.,

1983; Hongo and Nozaki, 2001). Thus, REE concentrations may vary significantly within the vent area resulting in a distinctly persistent Chondrite-normalized pattern of LREE enrichment and large positive Eu_{SN} excursion of two orders of magnitude higher than ambient seawater (Klinkhammer et al., 1983, 1994; Mills and Elderfield, 1995; Pichler et al., 1999).

A number of archives have been investigated for their reliability to carry REE compositions and trends of ancient oceans. Of those archives, biogenic apatite (e.g., ichthyoliths, conodonts and phosphatic brachiopods) has received the most attention in the last three decades (e.g., Wright e al., 1984, 1987; Grandjean et al., 1987, 1988; Bertram et al., 1992; Lécuyer et al., 1998, 2004; Armstrong et al., 2001; Girard and Lécuyer 2002; Picard et al., 2002; Kemp and Trueman 2003). Other biogenic archives such as foraminifers, corals and microbialites were also assessed for their REE uptake (e.g., Palmer, 1985; Sholkovitz and Shen, 1995; Webb and Kamber, 2000; Nothdurft et al., 2004; Olivier and Boyet, 2006; Roberts et al., 2012; Johannesson et al., 2014).

Brachiopods have an extended geological record and were most abundant during the Paleozoic (Logan, 2007). They fall into articulated and inarticulated categories, and they inhabit all seas and oceans of all latitudes and depths (Logan, 2007; Zezina, 2008). Articulated shells are constructed of a proteinaceous periostracum that covers an outer granular-calcite primary layer, an inner fibrous-calcite secondary layer, and occasionally a prismatic-calcite tertiary layer (Brand et al., 2003; Garbelli et al., 2015). The relative stability and high resistivity to diagenetic alteration of low-Mg calcite of articulated shells enables the secondary and tertiary layers to be utilized for assessing fluctuations in REEs

(cf. Brand and Veizer, 1980). Recently, the REE incorporation into modern shallow-water articulated brachiopods was evaluated by Azmy et al. (2011). They argued that those not affected by environmental conditions secrete their shells in REE equilibrium with ambient seawater.

In this study, we investigate the REE contents of deep-water (>500 m) articulated brachiopods from different seas and oceans to evaluate their potential as paleo-ocean chemistry proxies. Acquiring such aspect requires, 1) whether the REE compositions of brachiopod archives reflect, in a predictable way, the characteristic of the ambient water mass, 2) whether there is a reproducible tendency of analytical results among different marine organisms from similar oceanographic conditions, and 3) whether differences reflect physiochemical properties of their REE contents and/or mineralogy.

3.2. Sample localities

In order to minimize the influence of aeolian and riverine fluxes on seawater REEs, we studied brachiopods from below the neritic zone (>500 m; Logan, 2007). The shells were obtained at 18 stations of four seas; the Caribbean Sea and the North Atlantic, South Pacific and Southern Oceans (Fig. 3-1). Their taxonomy, geographic distribution, water depths and bathymetries are summarized in Table 3-1.

Specimens belonging to *Chlidonophora incerta* were obtained from two stations of the abyssal plain (~4000 m) of the Venezuela Basin in the Caribbean Sea (Fig. 3-2A). Although the two stations are about 100 km apart, they are located within the same sedimentological province (Richardson and Young, 1987).

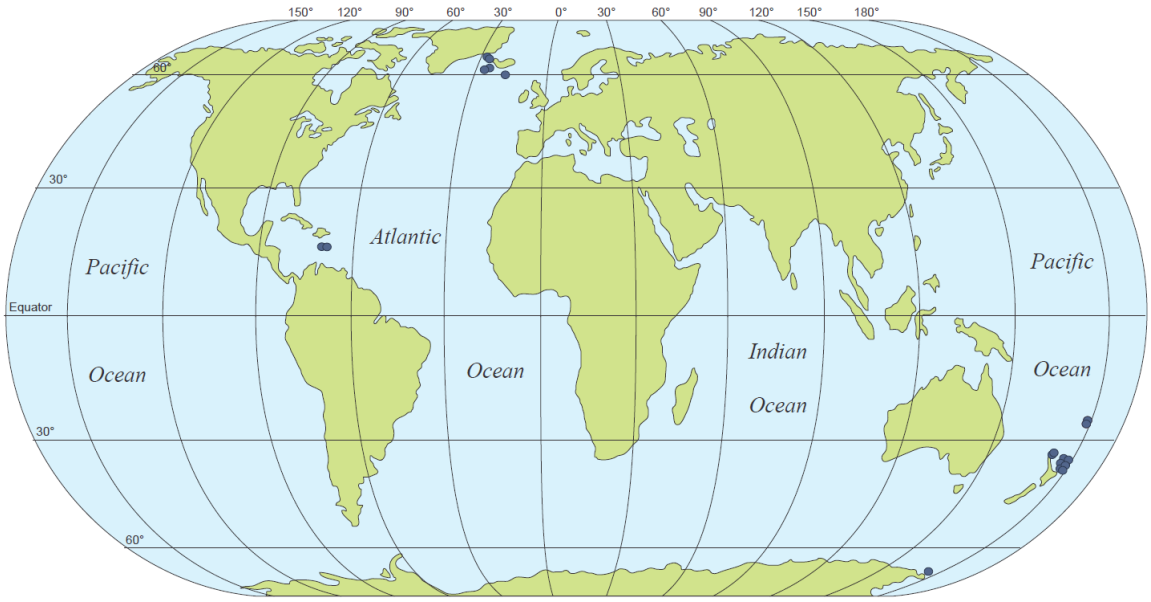

Figure 3-1. Locality diagram of the deep-water (>500 m) brachiopod sampling stations. Details of stations are summarized in Table 3-1.

The Reykjanes Ridge, of the Mid-Atlantic spreading system, is an active volcanic rift southwest of Iceland separating the North American and Eurasian Plates (e.g., Benediktsdóttir et al., 2012). The Irminger and Iceland Basins constitute the northern and southern borders of the ridge, respectively, while the Denmark Strait comprises the northeastern margin of the Irminger Basin. *Macandrevia cranium* shells were gathered live at four stations on the shelfs of the Denmark Strait and the Irminger Basin, and from one station in deep water of the Iceland Basin (Fig. 3-2B).

The actively widening Tonga-Kermadec and Lau-Havre Arc-Back-arc systems are situated on the Indo-Australian Plate in the South Pacific, northeast of New Zealand (Smith et al., 2003). The Tonga-Kermadec ridge constitutes its frontal volcanic ridge and the Lau Basin-Havre Trough its extensional back-arc basin (Karig, 1970; Bryan et al., 1972; Smith et al., 2003). The two basins are bordered on the west by the Lau–Colville Ridge, which is

known as the "third basin" (Karig, 1970; Smith and Price, 2006; Timm et al., 2012). To the west of the subduction zone, the Northland Plateau locates. It represents a submerged continent-ocean margin between the 1000 m deep Northland continental slope of New Zealand and the 3000 m deep Kupe abyssal plain of the South Fiji Basin (Mortimer et al., 2007, 2010; Schellart, 2007). *Abyssothyris wyvillei, Basiliola beecheri, B. pompholyx, Dallinia* sp., *D. triangularis, Goniobrochus ewingi, Liothyrella neozelanica* and *S. crosnieri* were collected from several seamounts and sites of the Lau and Colville Arcs, Kermadec Ridge, Havre Trough and the Northland Plateau (Fig. 3-2C).

Spreading along the Southeast Indian Ridge separates the Indo-Australian Plate to the north from the Antarctic Plate to the south (Cande et al., 2000). *Magellania fragilis* samples were acquired from the northeastern knoll of the Admiralty Seamount, which is located within the Balleny Fracture Zone of the spreading system and north of the Ross Sea in the Southern Ocean (Fig. 3-2D).

Table 3-1. Location, setting and depth of the investigated brachiopod samples and their orders and species.

Locality	Station No.[a]	Sample No.	Order	Species	Coordinates	Setting	Depth (m)
1- CARIBBEAN SEA							
Venezuela Basin							
VB1	1	VB-St1-1	T	*Chlidonophora incerta*	15.6571°N, 69.1943°W	Deep sea	3986
		VB-St1-2	″	″			″
		VB-St1-3	″	″			″
VB2	2	VB-St2-1	″	″	15.7370°N, 69.8180°W	"	3998
		VB-St2-2	″	″			″
		VB-St2-3	″	″			″
2- NORTH ATLANTIC OCEAN							
Denmark Strait							
1090	3	DS-S-St1-1	″	*Macandrevia cranium*	66.0005°N, 25.0530°W	Continental shelf	603.1-742.5
1119	4	DS-S-St2-1	″	″	67.2135°N, 26.2417°W	"	696.9-706.4
Irminger Basin							
1086	5	IrB-S-St1-1	″	″	63.7088°N, 26.3842°W	"	678.5-698.1
		IrB-S-St1-2	″	″			
		IrB-S-St1-3	″	″			
		IrB-S-St1-4	″	″			
1082	6	IrB-S-St2-1	″	″	63.7017°N, 23.4497°W	"	704.9-724.4
Iceland Basin							
983	7	IcB-D-1	″	″	60.3573°N, 18.1357°W	Deep sea	2567.7-2568.5
		IcB-D-2	″	″			
		IcB-D-3	″	″			
3- SOUTH PACIFIC OCEAN							
Lau Arc							
P948	8	LA-1	″	*Terebratulida* sp.	24.2950°S , 178.8350°W	Volcanic Arc	589
		LA-2	″	″			
		LA-3	R	*Basiliola beecheri*			
		LA-4	″	″			
Colville Arc							
CA	9	CA-1	T	*Dallina* sp.	25.9833°S, 179.3000°W	"	660
		CA-2	″	″			
Havre Trough							
TAN0205/102	10	HT-St1-1	″	*Liothyrella neozelanica*	34.7098°S, 178.5748°E	Seamount west of Volcano L	1115-1172
		HT-St1-2	″	″			
		HT-St1-3	″	″			
		HT-St1-4	″	″			
		HT-St1-5	″	″			
		HT-St1-6	″	″			
		HT-St1-7	″	″			
		HT-St1-8	″	″			
		HT-St1-9	″	″			
TAN1104/39	11	HT-St2-1	″	*Goniobrochus ewingi*	35.3335°S, 178.4292°E	Seamount west of Rumble II West	1520
Kermadec Arc							
TAN1007/123	12	KA-St1-1	″	*Stenosarina crosnieri*	35.2838°S, 178.8627°E	Thomson Seamount	1244
TAN1104/19	13	KA-St2-1	″	*Dallina triangularis*	36.4762°S, 177.8918°E	Clark Seamount, south cone	1460
		KA-St2-2	″	*Stenosarina crosnieri*			
TAN1104/9	14	KA-St3-1	″	*Dallina triangularis*	36.5042°S, 177.8770°E	Clark Seamount, south flank	1583
Z15337	15	KA-St4-1	″	*Goniobrochus ewingi*	34.8735°S, 179.0541°E	Brothers Seamount West	1740
Northland Plateau							
P70	16	NB-St.1-1	R	*Basiliola pompholyx*	34.1167°S, 174.8699°E	Ballance Seamount	1293
		NB-St.1-2	″	″			
		NB-St.1-3	″	″			
P73	17	NB-St.2-1	T	*Abyssothyris wyvillei*	33.6283°S, 175.5267°E	Unnamed volcanic peak	1538
4- SOUTHERN OCEAN							
Balleny Fracture Zone							
TAN0802/296	18	SO-S-1	″	*Magellania fragilis*	66.9367°S, 170.8297°E	Admiralty Seamount	547
		SO-S-2	″	″			
		SO-S-3	″	″			
		SO-S-4	″	″			
		SO-S-5	″	″			

Brachiopod Orders: T (*Terebratulida*) and R (*Rynchonellida*).
[a] Numbers on Fig. 3-2.

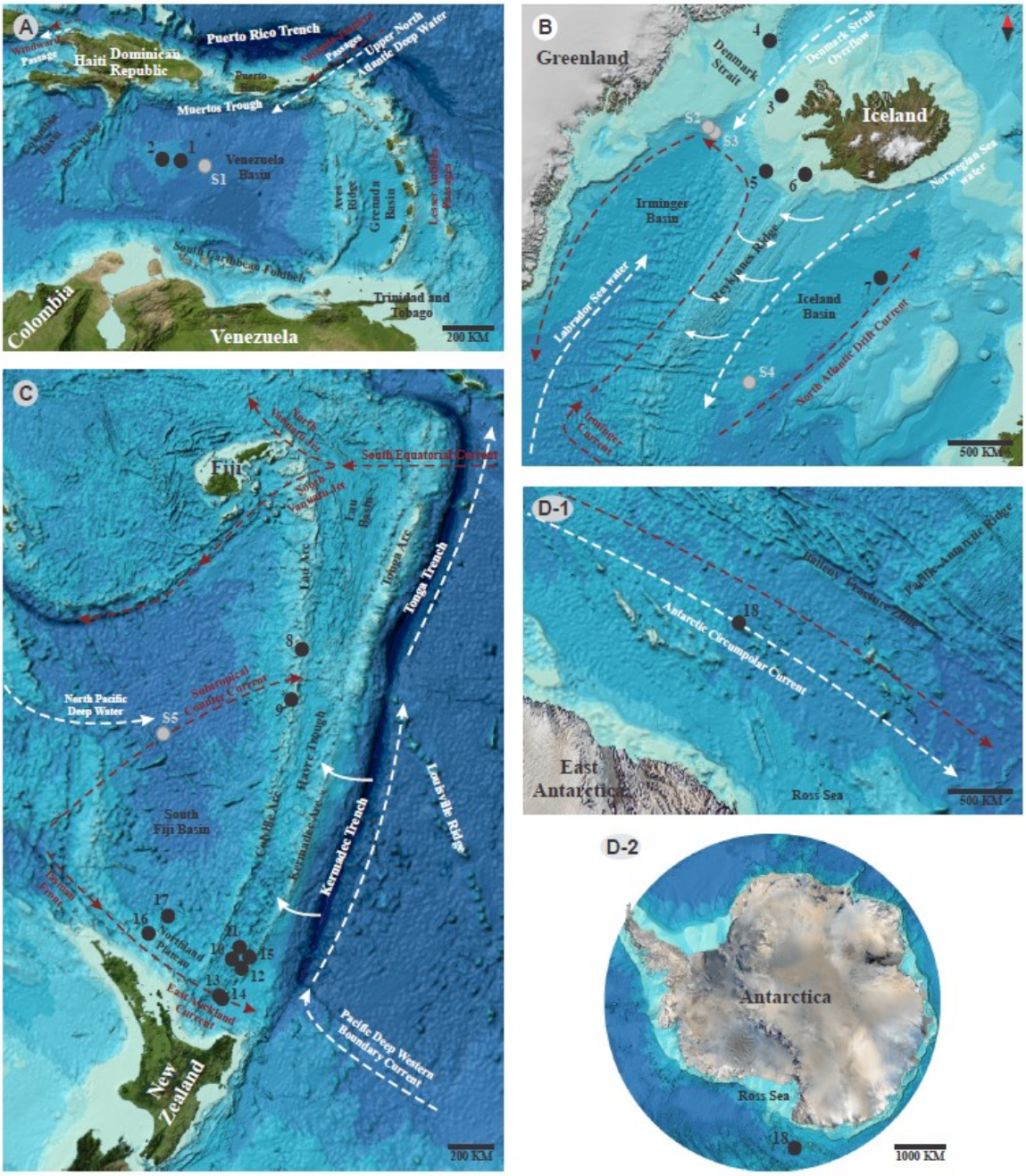

Figure 3-2. GEBCO-bathymetric maps of the different regions showing surface (red) and deep (white) currents, brachiopod (black circle) and seawater (gray circle) stations, and the main tectonic features in (A) Caribbean Sea, (B) North Atlantic around Iceland, (C) South Pacific between the south of Tonga and the north New Zealand, and (D-1) Ross Sea in the Southern Ocean. The seawater stations S1, S2, S3, S4 and S5 represent Station 220-1&2 (Osborne et al., 2015), Stations 14, 15 and 12 (Lacan and Jeandel, 2005), and Station SA-12 (Zhang and Nozaki, 1996), respectively, while, the numbers of the brachiopod stations are illustrated on Table 3-1. D-2 shows the locality of the Southern Ocean brachiopod station on the GEBCO-polar Stereographic Projection of Antarctica.

3.3. Methodology

Following the protocol advanced by Zaky et al. (2015); brachiopod shells were cleaned of pedicles, organic tissue and attached sediment using a sharp stainless-steel blade. Encrusting epibionts and other organic remnants were removed by submerging the shells in 2.5% hydrogen peroxide for three days. The primary layer and remaining surface contaminants were removed by immersing shells in 10% HCl. Subsequently, shells were rinsed with de-ionized water and air-dried at room temperature and then powdered in an agate mortar.

About 10 mg of each sample, weighed to four decimals, was spiked with 0.05 mL of 8N HNO_3 and then digested in 10mL of distilled 0.2N HNO_3 for about a week. After that, 2 mL of the sample solution was diluted with 3 mL 0.2N HNO_3 and then the final solution was analyzed for their REE compositions at the CREAIT facility of Memorial University of Newfoundland using a Perkin Elmer Sciex inductively coupled plasma mass spectrometer (ICP-MS). The samples were analyzed in eight different runs between 2014 and 2015; the measurements of blanks, standards and the detection limit of each element of the different runs as well as the relative standard deviation (RSD) percentages are reported in Appendix 3-1. The relative uncertainties of the measurements compared to internal (Indium) and standard reference materials (NBS 88a and CCH-1) are better than 3% (Appendix 3-1).

3.4. Results

The REE concentrations of the articulated brachiopods are listed in Appendix 3-1 and their statistics are summarized in Appendix 3-2. The REE concentrations were shale

normalized to the Post-Archean Australian Shale (PAAS) values of McLennan (1989). The Ce/Ce^{*} (Ce anomaly) was calculated with the de Baar et al. (1988) equation; $[Ce/Ce^{*}=3(Ce_{Sample}/Ce_{Shale})/(2La_{Sample}/La_{Shale}+Nd_{Sample}/Nd_{Shale})]$.

For evaluating the enrichments or depletions of the HREEs (Ho to Lu) relative to LREEs (La to Nd) and MREEs (Sm to Dy) on the shale normalized patterns of the investigated brachiopod shells, the $(LREE:HREE)_{SN}$ and $(MREE:HREE)_{SN}$ formulas were used, respectively. They have been calculated by dividing the sum of the $LREE_{SN}$ in the former or the $MREE_{SN}$ in the later to those of the $HREE_{SN}$. However, due to the tendency of Ce (one of the LREEs) to vary in response to changing redox conditions, it has been excluded from the calculation. Consequently, the sum of the $HREE_{SN}$ was multiplied by 3/5 in the first formula to equalize the equation; the total number of elements in the LREE group is 3, while for the HREE it is 5. For assessing the MREEs relative to LREEs, the $(LREE:MREE)_{SN}$ formula was utilized. The sum of the $MREE_{SN}$ was multiplied by 3/5 to equalize the equation; the total number of elements in the group is 5. Overall, values less than or close to unity indicate enrichment, while values larger than unity reflect depletion; the smaller the value, the more pronounced the enrichment.

Table 3-2. Mean $(LREE:MREE)_{SN}$, $(LREE:HREE)_{SN}$, $(MREE:HREE)_{SN}$ and Ce/Ce* values, and the REE concentrations (in ppm) of the investigated brachiopod shells of the different localities and their ambient water masses.

	$(LREE:MREE)_{SN}$	$(LREE:HREE)_{SN}$	$(MREE:HREE)_{SN}$	Ce/Ce*				∑REEs[1]			
				Average[2]	Stdev	Max.	Min.	Average	Stdev	Max.	Min.
Seawater											
Subpolar Mode Water (500-1000 m)[a]	0.56	0.28	0.29	0.17	0.06	0.37[g]	0.12	1.22	0.06	1.30	1.17
North Pacific Deep Water (500-1000 m)[b]	0.59	0.22	0.19	0.16	0.01	0.25[h]	0.10	0.62	0.09	0.69	0.56
Low-oxygenated Upper Circumpolar Deep Water (500-1000 m)[c]	0.68	0.30	0.23	0.13	0.11	0.46[i]	0.08	1.23	0.25	1.82	0.96
Iceland Scotland Overflow Water (>1000 m)[d]	0.54	0.31	0.32	0.16	0.01	0.18[j]	0.16	1.18	0.08	1.24	1.12
North Pacific Deep Water (1000-2000 m)[e]	0.66	0.24	0.19	0.05	0.03	0.18[k]	0.03	0.95	0.15	1.10	0.81
Upper North Atlantic Deep Water (>3000 m)[f]	0.46	0.27	0.33	0.14	0.01	0.31[L]	0.13	1.32	0.01	1.33	1.32
Brachiopods											
Caribbean Sea											
Venezuela Basin (3986 m)	0.53	0.36	0.67	0.49	0.08	0.57	0.37	0.24	0.15	0.46	0.08
North Atlantic											
Denmark Strait (603.1-742.5 m)	0.51	0.54	1.00	0.30	0.05	0.34	0.27	0.94	0.44	1.25	0.63
Irminger Basin (678.5-698.1 m)	0.50	0.49	0.99	0.46	0.14	0.66	0.33	0.93	0.46	1.45	0.52
Iceland Basin (2567.7-2568.5 m)	0.52	0.44	0.82	0.17	0.01	0.17	0.15	0.80	0.14	0.94	0.66
South Pacific											
Lau and Colville Arcs (589-660 m)	0.54	0.45	0.83	0.53	0.21	0.74	0.25	0.85	0.32	1.21	0.30
Havre Trough (1115-1520 m)	0.50	0.40	0.80	0.20	0.05	0.28	0.13	0.35	0.28	0.87	0.09
Kermadec Arc (1244-1740 m)	0.55	0.47	0.87	0.18	0.03	0.23	0.14	1.45	0.44	2.00	1.08
Northland Plateau (1293-1583 m)	0.50	0.41	0.83	0.22	0.05	0.28	0.18	0.62	0.38	1.11	0.20
Southern Ocean											
Ross Sea (547 m)	0.53	0.50	0.94	0.31	0.11	0.51	0.25	0.24	0.12	0.38	0.04

$_{SN}$ Values normalized to Post Achaean Australian Shale (PAAS; McLennan, 1989).
$(LREE:MREE)_{SN}$ = Sum of $(LREEs)_{SN}$ / 3/5 Sum of $(MREEs)_{SN}$.
$(LREE:HREE)_{SN}$ = Sum of $(LREEs)_{SN}$ / 3/5 Sum of $(HREEs)_{SN}$.
$(MREE:HREE)_{SN}$ = Sum of $(MREEs)_{SN}$ / Sum of $(HREEs)_{SN}$.
$Ce/Ce^* = 3(Ce)_{SN}/ 2(La)_{SN} + (Nd)_{SN}$ (de Baar et al., 1988)
[1] Seawater REE concentrations are multiplied by 10^5.
[2] Average Ce anomaly value of the a) corresponding composite in the seawater section, or b) the modern shells in the brachiopod section.
[a] Composite of Stations 14 & 15 in Irminger Basin (500-1000 m, *n*= 4 samples; Lacan and Jeandel, 2005)
[b] Composite of Station SA-12 in the South Pacific Ocean (500-1000 m, *n*=2 samples; Zhang and Nozaki, 1996).
[c] Composite of Stations C5, C11, B11, A11 & KERFIX in the Southern Ocean (500-1000 m, *n*=9 samples; Zhang et al., 2008).
[d] Composite of Station 12 in Iceland Basin (>1000 m, *n*= 2 samples; Lacan and Jeandel, 2005).
[e] Composite of Station SA-12 in the South Pacific Ocean (1000 -2000 m, *n*=3 samples; Zhang and Nozaki, 1996).
[f] Composite of Station 220-1&2 in Venezuela Basin (>3000 m, *n*= 2 samples; Osborne et al., 2015).
[g] 901m water depth value at Station 8 in the Irminger Basin (Lacan and Jeandel, 2005).
[h] 795m water depth value at SA-7 in the South Pacific Ocean (Zhang and Nozaki, 1996).
[i] 600m water depth value at KERFIX station in the Southern Ocean (Zhang et al., 2008).
[j] 2020m water depth value at Station 12 in the Iceland Basin (Lacan and Jeandel, 2005).
[k] 1980m water depth value at SA-7 in the South Pacific Ocean (Zhang and Nozaki, 1996).
[L] 4033m water depth value at Station 162-1 in the Caribbean Sea (Osborne et al., 2015).

3.4.1 REE_{SN} patterns

All brachiopods display gradual enrichment patterns with $(LREE:HREE)_{SN}$ values consistently less than 1 (Table 3-2). The enrichments are well pronounced in the shells from the Venezuela Basin (average= 0.36), moderately pronounced in those from the Iceland Basin, Lau and Colville Arcs, Havre Trough, Kermadec Arc and Northland Plateau (averages= 0.44, 0.45, 0.40, 0.47 and 0.41, respectively), and less pronounced in the samples from the Denmark Strait, Irminger Basin and Ross Sea (averages= 0.54, 0.49 and 50, respectively; Table 3-2). Their REE trends are prominently punctuated with negative Ce excursions.

The magnitude of the MREE enrichment relative to that of the LREEs are invariant; the brachiopods display relatively comparable $(LREE:MREE)_{SN}$ values that vary around a minimum of 0.50 and maximum of 0.55 (Table 3-2). In contrast, enrichment of HREEs relative to MREEs differs dramatically between locations and water masses. They are prominent in the Venezuela Basin samples with $(MREE:HREE)_{SN}$ value of 0.67, less prominent in those from the Iceland Basin, Lau and Colville Arcs, Havre Trough, Kermadec Arc and Northland Plateau with averages of 0.82, 0.83, 0.80, 0.87 and 0.83, respectively, but are invariant for those from the Denmark Strait, Irminger Basin and Ross Sea exhibiting means close to unity (1.00, 0.99 and 0.94, respectively; Table 3-2).

3.4.2 Ce/Ce*

The Ce/Ce^* values of all shells from the different water masses are consistently less than 1 (Table 3-2). However, the values may vary within the same area, for example the North Atlantic and South Pacific. Shells from the Lau and Colville Arcs display the highest

average value of 0.53 ranging from 0.25 to 0.74 (Table 3-2). In contrast, Iceland Basin, Havre Trough, Kermadec Arc and the Northland Plateau brachiopods have lower average values with 0.17, 0.20, 0.18 and 0.20, respectively as well as smaller ranges of 0.15 to 0.17, 0.13 to 0.28, 0.14 to 0.23, and 0.18 to 0.23, respectively (Table 3-2). Specimens from the other locations such as the Venezuela Basin, Denmark Strait, Irminger Basin, and Ross Sea have intermediate average values of 0.49, 0.30, 0.46 and 0.31, respectively and variable ranges of 0.37 to 0.57, 0.27 to 0.34, 0.33 to 0.66, and 0.25 to 0.51, respectively (Table 3-2).

3.4.3 ∑REE concentrations

The ∑REE concentrations of the investigated brachiopods vary significantly between water masses. The Venezuela Basin and Ross Sea samples have the lowest concentrations ranging from 0.08 to 0.46 and 0.04 to 0.38 ppm, respectively, and averages of 0.24 (Table 3-2). Havre Trough specimens have comparable average concentration of 0.35 ppm but with large range varying from 0.09 to 0.87 ppm. On the other hand, Kermadec Arc shells have the highest concentrations with a range between 2.0 and 1.08 ppm and an average of 1.45 ppm (Table 3-2). Similarly, Denmark Strait, Irminger Basin, Iceland Basin, Lau and Colville Arcs and Northland Plateau brachiopods have comparable concentrations of 0.63 to 1.25, 0.51 to 1.45, 0.66 to 0.94, 0.30 to 1.21, and 0.20 to 1.11 ppm, respectively and averages of 0.94, 0.93, 0.80, 0.85 and 0.62 ppm, respectively (Table 3-2).

3.5. Discussion

Evaluating the REE compositions of modern brachiopod calcite was done in conjunction with seawater parameters. Accordingly, we compiled from the literature the

REE compositions of ambient seawater, normalized to PAAS, and correlated them to the brachiopod results to visualize differences and similarities in environmental influences. Brachiopod REE concentrations are elevated relative to those of their ambient seawater at each locality by a number (enrichment factor; section 5.2) listed with the respective component (Table 3-3), and additional water mass and current information at each locality are summarized in Appendix 3-3.

3.5.1. Water Mass Evaluations

3.5.1.1. Caribbean Sea

The REE_{SN} patterns of deep-water brachiopods (~4000m) from the Venezuela Basin depict gradual enrichment trends with $(LREE:HREE)_{SN}$ and $(LREE:MREE)_{SN}$ values of 0.36 and 0.53, respectively, similar to that of ambient Upper North Atlantic Deep Water (Table 3-2; Fig. 3-3). However, the magnitude of their HREE enrichment relative to the MREEs ($(MREE:HREE)_{SN}$= 0.67; Table 3-2) and Ce excursions are less pronounced compared to those of the ambient seawater. In addition, the average Ce/Ce* of the brachiopods (0.49) is higher than that of the seawater (0.14; Table 3-2).

The Venezuela Basin, at depth (> 2800 m), is semi-isolated from the North Atlantic Ocean and is separated tectonically from the neighboring eastern and western basins (Colombia and Grenada) by Beata and Aves ridges (Matthews and Holcombe, 1985). The dissolved oxygen content of Upper North Atlantic Deep Water, which enters from the Anegada-Jungfern Passages, decreases gradually from >6 mL/L (Metcalf, 1976)

Table 3-3. Average REE concentrations (ppm) in brachiopod shells of the different localities and their ambient water masses.

	La	Ce	Pr	Nd	Sm	Eu	Gd	Tb	Dy	Ho	Er	Tm	Yb	Lu	Enrichment factor x (10^5)
Seawater*															
Subpolar Mode Water (500-1000 m)[a]	0.333	0.113	0.060	0.260	0.050	0.010	0.073	0.010	0.095	0.025	0.088	0.010	0.080	0.010	
North Pacific Deep Water (500-1000 m)[b]	0.177	0.034	0.025	0.110	0.022	0.006	0.037	0.007	0.054	0.017	0.059	0.009	0.058	0.011	
Low-oxygenated Upper Circumpolar Deep Water (500-1000 m)[c]	0.373	0.100	0.051	0.231	0.043	0.012	0.067	0.011	0.088	0.025	0.094	0.014	0.103	0.019	
Iceland Scotland Overflow Water (>1000 m)[d]	0.335	0.105	0.055	0.245	0.050	0.010	0.075	0.010	0.095	0.020	0.080	0.010	0.080	0.010	
North Pacific Deep Water (1000-2000 m)[e]	0.289	0.026	0.036	0.171	0.033	0.009	0.054	0.010	0.082	0.025	0.090	0.014	0.096	0.018	
Upper North Atlantic Deep Water (>3000 m)[f]	0.348	0.097	0.061	0.289	0.062	0.018	0.091	0.014	0.103	0.028	0.096	0.015	0.085	0.017	
Brachiopods															
Caribbean Sea															
Venezuela Basin (3986 m)	0.052	0.051	0.010	0.051	0.011	0.002	0.012	0.002	0.017	0.004	0.011	0.001	0.011	0.002	**0.15**
North Atlantic															
Denmark Strait (603.1-742.5 m)	0.230	0.157	0.051	0.228	0.045	0.014	0.059	0.011	0.059	0.012	0.035	0.005	0.035	0.004	**0.88**
Irminger Basin (678.5-698.1 m)	0.200	0.189	0.049	0.223	0.047	0.014	0.058	0.009	0.055	0.011	0.032	0.005	0.027	0.005	**0.88**
Iceland Basin (2567.7-2568.5 m)	0.229	0.075	0.045	0.202	0.040	0.011	0.051	0.008	0.054	0.012	0.032	0.005	0.036	0.005	**0.79**
South Pacific															
Lau and Colville Arcs (589-660 m)	0.200	0.211	0.040	0.168	0.033	0.009	0.047	0.008	0.049	0.011	0.033	0.004	0.032	0.004	**1.34**
Havre Trough (1115-1520 m)	0.089	0.037	0.019	0.087	0.020	0.005	0.021	0.004	0.024	0.006	0.017	0.002	0.018	0.002	**0.46**
Kermadec Arc (1244-1740 m)	0.402	0.149	0.083	0.357	0.076	0.020	0.089	0.016	0.101	0.022	0.065	0.009	0.056	0.008	**1.83**
Northland Plateau (1293-1583 m)	0.158	0.071	0.035	0.146	0.032	0.009	0.047	0.007	0.039	0.010	0.027	0.004	0.028	0.005	**0.81**
Southern Ocean															
Ross Sea (547 m)	0.064	0.042	0.013	0.050	0.013	0.003	0.016	0.002	0.015	0.003	0.011	0.002	0.007	0.001	**0.21**

Enrichment factor: sum of the concentration of each of the light (except Ce) and MREEs in the brachiopod shells to the corresponding value of the nearby seawater divided by their number.

* Seawater REE concentrations are multiplied by 10^5.

[a] Composite of Stations 14 & 15 in Irminger Basin (500-1000 m, *n*= 4 samples; Lacan and Jeandel, 2005).

[b] Composite of Station SA-12 in the South Pacific Ocean (500-1000 m, *n*=2 samples; Zhang and Nozaki, 1996).

[c] Composite of Stations C5, C11, B11, A11 & KERFIX in the Southern Ocean (500-1000 m, *n*=9 samples; Zhang et al., 2008).

[d] Composite of Station 12 in Iceland Basin (>1000 m, *n*= 2 samples; Lacan and Jeandel, 2005).

[e] Composite of Station SA-12 in the South Pacific Ocean (1000 -2000 m, *n*=3 samples; Zhang and Nozaki, 1996).

[f] Composite of Station 220-1&2 in Venezuela Basin (>3000 m, *n*= 2 samples; Osborne et al., 2015).

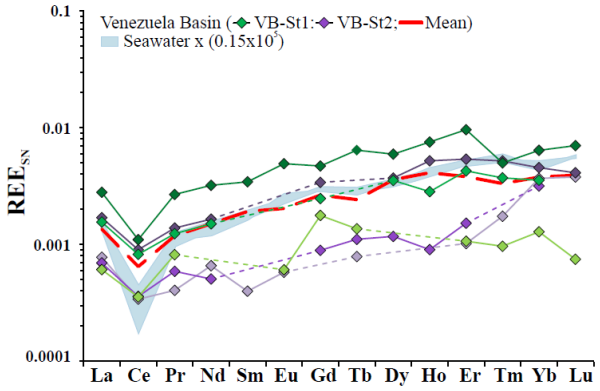

Fig. 3-3: REE_{SN} patterns of Caribbean Sea (Venezuela Basin) brachiopods relative to the Upper North Atlantic Deep Water. Samples of VB1 Station are in green and those of VB2 station are in the purple (Table 3-1) and seawater is compiled in Table 3-2.

in the Virgin Islands Basin, close by the sill, to ~5.1 mL/L in the north of the Venezuela Basin (Williams et al., 1986; Briggs et al., 1996). These redox factors most likely influenced the Ce/Ce* of the brachiopods within the Caribbean Sea (Osborne et al., 2015).

3.5.1.2. North Atlantic Ocean

North Atlantic shelf brachiopods from the Irminger Basin and Denmark Strait are grouped together, and their REE_{SN} patterns correspond well with that of the ambient Subpolar Mode Water (Fig. 3-4A). Although, the Denmark Strait and Irminger Basin brachiopods are from two different water masses (Denmark Strait Over Flow Water and Subpolar Mode Water, respectively), their REE_{SN} patterns are almost identical ($(LREE:MREE)_{SN}$= 0.51 and 0.50, $(MREE:HREE)_{SN}$= 1 and 0.99, Table 3-2; Fig. 3-4A). In contrast, the higher Ce/Ce* of Irminger Basin brachiopods (0.46) relative to those from the Denmark Strait (0.30) reflect differences in redox of the water mass at the two localities. Lacan and Jeandel (2005) investigated the REE compositions of several other locations within the Subpolar Gyre of the Irminger Sea and showed that within the topmost 1000 m, the Ce/Ce*values vary significantly due to deep ocean convection (Lazier et al., 2001; de Jong et al., 2012), reaching the value of 0.37 in some places (normally, the Ce anomaly is relatively high in the shallow water and decreases with depth; Table 3-2). In addition, the

seawater sample locations are ~400 km from those of the brachiopods, suggesting that the observed Ce/Ce* differences between seawater (0.17; Table 3-2) and brachiopods reflect variations in the ambient environmental conditions.

The REE_{SN} patterns of deep-water brachiopods from the Iceland Basin and Iceland Scotland Overflow Water (Lacan and Jeandel, 2005) are displayed on Fig. 3-4B. The REE trends of the Iceland Basin brachiopods show gradual enrichments similar to that of the ambient seawater even between Dy and Lu ($(LREE:HREE)_{SN}$ and $(LREE:MREE)_{SN}$= 0.44 and 0.52, respectively; Table 3-2). Nevertheless, the magnitude of the HREE enrichment is slightly less pronounced ($(MREE:HREE)_{SN}$=0.82; Table 3-2). On the other hand, the average Ce/Ce* of the brachiopods (0.17) is almost identical to that of the seawater (0.16; Table 3-2).

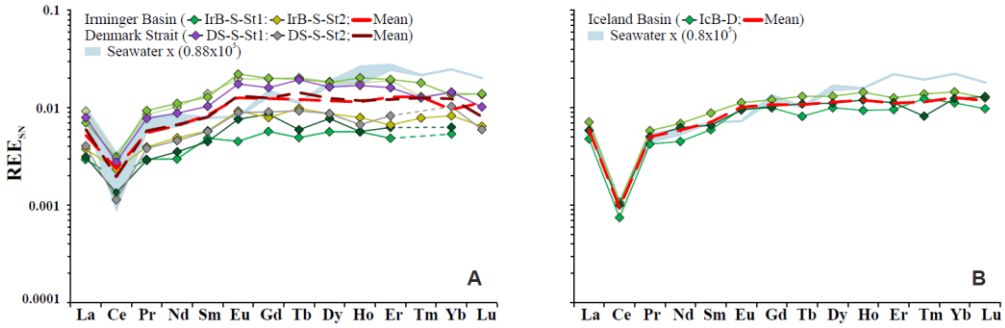

Fig. 3-4: REE_{SN} patterns of North Atlantic brachiopods relative to ambient seawater masses (Seawater information in Table 3-2). (A) Denmark Strait and Irminger Basin brachiopods matched to Subpolar Mode Water (Lacan and Jeandel, 2005). (B) Iceland Basin shells matched to Iceland Scotland Overflow Water (Lacan and Jeandel, 2005). Shells of the Irminger Basin 1086 and 1082 station are in green and yellow shades, while those of the Denmark Strait 1090 and 1119 station are represented by the purple and the gray colors panel A, respectively (Table 3-1).

3.5.1.3. South Pacific Ocean

The average REE_{SN} trend of the relatively shallower brachiopods (<1000 m) from the Lau and Colville Arcs is similar to those from the North Atlantic (Figs. 3-4A, 3-5A). It displays gradual enrichment for $(LREE:MREE)_{SN}$ similar to that of ambient North Pacific

Deep Water mass between La and Dy ($(LREE:MREE)_{SN}$= 0.54), but then the enrichments are less pronounced ($(MREE:HREE)_{SN}$= 0.83; Table 3-2). On the other hand, the average Ce/Ce* of Lau and Colville brachiopods (0.53) is higher than of their ambient seawater (0.16; Table 3-2). However, the North Pacific Deep Water mass in the western South Pacific Ocean displays variation in the Ce anomaly at depths between 500 and 1000m reaching value of 0.25 in the Coral Sea (Table 3-2; Zhang and Nozaki, 1996). Meanwhile, the oxygen maximum zone in the South Pacific starts below 600 m in the northwest near the seawater sampling station, and depletes with depth southeastward toward New Zealand; reaching depths below 800 m close to the brachiopod stations (Wyrtki, 1962). In addition, the North Pacific Deep Water mixes with the relatively more oxic Antarctic Intermediate Water at some locations in the South Fiji Basin close to the seawater station (Zhang and Nozaki, 1996). Thus, the higher Ce/Ce* value of the brachiopods reflects the lower dissolved oxygen content in their ambient seawater relative to that where the seawater station locates.

Furthermore, the average REE_{SN} patterns of the relatively deeper brachiopods (>1000 m) from the other three localities in the South Pacific (Havre Trough, Kermadec Arc and the Northland Plateau) are notably similar to each other ($(LREE:MREE)_{SN}$= 0.50, 0.55 and 0.50, respectively; Table 3-2), and insignificantly different from those of their ambient water mass except in the HREE sections ($(MREE:HREE)_{SN}$= 0.80, 0.87 and 0.83; Table 3-2) where the enrichment patterns of the brachiopods are less pronounced (Fig. 3-5B, C, D). Meanwhile, the mean Ce anomaly values from Havre Trough (0.20), Kermadec Arc (0.18) and the Northland Plateau (0.22) brachiopods are similar but higher than that of

the ambient North Pacific Deep Water mass (0.05; Table 3-2). However, besides fact that the brachiopod sampling stations are extremely far to the south from the water station and dissolved oxygen content decreases southward (Wyrtki, 1962), the deep water of the South Pacific Ocean north of New Zealand is impacted by the deep flow of the Pacific Deep Western Boundary Current which transfers the remnant of North Atlantic Deep Water into the deep of South Fiji Basin (Hogg, 2001; Bostock et al., 2011; Lörz et al., 2012). Consequently, the Ce anomaly of North Pacific Deep Water mass is inconsistent around 0.05, but increases to a value of 0.18 (e.g., 1980 m water depth of Station SA-7 in the Coral Sea; Zhang and Nozaki, 1996). The Ce/Ce* values of brachiopod shells from the Havre Trough, Kermadec Arc and Northland Plateau, thus, reflect the natural variation of Ce within and between water masses.

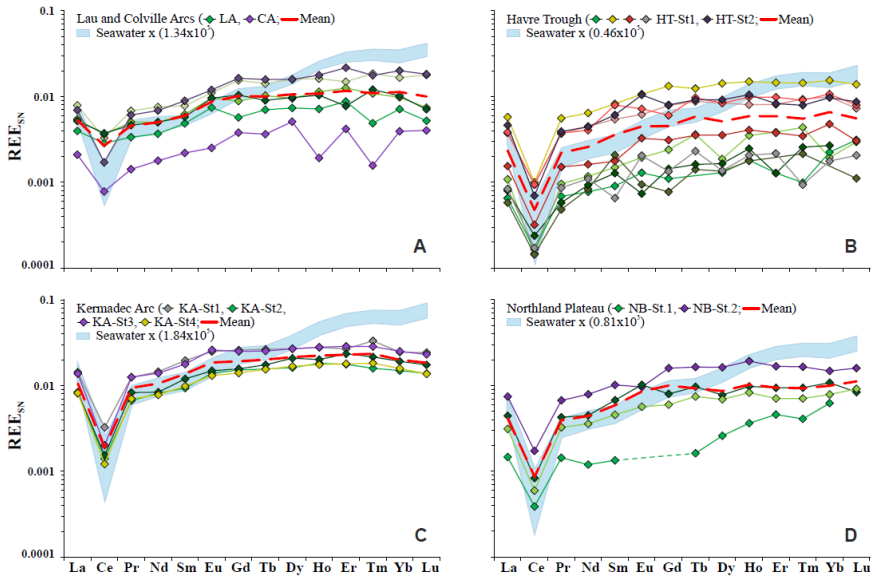

Fig. 3-5: REE_{SN} patterns of South Pacific brachiopods from (A) Lau and Colville Arcs, (B) Havre Trough, (C) Kermadec Arc, and (D) Northland Plateau shells matched to North Pacific Deep Water (Seawater information in Table 3-2). Specimens of Lau and Colville Arc P948 and CA are in green and purple shades on panel A. Those of Havre Through TAN0205/102 Station are represented by green, yellow, dark red and gray shades, while those of TAN1104/39 Station are in purple color on Panel B. Shells of Kermadec Arc TAN1007/123, TAN1104/19, TAN1104/9 and Z15337 stations are represented by gray, green, purple and the yellow colors on Panel C (Table 3-1), and those of the Northland Plateau P70 and P3 stations are in green and purple shades on Panel D (Table 3-1).

Furthermore, the average REE_{SN} patterns of the relatively deeper localities (>1000 m) in the South Pacific Ocean (Havre Trough, Kermadec Arc and the Northland Plateau) are notably similar to each other ($(LREE:MREE)_{SN}$= 50, 55 and 50, respectively; Table 3-2), and insignificantly different from those of their ambient water mass except in the HRRE sections ($(MREE:HREE)_{SN}$ = 80, 87 and 83; Table 3-2) where the enrichment patterns of the brachiopods are less pronounced (Fig. 3-5B, C, D). Meanwhile, the mean Ce anomaly values from Havre Trough= 0.20, Kermadec Arc= 0.18 and the Northland Plateau= 0.22 brachiopods are similar but higher than that of the ambient North Pacific Deep Water mass (0.05; Table 3-2). Ce anomaly of North Pacific Deep Water mass is inconsistent and increases to a value of 0.18 (e.g., 1980 m water depth of Station SA-7 in the Coral Sea; Zhang and Nozaki, 1996). Accordingly, the Ce anomaly of the brachiopods from the Havre Trough, Kermadec Arc and the Northland Plateau also reflect the natural variation of the Ce anomaly within the water body.

3.5.1.4. Southern Ocean

The REE_{SN} patterns of the Ross Sea specimens and the low-oxygenated Upper Circumpolar Deep Water of the Kerguelen Plateau are illustrated on Fig. 3-6. The average REE_{SN} trend of the brachiopods is insignificantly different from that of the seawater between La and Tm showing corresponding enrichments ($(LREE:MREE)_{SN}$ = 0.53; Table 3-2). However, the magnitudes of the enrichments after Dy are less pronounced except for Er and Tm ($(MREE:HREE)_{SN}$= 0.94; Table 3-2). In contrast, the mean Ce/Ce* of shells from the Ross Sea (0.31) is higher than that of the seawater (0.13; Table 3-2).This may be a result of winter convection that takes place in the Southern Ocean (Toole, 1981; Matear

et al., 2000; Aoki et al., 2007), and consequently the Upper Circumpolar Deep Water is highly variable in Ce/Ce* with values ranging between 0.09 and 0.46 (Zhang et al., 2008). Moreover, it is as a water body characterized by low dissolved oxygen content (Matthias and Godfrey, 2003). Accordingly, the Ce anomaly of the brachiopods is within the range of local seawater and it reflects variations in the environment.

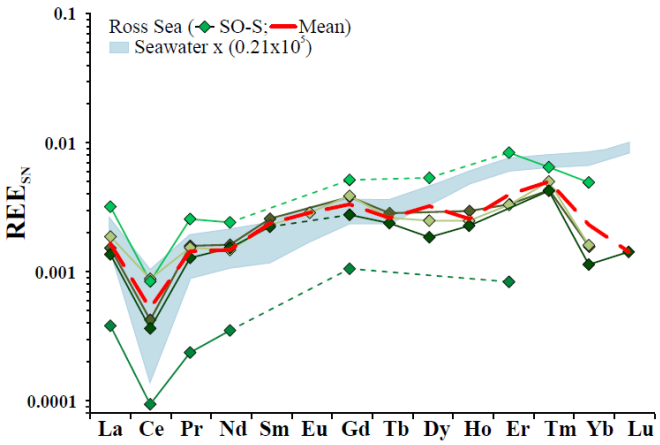

Fig. 3-6: REE_{SN} patterns of Southern Ocean (Ross Sea) brachiopods relative to the low-oxygenated Upper Circumpolar Deep Water (Seawater information in Table 3-2).

3.5.2. ∑REE enrichment

REEs incorporated into the calcite crystal lattice of deep-water brachiopods are elevated in their concentrations relative to their ambient water masses by three or four orders of magnitude (Fig. 3-7). The magnitude of the enrichments was calculated by dividing the sum of the average REE concentration of each shell by that of their ambient water mass (Table 3-3). To minimize undue influences, the HREE and Ce concentrations were excluded from the calculations due to their response to changes in environmental parameters such as dissolved oxygen and depth (sections 5.4 and 5.5).

The brachiopods display comparable enrichment factors (Table 3-3) with an average of 0.81×10^5 and a geometric mean of 0.61×10^5. Caribbean Sea and Southern Ocean

samples have the lowest enrichment factors of $0.15x10^5$ and $0.21x10^5$. Shells from the North Atlantic exhibit insignificantly different values of $0.88x10^5$ for the Denmark Strait and Irminger Basin, and $0.79x10^5$ in the Iceland Basin. On the other hand, South Pacific specimens show a wider range of enrichment factors of $0.46\ x10^5$ in Havre Through and $1.83\ x10^5$ in the Kermadec Arc with in between values of $0.81\ x10^5$ and $1.34\ x10^5$ in the Northland Plateau and Lau and Colville Arcs, respectively. These differences in enrichment factors may be attributed to either environmental factors such as greater complexity of the ambient water masses or an insufficient database.

3.5.3. Distribution Coefficients and Fractionation

REE concentrations in the calcite crystal lattices of brachiopods from the Caribbean Sea, the North Atlantic, South Pacific and Southern Oceans are elevated relative to those of their ambient water masses (Fig. 3-7). We utilized the equations used by Palmer (1985) and Haley et al. (2005), to calculate the log K_D value for each sample relative to its neighboring water mass while assuming 10.46 mmol/L Ca for all water masses (Haley et al., 2005; Appendix 3-4). The log K_D values of the two main brachiopod orders *Terebratulida* and *Rynchonellida* overlap (Table 3-4, Fig. 3-8). The consistency of the values among all shells of the two orders, despite differences in localities, water depth and water mass origins, eliminates the possibility of a biological "vital" control over their REE incorporation. Furthermore, the brachiopod log K_D values are similar to values documented for foraminferal calcite (Palmer, 1985; Haley et al., 2004; Table 3-4). This suggests that brachiopods are consistent with other calcitic archives in their tendency to incorporate REEs preferentially into their crystal lattice and without a vital effect.

Speciation of REEs results from changes in their ionic radii due to the progressive filling of the inner 4f electrons with increasing atomic number and variations in binding energy of the nucleus as a function of neutron and proton number (Cantrell and Byrne, 1987; Elderfield et al., 1988). The enhanced correlation between distribution coefficients and REEs from La to Gd (Fig. 3-8) reflects the control of the ionic radii of the REE cations regarding their placement in the calcite crystal lattice which is governed by their binding energies. Thus cations with similar ionic radius to Ca^{2+} (0.990) such Ce (1.01), Pr (0.997), Nd (0.983) Sm (0.958), Eu (0.947) and Gd (0.938) are preferentially incorporated into the lattice over those with relatively smaller radii than 0.91 (i.e. HREEs; Ho (0.901), Er (0.89), Tm (0.88), Yb (0.868) and Lu (0.861); Fig. 3-8; Palmer, 1985; Palmer and Elderfield, 1986; Kuss et al., 2001). Normalization of the brachiopods to their ambient water masses (Fig. 3-7) confirms that radii of cations are the controlling factor in Ca substitution within the calcite lattice. The enrichments in the shells' REEs appear as a mirror image of the shell of the shells log K_D values (Fig. 3-8).

Haley et al. (2005) argued that the binding efficiency of free REE ions in the ambient water with the shells protein is the main reason for the elevated log K_D in biogenic calcite archive relative to seawater. Palmer (1985), on the other hand, attributed the distribution coefficient enrichment to the solubility product of the REE carbonate salts. Consequently, he calculated their K_{DSS} based on the solid-solution theory equation and, surprisingly, noticed that the theoretically calculated values are insignificantly different from the values observed in the calcite archives.

Table 3-4. Distribution coefficients of REEs in the calcite crystal lattice of deep-water brachiopods relative to published values in foraminiferal calcite.

	La	Ce	Pr	Nd	Sm	Eu	Gd	Tb	Dy	Ho	Er	Tm	Yb	Lu
log K_D														
Terebratulida	1.788	2.349	1.964	1.949	2.026	2.056	1.873	1.920	1.764	1.662	1.552	1.562	1.528	1.517
Rhynchonellida	1.829	2.643	2.035	1.992	2.020	2.122	1.938	1.862	1.729	1.607	1.493	1.464	1.523	1.393
Planktonic foraminifera[a]	2.097	1.851	-	2.100	2.068	2.114	2.076	-	1.924	-	1.845	-	1.863	-
Planktonic foraminifera[b]	2.806	2.782	-	2.831	2.833	2.919	2.767	-	2.799	-	2.638	-	2.670	2.646
Benthic foraminifera (Epifaunal)[c]	2.312	2.919	2.470	2.398	2.623	2.491	2.538	2.332	2.498	2.342	2.362	2.672	2.176	2.079
Benthic foraminifera (Infaunal)[c]	2.568	3.009	2.556	2.607	2.477	2.568	2.447	2.398	2.371	2.332	2.290	2.491	2.114	1.978

[a] From Palmer (1985).
[b] Average of N. Dutertrei calculations relative to the surface seawaters of AJAX 47 and TPS 47: 39-1 (Haley et al., 2005)
[c] From Haley et al. (2005).

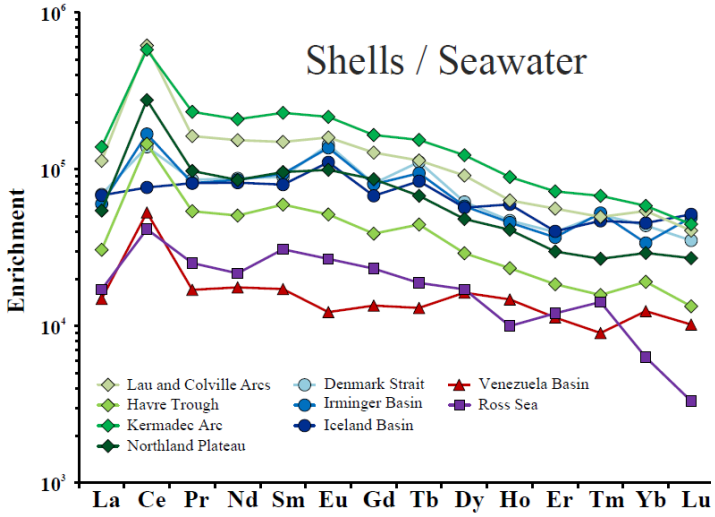

Fig. 3-7: Average REE enrichment in brachiopod calcite at each locality calculated by normalizing the shells REE concentrations to those of their ambient water masses (Table 3-2).

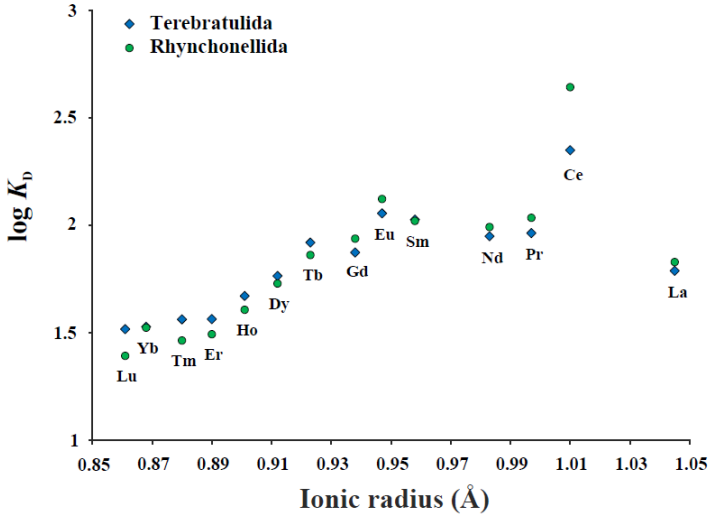

Fig. 3-8: Distribution diagram of calculated log K_D values for the *Terebratulida* and *Rhynchonellida* specimens and the corresponding ionic radii of the REEs.

3.5.4. Seawater Ce/Ce* profile

The Ce anomalies recorded in various marine phases have been utilized as a paleoceanographic indicator of paleoredox (c.f. German and Elderfield, 1990; Nothdurft et al., 2004; Neuweiler and Bernoulli, 2005; Pattan et al., 2005; Olivier and Boyet, 2006; Garbelli et al., 2015). In modern seawater, Ce concentrations are elevated in shallow water (e.g. Elderfield et al., 1988; Holser, 1997; Nozaki and Alibo, 2003). However, oxidation of

Ce^{3+} is rapid and takes place through bacterial mediation (Nozaki, 2001). The resultant Ce^{+4} reacts with dissolved oxygen to produce insoluble cerium oxide (CeO_2), which gets removed by scavenging of sinking ferromanganese nodules and particulate matters causing Ce depletion in correspondingly dissolved fraction (Elderfield and Greaves, 1982; Sholkovitz and Schneider, 1991; Piepgras and Jacobsen, 1992; German et al., 1995; Byrne and Sholkovitz, 1996, Nozaki, 2001). Accordingly, the vertical profile of Ce is different from that of other REEs displaying a stepwise decline with increasing depth from high values in surface water to nearly steady and low ones in deep water (Haley et al., 2005).

However, for brachiopods to serve as paleoceanographic indicators they should have the tendency to record the depth profile of Ce in seawater. Figure 3-9 illustrates the correlation of the Ce/Ce* values of the investigated brachiopod shells with their water depths. Aside from the Caribbean Sea specimens, which are from a semi-isolated deep water body, the other deep-water brachiopods define a Ce/Ce* trend that is consistent to that of the Ce vertical profile in seawater in both stepwise declination with increasing depths and of nearly constant low values in deeper water. This lends strong support to their reliability as a geochemical proxy recording redox conditions of seawater.

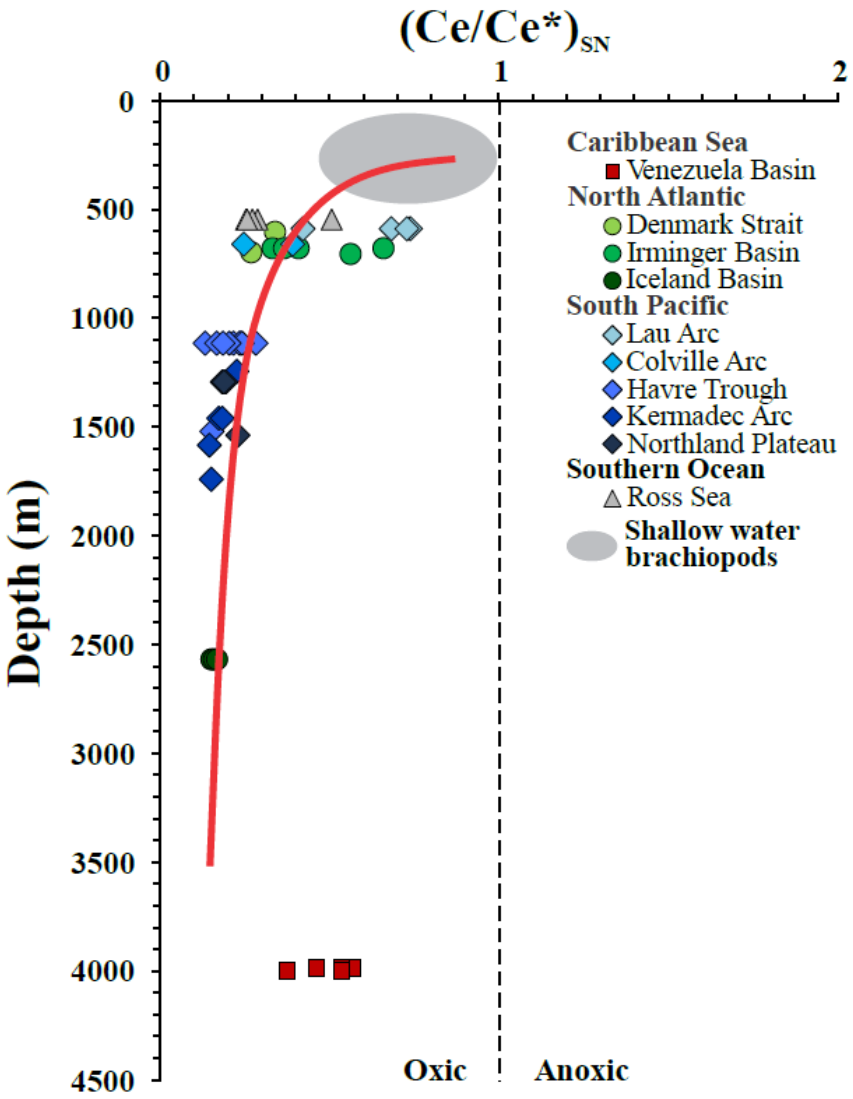

Fig. 3-9: Distribution diagram of Ce/Ce* of brachiopod shells with water depth; values calculated with the de Baar et al. (1988) equation. Shallow water brachiopod field are Ce/Ce* values from Zaky et al. (2016).

3.5.5. Deep-water REE archives

We subcategorized the South Pacific *Cibicidoides* of Haley et al. (2005), which adopt epifaunal habitats similar to those of the investigated brachiopods, into three different groups; those from 1000-2000 m (6 samples from Station 54MC), those from 2000-3000 m (2 samples from Stations 64MC and 66MC) and those from >3000m (1 sample from

Station 50MC). Likewise, the deep-water brachiopods were subdivided into three similar intervals in addition to an extra group to represent those from a depth of 500 m to 1000 m (Fig. 3-10, Table 3-5).

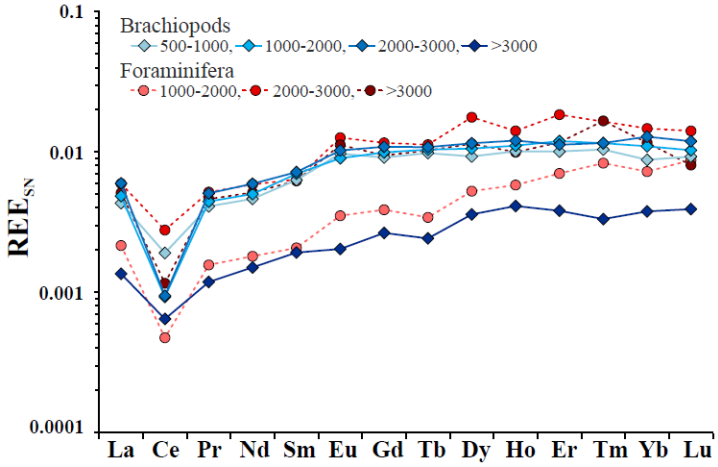

Fig. 3-10: Average REE_{SN} patterns for deep-water modern brachiopods (blue) and epifaunal foraminifera (red) from Haley et al. (2005).

The deep-water brachiopods display gradual enrichments in REE_{SN} patterns that get more pronounced with increasing depth (Fig. 3-10). In order to quantify the magnitude of the enrichment, the $(LREEs:HREE)_{SN}$ and $(MREE:HREE)_{SN}$ ratios of each group from specific depth intervals has been calculated. The lower the ratio the greater the enrichment and vice versa, while a ratio of greater than unity indicates depletion in HREEs. Enrichment of HREEs relative to that of LREEs is gradual in brachiopod calcite with increasing water depth. The shells display gradual depletions in their $(LREE:HREE)_{SN}$ values from 0.46 at depth of 500-1000 m, to 0.44 at 1000-2000 m and 2000-3000 m, and then decrease to 0.36 at depths greater than 3000 m (Table 3-5). In addition the $(MREE:HREE)_{SN}$ ratio decreases with increasing water depth from values close to unity (0.96 at 500-1000 m depth, to 0.83 and 0.82 at depths of 1000-2000 m and 2000-3000 m, with a value of 0.67 in deeper (>3000 m) depths (Table 3-5).

The observed variation in the $(MREE:HREE)_{SN}$ values suggests that the $HREE_{SN}$ enrichment of the deep water brachiopods defines a seawater-depth relationship trend. Its slope varies from flat to upward position with depth. It is most likely attributable to the interplay of the aquatic chemistry of REEs and their co-precipitation into the calcite crystal lattice of brachiopods. The ionic radii of the trivalent REE cations play an important role in their exchange with Ca^{+2} and consequently govern their distribution coefficients in the calcite crystal lattice (Palmer, 1985, Zhong and Mucci 1995). HREEs with smaller ionic radii than Ca^{+2} (i.e. HREEs) are discriminated against relative to MREEs and LREEs (Palmer, 1985; Palmer and Elderfield, 1986; Kuss et al., 2001). This is perhaps the main reason for the higher $(MREE:HREE)_{SN}$ ratio (i.e. the relatively flat $HREE_{SN}$ trend) of the shallower (500-1000 m) brachiopod shells (Table 3-5).

Speciation of the REEs in the seawater is initiated primarily as a direct result of their complexation chemistry in solution and surface bindings (Elderfield et al., 1988). The vertical concentration of each of the REEs in the ocean, except Ce, reflects its affinity to complex with seawater carbonate ligands, which increases systematically across the lanthanide series with increasing the atomic numbers (Cantrell and Byrne, 1987). Meanwhile, the stability of these complexes in solution increases systematically from LREEs to HREEs with increasing atomic number which in turn causes gradual enrichments of the HREEs with depth (Millero, 1992; Lee and Byrne 1992, 1993; Kuss et al., 2001). The downward transportation of the REEs-carbonate ligands and their free ions as well as the regeneration of the HREE ions adsorbed from the surface water by the sinking particulates enhance the HREE concentrations of the deep water (Elderfield et al., 1988;

Nozaki, 2001; Dubinin, 2004). The gradual propagation of the $HREE_{SN}$ pattern of brachiopod calcite with increasing depths is probably a reflection of the general increase in the seawater HREE concentrations and their higher availability over the other REEs.

The REE concentrations of modern deep water brachiopod shells fall within the same range as those documented in benthic foraminifera (Fig. 3-10; Haley et al., 2005). Although the REE_{SN} patterns of the two archives are visually similar, some differences exist. The $(MREE:HREE)_{SN}$ ratio of the benthic foraminifera increases downward from 0.49 in the 1000-2000 m to 0.84 in the >3000 m depth intervals imparting a gradual HREE depletion with increasing depth (Table 3-5). However the observed difference between the brachiopod and foraminifera might have been influenced by the limited database of the latter.

Table 3-5. Average REE concentrations (ppm) in the different depth intervals of the deep-water brachiopods and epifaunal foraminifera (Haley et al., 2005).

	La	Ce	Pr	Nd	Sm	Eu	Gd	Tb	Dy	Ho	Er	Tm	Yb	Lu	∑REEs	Ce/Ce*	$(LREE:HREE)_{SN}$	$(MREE:HREE)_{SN}$
Brachiopods																		
500-1000 m	0.166	0.152	0.036	0.157	0.035	0.011	0.043	0.008	0.046	0.010	0.028	0.004	0.025	0.004	0.720	0.43	0.46	0.96
1000-2000 m	0.186	0.074	0.039	0.170	0.037	0.010	0.044	0.008	0.047	0.011	0.032	0.004	0.031	0.004	0.699	0.20	0.44	0.83
2000-3000 m	0.229	0.075	0.045	0.202	0.040	0.011	0.051	0.008	0.054	0.012	0.032	0.005	0.036	0.005	0.804	0.17	0.44	0.82
>3000 m	0.052	0.051	0.010	0.051	0.011	0.002	0.012	0.002	0.017	0.004	0.011	0.001	0.011	0.002	0.237	0.49	0.36	0.67
Foraminifera[1]																		
1000-2000 m	0.082	0.038	0.014	0.061	0.012	0.004	0.018	0.003	0.025	0.006	0.020	0.003	0.020	0.004	0.310	0.23	0.25	0.49
2000-3000 m	0.228	0.221	0.046	0.200	0.035	0.014	0.054	0.009	0.083	0.014	0.053	-	0.042	0.006	1.004	0.42	0.37[a]	0.78[b]
>3000 m	0.196	0.092	0.041	0.175	0.035	0.012	0.044	0.008	0.054	0.010	0.033	0.007	0.033	0.003	0.743	0.23	0.43	0.84

$_{SN}$: Values normalized to Post Achaean Australian Shale (PAAS; McLennan, 1989).
$Ce/Ce^* = 3(Ce)_{SN}/ 2(La)_{SN} + (Nd)_{SN}$ (de Baar et al., 1988).
$(LREE:HREE)_{SN}$ = Sum of $(LREEs)_{SN}$ / 3/5 Sum of $(HREEs)_{SN}$.
$(MREE:HREE)_{SN}$ = Sum of $(MREEs)_{SN}$ / Sum of $(HREEs)_{SN}$.
[1] Core top and bottom core epifaunal analyses from Stations 50MC, 54MC, 64MC & 66MC (Haley et al., 2005).
[a] Value of Tm, third HREEs, is absent therefore the HREE multiplied by 3/4 to even the equation.
[b] Value of Tm, third HREEs, is absent therefore the value of the third MREEs (Gd) has been excluded.

3.6. Conclusion

Modern *Terebratulida* and *Rynchonellida* shells recovered from deep-water of the Caribbean Sea, North Atlantic, South Pacific and Southern Oceans were evaluated for their REE contents.

1- REE distribution coefficients, irrespective of location and depth, for calcite of the two brachiopod orders are remarkably similar, which, in turn, eliminates a biological control for their uptake. The log K_D values vary between 2.6 and 1.3 and are consistent with results based on foraminiferal calcite.

2- Brachiopod shells are enriched in ∑REE concentrations relative to ambient seawater. Enrichment varies depending on water mass ranges from $0.15x10^5$ in shells from the Caribbean to $1.83x10^5$ in those from the South Pacific; with average and geometric mean values of $0.81x10^5$ and $0.61\ x10^5$.

3- The $LREE_{SN}$ and $MREE_{SN}$ of the brachiopod shells of the four main localities show gradual enrichment patterns similar to those of their ambient water masses, but their $HREE_{SN}$ define a seawater-depth relationship trend.

4- The Ce/Ce* of the brachiopods are consistently less than unity and vary in a manner that reflects local oceanographic redox conditions. Meanwhile, open-water shells define a vertical Ce/Ce* profile matching the Ce trend in seawater.

5- Overall, the results support the robustness of REE compositions of deep-water brachiopod as proxies for paleoceanography such as water mass identification and redox conditions

Acknowledgments

We are grateful to the National Institute of Water and Atmospheric research (NIWA) for supplying us with some brachiopods, and to PEEP (Petroleum Exploration Enhancement Program) for support to Karem Azmy, and NSERC (7961-09) for financial support to Uwe Brand.

References

Ainley, D.G., and Jacobs, S.S. (1981). Sea–bird affinities for ocean and ice boundaries in the Antarctic. *Deep Sea Research Part A. Oceanographic Research Papers*, *28*(10), 1173–1185.

Alibo, D.S., and Nozaki, Y. (1999). Rare earth elements in seawater: particle association, shale normalization, and Ce oxidation. *Geochimica et Cosmochimica Acta,* 63, 363–372.

Alibo, D.S., and Nozaki, Y. (2000). Dissolved rare earth elements in the South China Sea: Geochemical characterization of the water masses. *Journal of Geophysical Research: Oceans (1978–2012)*, *105*(C12), 28771–28783.

Alibo, D.S., and Nozaki, Y. (2004). Dissolved rare earth elements in the eastern Indian Ocean: chemical tracers of the water masses. *Deep–Sea Research I*, *51*, 559–576.

Alvera–Azcárate, A., Barth, A., and Weisberg, R.H. (2009). The surface circulation of the Caribbean Sea and the Gulf of Mexico as inferred from satellite altimetry. *Journal of Physical Oceanography*, *39*(3), 640–657.

Armstrong, H.A., Pearson, D.G., and Griselin, M. (2001). Thermal effects on rare earth and strontium isotope chemistry in single conodont element. *Geochimica et Cosmochimica Acta, 65*, 435–441.

Arrigo, K.R., and van Dijken, G.L. (2004). Annual changes in sea–ice, chlorophyll a, and primary production in the Ross Sea, Antarctica. *Deep Sea Research Part II: Topical Studies in Oceanography*, *51*(1), 117–138.

Azmy, K., Poty, E., and Brand, U. (2009). High–resolution isotope stratigraphy of the Devonian–Carboniferous boundary in the Namur–Dinant Basin, Belgium. Sedimentary *Geology*, *216*(3), 117–124.

Azmy, K., Brand, U., Sylvester, P., Gleeson, S., Logan, A., and Bitner, M.A. (2011). Biogenic low–Mg calcite (brachiopods): proxy of seawater–REE composition, natural processes and diagenetic alteration. *Chemical Geology*, *280*, 180–190.

Bacon, S., Gould, W.J., and Jia, Y. (2003). Open–ocean convection in the Irminger Sea. *Geophysical research letters*, *30*(5), 1–4.

Bau, M., and Dulski, P. (1999). Comparing yttrium and rare earths in hydrothermal fluids from the Mid-Atlantic Ridge: implications for Y and REE behaviour during near-vent mixing and for the Y/Ho ratio of Proterozoic seawater. *Chemical Geology, 155*(1), 77–90.

Benediktsdóttir, A., Hey, R., Martinez, F., and Höskuldsson, Á. (2012). Detailed tectonic evolution of the Reykjanes Ridge during the past 15 Ma. *Geochemistry, Geophysics, Geosystems*, *13*(2), 1–27.

Bertram, C.J., and Elderfield, H. (1993). The geochemical balance of the rare earth elements and neodymium isotopes in the oceans. *Geochimica et Cosmochimica Acta*, *57*, 1957–1986.

Bertram, C.J., Elderfield, H., Aldridge, R.J., and Conway Morris, S. (1992). $^{87}Sr/^{86}Sr$, $^{143}Nd/^{144}Nd$ and REEs in Silurian phosphatic fossils. *Earth and Planetary Science Letters, 113*(1–2), 239–249.

Blindheim, J., Buch, E., Fogelqvist, E., Tanhua, T., and Østerhus, S. (1996). The R/V Johan Hjort 1994 NORDIC WOCE cruise: on hydrography and tracers. *ICES*.

Borenäs, K., and Nikolopoulos, A. (2000). Theoretical calculations based on real topography of the maximum deep–water flow through the Jungfern Passage. *Journal of marine research*, *58*(5), 709–719.

Bostock, H.C., Hayward, B.W., Neil, H.L., Currie, K.I., and Dunbar, G.B. (2011). Deep–water carbonate concentrations in the southwest Pacific. *Deep Sea Research Part I: Oceanographic Research Papers*, *58*(1), 72–85.

Bowen, M.M., Sutton, P.J., and Roemmich, D. (2006). Wind-driven and steric fluctuations of sea surface height in the southwest Pacific. *Geophysical research letters*, *33*(14), 1–4(L14617).

Bowles, F.A., and Fleischer, P. (1985). Orinoco and Amazon River sediment input to the eastern Caribbean Basin. *Marine Geology*, *68*(1), 53–72.

Brand, U., Logan, A., Hiller, N., and Richardson, J. (2003). Geochemistry of modern brachiopods: applications and implications for oceanography and paleoceanography. *Chemical Geology, 198*, 305–334.

Brand, U., Azmy, K., Griesshaber, E., Bitner, M.A., Logan, A., Zuschin, M., Ruggiero, E., and Colin, P.L. (2015). Carbon isotope composition in modern brachiopod calcite: A case of equilibrium with seawater?. *Chemical Geology*, *411*, 81–96.

Briggs, K.B., Richardson, M.D., and Young, D.K. (1996). The classification and structure of megafaunal assemblages in the Venezuela Basin, Caribbean Sea. *Journal of marine research*, *54*(4), 705–730.

Bright, C.A., Cruse, A.M., Lyons, T.W., MacLeod, K.G., Glascock, M.D., and Ethington, R.L. (2009). Seawater rare–earth element patterns preserved in apatite of Pennsylvanian conodonts?, *Geochimica et Cosmochimica Acta*, *73*, 1609–1624.

Bryan, W.B., Stice, G.D., and Ewart, A. (1972). Geology, petrography, and geochemistry of the volcanic islands of Tonga. *Journal of Geophysical Research*, *77*(8), 1566–1585.

Buch, E., Malmberg, S.A., and Kristmannsson, S.S. (1996). Arctic Ocean deep water masses in the western Iceland Sea. *Journal of Geophysical Research: Oceans (1978–2012)*, *101*(C5), 11965–11973.

Butt, J., and Lindstrom, E. (1994). Currents off the east coast of New Ireland, Papua New Guinea, and their relevance to regional undercurrents in the western equatorial Pacific Ocean. *Journal of Geophysical Research: Oceans (1978–2012)*, *99*(C6), 12503–12514.

Byrne, R.H., and Sholkovitz, E.R. (1996). Marine chemistry and geochemistry of the lanthanides. *Handbook on the physics and chemistry of rare earths*, *23*, 497–593.

Callahan, J.E. (1972). The structure and circulation of deep water in the Antarctic. In *Deep Sea Research*, *19*, 563–575.

Cande, S.C., Stock, J.M., Müller, R.D., and Ishihara, T. (2000). Cenozoic motion between east and west Antarctica. *Nature*, *404*(6774), 145–150.

Cantrell, K.J., and Byrne, R.H. (1987). Rare earth element complexation by carbonate and oxalate ions. *Geochimica et Cosmochimica Acta*, *51*(3), 597–605.

Carpenter, S.J., and Lohmann, K.C. (1995). $\delta^{18}O$ and $\delta^{13}C$ values of modern brachiopods. *Geochimica et Cosmochimica Acta*, *59*: 3749–3764.

Cofer–Shabica, N.B., and Peterson, L.C. (1985). Late Pleistocene carbonate dissolution in the Venezuela Basin, Caribbean Sea. *Geological Society of America Abstract Programs.*

de Baar, H.J., Bacon, M.P., Brewer, P.G., and Bruland, K.W. (1985a). Rare earth elements in the Pacific and Atlantic Oceans. *Geochimica et Cosmochimica Acta*, *49*(9), 1943–1959.

de Baar, H.J., Brewer, P.G., and Bacon, M.P. (1985b). Anomalies in rare earth distributions in seawater: Gd and Tb. *Geochimica et Cosmochimica Acta*, *49*(9), 1961–1969.

de Baar, H.J., German, C.R., Elderfield, H., and Van Gaans, P. (1988). Rare earth element distributions in anoxic waters of the Cariaco Trench. G *Geochimica et Cosmochimica Acta*, *52*(5), 1203–1219.

de Boer, C.J., and van Aken, H.M. (1995). A study of objective methods for water mass analysis, applied to the Iceland Basin. *Ocean Dynamics*, *47*(1), 5–22.

Dinniman, M.S., Klinck, J.M., and Smith, W.O. (2007). Influence of sea ice cover and icebergs on circulation and water mass formation in a numerical circulation model of the Ross Sea, Antarctica. *Journal of Geophysical Research: Oceans (1978–2012)*, *112*(C11). 1–13(C11013).

Dubinin A.V. (2004). Geochemistry of Rare Earth Elements in the Ocean. *Lithology and Mineral Resources*, *39*(4), 289–307. Translated from *Litologiya i Poleznye Iskopaemye*, *4*, 339–358.

Elderfield, H., and Greaves, M.J. (1982). The rare earth elements in seawater. *Nature, 296*, 214–219.

Elderfield, H., and Sholkovitz, E.T. (1987). Rare earth elements in the pore waters of reducing nearshore sediments. *Earth and Planetary Science Letters*, *82*(3), 280–288.

Elderfield, H., Whitfield, M., Burton, J.D., Bacon, M.P., and Liss, P.S. (1988). The oceanic chemistry of the rare–earth elements [and discussion]. *Philosophical Transactions of the Royal Society of London A: Mathematical, Physical and Engineering Sciences*, *325*(1583), 105–126.

Falina, A., Sarafanov, A., and Sokov, A. (2007). Variability and renewal of Labrador Sea Water in the Irminger Basin in 1991–2004. *Journal of Geophysical Research: Oceans (1978–2012)*, *112*(C1), 1-11(C01006).

Fratantoni, D.M., Zantopp, R.J., Johns, W.E., and Miller, J.L. (1997). Updated bathymetry of the Anegada–Jungfern Passage complex and implications for Atlantic inflow to the abyssal Caribbean Sea. *Journal of Marine Research*, *55*(5), 847–860.

Ganachaud, A., Cravatte, S., Gourdeau, L., Ridgway, K., Cai, W., Kessler, W., Williams, M., Roemmich D., Sprintall, J., and Qiu, B. (2005). Southwest Pacific Circulation and climate Experiment Southwest Pacific Ocean Circulation and climate Experiment "Workshop on the Southwest Pacific Ocean Circulation, 1–21.

Ganachaud, A., Kessler, W., Wijffels, S., Ridgway, K., Cai, W., Holbrook, N., Bowen, M., Sutton, P., Qiu, B., Timmermann, A., Roemmich, D., Sprintall, J., Cravatte, S., Gourdeau, L., and Aung, T. (2007). Southwest Pacific Ocean Circulation and Climate Experiment (SPICE)–part I. Scientific background, 1–46.

Ganachaud, P., Brassington, G., Kessler, W., Mechoso, C.R., Wijffels, S., Ridgway, K., Cai, W., Holbrook., N., Sutton, P., Bowen, M., Qiu, B., Timmermann, A., Roemmich, D., Sprintall, J., Neelin, D., Lintner, B., Lintner, H., Lintner, S., Gourdeau, L., Eastwood, P., and Aung., T. (2008). Southwest Pacific Ocean Circulation and Climate Experiment (SPICE): Part II. Implementation Plan, 1–42.

Ganachaud, A., Cravatte, S., Melet, A., Schiller, A., Holbrook, N.J., Sloyan, B.M., Widlansky, M.J., Bowen, M., Verron, J., Wiles, P., Ridgway, K., Sutton, P., Sprintall, J., Steinberg, C., Brassington, G., Cai, W., Davis, R., Gasparin, F., Gourdeau, L., Hasegawa, T., Kessler, W., Maes, C., Takahashi, K., Richards K.J., and Send, U. (2014). The Southwest Pacific Ocean circulation and climate experiment (SPICE). *Journal of Geophysical Research: Oceans*,*119* (11), 7660–7686.

Garbelli, C., Angiolini, L., Brand, U., Shen, S.Z., Jadoul, F., Posenato, R., Azmy, K., and Cao, C.Q. (2015). Neotethys seawater chemistry and temperature at the dawn of the end Permian mass extinction. *Gondwana Research*. In press.

Garcia–Solsona, E., Jeandel, C., Labatut, M., Lacan, F., Vance, D., Chavagnac, V., and Pradoux, C. (2014). Rare Earth Elements and Nd isotopes tracing water mass mixing and particle–seawater interactions in the SE Atlantic. *Geochimica et Cosmochimica Acta*, *125*, 351–372.

GEBCO – General Bathymetric Chart of the Oceans – (2014). IHO–IOC GEBCO cook book. In: Marks, K., ed. Monaco: International Hydrographic Organization. 294 p.

German, C.R., and Elderfield, H. (1990). Application of the cerium anomaly as a paleoredox indicator: the ground rules. *Paleoceanography*, *5*, 823–833.

German, C.R., Holliday, B.P., and Elderfield, H. (1991). Redox cycling of rare earth elements in the suboxic zone of the Black Sea. *Geochimica et Cosmochimica Acta*, *5*5(12), 3553–3558.

German, C.R., Masuzawa, T., Greaves, M.J., Elderfield, H., and Edmond, J.M. (1995). Dissolved rare earth elements in the Southern Ocean: Cerium oxidation and the influence of hydrography. *Geochimica et Cosmochimica Acta*, *59*(8), 1551–1558.

Girard, C., and Lécuyer, C. (2002). Variations in Ce anomalies of conodonts through the Frasnian/Famennian boundary of Poland (Kowala–Holy Cross Mountains): implications for the redox state of seawater and biodiversity. *Palaeogeography, Palaeoclimatology, Palaeoecology, 181*, 299–311.

Goldberg, E.D., Koide, M., Schmitt, R.A., and Smith, R.H. (1963). Rare-Earth distributions in the marine environment. *Journal of Geophysical Research*, *68*(14), 4209–4217.

Gordon, A.L., Taylor, H.W., and Georgi, D.T. (1977). Antarctic oceanographic zonation. *Polar oceans*, *682*.

Grandjean, P., Cappetta, H., Michard, A., and Albaréde, F. (1987). The assessment of REE patterns and $^{143}Nd/^{144}Nd$ ratios in fish remains. *Earth and Planetary Science Letters, 84*, 181–196.

Grandjean, P., Cappetta H., and Albaréde F. (1988). The REE and εNd of 40–70 Ma old fish debris from the west–African platform. *Geophysical Research Letters,* 15, 389–392.

Greaves, M.J., Rudnicki, M., and Elderfield, H. (1991). Rare earth elements in the Mediterranean Sea and mixing in the Mediterranean outflow. *Earth and Planetary Science Letters*, *103*(1), 169–181.

Greaves, M.J., Elderfield, H., and Sholkovitz, E.R. (1999). Aeolian sources of rare earth elements to the Western Pacific Ocean. *Marine Chemistry*, *68*(1), 31–38.

Haley, B.A., Klinkhammer, G.P., and McManus, J. (2004). Rare earth elements in pore waters of marine sediments. *Geochimica et Cosmochimica Acta*, *68*(6), 1265–1279.

Haley, B.A., Klinkhammer, G.P., and Mix, A.C. (2005). Revisiting the rare earth elements in foraminiferal tests. *Earth and Planetary Science Letters*,*239*(1), 79-97.

Hansen, B., and Østerhus, S. (2000). North Atlantic–Nordic Seas exchanges. *Progress in Oceanography*, *45*(2), 109–208.

Heath, R.A. (1985). Large–scale influence of the New Zealand seafloor topography on western boundary currents of the South Pacific Ocean. *Marine and Freshwater Research*, *36*(1), 1–14.

Hogg, N.G. (2001). Quantification of the deep circulation. *International Geophysics*, *77*, 259–270.

Holser, W.T. (1997). Evaluation of the application of rare–earth elements to paleoceanography. *Palaeogeography, Palaeoclimatology, Palaeoecology*, *132*(1), 309–323.

Hongo, Y., and Nozaki, Y. (2001). Rare earth element geochemistry of hydrothermal deposits and Calyptogena shell from the Iheya Ridge vent field, Okinawa Trough. *Geochemical Journal*, *35*, 347–354.

Hongo, Y., Obata, H., Gamo, T., Nakaseama, M., Ishibashi, J., Konno, U., Saegusa, S., Ohkubo, S., and Tsunogai, U. (2007). Rare Earth Elements in the hydrothermal system at Okinawa Trough back–arc basin. *Geochemical Journal*, *41*(1), 1–15.

Jacobs, S.S. (1991). On the nature and significance of the Antarctic Slope Front. *Marine Chemistry*, *35*(1), 9–24.

Jeandel, C., Delattre, H., Grenier, M., Pradoux, C., and Lacan, F. (2013). Rare earth element concentrations and Nd isotopes in the Southeast Pacific Ocean. *Geochemistry, Geophysics, Geosystems*, *14*(2), 328–341.

Johannesson, K.H., Telfeyan, K., Chevis, D.A., Rosenheim, B.E., and Leybourne, M.I. (2014). Rare earth elements in stromatolites–1. Evidence that modern terrestrial stromatolites fractionate rare earth elements during incorporation from ambient waters. In *Evolution of Archean Crust and Early Life,* Springer Netherlands, 385–411.

Johns, W.E., Townsend, T.L., Fratantoni, D.M., and Wilson, W.D. (2002). On the Atlantic inflow to the Caribbean Sea. *Deep Sea Research Part I: Oceanographic Research Papers*, *49*(2), 211–243.

Karig, D.E. (1970). Ridges and basins of the Tonga–Kermadec Island arc system. *Journal of geophysical research*, *75*(2), 239–254.

Kemp, R.A., and Trueman, C. (2003). Rare earth elements in Solnhofen biogenic apatite: geochemical clues to the paleoenvironment. *Sedimentary Geology*, *155*, 109–127.

Keys, H., and Fowler, D. (1989). Sources and movement of icebergs in the south–west Ross Sea, Antarctica. *Annals of glaciology*, *12*, 85–88.

Kim, J.H., Torres, M.E., Haley, B.A., Kastner, M., Pohlman, J.W., Riedel, M., and Lee, Y.J. (2012). The effect of diagenesis and fluid migration on rare earth element distribution in pore fluids of the northern Cascadia accretionary margin. *Chemical Geology*, *291*, 152–165.

Kinder, T.H., Heburn, G.W., and Green, A.W. (1985). Some aspects of the Caribbean circulation. *Marine Geology*, *68*(1), 25–52.

Klinkhammer, G., Elderfield, H., and Hudson, A. (1983). Rare earth elements in seawater near hydrothermal vents. *Nature*, *305*, 185–188.

Klinkhammer, G., German, C.R., Elderfield, H., Greaves, M.J., and Mitra, A. (1994). Rare earth elements in hydrothermal fluids and plume particulates by inductively coupled plasma mass spectrometry. *Marine Chemistry*, *45*(3), 179–186.

Kocsis, L., Vennemann, T.W., and Fontignie, D. (2007). Migration of sharks into freshwater systems during the Miocene and implications for Alpine paleoelevation. *Geology*, *35*(5), 451–454.

Kuss, J., Garbe-Schonberg, C.D., and Kremling, K. (2001). Rare earth elements in suspended particulate material of North Atlantic surface waters. *Geochimica et Cosmochimica Acta*, *65*, 187–199.

Lacan, F., and Jeandel, C. (2001). Tracing Papua New Guinea imprint on the central Equatorial Pacific Ocean using neodymium isotopic compositions and Rare Earth Element patterns. *Earth and Planetary Science Letters*, *186*(3), 497–512.

Lacan, F., and Jeandel, C. (2004). Neodymium isotopic composition and rare earth element concentrations in the deep and intermediate Nordic Seas: Constraints on the Iceland Scotland Overflow Water signature. *Geochemistry, Geophysics, Geosystems*, *5*(11), 1–10.

Lacan, F., and Jeandel, C. (2005). Acquisition of the neodymium isotopic composition of the North Atlantic Deep Water. *Geochemistry, Geophysics, Geosystems*, *6*(12), 1–20.

Lécuyer, C., Grandjean, P., Barrat, J.A., Emig, C.C., Nolvak, J., Paris, F., and Robardet, M. (1998). $\delta^{18}O$ and REE contents of phosphatic brachiopods: a comparison between modern and lower Paleozoic populations. *Geochimica et Cosmochimica Acta, 62*, 2429–2436.

Lécuyer, C., Reynard, B., and Grandjean, P. (2004). Rare earth element evolution of Phanerozoic seawater recorded in biogenic apatites. *Chemical Geology,* 204, 63–102.

Locarnini, R.A. (1994). Water masses and circulation in the Ross Gyre and environs. MS thesis. Texas A and M University, College Station. 87p.

Logan, A. (2007). Geographic distribution of extant articulated brachiopods. In: Selden, P. A. (ed.): Treatise on Invertebrate Paleontology, Part H (Revised), Brachiopoda, 6 (supplement), 3082–3115. The Geological Society of America and the University of Kansas, Boulder, Colorado and Lawrence, Kansas.

Lörz, A.N., Berkenbusch, K., Nodder, S., Ahyong, S., Bowden, D., McMillan, P., Gordon, Mills, S., and Mackay, K. (2012). A review of deep–sea benthic biodiversity associated with trench, canyon and abyssal habitats below 1500 m depth in New Zealand waters. New Zealand Aquatic Environment and Biodiversity Report No. 92. Ministry of Agriculture and Forestry, Wellington. 133p.

Magaldi, M.G., Haine, T.W.N., and Pickart, R.S. (2012). On the nature and variability of the East Greenland Spill Jet. *EGU General Assembly Conference Abstracts*, *14*, 13143.

Malmberg, S.A. (2004). The Iceland Basin: topography and oceanographic features. Marine Research Institute, *Reykjavik Report, 109*, 1–41.

Malmberg, S.A., and Valdimarsson, H. (2003). Hydrographic conditions in Icelandic waters, 1990–1999. *ICES Marine Science Symposia*, *219*, 50–60.

Matthews, J.E., and Holcombe, T.L. (1985). Venezuela Basin of the Caribbean Sea—Stratigraphy and sediment distribution. *Marine geology*, *68*(1), 1–23.

Matthias, T., and Godfrey J.S. (2003). Regional Oceanography: an Introduction 2nd edition. Elsevier.

McArthur, J.M., and Walsh, J.N. (1984). Rare–earth geochemistry of phosphorites. *Chemical Geology, 47*, 91–220.

McCartney, M.S., and Talley, L.D. (1984). Warm–to–cold water conversion in the northern North Atlantic Ocean. *Journal of Physical Oceanography*, *14*(5), 922–935.

McLennan, S.M. (1989). Rare earth elements in sedimentary rocks: influence of provenance and sedimentary processes. In: Lipin, B.R., McKay, G.A. (Eds.), Geochemistry and Mineralogy of Rare Earth Elements, *Mineralogical Society of America Review Mineralogy*, *21*, 169–200.

Metcalf, W.G. (1976). Caribbean-Atlantic water exchange through the Anegada-Jungfern passage. *Journal of Geophysical Research*, *81*(36), 6401–6409.

Mills, R.A., and Elderfield, H. (1995). Rare earth element geochemistry of hydrothermal deposits from the active TAG Mound, 26 N Mid–Atlantic Ridge. *Geochimica et Cosmochimica Acta*, *59*(17), 3511–3524.

Mitra, A., Elderfield, H., and Greaves, M.J. (1994). Rare earth elements in submarine hydrothermal fluids and plumes from the Mid–Atlantic Ridge. *Marine Chemistry*, *46*(3), 217–235.

Mortimer, N., Herzer, R.H., Gans, P.B., Laporte–Magoni, C., Calvert, A.T., and Bosch, D. (2007). Oligocene–Miocene tectonic evolution of the South Fiji Basin and Northland Plateau, SW Pacific Ocean: evidence from petrology and dating of dredged rocks. *Marine Geology*, *237*(1), 1–24.

Mortimer, N., Gans, P.B., Palin, J.M., Meffre, S., Herzer, R.H., and Skinner, D.N.B. (2010). Location and migration of Miocene–Quaternary volcanic arcs in the SW Pacific region. *Journal of volcanology and geothermal research*, *190*(1), 1–10.

Müller–Karger, F.E., McClain, C.R., Fisher, T.R., Esaias, W.E., and Varela, R. (1989). Pigment distribution in the Caribbean Sea: Observations from space. *Progress in Oceanography*, *23*(1), 23–64.

Neil, H.L., Carter, L., and Morris, M.Y. (2004). Thermal isolation of Campbell Plateau, New Zealand, by the Antarctic Circumpolar Current over the past 130 kyr. *Paleoceanography*, *19*(4), 1-17(PA4008).

Neuweiler, F., and Bernoulli, D. (2005). Mesozoic (Lower Jurassic) red stromatactis limestones from the Southern Alps (Arzo, Switzerland): calcite mineral authigenesis and syneresis–type deformation. *International Journal of Earth Sciences*, *94*(1), 130–146.

Nothdurft, L.D., Webb, G.E., and Kamber, B.S. (2004). Rare earth element geochemistry of Late Devonian reefal carbonates, Canning Basin, Western Australia: confirmation of a seawater REE proxy in ancient limestones. *Geochimica et Cosmochimica Acta*, *68*(2), 263–283.

Nozaki, Y. (2001). Rare Earth Elements and their Isotopes in the Ocean. Encyclopedia of Ocean Sciences, *4*, 2354–2366.

Nozaki, Y., and Alibo, D. (2003). Dissolved rare earth elements in the Southern Ocean, southwest of Australia: Unique patterns compared to the South Atlantic data. *Geochemical Journal*, *37*, 47–62.

Nozaki, Y., Zhang, J., and Amakawa, H. (1997). The fractionation between Y and Ho in the marine environment. *Earth and Planetary Science Letters*, *148*(1), 329–340.

Nozaki, Y., Alibo, D., Amakawa, H., Gamo, T., and Hasumoto, H. (1999). Dissolved rare earth elements and hydrography in the Sulu Sea, *Geochimica et Cosmochimica Acta*, *63*(15), 2171–2181.

Olivier, N., and Boyet, M. (2006). Rare earth and trace elements of microbialites in Upper Jurassic coral–and sponge–microbialite reefs. *Chemical Geology*, *230*(1), 105–123.

Orsi, A.H., and Wiederwohl, C.L. (2009). A recount of Ross Sea waters. *Deep Sea Research Part II: Topical Studies in Oceanography*, *56*(13), 778–795.

Orsi, A.H., Whitworth, T., and Nowlin, W.D. (1995). On the meridional extent and fronts of the Antarctic Circumpolar Current. *Deep Sea Research Part I: Oceanographic Research Papers*, *42*(5), 641–673.

Osborne, A.H., Haley, B.A., Hathorne, E.C., Flögel, S., and Frank, M. (2014). Neodymium isotopes and concentrations in Caribbean seawater: Tracing water mass mixing and continental input in a semi–enclosed ocean basin. *Earth and Planetary Science Letters*, *406*, 174–186.

Osborne, A.H., Haley, B.A., Hathorne, E.C., Plancherel, Y., and Frank, M. (2015). Rare earth element distribution in Caribbean seawater: Continental inputs versus lateral transport of distinct REE compositions in subsurface water masses. *Marine Chemistry, 177,* 172-183.

Pahnke, K., Van de Flierdt, T., Jones, K.M., Lambelet, M., Hemming, S.R., and Goldstein, S.L. (2012). GEOTRACES intercalibration of neodymium isotopes and rare earth element concentrations in seawater and suspended particles. Part 2: Systematic tests and baseline profiles. *Limnology and Oceanography: Methods*, *10*(4), 252–269.

Palmer, M.R. (1985). Rare earth elements in foraminifera tests. *Earth and Planetary Science Letters, 73*, 285–298.

Palmer, M.R., and Elderfield, H. (1986). Rare earth elements and neodymium isotopes in ferromanganese oxide coatings of Cenozoic foraminifera from the Atlantic Ocean. *Geochimica et Cosmochimica Acta*, *50*(3), 409–417.

Parkinson, D., Curry, G.B., Cusack, M., Fallick A.E. (2005). Shell structure, patterns and trends of oxygen and carbon stable isotopes in modern brachiopod shells. *Chemical Geology*, *219*, 193–235.

Pattan, J.N., Pearce, N.J.G., and Mislankar, P.G. (2005). Constraints in using Cerium–anomaly of bulk sediments as an indicator of paleo bottom water redox environment: A case study from the Central Indian Ocean Basin. *Chemical Geology*, *221*(3), 260–278.

Pedersen, S.A., Madsen, J., and Dyhr–Nielsen, M. (2004). Global International Waters Assessment. Arctic Greenland, East Greenland Shelf, West Greenland Shelf. *GIWA Regional assessment 1b,15,16*. University of Kalmar on behalf of United Nations Environment Program.

Picard, S., Lécuyer, C., Barrat, J.A., Garcia, J.P., Dromart, G., and Sheppard, S.M.F. (2002). Rare earth element contents of Jurassic fish and reptile teeth and their potential relation to seawater composition (Anglo–Paris Basin, France and England). *Chemical Geology*, *186*, 1–16.

Pichler, T., Veizer, J., and Hall, G.E. (1999). The chemical composition of shallow–water hydrothermal fluids in Tutum Bay, Ambitle Island, Papua New Guinea and their effect on ambient seawater. *Marine Chemistry*, *64*(3), 229–252.

Pickart, R.S., Spall, M.A., Ribergaard, M.H., Moore, G.W.K., and Milliff, R.F. (2003). Deep convection in the Irminger Sea forced by the Greenland tip jet.*Nature*, *424*(6945), 152–156.

Piepgras, D.J., and Jacobsen, S.B. (1992). The behavior of rare earth elements in seawater: Precise determination of variations in the North Pacific water column. *Geochimica et Cosmochimica Acta*, *56*(5), 1851–1862.

Raddatz, J., Rüggeberg, A., Liebetrau, V., Foubert, A., Hathorne, E. C., Fietzke, J., and Dullo, W. C. (2014). Environmental boundary conditions of cold–water coral mound growth over the last 3 million years in the Porcupine Seabight, Northeast Atlantic. *Deep Sea Research Part II: Topical Studies in Oceanography*, *99*, 227–236.

Richardson, M.D., and Young, D.K. (1987). Abyssal benthos of the Venezuela Basin, Caribbean Sea: standing stock considerations. *Deep Sea Research Part A. Oceanographic Research Papers*, *34*(2), 145–164.

Ridgway, K.R. (2007). Long-term trend and decadal variability of the southward penetration of the East Australian Current. *Geophysical Research Letters*,*34*(13), 1–16.

Rintoul, S.R. (2010). Antarctic circumpolar current. *Ocean Currents: A Derivative of the Encyclopedia of Ocean Sciences*, 196.

Rintoul, S.R., Sokolov, S., and Church, J.A. (2001). Ocean Circulation and Climate. *Observing and Modelling the Global Ocean*, Academic Press, 103.

Roberts, N.L., Piotrowski, A.M., Elderfield, H., Eglinton, T.I., and Lomas, M.W. (2012). Rare earth element association with foraminifera. *Geochimica et Cosmochimica Acta*, *94*, 57–71.

Roemmich, D., Gilson, J., Davis, R., Sutton, P., Wijffels, S., and Riser, S. (2007). Decadal spinup of the South Pacific subtropical gyre. *Journal of Physical Oceanography*, *37*(2), 162–173.

Schellart, W.P. (2007). North-eastward subduction followed by slab detachment to explain ophiolite obduction and Early Miocene volcanism in Northland, New Zealand. *Terra Nova*, *19*(3), 211–218.

Sholkovitz, E.R., and Schneider, D. L. (1991). Cerium redox cycles and rare earth elements in the Sargasso Sea. *Geochimica et Cosmochimica Acta*, *55*(10), 2737–2743.

Sholkovitz, E.R., and Shen, G.T. (1995). The incorporation of rare–earth elements in modern coral. *Geochimica et Cosmochimica Acta*, *59*, 2749–2756.

Smith, I.E., and Price, R.C. (2006). The Tonga–Kermadec arc and Havre–Lau back–arc system: their role in the development of tectonic and magmatic models for the western Pacific. *Journal of volcanology and geothermal research*, *156*(3), 315–331.

Smith, I.E., Worthington, T.J., Stewart, R.B., Price, R.C., and Gamble, J.A. (2003). Felsic volcanism in the Kermadec arc, SW Pacific: crustal recycling in an oceanic setting. *Geological Society, London, Special Publications*, *219*(1), 99–118.

Stanton, B., Roemmich, D., and Kosro, M. (2001). A shallow zonal jet south of Fiji. *Journal of physical oceanography*, *31*(10), 3127–3130.

Stein, M. (1988). Revision of list of NAFO standard oceanographic sections and stations. *NAFO SCR Doc*, *88*(01), 1–9.

Stein, M. (2005). North Atlantic subpolar gyre warming–impacts on Greenland offshore waters. *Journal of Northwest Atlantic Fishery Science,36*, 43–54.

Straneo, F. (2006). Heat and Freshwater Transport through the Central Labrador Sea*. *Journal of Physical Oceanography*, *36*(4), 606–628.

Straneo, F., Pickart, R.S., and Lavender, K. (2003). Spreading of Labrador Sea water: An advective–diffusive study based on Lagrangian data. *Deep Sea Research Part I: Oceanographic Research Papers*, *50*(6), 701–719.

Sutherland, D.A., and Pickart, R.S. (2008). The East Greenland coastal current: Structure, variability, and forcing. *Progress in Oceanography*, *78*(1), 58–77.

Sutton, P.J., and Roemmich, D. (2001). Ocean temperature climate off north-east New Zealand. *New Zealand Journal of Marine and Freshwater Research*,*35*(3), 553–565.

Sutton, P.J., Bowen, M., and Roemmich, D. (2005). Decadal temperature changes in the Tasman Sea. *New Zealand journal of marine and freshwater research*, *39*(6), 1321–1329.

Talley, L.D. (1999). Mode waters in the subpolar North Atlantic in historical data and during the WOCE period. *International WOCE Newsletter*, *37*, 3–6.

Talley, L.D. (2011). Descriptive physical oceanography: an introduction. Academic press.

Timm, C., de Ronde, C.E., Leybourne, M.I., Layton–Matthews, D., and Graham, I.J. (2012). Sources of Chalcophile and Siderophile Elements in Kermadec Arc Lavas. *Economic Geology*, *107*(8), 1527–1538.

Våge, K., Pickart, R.S., Moore, G.W.K., and Ribergaard, M.H. (2008). Winter mixed layer development in the central Irminger Sea: The effect of strong, intermittent wind events. *Journal of Physical Oceanography*, *38*(3), 541–565.

Våge, K., Pickart, R.S., Sarafanov, A., Knutsen, Ø., Mercier, H., Lherminier, P., van Aken, H.M., Meincke, J., Quadfasel, D., and Bacon, S. (2011). The Irminger Gyre: Circulation, convection, and interannual variability. *Deep Sea Research Part I: Oceanographic Research Papers*, *58*(5), 590–614.

Van Woert, M.L., Johnson, E.S., Langone, L., Worthen, D.L., Monaghan, A., Bromwich, D.H., Meloni, R., and Dunbar, R.B. (2003). The Ross Sea circulation during the 1990s. *Biogeochemistry of the Ross Sea*, 5–34.

Veizer, J., Ala, D., Azmy, K., Bruckschen, P., Buhl, D., Bruhn, F., Carden, G.A., Diener, A., Ebneth, S., Godderis, Y., Jasper, T., (1999). $^{87}Sr/^{86}Sr$, $\delta^{13}C$ and $\delta^{18}O$ evolution of Phanerozoic seawater. *Chemical geology, 161*(1), 59-88.

Warren, B.A., Whitworth, T., Moore, M.I., and Nowlin, W.D. (1994). Slight northwestward inflow to the deep South Fiji Basin. *Deep Sea Research Part I: Oceanographic Research Papers*, *41*(5), 953–956.

Webb, D.J. (2000). Evidence for shallow zonal jets in the South Equatorial Current region of the southwest Pacific. *Journal of Physical Oceanography*,*30*(4), 706–720.

Webb, G.E., and Kamber, B.S. (2000). Rare earth elements in Holocene reefal microbialites: a new shallow seawater proxy. *Geochimica et Cosmochimica Acta*, *64*(9), 1557–1565.

White, W.B., and Peterson, R.G. (1996). An Antarctic circumpolar wave in surface pressure, wind, temperature and sea–ice extent. *Nature*, *380*(6576), 699–702.

Whitworth III, T., Orsi, A.H., Kim, S.J., Nowlin, W.D., and Locarnini, R.A. (1998). Water masses and mixing near the Antarctic Slope Front. *Ocean, ice, and atmosphere: interactions at the Antarctic continental margin*, 1–27.

Whitworth III, T., Warren, B.A., Nowlin Jr, W.D., Rutz, S.B., Pillsbury, R.D., and Moore, M.I. (1999). On the deep western–boundary current in the Southwest Pacific Basin. *Progress in Oceanography*, *43*(1), 1–54.

Williams, R.T., Sarmiento, J.L., Rhines, P., Smethie, W.M., Rooth, C.G.H., Key, R.M., Takahashi, T., and Collins, C. (1986). Transient tracers in the ocean. Tropical Atlantic study, 1 December 1982–18 February 1983. Shipboard Physical and Chemical Data Report. *Physical & Chemical Oceanographic Data Facility, Scripps Institution of Oceanography*. University of California. (86–16), 310.

Wright, J., Seymour, R.S., and Shaw, H.F. (1984). REE and Nd isotopes in conodont apatite: variations with geological age and depositional environment. *Geological Society of America Special Papers*, *196*, 325–340.

Wright, J., Schrader, H., and Holser, W.T. (1987). Paleoredox variations in ancient oceans recorded by rare earth elements in fossil apatite. *Geochimica et Cosmochimica Acta*, *51*(3), 631–644.

Wüst, G. (1964). The major deep–sea expeditions and research vessels 1873–1960: a contribution to the history of oceanography. *Progress in Oceanography*,*2*, 1–52.

Wyrtki, K. (1961). The flow of water into the deep sea basins of the western South Pacific Ocean. *Marine and Freshwater Research*, *12*(1), 1–16.

Wyrtki, K. (1962). The subsurface water masses in the western South Pacific Ocean. *Marine and Freshwater Research*, *13*(1), 18–47.

Yashayaev, I. (2007). Hydrographic changes in the Labrador Sea, 1960–2005.*Progress in Oceanography*, *73*(3), 242–276.

Young, D.K., Jahn, W.H., Richardson, M.D., and Lohanick, A.W. (1985). Photographs of deep–sea lebensspuren: a comparison of sedimentary provinces in the Venezuela Basin, Caribbean Sea. *Marine geology*, *68*(1), 269–301.

Zaky, A.H., Brand, U., and Azmy, K., (2015). A new sample processing protocol for procuring seawater REE signatures in biogenic and abiogenic carbonates. *Chemical Geology*, *416*, 36-50.

Zezina, O.N. (2008). Biogeography of the recent brachiopods. *Paleontological Journal*, *42*(8), 830–858.

Zhang, J., and Nozaki, Y. (1996). Rare earth elements and yttrium in seawater: ICP–MS determinations in the East Caroline, Coral Sea, and South Fiji basins of the western South Pacific Ocean. *Geochimica et Cosmochimica Acta*, *60*(23), 4631–4644.

Zhang, Y., Lacan, F., and Jeandel, C. (2008). Dissolved rare earth elements tracing lithogenic inputs over the Kerguelen Plateau (Southern Ocean). *Deep–Sea Research II*, *55*, 638–652.

Zilberman, N.V., Roemmich, D.H., and Gille, S.T. (2013). The mean and the time variability of the shallow meridional overturning circulation in the tropical South Pacific Ocean. *Journal of Climate*, *26*(12), 4069–4087.

CHAPTER 4

RARE EARTH ELEMENTS OF SHALLOW-WATER ARTICULATED BRACHIOPODS: A BATHYMETRIC SENSOR

(*Palaeogeography, Palaeoclimatology, Palaeoecology* – Accepted manusript with moderat revision)

Amir H. Zaky[a], Uwe Brand[b], Karem Azmy[a], Alan Logan[c] and Jörundur Svavarsson[d]

[a] Department of Earth Sciences, Memorial University of Newfoundland, St. John's, NL, A1B 3X5 Canada.
[b] Department of Earth Sciences, Brock University, St. Catharines, ON, L2S 3A1 Canada.
[c] Centre for Coastal Studies, University of New Brunswick, Saint John, New Brunswick E2L 4 L5, Canada.
[d] Institute of Biology, University of Iceland, Askja, Sturlugata 7, 101 Reykjavík, Iceland.

ABSTRACT

Variations in environmental physicochemical parameters result in corresponding changes in seawater REE distributions. For an archive to be utilized in paleoceanographic and paleoenvironmental reconstructions, it must record oceanographic REE changes and variations.

Articulated brachiopods of several shallow water localities (<500 m) of different water masses were evaluated for their REE contents. The effects of the variation in modern oceanographic factors such as depth, salinity, and temperature were investigated on shells' REE uptake. The REE uptake of brachial and pedicle valves of articulated shells are equivocal, whereas shells of the *Thecideidines*, the umbo region and the primary layer of the *Terebratulids* are anomalous, and should be avoided. Temperature and salinity appear to have a minor impact on REE contents on shells from shallow-water settings.

The mean REE_{SN} pattern of shallow water brachiopods is remarkably different from that of their deep water counterparts, displaying less pronounced enrichments in LREEs and MREEs but greater depletions in HREE sections. Depth exercises a major control on LREE and MREE fractionation with a milder one on HREE fractionation. The Ce/Ce* anomaly is not affected by either of these parameters in shallow-water settings, but in deep settings the depth effect dominates. Due to the importance of depth on REE fractionation in the shells from shallow settings, their REE_{SN} determination for the bathymetric sensor was divided into six discrete intervals. This bathymetric sensor was applied to some fossils and whole rock in order to estimate their paleodepths. The evaluation was successful in placing the Permian Gyanyima, the Pennsylvanian Naco, Boggy and the Silurian Chicotte, Becscie and Jupiter formations in shallow depths (<15-50 m), which is very consistent with the paleoenvironmental settings (epeiric seas) suggested for those Paleozoic brachiopods.

4.1. Introduction

Ancient epeiric seas were widespread during the Phanerozoic and carbonate successions experienced a wide range of salinity, temperature and depth variations (c.f. Holmden et al., 1998). The accurate interpretation of paleo physico-chemical parameters requires evaluating the impact of prevalent environmental and oceanographic conditions on modern carbonate archives. Modern brachiopods are well suited for such purpose, in addition to their ubiquity, diversity and abundance in Phanerozoic strata, they secrete multi-layer shells of low Mg-calcite that are relatively resistant to diagenesis and proven to precipitate shells in isotopic equilibrium with their ambient seawater (cf. Carpenter and Lohmann, 1995; Parkinson et al., 2005; Brand et al., 2003, 2013, 2015). Meanwhile, their

modern representatives populate almost all latitudes, depths and salinities of seas and oceans from the Arctic to the Southern Ocean (Ruppert and Fox 2004; Logan, 2007; Zezina, 2008). However, only 30% of species inhabit depths below the neritic zone; thus they preferentially dwell in the first 200 m of the water column (Logan 2007). Their growth rate is generally slow and differ seasonally (e.g, Peck et al., 1986; Thayer, 1986), and their low metabolic rate and ability to consume stored proteins to fuel metabolism enable brachiopods to survive oligotrophic conditions (Shumway, 1982; Peck et al., 1986, 1987; Thayer, 1986; Peck and Holmes, 1990; James et al., 1992).

Fractionation and distribution of the naturally occurring 14 lanthanides of the rare earth element (REE) group in marine geochemical processes are governed primarily by their redox state and prevailing ambient oceanographic conditions (cf. de Baar et al., 1985 a, b, 1988; Nozaki, 2001). Consequently, they are used widely for modeling major oceanographic events, reconstructing paleoenvironmental settings, and investigating mass extinctions (cf. Lécuyer et al. 1998, 2003, 2004; Webb and Kamber 2000; Kemp and Trueman 2003; Garbelli et al. 2015). With the exception of Ce, which adopts a +4 oxidization state in well-oxygenated conditions, REEs occur essentially in the +3 state in seawater (cf. Elderfield et al., 1988, German et al., 1991, Holser, 1997).

Weathering of the continental crust is the ultimate source of REEs in the water reservoirs, whereas riverine discharge and atmospheric deposition are the primary fluxes (Greaves et al., 1994; Sholkovitz et al., 1999; Goldstein and Hemming, 2003; Hagedorn et al., 2011). The terrigenous source and mechanism of transportation impact mainly the REE contents and partly the distribution in the aquatic system (Nozaki, 2001; Alibo and Nozaki,

2004). In general, the ∑REE concentrations in fluvial water are notably higher than in seawater (Nozaki et al., 2000 a; Alibo and Nozaki, 2004). However, their extensive removal in low-salinity zones controls the riverine input into seawater (Sholkovitz et al., 1999; Sholkovitz and Szymczak, 2000; Lawrence and Kamber, 2006; Kulaksiz and Bau, 2007). In contrast to the fluvial flux, which enters oceans at the land-sea interface, winds are capable of transporting terrestrial REEs over long distances (Greaves et al., 1994; 1999). The fallout of the carried dust and its solubilization in seawater impacts the REE composition of surface waters in coastal areas as well as in the middle of the ocean (Nozaki, 2001). Erosion of volcanic islands, remineralization of bottom sediments and hydrothermal fluids from vent areas are potential sources of oceanic REEs; but are of lesser importance (Mills and Elderfield, 1995; Sholkovitz et al., 1999; Sholkovitz and Szymczak., 2000; Alibo and Nozaki, 2004). The common shale normalized (SN) pattern of open ocean seawater REEs exhibits gradual enrichments with increasing atomic number accompanied by a negative Ce excursion (Elderfield and Greaves, 1982; Goldstein and Jacobsen, 1988; Elderfield et al., 1988).

Although most shallow water biogenic archives (e.g. foraminifera, corals and microbialites) yield heavy REE_{SN} ($HREE_{SN}$) enrichment patterns (Palmer, 1985, Sholkovitz and Shen, 1995, Wyndham et al., 2004, Webb and Kamber, 2000; Haley et al. 2004), corals from low salinity, bivalves and stromatolites display significantly different REE_{SN} trends with middle REE (MREE) enrichments relative to the light REEs (LREEs) but slight to extensive depletions in HREEs (Akagi et al., 2004; Bau et al., 2010; Johannesson et al., 2014; Merschel and Bau, 2015; Ponnurangam et al., 2015). Meanwhile,

inorganic precipitates as well as non-lithogenic $CaCO_3$ particulates in seawater exhibit $HREE_{SN}$ depletion (Palmer, 1985, Palmer and Elderfield, 1986 and Kuss et al., 2001). In addition, the previous investigation on the REE incorporation by deep water articulated brachiopods showed that their carbonate yielded $LREE_{SN}$ and $MREE_{SN}$ characteristic of the ambient water masses but with significant variations in their $HREE_{SN}$ patterns (Zaky et al., 2016).

The main objectives of this study are to (1) assess the REE incorporation into shells of shallow-marine articulated brachiopods, (2) evaluate the effect of variation in physicochemical parameters such as temperature and salinity of their ambient environment on their REE distribution, and (3) establish parameters for interpreting paleoceanographic conditions such as changes with water depth.

4.2. Sample localities

The study involves modern shallow water (<500 m) articulated brachiopods recovered from eight localities; three of them are from Iceland (Norwegian and Irminger Seas, and the Denmark Strait), two from Canada (Bonne Bay and Bay of Fundy), one from the U.S.A. (Friday Harbor), and two from the Ross Sea (Antarctica; Fig. 4-1). Species, number of specimens, the coordinates of their locations, and their ambient seawater parameters (temperature, salinity and depth) are shown on Table 4-1.

The study also includes fossil brachiopod shells and whole rock samples (Table 4-1) from units 9, 8, 7 and 6 of the Uppermost Lopingian (Upper Permian) Gyanyima Formation of Tibet, China (Garbelli et al. 2015), Upper Desmoinsian (Middle Pennsylvanian) Naco Formation of Arizona, U.S.A. (Brand 1989b), Middle Desmoinesian

(Middle Pennsylvanian) Boggy Formation of Oklahoma, U.S.A. (Brand 1987, 1989a, 1991; Smith et al. 1994), and the Llandovery (Lower Silurian) Chicotte, Jupiter and Becscie formations of Anticosti Island, Quebec, Canada (Azmy et al. 1998, 2011). The Permian materials are adopted from Garbelli et al. (2015), while those of the Pennsylvanian and the Silurian are from Zaky et al. (2015). Their degrees of preservation were evaluated by the original authors. For the comparison aspect, the modern deep water articulated brachiopods of Zaky et al. (2016) are included in the environmental impact section along with the oceanic parameters of their water masses (Fig. 4-1).

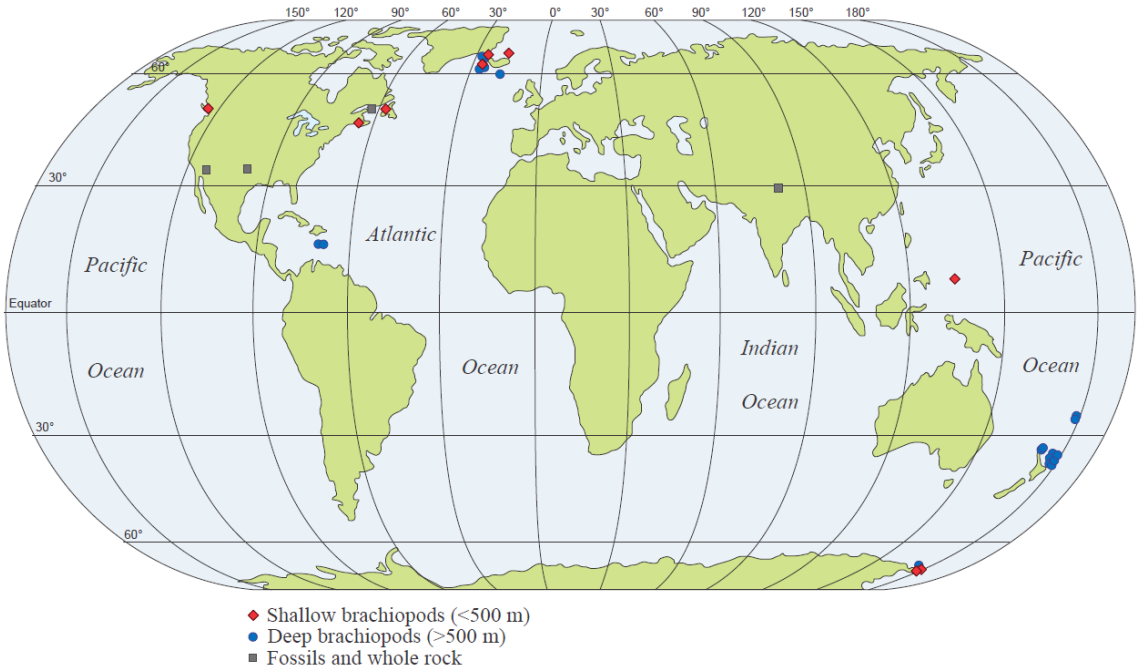

Figure 4-1. Locality diagram of the modern shallow (<500 m) and deep (>500 m; Zaky et al., 2016) water brachiopods, and fossil brachiopod and whole rock sample.

Table 4-1. Species, number of specimens, localities and ambient seawater parameters of temperature, salinity and depth for modern shells, or formation and epoch for the fossil shells.

Species	N	Depth [m]	Salinity [psu]	Temperature [°C]	Locality	Co-ordinates
Modern						
Macandrevia sp.	9*	353	34.7[d]	-1.5[d]	Ross Sea-1, Antarctica (St. E188)	72.17919° S, 170.80670° E
Macandrevia cranium	4*	318.1-316.5	34.63	0.71	Denmark Strait, Iceland (St. 1132)	67.64133° N, 26.75467° W
	4*	315.9-316.6	34.85	1.36	Norwegian Sea, Iceland (St. 1209)	66.53816° N, 12.86483° W
	28*	213.9-224.9	35.19	7.42	Irminger Sea, Iceland (St. 1043)	63.92433° N, 25.96100° W
Magellania joubini	6*	130	34.55[d]	-1.2[d]	Ross Sea-2, Antarctica (St. TAN0402/47)	72.31533° S, 170.36099° E
Terebratalia transversa	6*	85	30.5	8	Friday Harbour, Washington	48.54825° N, 122.98485° W
Terebratulina septentrionalis	12*	10-15	32.2	6.2	Bay of Fundy, New Brunswick	45.0207° N, 66.91162° W
	13*	30	31.1	5.6	Bonne Bay, Newfoundland	49.50965° N, 57.86893° W
Thecidellina congregata	4*	2	34.4	29.5	Philippine Sea, Palau	7.28397° N, 134.38057° E
		Formation		**Epoch**		
Fossil						
Late Permian						
Costiferina indica	2[a]	Units 7 & 8, Gyanyima		Latest Lopingian	Tibet, China	30.71067° N, 80.6951° E
C. spiralis	1[a]	Unit 8, "		"	"	"
Dielasma sp.	1[a]	Unit 6, "		"	"	"
Marginalosa sp.	1[a]	Unit 9, "		"	"	"
Martinia sp.	1[a]	Unit 7, "		"	"	"
Neospirifer sp.	1[a]	Unit 6, "		"	"	"
Permophricodothyris sp.	2[a]	Units 6 & 7, "		"	"	"
Richthofenia lawrenciana	1[a]	Unit 6, "		"	"	"
Middle Pennsylvanian						
Composita subtilita	3[b]	Naco		Late Desmoinsian	Arizona, USA	34.3261°N, 111.1140°W
Marginifera muricatina	3[b]	Boggy		Middle Desmoinesian	Oklahoma, USA	34.4456°N, 96.9614°W
Early Silurian						
Gotatrypa gibbosa	2[b,c]	Chicotte		Llandovery	Quebec, Canada	49.3631°N, 62.8344°W
Gotatrypa sp.	6[b,c]	Jupiter		"	"	49.3128°N, 62.8750°W &
	5[b]					49.3631°N, 62.8344°W
Virgiana barrandii	1[b]	Becscie		"	"	49.3631°N, 62.8344°W

Note: (N) number of samples.
*: new data in this study.
[a]: from Zaky et al. (2015).
[b]: from Garbelli et al. (2015).
[c]: from Azmy et al. (2011).
[d]: from Jacobs and Giulivi (1999)

4.3. Methodology

With the exception of those included in the protocol assessment and sample evaluation sections, cleaning of the investigated shells followed the protocol of Zaky et al. (2015). In summary, pedicles, organic tissue, proteinous periostracum and adhered inorganic particulate matter were eliminated using an acid washed sharp stainless-steel blade. Other organic remnants, including encrusting epibionts and organic nano-particulates in shell punctuate, were removed by submerging specimens in 2.5% hydrogen peroxide for three days. Potential inorganic surface contaminants and the primary layers were removed by leaching the shells in dilute hydrochloric acid (10%) for 10-30 seconds. Subsequently, all specimens were washed with de-ionized water and air-dried at room temperature.

The specimens were powdered in a small agate mortar, and 10 mg of each (weighed to four decimals) were placed in an acid washed test tube, spiked with a single drop of 8N HNO_3 then digested for a whole week in 10 mL distilled 0.2N HNO_3. From each sample solution, 2 mL were separated using an acid washed automatic pipette, diluted in another 3mL of 0.2N HNO_3 and analyzed for its trace element and REE contents using a Perkin Elmer Sciex inductively coupled plasma mass spectrometer (ICP-MS) at the CREAIT facility of Memorial University of Newfoundland. Relative uncertainties of the measurements compared to internal (Indium) and standard (DLS 88a and CCH-1) are better than 5%.

Concentrations of REEs were shale normalized (SN) to the Post-Archean Australian Shale (PAAS) values of McLennan (1989), whereas Ca, Mg, Mn, Fe and U were adjusted

to a 100% carbonate basis (cf. Brand and Veizer, 1980). The enrichment and/or the depletion in $HREE_{SN}$ (Ho to Lu) relative to $LREE_{SN}$ (La to Nd) and $MREE_{SN}$ (Sm to Dy), as well as in the $MREE_{SN}$ relative to $LREE_{SN}$ were quantified using the $LREE_{SN}$ to $HREE_{SN}$ (L:H), MREE $_{SN}$ to $HREE_{SN}$ (M:H) and $LREE_{SN}$ to $MREE_{SN}$ (L:M) ratios, respectively (e.g., Zaky et al., 2016). They have been calculated by dividing the sum of the $LREE_{SN}$ values in the (L:H) or the $MREE_{SN}$ in the (M:H) to those of the $HREE_{SN}$, while in the (L:M) by dividing the sum of the $LREE_{SN}$ values to those of the $MREE_{SN}$. Cerium was eliminated from the calculation due to its tendency to vary in response to changing in redox conditions. Because of the total number of elements in the MREE or the HREE groups is 5 while in the LREE group after excluding the Ce is 3, the sum of the $HREE_{SN}$ in the (L:H) and $MREE_{SN}$ in the (L:M) formulas were multiplied by 3/5 to equalize the equations. The ratios are inversely proportional to the enrichments; values higher than unity indicate depletion. The Ce excursion was evaluated by calculating the Ce anomaly (Ce/Ce^{*}) using the de Baar et al. (1988) equation;

$$Ce/Ce^{*}=[3(Ce_{Sample}/Ce_{Shale})] / [(2La_{Sample}/La_{Shale})+(Nd_{Sample}/Nd_{Shale})].$$

4.4. Protocol reproducibility assessment

Recently, a new sample processing protocol for acquiring robust REE signals from calcite archives was proposed by Zaky et al. (2015). The protocol was based on modern brachiopod specimens from deep waters (>500 m) of open ocean settings and tested on some Palaeozoic shells and whole rock. In contrast, most fossil archives lived in shallow water habitats in epeiric seas and it is therefore crucial to evaluate its reproducibility and consequently confirm its validity on specimens populating analogous modern shelf

environments. Accordingly, four of the five procedures (P-1, P-2, P-3 and P-5) were applied to 6 whole *M. cranium* shells dredged alive from depths between 213.9 and 224.9 m on the Irminger Sea shelf (North Atlantic).

The Mn, Fe, U and particularly the ∑REEs, LREEs and MREEs are remarkably elevated in the P-1 segments compared with segments of other cleaning procedures (Fig. 4-2; Table 4-2). They disclose a nearly flat REE_{SN} pattern that gets depleted slightly after Gd and remarkably after Dy (Fig. 4-2). Meanwhile, their mean Ce excursion is in the opposite direction (positive excursion) to that of their ambient seawater with an average Ce/Ce* value of 1.15 (Fig. 4-2). The P-2 and P-3 segments yielded remarkable depletions in the concentrations of the ∑REEs in general and LREEs in particular but slight depletions in Mn, U and MREEs and HREEs with Fe concentrations are still significantly elevated only in the P-2 in comparison with corresponding values in the P-1 fragments (Fig. 4-2; Table 4-2). The REE_{SN} patterns of the P-2 and P-3 segments display gradual enrichments in the LREE and MREE sections followed by depletions in the HREE (Fig. 2). However, the magnitudes of the enrichments on the two patterns are different; they are less pronounced on that of P-3 (Fig. 2). Their Ce excursions, on the other hand, are crucially different; they diverge in direction contradicts with that of P-1, but coincides with those of the ambient Subpolar Mode Water (negative excursion; Fig. 4-2). On the other hand, the excursion magnitudes differ significantly from slightly flat in P-3 (Ce/Ce*= 0.91) to remarkably negative in P-2 segments (Ce/Ce*= 0.59; Fig. 2; Table 2). Segments of P-5 yielded remarkable depletions in their Fe, Mn. U, LREE, MREE and HREE concentrations relative to the other segments. Their mean Ce excursion diverges in the same direction of

that of the Subpolar Mode Water, with relatively comparable amplitude to those of P-2 (Ce/Ce*= 0.55; Fig. 4-2; Table 4-2).

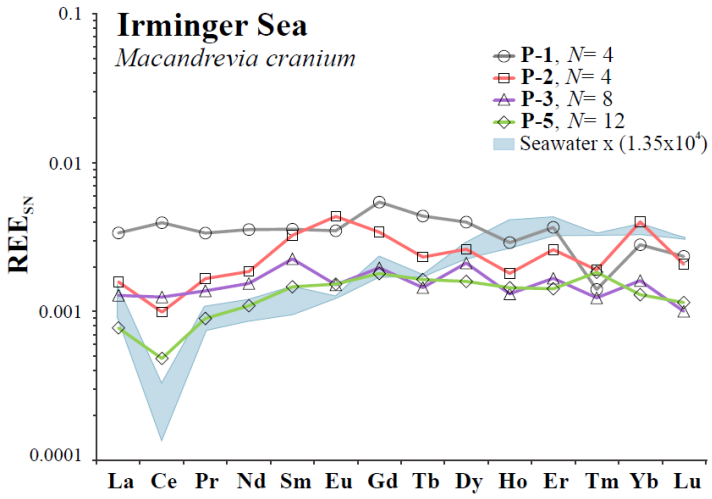

Figure 4-2. Average REE_{SN} patterns of the four cleaning procedures of the Irminger Sea's *Macandrevia cranium* shells and the Subpolar Mode Water (blue shaded area) represented by composite of the REE contents in stations 8, 9, 14, 15 and 16 in the Irminger Sea multiplied by 10^4 and normalized to PAAS (20-401 m, *n*= 10 samples; Lacan and Jeandel, 2005).

The LREEs and MREEs are scavenged fundamentally from the water column by the adsorptive particulate matters of Mn, Fe and U oxides (de Baar et al. 1988; Elderfield et al., 1990), whereas Ce is scavenged basically by the organically-coated particulates and organic matter (Haley et al. 2004). The non-removal of the sinking inorganic particulates attached to the shells' surfaces increased significantly the REE compositions of the P-1 segments, particularly their LREEs and MREEs. Meanwhile, the adsorbed REEs and the accumulated particulates on the shells' proteinous periostracum, the encrusting organisms and the organic remnants enhanced generally their REE compositions and overprinted their Ce contents (Fig. 4-2). Immersing the specimens in H_2O_2 for 3 continuous days successfully eliminated the periostracum and the other organic remnants, which have caused remarkable reduction in the REE concentrations and Ce anomalies of the P-2 segments. However, the adhered inorganic particulates (particularly the Fe oxides nano-particulates) caused the

abrupt elevation in their MREEs and LREEs (Fig. 4-2; Table 4-2). Scrapping the shells mechanically with a sharp stainless-steel blade eliminated fundamentally the adhered inorganic particulate matters and a notable percentage of the periostracum, which in turn depleted the Fe contents and the MREEs of the P-3 segments relative to those of the P-2. However, residues of the periostracum as well as the organically-coated particulates within the shells' punctuates deceptively enhanced their Ce excursions and consequently raised their Ce anomalies, while the presence of the primary layer increased their LREEs and MREEs slightly relatively to those of P-5 (Fig. 4-2; Table 4-2). Hydrochloric acid immersion dissolved mainly the shells' outer layer "primary layer" along with the surface-attached contaminants. Although it depleted slightly the Mn, Fe and U contents of P-5 segments relative to those of P-3, it reduced remarkable their LREEs and consequently their ∑REE concentrations (Fig. 4-2; Table 4-2).

Also, it is necessary to visualize differences between REE patterns of cleaned (P-5) and non-cleaned specimens of the other localities. We evaluated procedures P-1, P-3 and P-5 on *T. septentrionalis* from Bonne Bay and the Bay of Fundy (Fig. 4-3). The P-1 and P-3 specimens of the two localities yielded higher Fe, Mn and REE contents, and slightly to significantly different REE_{SN} patterns relative to their P-5 (Fig. 4-3; Table 4-2).

Specimens from Bonne Bay and Bay of Fundy were recovered alive from their habitats, and organic matter and periostracum membranes were removed right after collection. The absence of organic remnants, which scavenge Ce from seawater (Haley et al. 2004), explains the downward Ce excursion (Fig. 4-3) and negative Ce anomalies of the P-1 and P-3 specimens. The results confirm that P-5 is the optimal cleaning procedure for

acquiring robust REE signatures from calcite archives. The similarity between the outcome of this evaluation task and that of Zaky et al. (2015) emphasizes the reliability and reproducibility of the proposed cleaning protocol, and its applicability on specimens from significantly different settings.

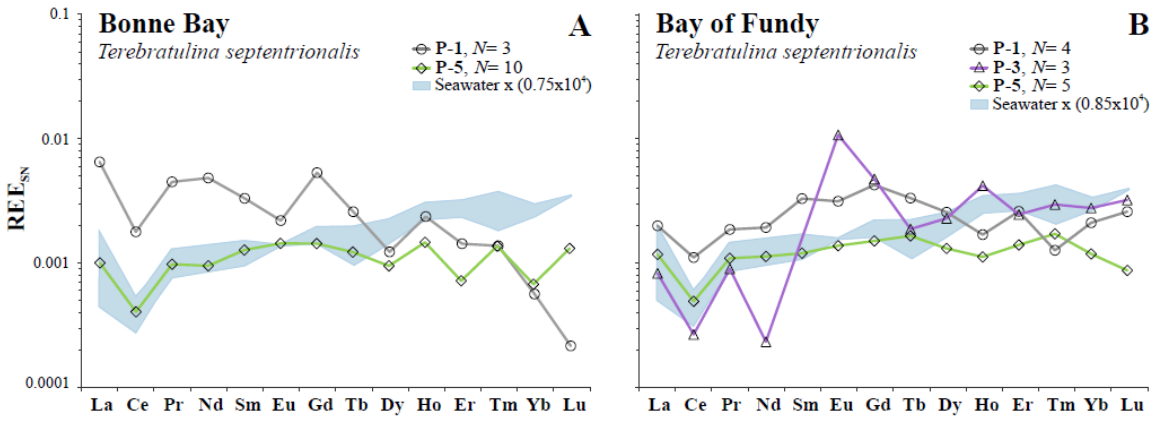

Figure 4-3. Average REE_{SN} patterns of the uncleaned (P-1 and P3) and cleaned (P-5) *Macandrevia cranium* shells from Bonne Bay (A) and Bay of Fundy (B) relative to the Subpolar Mode Water of the Irminger Sea (blue shaded area) represented by composite of the REE contents in stations 4, 5 and 6 (7-26 m, *n*= 4 samples; Lacan and Jeandel, 2004), values are normalized to PAAS and multiplied by 10^4.

4.5. Results

The trace element and REE concentrations in the modern shells from the different localities are listed in Appendix 4-1, their statistics are summarized in Appendix 4-2, and the geochemical compositions of the Paleozoic fossils and whole rock are presented in Appendix 4-3.

4.5.1. ∑REE concentrations

The P-5 fragments from the nine localities yielded low ∑REE contents in comparison to deep water counterparts (>500 m; Zaky et al., 2016). Shells from the Philippine Sea have the lowest ∑REE concentrations of 0.01 ppm, whereas those from the

Ross Sea-2 have the highest concentrations of 0.30 ppm (Table 4-2). On the other hand, specimens from the Denmark Strait, Norwegian Sea, Irminger Sea, Bonne Bay, Friday Harbor, Bay of Fundy and Ross Sea-1 have comparable concentration ranges (0.10 to 0.19 ppm, Table 4-2).

Shallow water brachiopods incorporate higher concentrations of REEs into their crystal lattice relative to ambient seawater. Such enrichments were quantified by correlating the average ∑REE concentrations of the shells (Table 4-2) to those of their nearby seawater (Table 4-3). However, due to variations in Ce and HREE concentrations in the brachiopod calcite in response to corresponding changes in environmental conditions such as dissolved oxygen and depth, they were excluded from the calculations (cf. Zaky et al., 2016).

Specimens from the Ross Sea-2 yielded the highest REE enrichments of $2.5x10^4$ (Fig. 4-4), whereas those from the Philippine Sea, Bonne Bay and Bay of Fundy had the lowest enrichments of 0.65, 0.75 and 0.85 x (10^4), respectively (Figs. 4-3, 4-5). Those of Friday Harbor, Irminger Sea, Denmark Strait, Norwegian Sea and Ross Sea-1 had intermediate enrichments of 1.05, 1.35, 1.65, 1.8 and 1.85 x (10^4), respectively (Figs. 4-2, 4-4, 4-5).

4.5.2. REE_{SN} patterns

The P-5 segments of the different localities display gradual $HREE_{SN}$ enrichment patterns with L:H ratios consistently less than unity (Table 2). However, the magnitudes of their enrichments are distinctly smaller than those of their nearby seawater (Table 3) or those of their deep-water counterparts (>500m; Zaky et al., 2016). The enrichments are less

pronounced in the specimens of Bonne bay, Friday Harbour, Bay of Fundy, and Ross Sea-2 (0.882, 0.797, 0.900 and 0.724), moderately pronounced in those of Denmark Strait, Norwegian Sea, Irminger Sea, and Ross Sea-1 (0.598, 0.564, 0.645 and 0.518), but well pronounced in the Philippine Sea samples (0.121; Table 2).

The magnitude of the $MREE_{SN}$ enrichments relative to the $LREE_{SN}$ varies between the shells of the different locations. The P-5 specimens of the Denmark Strait, Norwegian, Irminger and Philippine Seas and Ross Sea-1 yielded moderate L:M ratios (0.574, 0.544, 0.574, 0.451, 0.565 and 0.583), while those of Bonne Bay, Friday Harbour and Bay of Fundy yielded elevated ratios (0.773, 0.694 and 0.803; Table 2). With the exception of those of the Philippine Sea and Ross Sea-2, which display gradual $HREE_{SN}$ enrichments relative to the $MREE_{SN}$ (M:H= 0.267 and 0.916; Table 2), all the P-5 samples of the other localities display depletions in their M:H ratios. However, the depletion magnitudes vary; they are prominent in those of the Irminger Sea, Bonne Bay, Friday Harbour, Bay of Fundy and Ross Sea-2 (M:H= 1.123, 1.140, 1.147, 1.120 and 1.242), but less obvious in those of the Denmark Strait and Norwegian Sea (M:H= 1.042, 1.037; Table 2).

Only the P-5 shells of the Philippine Sea yielded gradual enrichment $HREE_{SN}$ pattern (Fig. 5A), that is insignificantly different from those of their ambient Tropical Surface Water (L:H= 0.190, L:M= 0.345 and M:H= 0.550; Table 3). Those of the Irminger Sea, the Denmark Strait, the Norwegian Sea and Ross Sea-1 display gradual $LREE_{SN}$ and $MREE_{SN}$ enrichments similar to those of their ambient water masses of the Subpolar Mode Water in the Irminger Sea, Iceland Sea Arctic Intermediate Water and the Low-oxygenated Upper Circumpolar Water (L:M= 0.584, 0.491 and 0.580, respectively; Figs. 2, 4; Table

3). But, in contradict to their water masses' $HREE_{SN}$ enrichment patterns (L:H= 0.304, 0.259 and 0.211, and M:H= 0.519, 0.527 and 0.365; respectively), they display slight $HREE_{SN}$ depletions on their patterns (Figs. 2, 4; Table 3). On the other hand, the P-5 specimens of Bonne Bay, Bay of Fundy, Friday Harbour and Ross Sea-2 disclose relatively flat REE_{SN} patterns, whereas their ambient water masses of the Subpolar Mode Water in the Labrador Sea and west of the North Atlantic, Pacific Subarctic Upper Water and Antarctic Surface Water disclose gradual $HREE_{SN}$ enrichment patterns with significantly depleted L:H (0.380, 0.334 and 0.221), L:M (0.663, 0.550 and 0.581) and M:H values (0.574, 0.608 and 0.380, respectively; Figs.3, 4, 5; Table 3).

Table 4-2. The mean Mn, Fe, U and the REE concentrations (in ppm), and L:H, L:M, M:H and Ce/Ce* values in the samples of the different cleaning procedures. Trace element results were normalized to a 100 % carbonate basis (cf. Brand and Veizer, 1980).

Procedure	N	Mn	Fe	U	LREEs	MREEs	HREEs	L:H	L:M	M:H	∑REEs	Ce/Ce*
Denmark Strait, Iceland												
P-5	4	33.8	140.5	0.015	0.122	0.029	0.013	0.60	0.57	1.04	0.15	0.44
Norwegian Sea, Iceland												
P-5	4	41.2	50.0	0.015	0.146	0.036	0.016	0.56	0.54	1.04	0.19	0.52
Irminger Sea, Iceland												
P-1	4	50.5	706.3	0.032	0.599	0.072	0.023	1.31	0.82	1.59	0.69	1.15
P-2	4	45.7	1,057.2	0.021	0.219	0.053	0.022	0.69	0.53	1.29	0.28	0.59
P-3	8	20.9	40.8	0.017	0.215	0.035	0.012	1.03	0.75	1.36	0.25	0.91
P-5	12	14.0	15.6	0.013	0.114	0.027	0.010	0.65	0.57	1.12	0.14	0.55
Bonne Bay, Newfoundland												
P-1	3	13.4	502.3	0.009	0.595	0.053	0.009	4.44	1.80	2.46	0.65	0.39
P-5	10	6.4	6.3	0.015	0.111	0.021	0.007	0.88	0.77	1.14	0.13	0.41
Friday Harbour, Washington												
P-5	5	39.1	49.8	0.018	0.082	0.017	0.007	0.80	0.69	1.15	0.10	0.42
P-5 (Umbo)	1	22.7	56.5	0.010	0.017	0.004	0.002	0.13	0.23	0.57	0.02	0.64
Bay of Fundy, New Brunswick												
P-1	4	26.0	427.4	0.026	0.247	0.056	0.017	0.94	0.58	1.62	0.31	0.56
P-3	3	9.2	13.0	0.006	0.068	0.046	0.022	0.21	0.13	1.58	0.10	0.28
P-5	5	9.0	18.2	0.016	0.132	0.023	0.010	0.90	0.80	1.12	0.16	0.42
Philippine Sea, North Pacific Ocean												
P-5	3	2.7	66.3	0.025	0.009	0.002	0.003	0.12	0.45	0.27	0.01	0.58
P-5 (Umbo)	1	7.3	63.8	0.065	0.019	0.003	0.005	0.15	0.15	1.01	0.03	0.77
Ross Sea-1, Antarctica												
P-5	9	63.6	27.3	0.009	0.144	0.035	0.015	0.52	0.57	0.92	0.18	0.40
Ross Sea-2, Antarctica												
P-5	6	58.2	40.2	0.017	0.237	0.051	0.020	0.72	0.58	1.24	0.30	0.64

Note: (N) number of samples.
(Av.) Average.
(Std.) standard deviation.
LREEs= Sum of La:Nd concentrations.
MREEs= Sum of Sm:Dy concentrations.
HREEs= Sum of Ho:Lu concentrations.
L:H = Sum of $(LREEs)_{SN}$ / 3/5 Sum of $(HREEs)_{SN}$.
L:M = Sum of $(LREEs)_{SN}$ / 3/5 Sum of $(MREEs)_{SN}$.
M:H = Sum of $(MREEs)_{SN}$ / Sum of $(HREEs)_{SN}$.

Table 4-3. Mean REE concentrations (in ppm x 10^5), and L:H, L:M, M:H and Ce/Ce* values in water masses.

Water Mass	LREEs	MREEs	HREEs	L:H	L:M	M:H	∑REEs	Ce/Ce*		
								Av.	Max.	Min.
Subpolar Mode Water in the Irminger Sea[1]	0.768	0.230	0.201	0.30	0.58	0.52	1.20	0.18	0.25	0.14
Iceland Sea Arctic Intermediate Water[2]	0.752	0.236	0.204	0.26	0.49	0.52	1.19	0.25	0.31	0.20
Subpolar Mode Water in the Labrador Sea and west of the North Atlantic[3]	1.570	0.343	0.265	0.38	0.66	0.57	2.18	0.38	0.51	0.31
Pacific Subarctic Upper Water[4]	0.930	0.231	0.167	0.33	0.55	0.61	1.33	0.33	0.60	0.10
Tropical Surface Water in the Pacific Ocean[5]	0.170	0.070	0.059	0.19	0.35	0.55	0.30	0.38	1.28	0.13
Antarctic Surface Water[6]	0.693	0.187	0.216	0.22	0.58	0.38	1.10	0.20	0.42	0.07
Low-oxygenated Upper Circumpolar Water[7]	0.681	0.192	0.230	0.21	0.58	0.37	1.10	0.15	0.15	0.07

Note: (N) number of samples.
(Av.) Average.
(Std.) standard deviation.
LREEs= Sum of La:Nd concentrations.
MREEs= Sum of Sm:Dy concentrations.
HREEs= Sum of Ho:Lu concentrations.
L:H = Sum of $(LREEs)_{SN}$ / 3/5 Sum of $(HREEs)_{SN}$.
L:M = Sum of $(LREEs)_{SN}$ / 3/5 Sum of $(MREEs)_{SN}$.
M:H = Sum of $(MREEs)_{SN}$ / Sum of $(HREEs)_{S\,N}$.
[1]: Composite of stations 8, 9, 14, 15 & 16 in the Irminger Sea (20-401 m, *n*= 10 samples; Lacan and Jeandel, 2005).
[2]: Composite of stations 20 & 21 in the Norwegian Sea (20-331 m, *n*= 3 samples; Lacan and Jeandel, 2005).
[3]: Composite of stations 4, 5 & 6 in the Labrador Sea (7-26 m, *n*= 4 samples; Lacan and Jeandel, 2004).
[4]: Composite of stations SAP ssw-8, 9, 10, 11, 12, 13 and 14, YERTEX II & Saanich Inlet in the west North Pacific and fjords of British Columbia (3-400 m, *n*= 33 samples; de Baar et al., 1985; German and Elderfield 1989; Hongo et al., 2006).
[5]: Composite of stations 5, 7 &12 in the South Pacific Ocean (0-200 m, *n*= 14 samples; Zhang and Nozaki 1996).
[6]: Composite of stations C1, C5, C11, B1, B5, B11, A3, A3', A11 & KERFIX in the Southern Ocean (0-200 m, *n*= 45 samples; Zhang et al., 2008).
[5]: Composite of stations C5, C11, B1, B5, B11, A3, A3', A11 & KERFIX in the Southern Ocean (200-480 m, *n*= 21 samples; Zhang et al., 2008).

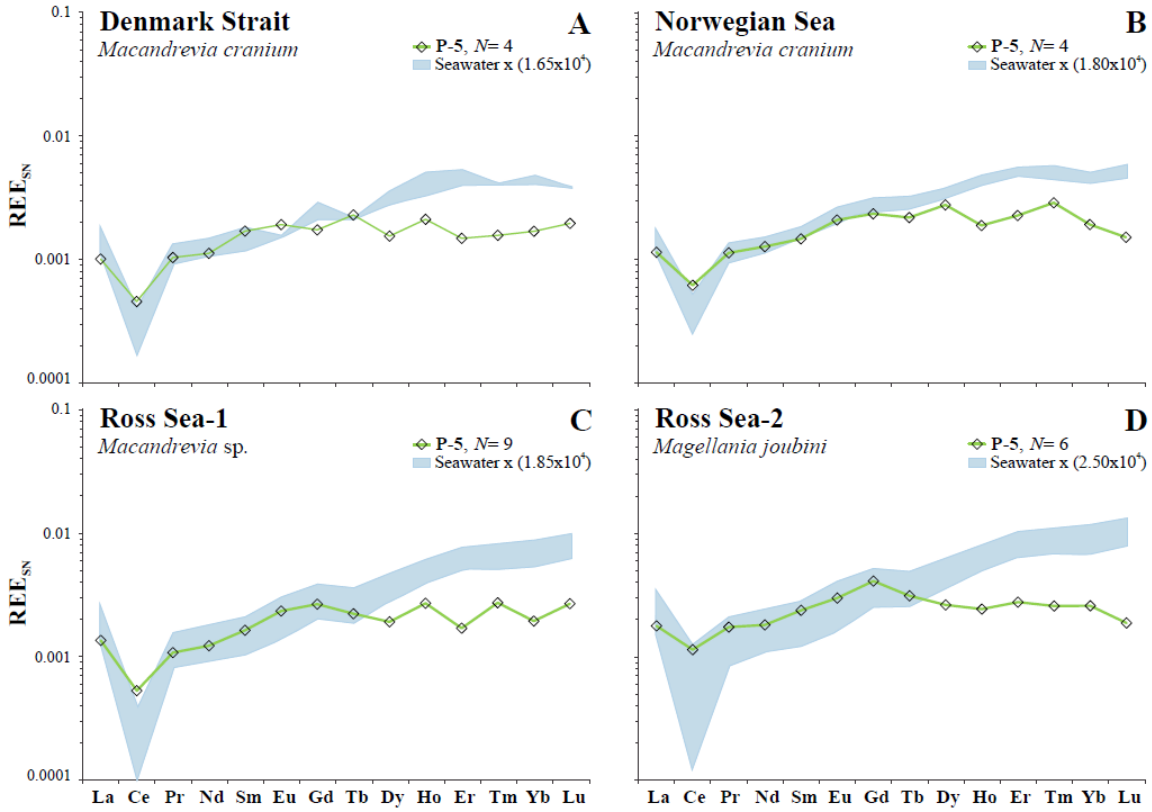

Figure 4-4. Average REE_{SN} patterns of the P-5 cleaned brachiopods and their ambient water masses (blue shaded areas). *Macandrevia cranium* shells of the Denmark Strait (A) and the Norwegian Sea (B) relative to Subpolar Mode Water and Iceland Sea Arctic Intermediate Water, respectively. *Macandrevia* sp. shells (C) and the Low-oxygenated Upper Circumpolar Water. *Magellania joubini* shells (D) and the Antarctic Surface Water. The REE contents of the Denmark Strait are from stations 8, 9, 14, 15 and 16 in the Irminger Sea (20-401 m, *n*= 10 samples; Lacan and Jeandel, 2005), those of Norwegian Sea are from stations 20 and 21 in the Norwegian Sea (20-331 m, *n*= 3 samples; Lacan and Jeandel, 2005), while those of the Ross Sea -1 and -2 are from stations C5, C11, B1, B5, B11, A3, A3', A11 and KERFIX (200-480 m, *n*= 21 samples; Zhang et al., 2008) and C1, C5, C11, B1, B5, B11, A3, A3', A11 and KERFIX (0-200 m, *n*= 45 samples; Zhang et al., 2008) in the Southern Ocean, respectively; values are normalized to PAAS and multiplied by 10^4.

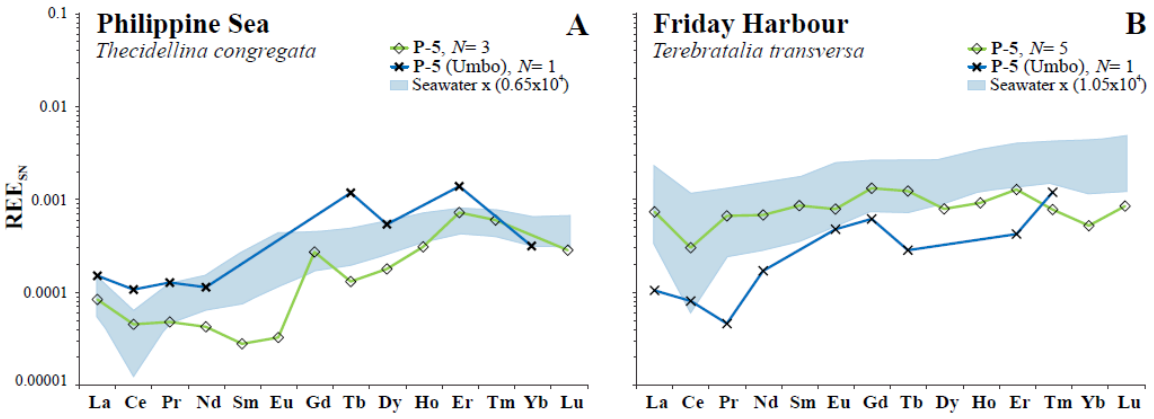

Figure 4-5. Average REE_{SN} patterns of the P-5 cleaned *Thecidellina congregata* (A) and *Terebratalia transversa* (B) shells and their umbo regions recovered from the Philippine Sea and Friday Harbor, respectively, relative to the Tropical Surface Water (A) and the Pacific Subarctic Upper Water (B). The REE contents of the Philippine Sea seawater are from stations 5, 7 and 12 in the South Pacific Ocean (0-200 m, *n*= 14 samples; Zhang and Nozaki 1996), while those of Friday harbor are from stations SAP ssw-8, 9, 10, 11, 12, 13 and 14, YERTEX II and Saanich Inlet in the west North Pacific and fjords of British Columbia (3-400 m, *n*= 33 samples; de Baar et al., 1985; German and Elderfield 1989; Hongo et al., 2006), values are normalized to PAAS and multiplied by 10^4.

4.5.3. Ce/Ce*

The P-5 specimens from the Ross Sea-2 and the Philippine Sea yielded the highest Ce/Ce* averages of 0.64 and 0.58 whereas those of the Ross Sea-1 yielded the lowest average of 0.40 (Table 4-2). Specimens from the Denmark Strait, Bonne Bay, Friday Harbor and Bay of Fundy yielded relatively similar Ce anomalies with averages of 0.44, 0.41, 0.42 and 0.42, respectively, while those of the Norwegian and Irminger Seas have slightly elevated averages of 0.52 and 0.55 (Table 4-2).

Overall, shallow-water brachiopod Ce/Ce* are representative of their respective ambient seawater. Cerium anomalies of specimens from the different localities are consistently negative, but slightly higher than those of their modern deep-water

counterparts (>500 m; Zaky et al., 2016) and their nearby seawater (Table 4-3). However, ambient water masses at shallow depths display high variations in Ce anomalies with values sometimes higher than those of the brachiopods shells.

4.6. Discussion

4.6.1. Species variation

With the exception of *Thecidellina congregata* which belong to the order Thecideida, the species *Macandrevia* sp., *M. cranium*, *Magellania joubini*, *Terebratalia transversa* and *Terebratulina septentrionalis* belong to the order Terebratulida.

The partition coefficient values of the investigated shallow water (<500 m) shells are summarized in Appendix 4-4. They were calculated using Palmer (1985) and Haley et al. (2005) equations assuming 10.46 mmol/L Ca for all water masses (Haley et al., 2005). The log K_D values of the shallow water (<500 m) *Terebratulida* are depleted relative to those of their deep water (>500 m) counterparts (Table 4-4). However, they exhibit the same incorporation pattern but with slight depletions in the HREEs (Fig. 4-6A). This in turn, confirms the previous suggestion that the ionic radii control the REE incorporation into the calcitic lattice of the articulated brachiopod shells, while the HREEs are impacted by the gradual increase in the amount of their free ions with depth (Zaky et al., 2016).

Table 4-4. The partion coefficients of REE in the calcite lattice of Terebratulida, and Rhynchonellida orders, and the different shell structure of *M. cranium, T. transversa, T. septentrionalis* and *T. congregata* species.

	La	Ce	Pr	Nd	Sm	Eu	Gd	Tb	Dy	Ho	Er	Tm	Yb	Lu
log K_D														
Terebratulida (<500 m)	1.130	1.547	1.290	1.252	1.337	1.297	1.243	1.226	1.009	0.935	0.801	0.953	0.764	0.755
Terebratulida (>500 m)[a]	1.788	2.349	1.964	1.949	2.026	2.056	1.873	1.920	1.764	1.662	1.552	1.562	1.528	1.517
Rhynchonellida (>500 m)[a]	1.829	2.643	2.035	1.992	2.020	2.122	1.938	1.862	1.729	1.607	1.493	1.464	1.523	1.393
Macandrevia cranium														
Secondary layer (<500 m)	1.096	1.584	1.254	1.254	1.308	1.320	1.172	1.222	1.045	0.957	0.810	1.017	0.842	0.901
Secondary layer (>500 m)[a]	1.837	2.154	1.945	1.958	1.976	2.144	1.913	2.005	1.796	1.729	1.613	1.727	1.623	1.697
Primary & secondary layers (2504.7–2531.8 m)[a]	1.022	1.853	1.114	1.203	1.338	1.564	1.148	1.132	0.944	0.770	0.438	0.734	0.576	1.047
Primary & secondary layers (213.9-224.9 m)	1.273	2.035	1.427	1.406	1.514	1.321	1.225	1.167	1.153	0.886	0.866	0.783	0.907	0.777
Terebratalia transversa														
Secondary layer	0.930	1.065	1.268	0.995	1.026	0.849	0.987	1.086	0.715	0.785	0.779	0.620	0.437	0.574
Umbo	0.086	0.486	0.107	0.396		0.633	0.659	0.467			0.307	0.812		
Terebratulina septentrionalis														
Secondary layer	0.992	1.026	1.028	0.985	1.027	1.007	0.959	0.910	0.749	0.720	0.530	0.799	0.533	0.502
Primary & secondary layers	0.813	0.742	0.901	0.280		1.815	1.399	0.972	1.015	1.158	0.895	1.034	0.954	0.900
Thecidellina congregata														
Primary layer	0.929	1.059	0.743	0.531	0.239	0.115	0.949	0.572	0.638	0.785	1.073	1.030		0.737
Umbo	1.114	1.363	1.080	0.926				1.483	1.041		1.287		0.762	

Note: [a]: from Zaky et al., 2016

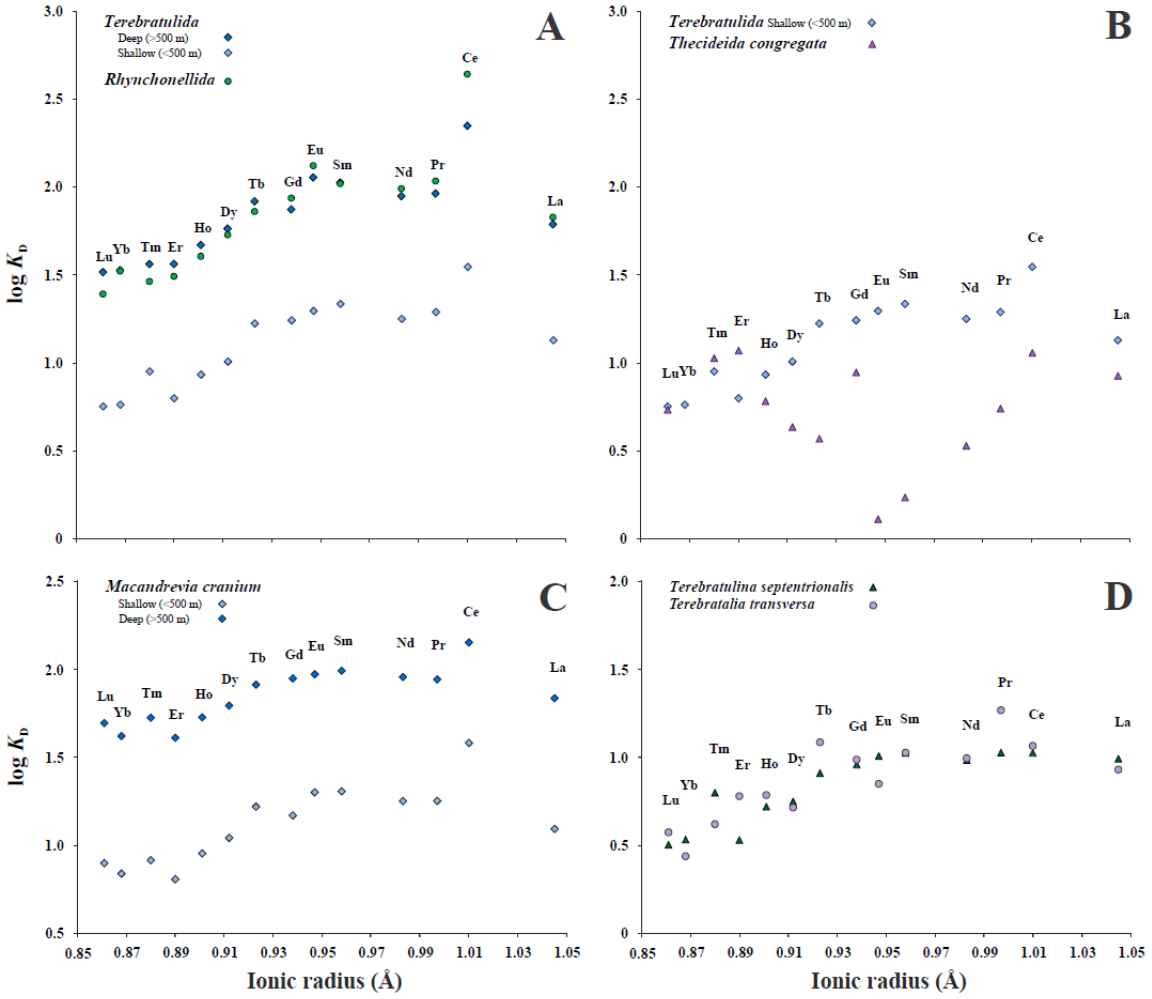

Fig. 4-6. Distribution diagram of the ionic radii of the REEs Vs. the calculated log K_D values for the shells of 1) Terebratulida from shallow (<500 m) and deep (>500 m) settings, and Rhynchonellida orders, 2) Terebratulida order from shallow setting (<500 m) and *T. congregata* species, 3) *M. cranium* species from shallow (<500 m) and deep (>500 m) settings, and 4) *T. septentrionalis* and *T. transversa* species.

4.6.1.1. *Thecidellina congregata*

The shell structure of Thecideidines is significantly different from that of other articulated brachiopods in the virtual suppression of the secondary layer (cf. Williams, 1966). Consequently, their shells are made almost exclusively of a granular laminae or blocky rhombohedra primary layer, which can be more than 100 µm thick in mature valves

(Cusack and Williams, 2003). On the other hand, sporadic traces of secondary fibrous can be traced only on cardinalia and valve floors (Williams, 1973).

The predominant primary layer shell structure of the *T. congregata* is reflected in the different trace element and REE contents, and the REE_{SN} pattern of the Philippine Sea specimens relative to those from the other localities. Although, they display noticeably gradual HREE enrichments similar to those of their ambient Tropical Surface Water (L:H= 0.19, L:M= 0.35 and M:H= 0.55; Table 4-3), their Pr, Nd, Sm and Eu present downward excursions (Fig. 4-5). Quantifying the magnitudes of those excursions by correlating the normalized values of these elements to that of the La show that, the Pr excursion (Pr_{SN}/La_{SN}= 0.57) is relatively similar to that of the Ce (Ce_{SN}/La_{SN}= 0.54), while those of the Nd (Nd_{SN}/La_{SN}= 0.31), Sm (Sm_{SN}/La_{SN}= 0.33) and Eu (Eu_{SN}/La_{SN}= 0.39) are more pronounced. In addition, they display significantly different partition coefficient values (Table 4-4) and pattern (Fig. 4-6B) from their counterparts of the shallow water (<500 m) habitat, which secrete secondary layer (i.e. *Terebratulida*).

4.6.1.2. *Macandrevia cranium*

Shallow water specimens of *M. cranium* from the Denmark Strait, and Norwegian and Irminger seas are depleted in LREE, MREE, HREE and ∑REE contents in comparison to their deep water counterparts (>500m) from the Denmark Strait, and Irminger and Iceland basins (Tables 4-2, 4-5; Zaky et al., 2016). *M. cranium* shells exhibit consistently negative Ce anomalies, however, values of the shallow water specimens in the Denmark Strait (0.44), and the Norwegian (0.52) and the Irminger seas (0.55) are slightly higher than

those from deeper waters (Ce/Ce*= 0.31, 0.42 and 0.17, in the Denmark Strait, and the Irminger and the Iceland basins; Zaky et al., 2016; Tables 4-2, 4-5).

Table 4-5. The mean REE concentrations (in ppm), and L:H, L:M, M:H and Ce/Ce* values in the primary and secondary layers of deep-water *Macandrevia cranium* shells, and their locations and water depths.

	N	Depth	LREEs	MREEs	HREEs	L:H	L:M	M:H	∑REEs	Ce/Ce*
Primary layer										
Irminger Basin[1]	2	2504.7–2531.8	0.154	0.032	0.008	0.69	0.45	1.52	0.19	0.99
Secondary layer										
Denmark Strait[2]	2	603.1-742.5	0.666	0.188	0.088	0.54	0.51	1.06	0.94	0.31
Irminger Basin[2]	5	678.5-724.4	0.661	0.183	0.077	0.51	0.50	1.01	0.93	0.42
Iceland Basin[2]	3	2567.7-2568.5	0.550	0.164	0.090	0.44	0.52	0.83	0.81	0.17

Note: (N) number of samples.
LREEs= Sum of La:Nd concentrations.
MREEs= Sum of Sm:Dy concentrations.
HREEs= Sum of Ho:Lu concentrations.
L:H = Sum of $(LREEs)_{SN}$ / 3/5 Sum of $(HREEs)_{SN}$.
L:M = Sum of $(LREEs)_{SN}$ / 3/5 Sum of $(MREEs)_{SN}$.
M:H = Sum of $(MREEs)_{SN}$ / Sum of $(HREEs)_{SN}$.
[1]: from Zaky et al. (2015).
[2]: from Zaky et al. (2016).

All segments display relatively similar REE_{SN} patterns of HREE enrichment but with lower magnitude for the shallower (L:H= 0.60, 056 and 0.65) to the deeper samples (L:H= 0.54, 0.51 and 0.44, respectively; Tables 4-2, 4-5; Zaky et al., 2016). The magnitudes of the $MREE_{SN}$ enrichments relative to the $LREE_{SN}$ also vary, but insignificantly between the shallow (L:M= 0.57, 054 and 0.57) and the deep-water shells (L:M= 0.51, 0.50 and 0.52, respectively; Tables 4-2, 4-5; Zaky et al., 2016).

The variations in the $HREE_{SN}$ relative to the $MREE_{SN}$, on the other hand, define relatively different patterns that vary by locality. Shallow water specimens of the Irminger Sea yielded the highest M:H value of 1.12 documenting depletion in HREEs (Fig. 4-7; Table 4-2). Those from the Norwegian Sea, shallow and deep Denmark Strait yielded lower M:H ratios of 1.04, 1.04 and 1.06 presenting less HREE depletion, while those of the deep Irminger Basin yielded M:H ratio closer to the unity (1.01) displaying a flat pattern after the MREEs (Fig. 4-7; Tables 4-2, 4-5). On the opposite, those of the Iceland Basin present

an invariant trend of slight $HREE_{SN}$ enrichments (M:H= 0.83; Fig. 4-7; Table 4-5). The partition coefficient values of the shallow-water (<500 m) locations are slightly depleted relative to those of the deeper (>500 m) locations (Table 4- 4), but their patterns are similar (Fig. 4-6C).

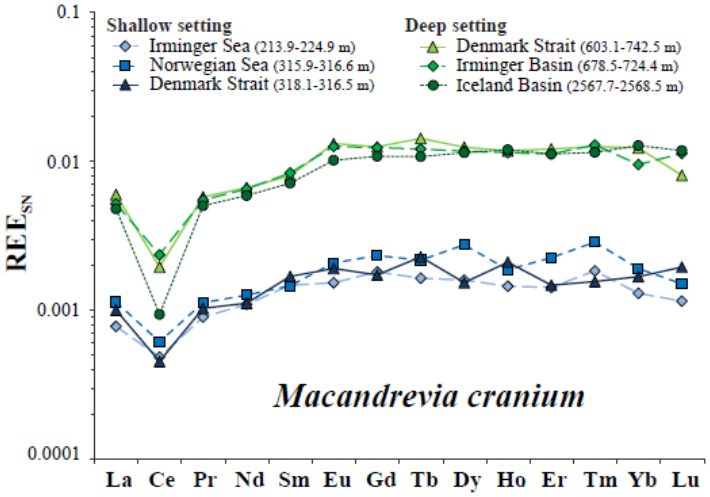

Figure 4-7. Average REE_{SN} patterns of the *Macandrevia cranium* shells of the shallow (<500 m; this study) and the deep settings (>500 m; Zaky et al., 2016).

The intraspecific variations in REE contents and Ce anomalies of *M. cranium* in general, and the HREE enrichments on REE_{SN} pattern of those from the Iceland Basin in particular, suggest that REE uptake by members of this species may be influenced to some degree by external environmental factor(s).

4.6.1.3. *Terebratulina septentrionalis* and *Terebratalia transversa*

The LREE, MREE, HREE and ∑REE concentrations in the specimens from Bonne Bay and Bay of Fundy are similar (Table 4-2). Their REE_{SN} patterns (Fig. 4-3) are also similar; they display flat trends with L:H ratios close to unity (0.88 and 0.90; Table 4-2). Their L:M (0.77 and 0.80), M:H (1.14 and 1.12) and Ce/Ce* (0.41 and 0.42) values are conspicuously close as well (Table 4-2).

Such resemblance in the REE compositions and REE_{SN} patterns of the brachiopods from the two localities does not represent a species dependence but similarity in the environmental conditions. The shells of the two localities arefom bay habitat, and from comparable depths (30 and 10-15 m), salinity (31.1 and 32.2) and temperatures (5.6 and 6.2° C; Table 4-1). In addition, *T. septentrionalis* shells from Friday Harbor with similar environmental settings (depth= 75 m, salinity= 30.5 and temperature= 8° C; Table 4-1), display a similar REE_{SN} pattern (Fig. 4-5), LREE, MREE, HREE and ∑REE compositions, and L:H, L:M, M:H and Ce/Ce* ratios (Table 4-2).

The insignificant variations between the partition coefficient values (Table 4- 4) and patterns of the *T. septentrionalis* and *T. septentrionalis* (Fig. 4-6D) confirm that the environmental conditions are the main controller on their REE incorporation not their species.

4.6.2. Shell fractionation

Shells of articulated brachiopods consist of two opposing bilaterally symmetrical valves that are predominantly dissimilar in size with brachial (dorsal) valve normally smaller than the pedicle (ventral) valve (MacFarlan et al., 2009). The two valves are hinged posteriorly near the umbo (the most prominent and the oldest part of the valve) through a series of teeth and sockets, and simple opening and closing muscles (James et al., 1992). The shell is secreted as multi-layers consisting of low-Mg calcite and a proteinaceous periostracum membrane succeeded by an outer granular calcite primary layer and an inner fibrous calcite secondary layer, and occasionally a stacked prismatic calcite tertiary layer

in some species (Azmy et al., 1998; 2011; Auclair et al., 2003; Brand et al., 2003, 2013, 2015; Parkinson et al., 2005).

4.6.2.1. Umbo region

Specialized shell structures of modern brachiopods such as umbonal regions present anomalous Mg distributions and have their own isotopic compositions which have been attributed to their higher organic content (cf. Carpenter and Lohmann, 1995; Brand et al., 2003, 2013, 2015; Cusack et al., 2007; Pérez Huerta et al., 2008). In order to evaluate their REE fractionation, umbo areas of *T. congregata* and *T. transversa* from the Philippine Sea and Friday Harbor were separated, cleaned according to the Procedure-5 of Zaky et al. (2015) and analysed for their REE contents.

The umbo regions seem to incorporate REEs compositions and distributions that are different from the rest of the shells (Fig. 4-5; Table 4-2). In addition, their partition coefficient values and pattern are also significantly different (Table 4-4; Fig. 4-8 A & B). The inconsistency between REE contents within a brachiopod umbo-shell could be either species dependent during growth of the juvenile stage or a selective uptake of certain elements during their secretions. Consequently, REE contents of the umbo areas of brachiopods should not be considered for paleoenvironmental investigations.

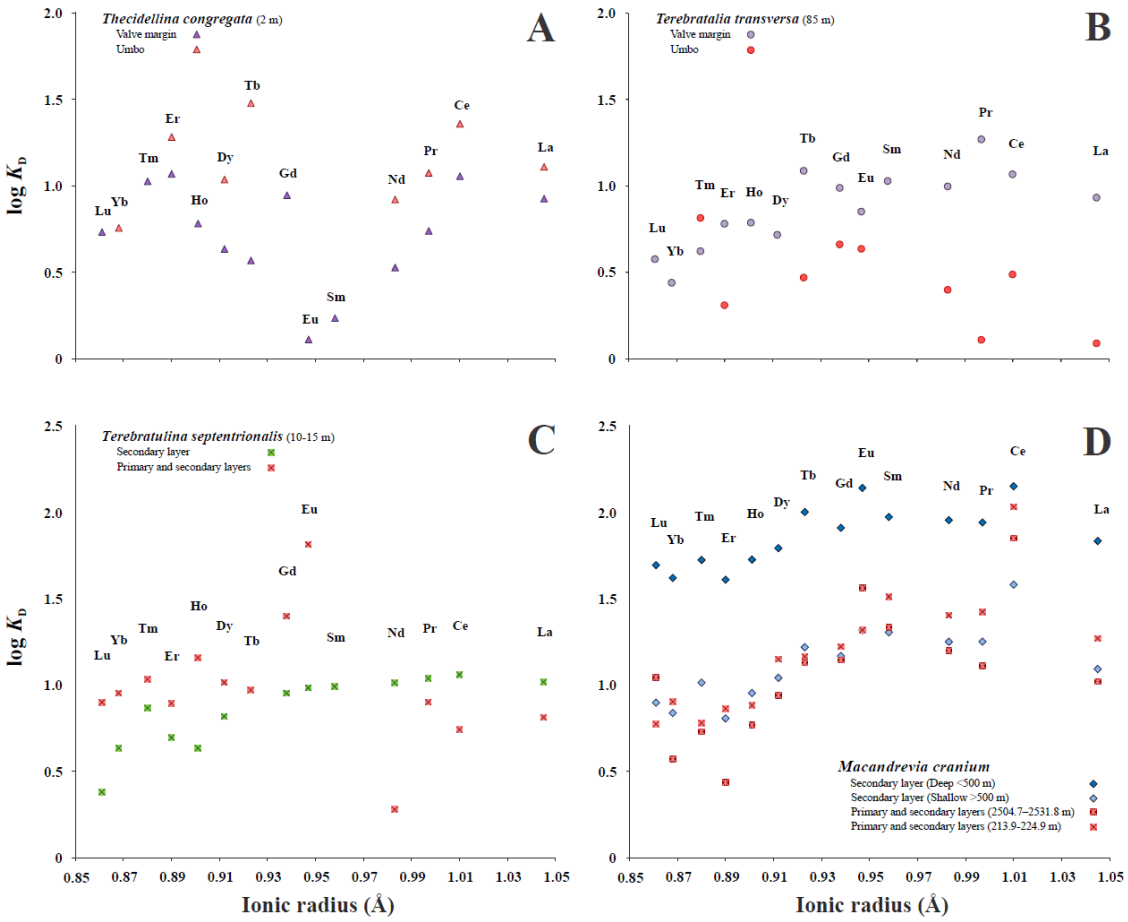

Fig. 4-8. Distribution diagram of the ionic radii of the REEs Vs. the calculated log K_D values for the shells of 1) the valve margin and the umbo of *T. congregata* species, 2) the valve margin and the umbo of *T. transversa* species, 3) primary and secondary layers of *T. septentrionalis* species, and *4)* primary and secondary layers of *M. cranium* species.

4.6.2.2. Primary layer

The primary layer of modern articulated brachiopods is precipitated in oxygen and carbon isotope disequilibrium with their ambient seawater (cf. Carpenter and Lohmann, 1995; Parkinson et al., 2005; Brand et al., 2003, 2013, 2015). In a previous study, Zaky et al. (2015) demonstrated that the primary layer of *M. cranium* from deep water of the Irminger Basin is remarkable elevated in its Ce (Ce/Ce*= 0.99) and MREE contents (L:H,

L:M and M:H= 0.69, 0.45 and 1.52: Table 4-5) relative to the secondary layer of deep-water counterparts of the Iceland Basin (Table 4-2).

For assessing the REE incorporation into the primary layer of shallow water articulated brachiopods, the P-3 segments of the *T. septentrionalis* and *M. cranium* from the Bay of Fundy and Irminger Sea were cleaned predominantly by abrasion of the external contaminants until they were deemed clean. The likelihood of success of the physical cleaning in removing adsorptive particulate matter of Mn, Fe and U oxides is reflected in the resemblance between the Mn, Fe and U concentrations in the P-3 (primary layer present) parts of the two species and their P-5 counterparts (primary layer removed; Table 4-2).

Higher MREE and HREE contents in P-3 segments from the Bay of Fundy relative to P-5 indicate their selective incorporation into the primary layer of the *T. septentrionalis* (Fig. 4-3; Table 4-2). On the other hand, the lower LREE, Sm, Eu and Gd contents in Irminger Sea P-5 specimens relative to those of the P-3 implies their preferentially incorporation into the primary layer of the shallow water *M. cranium* shells (Fig. 4-2; Table 4-2). The inconsistency of these results with those of the deep-water counterparts of Zaky et al. (2015) eliminates the "vital" effect on the REE incorporation of the primary layers of the modern articulated brachiopods. Instead, their partition coefficient values and pattern (Table 4-4; Fig. 4-8 C & D) suggest random, variable and incidental REE uptake during shell calcite secretion and implies that primary layers should be avoided for paleoenvironmental REE investigations.

4.6.2.3. Dorsal and venteral valves

In contrast to the primary layer, secondary and tertiary layers in modern brachiopods are secreted in near isotopic near equilibrium with their ambient seawater (Carpenter and Lohman, 1995; Brand et al., 2003, 2011, 2013, 2015; Parkinson et al., 2005). The ventral (pedicle) valves of *T. septentrionalis* from Bonne Bay are slightly depleted in their LREE, MREE, HREE, ∑REE, Fe and U contents, but slightly enriched in their Mn and Ce/Ce* values in comparison to dorsal (brachial) valves (Table 4-6). In contrast, the LREE, MREE, HREE, ∑REE and U concentrations in the ventral valves of *T. transversa* of Friday Harbor are slightly higher relative to those of the dorsal values, while their Fe, Mn and Ce/Ce* anomaly are lower (Table 4-6).

The dorsal and ventral valves of the *M. cranium* shells display variations from location to another. The ventral valves of those from Irminger Sea are enriched in their LREE, MREE, HREE, ∑REE, Mn, Fe and U contents relative to the dorsal valves. On the contrary, the dorsal valve of the Denmark Strait and Norwegian Sea shells are enriched relative to the ventral valve (Table 4-6). The ambivalence between elemental and REE compositions of the dorsal and ventral valves in the representatives of the different species and even within the same members discount the probability of selective REE uptake by a certain valve. Overall, the differences are small with most attributed to natural variation to the brachiopod's lattice incorporation process rather than a major environmental factor.

Table 4-6. Mean Mn, Fe, U and the REE concentrations (in ppm), and L:H, L:M, M:H and Ce/Ce* values in pedicle and brachial valves of different brachiopods. Trace element results were normalized to 100 % carbonate basis (cf. Brand and Veizer, 1980).

Valve	Location	N	Mn	Fe	U	LREEs	MREEs	HREEs	∑REEs	Ce/Ce*
Terebratulina septentrionalis										
Ventral	Bonne Bay	8	04.4	02.2	0.015	0.102	0.015	0.004	0.13	0.42
Dorsal		2	06.4	06.2	0.015	0.147	0.023	0.005	0.17	0.38
Terebratalia transversa										
Ventral	Friday Harbour	3	34.3	46.0	0.019	0.100	0.014	0.007	0.12	0.47
Dorsal		2	46.3	55.6	0.016	0.055	0.009	0.005	0.07	0.31
Macandrevia cranium										
Ventral	Denmark Strait	2	30.2	46.3	0.013	0.101	0.025	0.009	0.13	0.37
Dorsal		2	37.3	234.7	0.018	0.143	0.022	0.010	0.18	0.48
Ventral	Norwegian Sea	2	40.3	52.0	0.018	0.113	0.017	0.011	0.15	0.56
Dorsal		2	42.1	48.1	0.013	0.179	0.044	0.015	0.24	0.50
Ventral	Irminger Sea	6	17.5	18.4	0.016	0.152	0.032	0.012	0.20	0.55
Dorsal		6	07.9	06.1	0.010	0.064	0.014	0.004	0.09	0.65

Note: (N) number of samples.
LREEs= Sum of La:Nd concentrations.
MREEs= Sum of Sm:Dy concentrations.
HREEs= Sum of Ho:Lu concentrations.

4.6.3. Environmental impacts

To evaluate the temperature, salinity and depth influences on REE incorporation by articulated brachiopods, the REE contents of those from deeper depths (>500 m) of Zaky et al., 2016 are included in this section (Table 4-7). Meanwhile, due to the anomalous REE incorporation by the umbo and the suppression of REE in *T. congregata* species, only REEs of secondary/tertiary layers' specimens derived from dorsal and ventral valves are considered.

Table 4-7. The mean REE concentrations (in ppm), and L:H, L:M, M:H and Ce/Ce* values in modern deep water articulated brachiopod samples (Zaky et al., 2016), their locations, depth and the ambient water masses' parameters of temperature and salinity.

Location/Station	N	Depth [m]	Salinity [psu]	Temperature [°C]	LREEs	MREEs	HREEs	L:H	L:M	M:H	∑REEs	Ce/Ce*
Venezuela Basin												
Stations VB1 & VB2	6	3986-3998	34.97[a]	3.87[a]	0.156	0.027	0.027	0.36	0.53	0.67	0.24	0.49
Denmark Strait												
Station 1090	1	603.1-742.5	35.13	7.88	0.895	0.244	0.113	0.58	0.51	1.13	1.25	0.34
Station 1119	1	696.9-706.4	34.91	0.07	0.437	0.132	0.062	0.67	0.50	1.33	0.63	0.27
Irminger Basin												
Station 1086	4	678.5-698.1	35.10	6.20	0.693	0.197	0.082	0.48	0.50	0.96	0.98	0.39
Station 1082	1	704.9-724.4	35.10	6.20	0.535	0.128	0.056	0.57	0.51	1.12	0.72	0.56
Iceland Basin												
Station 983	3	2567.7-2568.5	35.00	2.66	0.550	0.164	0.090	0.44	0.52	0.82	0.80	0.17
Lau Arc												
Station P948	4	589	34.76[b]	10.18[b]	0.704	0.148	0.082	0.49	0.57	0.86	0.94	0.61
Colville Arc												
Station CA	2	660	34.5[b]	7.62[b]	0.450	0.142	0.089	0.38	0.49	0.78	0.68	0.28
Havre Trough												
Station TAN0205/102	9	1115-1172	34.47[b]	3.75[b]	0.212	0.067	0.039	0.39	0.51	0.77	0.32	0.21
Station TAN1104/39	1	1520	34.56[b]	2.95[b]	0.413	0.131	0.068	0.48	0.50	0.95	0.61	0.15
Kermadec Arc												
Station TAN1007/123	1	1244	34.47[b]	3.75[b]	1.404	0.403	0.197	0.50	0.56	0.91	2.00	0.23
Station TAN1104/19	2	1460	34.56[b]	2.95[b]	0.775	0.245	0.140	0.44	0.53	0.83	1.16	0.18
Station TAN1104/9	1	1583	34.56[b]	2.95[b]	1.265	0.388	0.202	0.50	0.55	0.91	1.86	0.14
Station Z15337	1	1740	34.63[b]	2.20[b]	0.731	0.224	0.126	0.46	0.55	0.83	1.08	0.15
Northland Plateau												
Station P70	3	1293	34.47[b]	3.75[b]	0.296	0.083	0.056	0.40	0.49	0.82	0.45	0.20
Station P73	1	1583	34.56[b]	2.95[b]	0.752	0.230	0.122	0.44	0.54	0.82	1.11	0.23
Ross Sea												
Station TAN0802/296	5	547	34.80[c]	-1.85[c]	0.168	0.036	0.018	0.50	0.53	0.94	0.24	0.31

[a]: from Osborne et al. (2015)
[b]: from Zhang and Nozaki (1996)
[c]: from Jacobs and Giulivi (1999)

4.6.3.1. Temperature

Earlier studies suggest that water temperature has some influence on seawater REEs. For example, the HREE content in the top 1000 m of the water column varies with temperature, but below that depth, HREE contents are invariant (Zhang and Nozaki, 1996). The low correlation coefficients (R^2) between seawater temperatures and the LREE, MREE, HREE and ∑REE concentrations in articulated brachiopods (0.02, 0.01, 0.01 and 0.012), as well as their L:H, L:M, M:H and Ce/Ce* ratios (0.01, 0.05, 0.00 and 0.04) reflect a lack of covariance.

The samples are from three temperature regimes; -5° C to 0° C, 0° C to 5° C and 5° C to 10° C. The correlation coefficients between the ambient seawater temperature and the REE partition coefficients of the brachiopods in general or shells of each regime are remarkably small (Fig. 4-9). It in turn suggests a limited temperature control on the REE fractionations in brachiopod calcite.

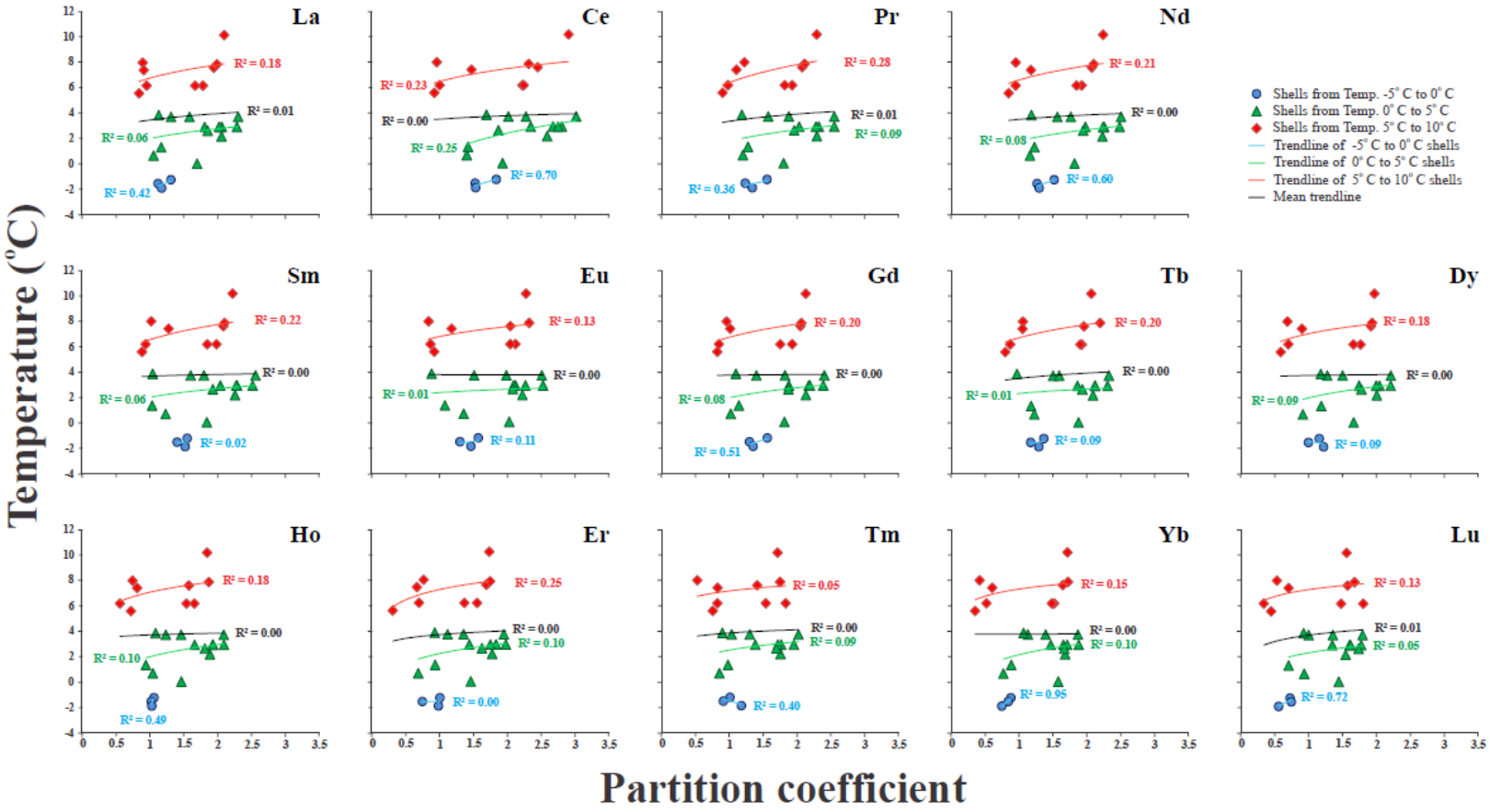

Fig. 4-9. Correlation plots between the water temperature and the log K_D values of the REEs in the shallow (<500 m; this study) and the deep (>500 m; Zaky et al., 2016) settings (Appendix 4-4). *Thecidellina congregata* shells of the Philippine Sea are excluded from the correlations.

4.6.3.2. Salinity

Geochemical reactions in low salinity regions (bays and estuaries) control fluxes of weathered REE into seawater and consequently influences the oceanic budget of REEs (Nozaki et al., 2000 a, b; Sholkovitz and Szymczak, 2000). Large-scale removal of the dissolved and suspended REEs (in particularly the LREEs) has been observed in the low salinity mixing zones by salt-induced coagulation of colloids and several other mechanisms including planktonic uptake and coprecipitation with iron hydroxides (Sholkovitz et al., 1999; Sholkovitz and Szymczak, 2000; Kulaksiz and Bau, 2007; Leybourne and Johannesson, 2008; Kessarkar et al., 2013). On the contrary, salinity seems to have no obvious impact on either the generation or the magnitude of Ce anomalies in seawater (Lawrence and Kamber, 2006). Concentrations of LREEs, MREEs, HREEs and ∑REEs in the brachiopods correlate poorly with salinity of their ambient water masses (R^2= 0.23, 0.26, 0.30 and 0.25).. On the other hand, the salinity displays moderate to good correlations with the L:H and L:M, but weak with the M:H and Ce/Ce* ratios of the articulated brachiopods (R^2= 0.40, 0.69, 0.10 and 0.02).

The shells represent two salinity levels; normal (~34 psu) and relatively low (30-32 psu). The correlation coefficients between the shells' partition coefficients of the REEs and the salinity of the ambient seawater of the two levels implies that, the salinity has a moderate to minor impact on the shells REE fractionation (Fig. 4-10).

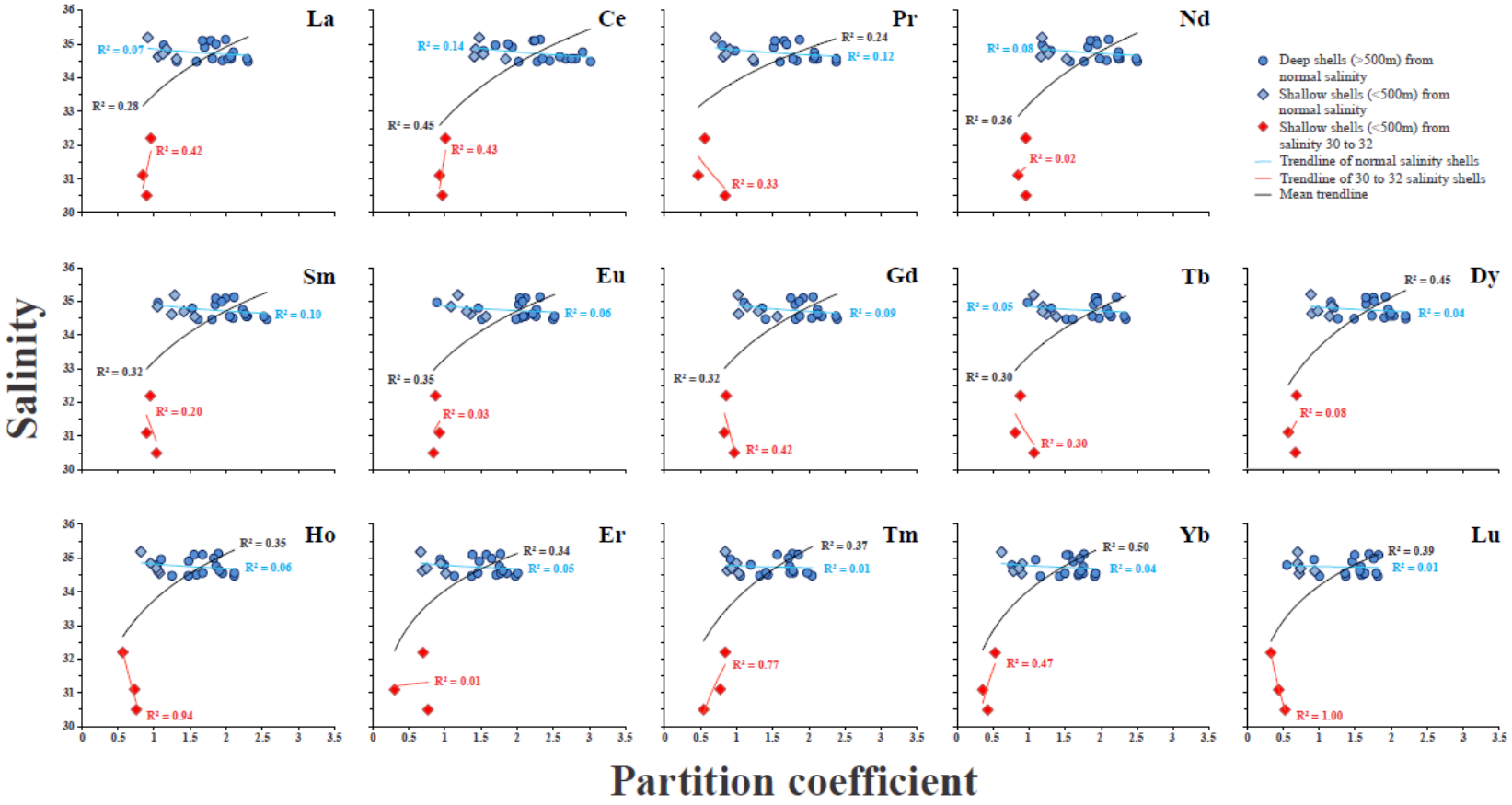

4-10. Correlation plots between the salinity and the log K_D values of the REEs in the shallow (<500 m; this study) and the deep (>500 m; Zaky et al., 2016) settings (Appendix 4-4). *Thecidellina congregata* shells of the Philippine Sea are excluded from the correlations.

4.6.3.3. Water Depth

Depth has a major control on the REE concentrations in seawater (cf. Elderfield et al., 1990). As a direct result of the progressive breakdown of particulate matter in the modern ocean, all REEs, with the exception of Ce, display a "nutrient-like" pattern with increasing depth (e.g., de Baar et al., 1985; Nozaki, 2001). Meanwhile, HREE concentrations at depth's are significantly elevated relative to those from shallow depth's due to the re-association of LREE complexes by scavenging particulates and the high solubility of HREE complexes (Goldberg et al., 1963; Haley et al., 2004). The oxidization state of Ce governs its concentration in shallow depth's; Ce^{+3} is oxidized rapidly through bacterial mediation into insoluble Ce^{+4} which in turn gets scavenged quickly by sinking particulate Fe- and Mn-oxides (Elderfield et al., 1988; Holser, 1997; Nozaki, 2001). Continuation of the scavenging process and the ease of adsorption of remaining Ce^{+3} on nano-particulates results in Ce depletion with increasing depth (Elderfield and Greaves, 1982; Sholkovitz and Schneider, 1991). Thus, the REE_{SN} distribution pattern of deeper seawater yields stronger Ce depletions and more pronounced HREE enrichments than in shallow water (de Baar et al., 1988; Haley et al., 2004; Kim et al., 2012).

Depth seems to have no direct impact on the REE concentrations of the articulated brachiopods in general (R^2= 0.08, 0.10, 0.15 and 0.10). It discloses insignificant correlation with the shells' LREE, MREE, HREE and ∑REE concentrations of the shallow (R^2= 0.01, 0.17, 0.30 and 0.04) and the deep settings (R^2= 0.02, 0.01, 0.00 and 0.02).

The correlation between depth and the L:H, L:M, M:H and Ce/Ce* ratios of all investigated shallow and deep-water brachiopods (R^2= 0.78, 0.71, 0.45 and 0.71) implies

that water depth may control brachiopod REE contents (Fig. 4-11). An individual assessment of each setting suggests that shallow water brachiopods display a strong correlation of depth with L:H and L:M (R^2= 0.88 and 0.93), mild with M:H (R^2= 0.25) but weak with Ce/Ce* (R^2= 0.10; Fig. 4-11). On the other hand, deep-water shells exhibit poor correlation of depth with the L:H and L:M ratios (R^2= 0.28 and 0.10), but moderate to good with M:H and Ce/Ce* (R^2= 0.36 and 0.68; Fig. 4-117). In addition, the correlation coefficients between the water depth and the shells' partition coefficients of the REEs are moderate to high in the two settings (shallow and deep; Fig. 4-12). This implies that water depth has a prominent impact on the LREE and MREE fractionations of shallow water shells and on the Ce anomaly of those from deep water.

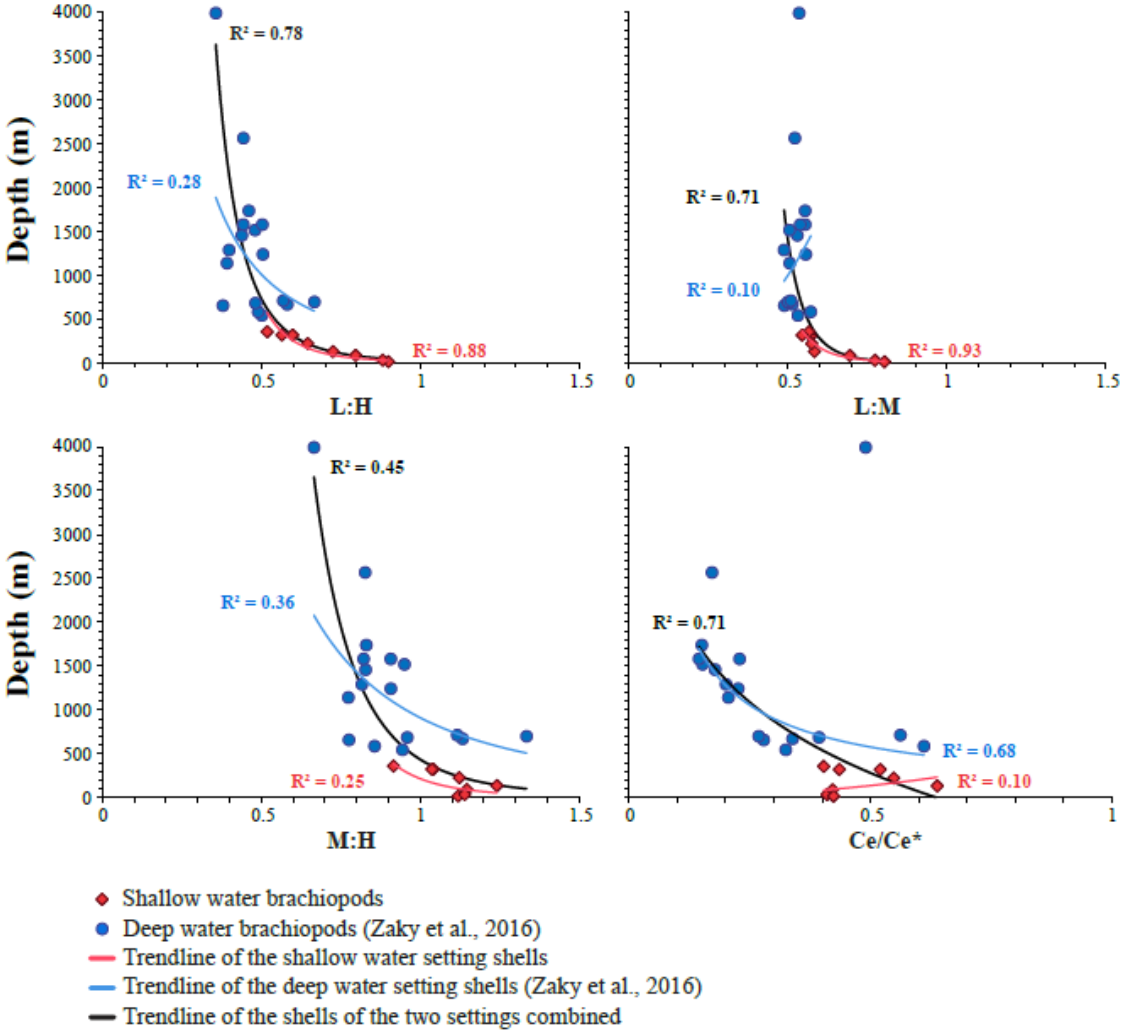

Figure 4-11. Correlation plots between the water depths (bathymetry) and shells' L:H, L:M and M:H ratios and Ce/Ce* anomalies of the shallow (<500 m; this study) and the deep (>500 m; Zaky et al., 2016) settings. *Thecidellina congregata* shells of the Philippine Sea are excluded from the correlations, and the mean Ce/Ce* value of the Venezuela Basin is plotted but eliminated from the correlation coefficient (R^2) calculation.

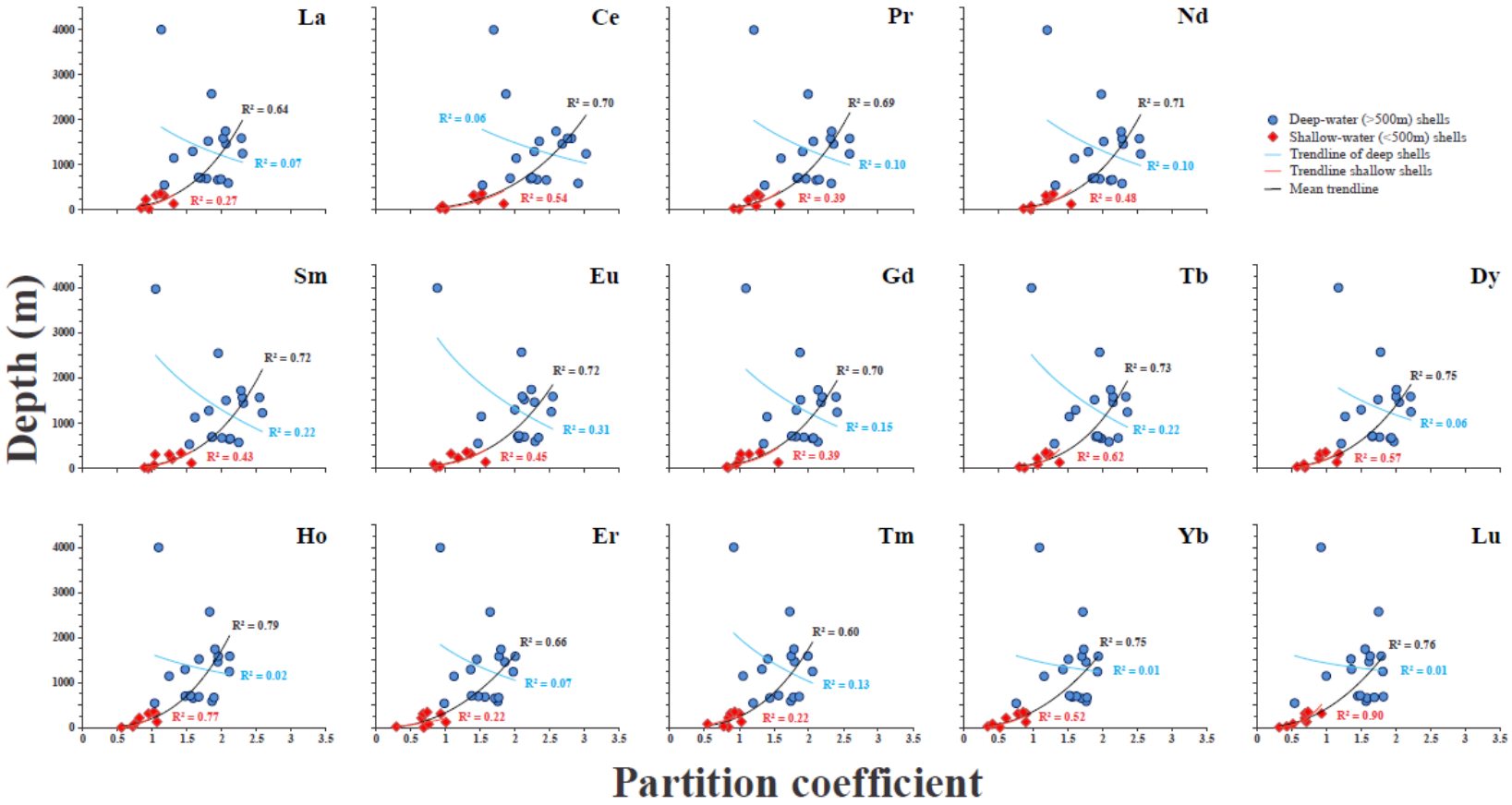

4-12. Correlation plots between the water depths (bathymetry) and the log K_D values of the REEs in the shallow (<500 m; this study) and the deep (>500 m; Zaky et al., 2016) settings (Appendix 4-4). *Thecidellina congregata* shells of the Philippine Sea are excluded from the correlations.

4.6.4. Paleobathymetric Sensor

Geochemical proxies are used to investigate and characterize paleoceanographic and paleoenvironmental conditions. Determining the paleobathymetry is a cornerstone of those investigations, and consequently numerous proxies have been recruited (cf. Immenhauser, 2009). The REEs represent a significant potential proxy of paleobathymetry, their shale normalized patterns vary significantly in seawater displaying pronounced $MREE_{SN}$ and $HREE_{SN}$ enrichments with increasing water depth (cf. Elderfield et al., 1988; Holser, 1997).

The L:H ratio of modern shallow water brachiopods exhibit strong correlation with water depth (R^2= 0.88; Fig. 4-11), and its values display systematic decrease with increasing depths (Table 4-8). Consequently, it has been utilized to to construct a water depth sensor that consists of six segments (Table 4-8). Due to a lack of suitable specimens, the first (shallowest) interval of < 15 m is represented by the upper limit of the second interval; i.e. location with the highest mean L:H value of the 15-50 m interval (Bay of Fundy); Table 4-8). The other five intervals were chosen to represent depths of 15-50 m, 50-150 m, 150-250 m, 250-350 m and 350-500 m (Table 4-8). Values of each bathymetric interval represent its lower limit; i.e. adopted from the location with the lowest mean L:H value of this interval (Table 4-2). We expect, with more analyses of shallow water brachiopods, that this depth sensor will be refined over the years. Also, we consider the L:H parameter to be of primary importance and the L:M one to be secondary and of a supportive role in determining water depths. In the meantime, we plan to test our proposed REE bathymetric sensor (RBS) on the REEs of fossil brachiopods and whole rock samples

from six different shallow water Paleozoic formations (Gyanyima, Naco, Boggy, Chicotte, Jupiter and Becscie) in an attempt to ascertain their paleowater depths.

Table 4-8. Bathymetric sensor using L:H parameter to characterize depth intervals based on $(LREE)_{SN}$ and $(HREE)_{SN}$ constituents.

Bathymetric intervals [m]	**LREEs [ppm]**	**HREEs [ppm]**	**∑REEs [ppm]**	**$(LREEs)_{SN}$**	**$(HREEs)_{SN}$**	**L:H**	**L:H[b]**
< 15[a]	0.13	0.01	0.16	0.003	0.006	**> 0.90**	
15-50	0.11	0.01	0.13	0.003	0.006	**0.88**	0.908
50-150	0.24	0.02	0.30	0.005	0.012	**0.72**	0.706
150-250	0.11	0.01	0.14	0.003	0.007	**0.65**	0.645
250-350	0.15	0.02	0.19	0.004	0.010	**0.56**	0.567
350-500	0.14	0.02	0.18	0.004	0.012	**0.52**	0.518

Note: Values of each bathymetric interval are adopted from the location with the lowest mean L:H value of the interval (Table 4-2).
[a] Values of this bathymetric interval are adapted from the location with highest mean L:H value of the 10-50 m interval (i.e. Bay of Fundy; Table 4-2)
[b] Mean values of each interval (Appendix 4-2).
$(LREEs)_{SN}$ = Sum of $(La)_{SN}$:$(Nd)_{SN}$ values.
$(HREEs)_{SN}$ = Sum of $(Ho)_{SN}$:$(Lu)_{SN}$ values.
L:H = Sum of $(LREEs)_{SN}$ / 3/5 Sum of $(HREEs)_{SN}$.

4.6.4.1. REE Paleobathymetric Sensor (RBS) Application

The Upper Permian samples are from four different horizons (6, 7, 8 and 9; Garbelli et al., 2015) that constitute the topmost part (just below the end of Permian extinction event) of the Lopingian Gyanyima Formation, southwestern Tibet, China. The formation consists of reefal carbonates interbedded with thick basalts representing a carbonate platform on a Neotethyan seamount that were deposited in a normal marine, subtidal environment (Shen et al., 2001, 2003, 2010). Horizons 6 and 9 are composed mainly of reefal limestone, horizon 7 of micritic limestone, whereas horizon 8 of cherty limestone (Garbelli et al., 2015).

The Upper Desmoinsean (Middle Pennsylvanian) Naco Formation in central Arizona is a predominantly marine limestone sequence interbedded with terrigenous

sedimentary rocks (Brew and Beus 1976). It is divided into 3 main members (alpha, beta and gamma), the middle beta member from which the samples were collected is a highly fossiliferous shallow marine unit of ledge-forming limestone interbedded with mudstones and calcareous shales (Brew 1970; Brand, 1989b, 1990). Its depth setting is assumed to be in the 10-30 m range. The lower-Middle Desmoinesian Boggy Formation exposed at the Buckhorn Asphalt Quarry in south Oklahoma consists of asphalt-impregnated shallow marine carbonates mixed with siliciclastics (Brand, 1987, 1989a, 1991; Smith et al., 1994; Seuß et al., 2009).

The richly fossiliferous Lower Silurian (Llandovery) sequence of Anticosti Island (Quebec, Canada) consists of six formations, from top to bottom, Chicotte, Jupiter, Gun River, Merrimack, Becscie and Ellis Bay formations (Ziegler et al., 1977; Scotese et al., 1985; Azmy et al., 1998). The succession was deposited during the eustatic sea-level rise that followed the late Ordovician glaciation on an open subtidal carbonate platform at the continental margin of shallow epeiric seas (Sami and Desrochers, 1992). The topmost Chicotte Formation, deposited in a shallow wave-agitated setting, consists of crinoidal grainstone with patch reefs (Long and Copper, 1994). The underlain Jupiter Formation is dominated mainly by lime mudstone, skeletal wackestone and grainstone with minor calcareous shale and rare sandy siliciclastics and reefal interbeeds mostly restricted to the topmost part (Copper and Long, 1990). The Becscie Formation consists of shallow marine limestone that grades from fossiliferous grainstone and packstone at the top into brachiopod packstone, rudstone, skeletal wackestone and lime mudstone at the bottom interbedded with green shale (Petryk, 1981; Barnes, 1989).

The Paleozoic brachiopod shells and whole rock samples have consistently negative Ce anomalies that are relatively comparable to modern shallow water counterparts, but they yield elevated ∑REE concentrations (Table 4-9). The variations between fossils and coeval whole rock trace element and REE compositions, and Ce/Ce* ratios were previously assessed by Zaky et al. (2015). Brachiopods of units 7 and 6 of the Gyanyima, Boggy and Jupiter formations exhibit gradual enrichment REE_{SN} patterns with mean L:H values of 0.68 and 0.81 (Table 4-9). In contrast, shells of units 9 and 8 of the Gyanyima , Naco and Chicotte and Becscie formations are HREE depleted relative to LREE with mean L:H values of 1.22 to 1.59 (Table 4-9). With the exception of units 7 and 6 of Gyanyima Formation, the whole rock samples of the same horizons disclose insignificantly different REE_{SN} patterns, albeit overall dramatically higher REE contents (Fig. 4-8) than those of their coeval fossils with relatively comparable L:H values (Table 4-9). Furthermore, the fossil brachiopod and whole rock REE_{SN} patterns and values are similar to modern shallow water counterparts.

Table 4-9. The mean ∑REE concentrations (in ppm), and L:H, L:M, M:H and Ce/Ce* values in the fossil brachiopod and whole rock samples, and their estimated paleodepths.

	N	L:H	L:M	M:H	∑REEs	Ce/Ce*	Paleodepth
Upper Lopingian (Upper Permian)							
Unit 9, Gyanyima Formation[a]							
Brachiopods	1	1.22	0.90	1.35	6.28	0.25	< 15 m
Whole rock	2	0.94	0.83	1.10	93.86	0.22	< 15 m
Unit 8, Gyanyima Formation[a]							
Brachiopods	2	1.59	1.01	1.58	6.28	0.31	< 15 m
Whole rock	2	1.24	0.96	1.27	26.26	0.33	< 15 m
Unit 7, Gyanyima Formation[a]							
Brachiopods	3	0.68	0.69	0.99	8.86	0.40	150-250 m
Whole rock	3	0.84	0.78	1.08	21.59	0.35	50-150 m
Unit 6, Gyanyima Formation[a]							
Brachiopods	4	0.81	0.83	0.98	8.11	0.39	50-150 m
Whole rock	4	0.90	0.82	1.08	15.77	0.37	15-50 m
Upper Desmoinesian (Middle Pennsylvanian)							
Naco Formation[b]							
Brachiopods	3	1.29	1.49	0.86	13.30	0.64	< 15 m
Whole rock	2	1.24	0.91	1.35	25.28	0.74	< 15 m
Middle Desmoinesian (Middle Pennsylvanian)							
Boggy Formation[b]							
Brachiopods	3	0.91	0.80	1.13	2.29	0.66	< 15 m
Whole rock	1	1.09	0.84	1.30	21.03	0.79	< 15 m
Llandovery (Lower Silurian)							
Chicotte Formation[b,c]							
Brachiopods	2	1.44	0.89	1.63	2.59	0.79	< 15 m
Whole rock	1	1.08	0.74	1.46	6.81	0.83	< 15 m
Jupiter Formation[b,c]							
Brachiopods	11	0.99	0.70	1.41	2.47	0.65	< 15 m
Whole rock	4	1.01	0.70	1.45	37.85	0.80	< 15 m
Becscie Formation[b]							
Brachiopods	1	1.15	0.73	1.57	0.72	0.78	< 15 m
Whole rock	1	0.92	0.68	1.37	5.15	0.89	< 15 m

(N) number of samples.
L:H = Sum of $(LREEs)_{SN}$ / 3/5 Sum of $(HREEs)_{SN}$.
L:M = Sum of $(LREEs)_{SN}$ / 3/5 Sum of $(MREEs)_{SN}$.
[a]: from Garbelli et al. (2015).
[b]: from Zaky et al. (2015).
[c]: from Azmy et al. (2011).

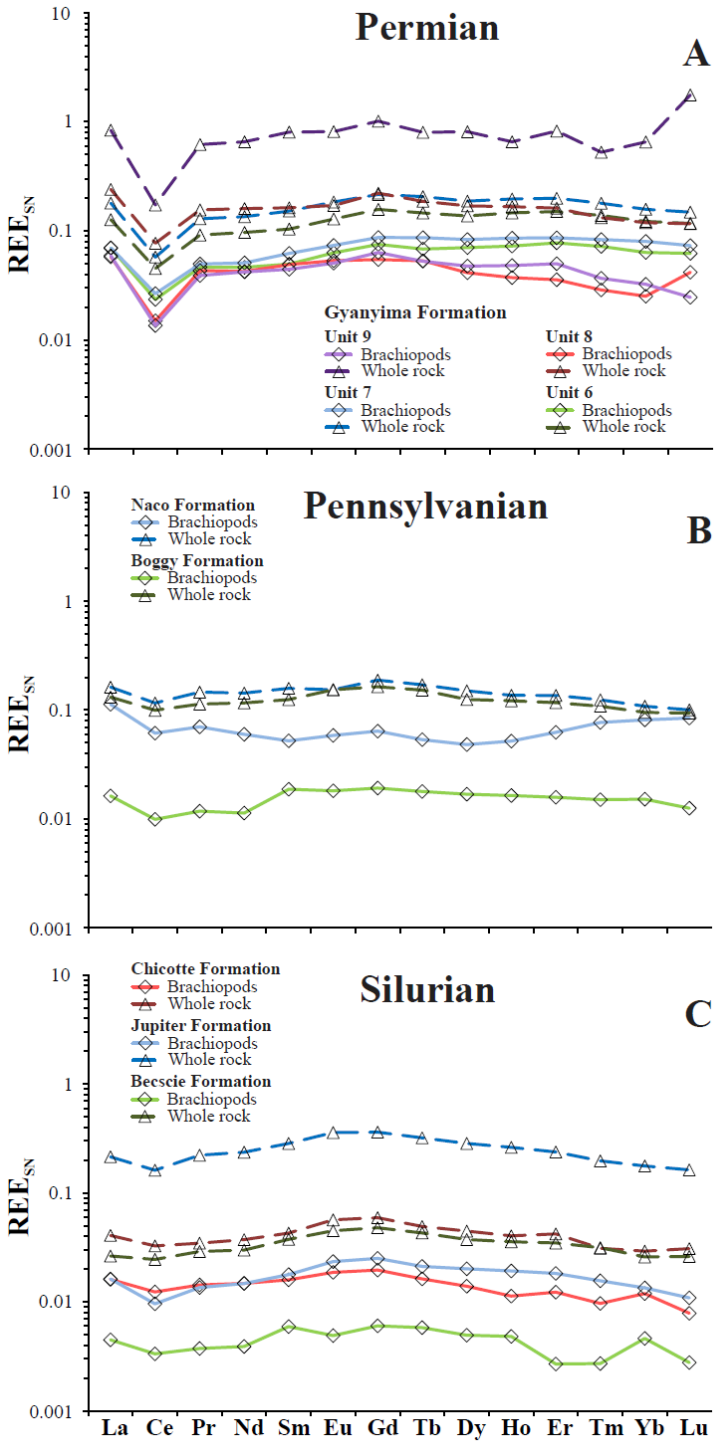

Figure 4-13. Average REE_{SN} patterns of the well-preserved fossil brachiopods and the whole rock samples from (A) the Upper Lopingian (Upper Permian) Gyanyima Formation of Tibet, (B) Middle and Upper Desmoinsian (Middle Pennsylvanian) Naco and Boggy Formations of Arizona and Oklahoma, and (C) Llandoverian (Lower Silurian) Chicotte, Jupiter and Becscie Formations of Anticosti Island.

Matching the L:H ratios to the six depth intervals established by the RBS (Table 4-8) of the fossil counterparts and whole rock samples confirms deposition of the six formations in shallow marine settings (Table 4-9). The L:H parameter suggests deposition in water depths of less than 50 m with two exceptions (units 7 and 6; Gyanyima Formation), but with many at < 15 m deep (Table 4-13). Although whole rock specimens were sampled from fresh fine-grained micritic surfaces, the chemistry of the diagenetic fluids sometimes alters and/or shifts the original geochemical compositions of the whole rock (Brand, 1994; Brand et al., 2011). The differences between the estimated paleodepths from the shells and their enclosing whole rock samples (e.g. units 7 and 6; Gyanyima Formation) imply that, in the absence of fossil brachiopods caution is required in utilizing the whole rock samples in paleobathymetric estimations.

The biofacies analyses suggest the deposition of Unit 8 of Gyanyima Formation in infralittoral shallow to open subtidal environments around fair-weather wave base but in depths deeper than those revealed from the paleodepth estimations (below 15 m; Garbelli et al., 2015; Shen et al., 2010; Wang et al., 2010). However, *C. indica* is a low-level epifaunal species lived close to the bottom-water interface (Garbelli et al., 2015), and thus their REE composition is impacted partly by the chemistry of the pore water. This in turn emphasises that the paleoecological parameters are of the importance of the diagenetic alteration, and thus should be taken in the consideration before utilizing the REEs in the paleodepth investigations.

4.7. Conclusions

Modern shallow water (<500 m) *Macandrevia* sp., *M. cranium*, *Magellania joubini*, *Terebratalia transversa*, *Terebratulina septentrionalis* and *Thecidellina congregata* from the Norwegian, Irminger and Ross seas, the Denmark Strait, Bonne Bay, Friday Harbor and Bay of Fundy were evaluated for their REE contents and oceanographic parameters of depth, salinity and temperature.

1- The REE contents of the umbo is equivocal and consequently should not be used in paleoenvironmental evaluations

2- The REE uptake of the shell's primary layer is variable, and found unreliable as a paleo-oceanographic indicator

3- Variations in REE concentrations between the brachial and pedicle valves are generally insignificant and within the natural variation of the brachiopod incorporation.

4- The elemental, REE compositions and the REE_{SN} patterns of the *thecideidines* shells are remarkably different from the other articulated brachiopods, reflecting the domination of the primary layers over the shell structures.

5- Temperature and salinity have minor impacts on the REE contents of shallow water brachiopods.

6- Shells' Ce/Ce* anomalies display no correlation with temperature, salinity and depth in shallow water although depth appears to have a significant control in deep water counterparts.

7- Shallow water shell L:H and L:M ratios were used to construct a reliable REE bathymetric sensor (RBS) scheme.

8-Testing the reliability of the L:H and L:M values and their corresponding depth intervals of the reconstructed RBS by determining the water depths of fossil brachiopods and their corresponding whole rock provided very consistent results.

Acknowledgments

This work was supported in part by an industry grant by the MITACS-Accelerate internship program in partnership with Husky Oil. The authors are also thankful to the National Institute of Water and Atmospheric research of New Zealand (NIWA) for supplying us with some brachiopods, and to NSERC (7961-09) for financial support to Uwe Brand and PEEP (Petroleum Exploration Enhancement Program).

References

Akagi, T., Hashimoto, Y., Fu, F.F., Tsuno, H., Tao, H., and Nakano, Y. (2004). Variation of the distribution coefficients of rare earth elements in modern coral–lattices: species and site dependencies. *Geochimica et Cosmochimica Acta*, *68*(10), 2265–2273.

Alibo, D.S., and Nozaki, Y. (2004). Dissolved rare earth elements in the eastern Indian Ocean: chemical tracers of the water masses. *Deep–Sea Research I*, *51*, 559–576.

Auclair, C., Joachimski, M.M., and Lecuyer C. (2003). Deciphering kinetic, metabolic and environmental controls on stable isotope fractionations between seawater and the shell of Terebratalia transversa (Brachiopoda). *Chemical Geology, 202*, 59–78.

Azmy, K., Veizer, J., Bassett, M.G., and Copper, P. (1998). Oxygen and carbon isotopic composition of Silurian brachiopods: implications for coeval seawater and glaciations. *Geological Society of America Bulletin*, *110*, 1499–1512.

Azmy, K., Poty, E., and Brand, U. (2009). High–resolution isotope stratigraphy of the Devonian–Carboniferous boundary in the Namur–Dinant Basin, Belgium. Sedimentary *Geology*, *216*(3), 117–124.

Azmy, K., Brand, U., Sylvester, P., Gleeson, S., Logan, A., and Bitner, M.A. (2011). Biogenic low–Mg calcite (brachiopods): proxy of seawater–REE composition, natural processes and diagenetic alteration. *Chemical Geology*, *280*, 180–190.

Azmy, K., Poty, E., and Mottequin, B. (2012). Biochemostratigraphy of the Upper Frasnian in the Namur–Dinant Basin, Belgium: Implications for a global Frasnian–Famennian pre–event, *Palaeogeography, Palaeoclimatology, Palaeoecology, 313–314*, 93–106.

Barnes, C.R. (1989). Lower Silurian chronostratigraphy of Anticosti Island, Québec. *A Global Analysis of the Ordovician–Silurian Boundary*, *9*, 101–108.

Bau, M., Balan, S., Schmidt, K., and Koschinsky, A. (2010). Rare earth elements in mussel shells of the Mytilidae family as tracers for hidden and fossil high–temperature hydrothermal systems. *Earth and Planetary Science Letters*, *299*(3), 310–316.

Brand, U. (1987). Biogeochemistry of nautiloids and paleoenvironmental aspects of Buckhorn seawater (Pennsylvanian), southern Oklahoma.*Palaeogeography, Palaeoclimatology, Palaeoecology*, *61*, 255–264.

Brand, U. (1989a). Aragonite–calcite transformation based on Pennsylvanian molluscs. *Geological Society of America Bulletin*, *101*(3), 377–390.

Brand, U. (1989b). Biogeochemistry of Late Paleozoic North American brachiopods and secular variation of seawater composition. *Biogeochemistry*, *7*(3), 159–193.

Brand, U. (1990). Chemical diagenesis and dolomitization of Paleozoic high–Mg calcite crinoids. *Carbonates and Evaporites*, *5*(2), 179–196.

Brand, U. (1991). Strontium isotope diagenesis of biogenic aragonite and low–Mg calcite. *Geochimica et Cosmochimica Acta*, *55*(2), 505–513.

Brand, U. (2004). Carbon, oxygen and strontium isotopes in Paleozoic carbonate components: an evaluation of original seawater–chemistry proxies. *Chemical Geology*, *204*(1), 23–44.

Brand, U., and Veizer, J. (1980). Chemical diagenesis of a multicomponent carbonate system–1: Trace elements. *Journal of Sedimentary Research*, 50(4), 1219–1236.

Brand, U., Logan, A., Hiller, N., and Richardson, J. (2003). Geochemistry of modern brachiopods: applications and implications for oceanography and paleoceanography. *Chemical Geology, 198*, 305–334.

Brand, U., Logan, A., Bitner, M.A., Ggriesshsaber, E., Azmy, K., and Buhl, D. (2011). What is the Ideal Proxy of Palaeozoic Seawater chemistry? *Memoirs of the Association of Australasian Palaeontologists*, *41*, 9–24.

Brand, U., Azmy, K., Bitner, M.A., Logan, A., Zuschin, M., Came, R., and Ruggiero, E. (2013). Oxygen isotopes and $MgCO_3$ in brachiopod calcite and a new paleotemperature equation. *Chemical Geology, 359*, 23–31.

Brand, U., Azmy, K., Griesshaber, E., Bitner, M.A., Logan, A., Zuschin, M., Ruggiero, E., and Colin, P.L. (2015). Carbon isotope composition in modern brachiopod calcite: A case of equilibrium with seawater?. *Chemical Geology*, *411*, 81–96.

Brew, D.C. (1970). The Naco Formation (Pennsylvanian) in central Arizona. *Plateau*, *42*(4), 126–138.

Brew, D.C., and Beus, S.S. (1976). A middle Pennsylvanian fauna from the Naco Formation near Kohl Ranch, central Arizona. *Journal of Paleontology*, 888–906.

Carpenter, S.J., and Lohmann, K.C. (1995). $\delta^{18}O$ and $\delta^{13}C$ values of modern brachiopods. *Geochimica et Cosmochimica Acta*, *59*: 3749–3764.

Copper, P., and Long, D.G.F. (1990). Stratigraphic revision of the Jupiter Formation, Anticosti Island, Canada: a major reference section above the Ordovician-Silurian boundary. *Newsletters on Stratigraphy*, 11–36.

Cusack, M., and Williams, A. (2003). Chemico–structural differentiation of the organocalcitic shells of rhynchonellate brachiopods. *Brachiopods*, 2–17.

Cusack, M., Parkinson, D., Perez–Huerta, A., England, J., Curry, G.B., and Fallick, A.E. (2007). Relationship between δ^{18} O and minor element composition of *Terebratalia transversa*. *Earth and Environmental Science Transactions of the Royal Society of Edinburgh*, *98*(3–4), 443–449.

de Baar, H.J., Bacon, M.P., Brewer, P.G., and Bruland, K.W. (1985). Rare earth elements in the Pacific and Atlantic Oceans. *Geochimica et Cosmochimica Acta*, *49*(9), 1943–1959.

de Baar, H.J., German, C.R., Elderfield, H., and Van Gaans, P. (1988). Rare earth element distributions in anoxic waters of the Cariaco Trench. G *Geochimica et Cosmochimica Acta*, *52*(5), 1203–1219.

Elderfield, H., and Greaves, M.J. (1982). The rare earth elements in seawater. *Nature, 296*, 214–219.

Elderfield, H., Whitfield, M., Burton, J.D., Bacon, M.P., and Liss, P.S. (1988). The oceanic chemistry of the rare–earth elements [and discussion]. *Philosophical Transactions of the Royal Society of London A: Mathematical, Physical and Engineering Sciences*, *325*(1583), 105–126.

Elderfield, H., Upstill–Goddard, R., and Sholkovitz, E.R. (1990). The rare earth elements in rivers, estuaries, and coastal seas and their significance to the composition of ocean waters. *Geochimica et Cosmochimica Acta*, *54*(4), 971–991.

Garbelli, C., Angiolini, L., Brand, U., Shen, S.Z., Jadoul, F., Posenato, R., Azmy, K., and Cao, C.Q. (2015). Neotethys seawater chemistry and temperature at the dawn of the end Permian mass extinction. *Gondwana Research*. In press.

German, C.R., and Elderfield, H. (1989). Rare earth elements in Saanich Inlet, British Columbia, a seasonally anoxic basin. Geochimica et Cosmochimica Acta, *53*(10), 2561–2571.

German, C.R., Holliday, B.P., and Elderfield, H. (1991). Redox cycling of rare earth elements in the suboxic zone of the Black Sea. *Geochimica et Cosmochimica Acta*, *5*5(12), 3553–3558.

Goldberg, E.D., Koide, M., Schmitt, R.A., and Smith, R.H. (1963). Rare-Earth distributions in the marine environment. *Journal of Geophysical Research*, *68*(14), 4209–4217.

Goldstein, S.L., and Hemming, S.R. (2003). Long–lived isotopic tracers in oceanography, paleoceanography and ice sheet dynamics, in: H. Elderfield (Ed.), *Treatise on Geochemistry*, V.6, Elsevier, Oxford, 453–489.

Goldstein, J., and Jacobsen, B. (1988). Rare earth elements in river waters. *Earth and Planetary Science Letters, 89*, 35–47.

Greaves, M.J., Statham, P.J., and Elderfield, H. (1994). Rare Earth Element Mobilization from Marine Atmospheric Dust into Seawater, *Marine Chemistry*, *46*, 255–260.

Greaves, M.J., Elderfield, H., and Sholkovitz, E.R. (1999). Aeolian sources of rare earth elements to the Western Pacific Ocean. *Marine Chemistry*, *68*(1), 31–38.

Hagedorn, B., Cartwright, I., Raveggi, M., and Maas, R. (2011). Rare earth element and strontium geochemistry of the Australian Victorian Alps drainage system: Evaluating the dominance of carbonate vs. aluminosilicate weathering under varying runoff. *Chemical Geology*, *284*, 105–126.

Haley, B.A., Klinkhammer, G.P., and McManus, J. (2004). Rare earth elements in pore waters of marine sediments. *Geochimica et Cosmochimica Acta*, *68*(6), 1265–1279.

Holmden, C., Creaser, R.A., Muehlenbachs, K.L.S.A., Leslie, S.A., and Bergström, S.M. (1998). Isotopic evidence for geochemical decoupling between ancient epeiric seas and bordering oceans: implications for secular curves. *Geology*, *26*(6), 567–570.

Holser, W. T. (1997). Evaluation of the application of rare-earth elements to paleoceanography. Palaeogeography, Palaeoclimatology, *Palaeoecology*,*132*(1), 309-323.

Hongo, Y., Obata, H., Alibo, D., and Nozaki, Y. (2006). Spatial Variations of Rare Earth Elements in North Pacific Surface Water. *Journal of Oceanography*, 62, 441–455.

Immenhauser, A. (2009). Estimating palaeo–water depth from the physical rock record. *Earth–Science Reviews*, *96*(1), 107–139.

Jacobs, S.S., and Giulivi, C.F. (1999). Thermohaline data and ocean circulation on the Ross Sea continental shelf. In *Oceanography of the Ross Sea Antarctica*, Springer Milan, 3–16.

James, M.A., Ansell, A.D., Collins, M.J., Curry, G.B., Peck, L.S., and Rhodes, M.C. (1992). Biology of living brachiopods. *Advances in Marine Biology*, *28*, 175–387.

Johannesson, K.H., Telfeyan, K., Chevis, D.A., Rosenheim, B.E., and Leybourne, M.I. (2014). Rare earth elements in stromatolites–1. Evidence that modern terrestrial stromatolites fractionate rare earth elements during incorporation from ambient waters. In *Evolution of Archean Crust and Early Life,* Springer Netherlands, 385–411.

Kemp, R.A., and Trueman, C. (2003). Rare earth elements in Solnhofen biogenic apatite: geochemical clues to the paleoenvironment. *Sedimentary Geology*, *155*, 109–127.

Kessarkar, P.M., Shynu, R., Rao, V.P., Chong, F., Narvekar, T., and Zhang, J. (2013). Geochemistry of the suspended sediment in the estuaries of the Mandovi and Zuari rivers, central west coast of India. *Environmental monitoring and assessment*, *185*(5), 4461–4480.

Kim, J.H., Torres, M.E., Haley, B.A., Kastner, M., Pohlman, J.W., Riedel, M., and Lee, Y.J. (2012). The effect of diagenesis and fluid migration on rare earth element distribution in pore fluids of the northern Cascadia accretionary margin. *Chemical Geology*, *291*, 152–165.

Kulaksız, S., and Bau, M. (2007). Contrasting behaviour of anthropogenic gadolinium and natural rare earth elements in estuaries and the gadolinium input into the North Sea. *Earth and Planetary Science Letters*, *260*(1), 361–371.

Kuss, J., Garbe-Schonberg, C.D., and Kremling, K. (2001). Rare earth elements in suspended particulate material of North Atlantic surface waters. *Geochimica et Cosmochimica Acta*, *65*, 187–199.

Lacan, F., and Jeandel, C. (2004). Neodymium isotopic composition and rare earth element concentrations in the deep and intermediate Nordic Seas: Constraints on the Iceland Scotland Overflow Water signature. *Geochemistry, Geophysics, Geosystems*, *5*(11), 1–10.

Lacan, F., and Jeandel, C. (2005). Acquisition of the neodymium isotopic composition of the North Atlantic Deep Water. *Geochemistry, Geophysics, Geosystems*, *6*(12), 1–20.

Lawrence, M.G., and Kamber, B.S. (2006). The behaviour of the rare earth elements during estuarine mixing—revisited. *Marine Chemistry*, *100*(1), 147–161.

Lécuyer, C., Grandjean, P., Barrat, J.A., Emig, C.C., Nolvak, J., Paris, F., and Robardet, M. (1998). $\delta^{18}O$ and REE contents of phosphatic brachiopods: a comparison between modern and lower Paleozoic populations. *Geochimica et Cosmochimica Acta, 62*, 2429–2436.

Lécuyer, C., Bogey, C., Garcia, J.P., Grandjean, P., Barrat, J.A., Bardet, N., and Pereda-Superbiola, X. (2003). Stable isotope composition and rare earth element content of vertebrate remains from the late Cretaceous of northern Spain (Lano): did the environmental record survive?, *Palaeogeography, Palaeoclimatology, Palaeoecology*, *193*, 457–471.

Lécuyer, C., Reynard, B., and Grandjean, P. (2004). Rare earth element evolution of Phanerozoic seawater recorded in biogenic apatites. *Chemical Geology,* 204, 63–102.

Leybourne, M.I., and Johannesson, K.H. (2008). Rare earth elements (REE) and yttrium in stream waters, stream sediments, and Fe–Mn oxyhydroxides: fractionation, speciation, and controls over REE+ Y patterns in the surface environment. *Geochimica et Cosmochimica Acta*, *72*(24), 5962–5983.

Logan, A. (2007). Geographic distribution of extant articulated brachiopods. In: Selden, P. A. (ed.): Treatise on Invertebrate Paleontology, Part H (Revised), Brachiopoda, 6 (supplement), 3082–3115. The Geological Society of America and the University of Kansas, Boulder, Colorado and Lawrence, Kansas.

Long, D.G.F., and Copper, P. (1994). The late Ordovician–early Silurian carbonate tract of Anticosti Island, Gulf of St. Lawrence, Eastern Canada. Geological *Association of Canada (GAC), Mineralogical Association of Canada (MAC)*, Joint Annual Meeting, Waterloo, Ontario, guidebook, Field trip B4: 69 p.

MacFarlan, D., Bradshaw, M., Campbell, H., Cooper, R., Lee, D., MacKinnon, D., Waterhouse, J., Wright, A.J. and Robinson, J. (2009). *Phylum Brachiopoda: lamp shells*, 255.

McLennan, S.M. (1989). Rare earth elements in sedimentary rocks: influence of provenance and sedimentary processes. In: Lipin, B.R., McKay, G.A. (Eds.), Geochemistry and Mineralogy of Rare Earth Elements, *Mineralogical Society of America Review Mineralogy*, *21*, 169–200.

Merschel, G., and Bau, M. (2015). Rare earth elements in the aragonitic shell of freshwater mussel Corbicula fluminea and the bioavailability of anthropogenic lanthanum, samarium and gadolinium in river water. *Science of The Total Environment*, *533*, 91–101.

Mills, R.A., and Elderfield, H. (1995). Rare earth element geochemistry of hydrothermal deposits from the active TAG Mound, 26 N Mid–Atlantic Ridge. *Geochimica et Cosmochimica Acta*, *59*(17), 3511–3524.

Nozaki, Y. (2001). Rare Earth Elements and their Isotopes in the Ocean. Encyclopedia of Ocean Sciences, *4*, 2354–2366.

Nozaki, Y., Lerche, D., Alibo, D.S., and Tsutsumi, M. (2000a). Dissolved indium and rare earth elements in three Japanese rivers and Tokyo Bay: evidence for anthropogenic Gd and In. *Geochimica et Cosmochimica Acta*,*64*(23), 3975–3982.

Nozaki, Y., Lerche, D., Alibo, D.S., and Snidvongs, A. (2000b). The estuarine geochemistry of rare earth elements and indium in the Chao Phraya River, Thailand. *Geochimica et Cosmochimica Acta*, *64*(23), 3983–3994.

Osborne, A.H., Haley, B.A., Hathorne, E.C., Plancherel, Y., and Frank, M. (2015). Rare earth element distribution in Caribbean seawater: Continental inputs versus lateral transport of distinct REE compositions in subsurface water masses. *Marine Chemistry, 177,* 172-183.

Palmer, M.R. (1985). Rare earth elements in foraminifera tests. *Earth and Planetary Science Letters, 73*, 285–298.

Palmer, M.R., and Elderfield, H. (1986). Rare earth elements and neodymium isotopes in ferromanganese oxide coatings of Cenozoic foraminifera from the Atlantic Ocean. *Geochimica et Cosmochimica Acta*, *50*(3), 409–417.

Parkinson, D., Curry, G.B., Cusack, M., Fallick A.E. (2005). Shell structure, patterns and trends of oxygen and carbon stable isotopes in modern brachiopod shells. *Chemical Geology*, *219*, 193–235.

Peck, L.S., and Holmes, L.J. (1990). Seasonal and ontogenetic changes in tissue size in the Antarctic brachiopod Liothyrella uva (Broderip, 1833). *Journal of experimental marine biology and ecology*, *134*(1), 25–36.

Peck, L., Morris, D., and Clarke, A. (1986). The caeca of punctate brachiopods: a respiring tissue not a respiratory organ. *Lethaia*, *19*(3), 232–232.

Peck, L.S., Clarke, A., and Holmes, L.J. (1987). Summer metabolism and seasonal changes in biochemical composition of the Antarctic brachiopod *Liothyrella uva* (Broderip, 1833). *Journal of experimental marine biology and ecology*, *114*(1), 85–97.

Pérez–Huerta, A., Cusack, M., Jeffries, T.E., and Williams, C.T. (2008). High resolution distribution of magnesium and strontium and the evaluation of Mg/Ca thermometry in Recent brachiopod shells. *Chemical Geology*, *247*(1), 229–241.

Petryk, A.A. (1981). Stratigraphy, sedimentology and paleogeography of the upper Ordovician–lower Silurian of Anticosti Island, Quebec. *Stratigraphy and Paleontology. Field Meeting, Anticosti–Gaspé, Québec*, *2*, 11–40.

Ponnurangam, A., Bau, M., Brenner, M., and Koschinsky, A. (2015). Mussel shells of *Mytilus edulis* as bioarchives of the rare earth elements and yttrium distribution in seawater and the potential impact of pH and temperature on the partitioning behaviour. *Biogeosciences Discussions*, *12*(17).

Ruppert, E.E., and Fox, R.S. (2004). Invertebrate zoology: a functional evolutionary approach, in Barnes R.D., *Invertebrate Zoology*, Brooks/Cole, Belmont, CA.

Sami, T., and Desrochers, A. (1992). Episodic sedimentation on an early Silurian, storm-dominated carbonate ramp, Becscie and Merrimack formations, Anticosti Island, Canada. *Sedimentology*, *39*(3), 355–381.

Scotese, C.R., Van der Voo, R., Barrett, S., Westoll, T.S., and Chaloner, W.G. (1985). Silurian and Devonian Base Maps [and Discussion]. *Philosophical Transactions of the Royal Society of London B: Biological Sciences*, *309*(1138), 57–77.

Seuß, B., Nützel, A., Mapes, R.H., and Yancey, T.E. (2009). Facies and fauna of the Pennsylvanian Buckhorn Asphalt Quarry deposit: a review and new data on an important Palaeozoic fossil Lagerstätte with aragonite preservation. *Facies*, *55*(4), 609–645.

Shen, S.Z., Cao, C.Q., Shi, G.R., Wang, X.D. and Mei, S.L. (2001). Lopingian (Late Permian) stratigraphy, sedimentation and palaeobiogeography in southern Tibet. *Newsletters on Stratigraphy, 39*, 157–179.

Shen, S., Dongli, S., and Shi, G.R. (2003). A biogeographically mixed late Guadalupian (late Middle Permian) brachiopod fauna from an exotic limestone block at Xiukang in Lhaze county, Tibet. *Journal of Asian earth sciences*, *21*(10), 1125–1137.

Shen, S.Z., Cao, C.Q., Zhang, Y.C., Li, W.Z., Shi, G.R., Wang, Y., Wu, Y.S., Ueno, K., Henderson, C.M., Wang, X.D. and Zhang, H. (2010). End–Permian mass extinction and palaeoenvironmental changes in Neotethys: Evidence from an oceanic carbonate section in southwestern Tibet. *Global and Planetary Change*, *73*(1), 3–14.

Sholkovitz, E.R., and Schneider, D. L. (1991). Cerium redox cycles and rare earth elements in the Sargasso Sea. *Geochimica et Cosmochimica Acta*, *55*(10), 2737–2743.

Sholkovitz, E.R., and Shen, G.T. (1995). The incorporation of rare–earth elements in modern coral. *Geochimica et Cosmochimica Acta*, *59*, 2749–2756.

Sholkovitz, E.R, and Szymczak, R. (2000). The estuarine chemistry of rare earth elements: comparison of the Amazon, Fly, Sepik and the Gulf of Papua systems. *Earth and Planetary Science Letters*, *179*(2), 299–309.

Sholkovitz, E.R., Elderfield, H., Szymczak, R., and Casey, K. (1999). Island weathering: River sources of rare earth elements to the Western Pacific Ocean. *Marine Chemistry*, *68*(1–2), 39–57.

Shumway, S.E. (1982). Oxygen consumption in brachiopods and the possible role of punctae. *Journal of Experimental Marine Biology and Ecology*, *58*(2), 207–220.

Smith, P.E., Brand, U., and Farquhar, R.M. (1994). U–Pb systematics and alteration trends of Pennsylvanian–aged aragonite and calcite. *Geochimica et cosmochimica acta*, *58*(1), 313–322.

Thayer, C.W. (1986). Respiration and the function of brachiopod punctae. *Lethaia*, *19*(1), 23–31.

Veizer, J., Ala, D., Azmy, K., Bruckschen, P., Bruhn, F., Buhl, D., Carden, G., Diener, A., Ebneth, S., Goddris, Y., Jasper, T., Korte, C., Pawellek, F., Podlaha, O., Strauss, H. (1999). $^{87}Sr/^{86}Sr$, $\delta^{13}C$ and $\delta^{18}O$ evolution of Phanerozoic seawater. *Chemical Geology*, *161*, 59–88.

Wang, Y., Ueno, K., Zhang, Y. C., and Cao, C. Q. (2010). The Changhsingian foraminiferal fauna of a Neotethyan seamount: the Gyanyima Limestone along the Yarlung-Zangbo Suture in southern Tibet, China. *Geological Journal, 45*(2-3), 308-318.

Webb, G.E., and Kamber, B.S. (2000). Rare earth elements in Holocene reefal microbialites: a new shallow seawater proxy. *Geochimica et Cosmochimica Acta, 64*, 1557–1565.

Williams, A. (1966). Growth and structure of the shell of living articulate bachiopods. *Nature*, *211*, 1146–1148.

Williams, A. (1973). The secretion and structural evolution of the shell of *thecideidine* brachiopods. *Philosophical Transactions of the Royal Society of London. Series B, Biological Sciences*, 439–478.

Wyndham, T., McCulloch, M., Fallon, S., and Alibert, C. (2004). High–resolution coral records of rare earth elements in coastal seawater: biogeochemical cycling and a new environmental proxy. *Geochimica et Cosmochimica Acta*, *68*(9), 2067–2080.

Zaky, A.H., Brand, U., and Azmy, K., (2015). A new sample processing protocol for procuring seawater REE signatures in biogenic and abiogenic carbonates. *Chemical Geology*, *416*, 36-50.

Zaky, A.H, Azmy, K., Brand, U. and Svavarsson, J. (2016). Rare earth elements in deep-water articulated brachiopods: Evaluation of seawater masses. *Chemical Geology*, In revision.

Zezina, O.N. (2008). Biogeography of the recent brachiopods. *Paleontological Journal*, *42*(8), 830–858.

Zhang, J., and Nozaki, Y. (1996). Rare earth elements and yttrium in seawater: ICP–MS determinations in the East Caroline, Coral Sea, and South Fiji basins of the western South Pacific Ocean. *Geochimica et Cosmochimica Acta*, *60*(23), 4631–4644.

Zhang, Y., Lacan, F., and Jeandel, C. (2008). Dissolved rare earth elements tracing lithogenic inputs over the Kerguelen Plateau (Southern Ocean). *Deep Sea Research Part II: Topical Studies in Oceanography*, *55*(5), 638–652.

Ziegler, A.M. (1976). Silurian continental distribution, paleogeography, climatology and biogeography (abs.): 25th Internat. *Geol. Cong., Sydney, Australia, Abs*, *3*, 729.

CHAPTER 5

SUMMARY

The reliable and definitive cleaning protocol that was established by the current study, consists of a combination of physical and chemical procedures for preparing different archives for geochemical analyses in general and the REEs in particular.

1- For achieving such aspect, a database of modern and fossil brachiopods was tested with five cleaning procedures (P-1 to P-5) for the robustness of their seawater REE signatures.

1.1- Washing the specimens with distilled water prior to geochemical analysis (P-1) resulted in extremely elevated and remarkably different REE concentrations and patterns from that stored in the calcite lattice caused by continued the presence of internal and external contaminants.

1.2- Immersion in hydrogen peroxide (P-2) eliminates primarily the organic remnants. However, the thickness of the proteinaceous periostracum membrane prevents its full elimination and at the same time blocks the removal of the adsorbed organic nano-particulates within the shells punctuates, which in turn resulted in partial depletions in the Ce/Ce* anomalies only. Meanwhile, the immersion for more than 3 continuous days does not remove the periostracums only, but dissolves the shell's layers as well.

1.3- Physical abrasion (P-3) removes mainly the scavenged inorganic nano-particulates, but only some of the periostracum sheet and the primary layer. It depletes the REE contents remarkably and improves slightly the REE_{SN} patterns.

1.4- Physical removal of the organic tissues and adhering surface contaminants followed by an acid leaching with 10% hydrochloric acid (P-4) resulted in REE contents consistent with seawater signatures.

1.5- Combining the different cleaning steps of mechanical abrasion, hydrogen peroxide immersion and hydrochloric acid leaching (P-5) gave REE results similar to that of P-4, but with depletions in the ∑REE contents.

2- Acquiring robust unaltered REE signatures requires the adherence to the cleaning steps outlined in procedure P-5 for modern biogenic archives, and to those in procedure P-4 for fossil archives, including whole rock.

3- The processing protocol is not infallible in removing the contaminants and its completion must be assessed in the light of the archives' elemental composition.

4- Correlating the elemental and the REE compositions of the properly cleaned and screened Paleozoic fossil brachiopods and enclosed near-micritic whole rock suggests that only samples with insignificantly to slightly elevated Mn and Fe concentrations should be considered reliable proxies of paleoredox.

5- The whole rock samples with Fe and Mn concentrations higher than 300 and 100 ppm respectively, their Ce/Ce* anomaly values should be adjusted by −13% prior to be utilized in the paleoredox studies.

The REE incorporations of the Terebratulida and Rynchonellida shells recovered from the deep waters (>500 m) of the Caribbean Sea, North Atlantic, South Pacific and Southern Oceans have been evaluated to assess their proxy potential for paleo-oceanic studies.

1- The brachiopods yielded remarkably elevated ∑REE concentrations compared to their ambient seawater. Their secondary layers are enriched by a factor that varies between the different water masses from as low as $0.15x10^5$ in shells of the Caribbean to as high as $1.83x10^5$ in those of the South Pacific; with average and geometric mean values of $0.81x10^5$ and $0.61\ x10^5$, respectively.

2- Calculating the distribution coefficients between the calcite lattice and the ambient seawater suggest insignificant variations in the REE incorporations of the two brachiopod orders. Their log K_D values differ within the REE series between 2.6 and 1.4, which are consistent with the results of foraminiferal calcite.

3- Variations in the prevalent oceanographic conditions seem to have remarkable impacts on the shells' Ce anomalies. Meanwhile, the open-water shells exhibit a vertical Ce/Ce* profile coupled with the Ce vertical curve in seawater.

4- Shells of the investigated four main localities display gradual $LREE_{SN}$ and $MREE_{SN}$ enrichments similar to those of their ambient water masses with average L:H and M:H ratios of about 0.45 and 0.52, respectively. On the other hand, their M:H ratios are in direct proportion with increasing depth defining a secondary seawater signature trend.

5- Evaluating the REE incorporation of the deep water (> 500m) articulated brachiopods strongly support the reliability of their shells as an REE proxy for paleoceanographic investigations.

Investigating the REE incorporation of the articulated brachiopod shells' structures implies that:

1- Precipitation of the umbo region is either with selective REE uptake or species dependency during the growth of the juvenile stage.

2- Primary layers are secreted with variable and incidental REE contents.

3- Inconsistent, but insignificant variations in the REE uptake of the secondary layers of the pedicle and brachial valves occur, with a small range of differences that falls within the natural variation of the brachiopod's lattice incorporation.

4- Domination of the primary layers over the shell structures of the thecideidines versus other articulated shells is reflected in the remarkable variations in their elemental, REE compositions and the REE_{SN} patterns.

Assessing the impacts of changes in the seawater physicochemical parameters on the REE fractionations and distributions of the shallow (<500 m) and deep-water (>500 m) brachiopods suggest that:

1- Depth plays a major rule on the shells' fractionations of LREEs and MREEs, but moderate on the HREEs.

2- Temperature has a small influence on the REE concentrations in the shells of the shallow water setting only.

3- Impacts of salinity on the compositions and the fractionations of the shallow water shells are moderate, whereas on the deep shells are weak.

4- The investigated parameters seem to have no effect on the shells' Ce/Ce* anomalies in the shallow water setting, but in the deep waters, the depth appears to have a significant control.

Shallow water shell L:H ratio was used to construct a REE bathymetric sensor (RBS) classification. The L:H values and corresponding depth intervals of the RBS were used to determine the water depths of fossil brachiopods and their corresponding whole rock.

Appendix 2-1. Geochemical data of the bulk and Standard samples, and investigated modern and Paleozoic brachiopods and whole rock, their Ce anomalies (Ce/Ce*) calculated based on de Baar et al. (1988) equation and their $(La/Yb)_{SN}$ Values.

	Sr	Mn	Fe	U	La	Ce	Pr	Nd	Sm	Eu	Gd	Tb	Dy	Ho	Er	Tm	Yb	Lu	∑REEs	Ce/Ce*	$(La/Yb)_{SN}$
Machine detection limit	0.00007	0.00005	0.00249	0.00023	0.00041	0.00020	0.00048	0.00071	0.00088	0.00028	0.00067	0.00026	0.00051	0.00014	0.00043	0.00020	0.00079	0.00022			
Bulk Samples																					
blank-1	0.768	N/A	N/A	0.012	0.037	0.076	0.008	0.031	0.008	0.000	0.004	N/A	0.001	0.000	N/A	N/A	0.004	N/A			
blank-2	0.393	N/A	N/A	0.004	0.004	0.005	N/A	N/A	N/A	N/A	N/A	N/A	N/A	N/A	N/A	N/A	N/A	N/A			
blank-3	0.209	N/A	N/A	0.003	0.005	0.009	N/A	N/A	N/A	N/A	N/A	N/A	N/A	N/A	N/A	N/A	N/A	N/A			
blank-4	0.121	0.231	9.734	0.001	0.000	N/A	N/A	N/A	N/A	N/A	N/A	N/A	0.007	0.000	0.002	0.001	0.004	0.000			
blank-5	0.078	0.076	18.858	N/A	N/A	0.000	N/A	N/A	N/A	0.000	N/A	N/A	N/A	N/A	N/A	N/A	N/A	N/A			
blank-6	0.094	0.122	N/A	0.006	N/A	N/A	N/A	N/A	0.001	N/A	N/A	N/A	N/A	N/A	N/A	0.000	0.001	0.000			
blank-7	N/A	0.003	N/A	0.007	0.003	0.001	N/A	0.003	0.007	N/A	0.010	N/A	N/A	N/A	0.002	N/A	N/A	N/A			
blank-8	0.047	0.119	14.240	0.005	0.001	0.002	N/A	N/A	N/A	0.002	N/A	N/A	0.004	N/A	N/A	N/A	0.000	N/A			
Standards																					
DLS 88a (Published values/ underline are internal values)	42.35	**232**	**1958**	0.16	1.42	2.56	0.36	1.46	0.30	0.07	0.32	0.05	0.29	0.06	0.17	0.02	0.14	0.02			
DLS 88a-1	45.441	219.080	1563.643	0.361	1.580	2.875	0.395	1.617	0.321	0.068	0.358	0.056	0.323	0.067	0.194	0.024	0.154	0.022			
DLS 88a-2	40.304	203.109	1708.808	0.184	1.626	2.918	0.393	1.698	0.362	0.096	0.426	0.068	0.375	0.087	0.241	0.030	0.190	0.028			
DLS 88a-3	35.575	192.980	1557.722	0.173	1.608	2.914	0.406	1.711	0.345	0.079	0.413	0.064	0.360	0.072	0.210	0.026	0.172	0.022			
DLS 88a-4	32.514	140.681	916.232	0.076	1.040	1.808	0.253	1.043	0.210	0.051	0.238	0.036	0.210	0.045	0.116	0.015	0.105	0.015			
DLS 88a-5	29.195	165.833	1068.970	0.093	1.406	2.481	0.343	1.423	0.288	0.063	0.306	0.049	0.281	0.062	0.168	0.021	0.127	0.017			
DLS 88a-6	37.435	179.397	1331.512	0.095	1.311	2.343	0.328	1.348	0.263	0.063	0.305	0.048	0.262	0.058	0.164	0.022	0.129	0.018			
DLS 88a-7	36.998	181.675	1370.782	0.104	1.307	2.314	0.327	1.300	0.275	0.065	0.285	0.044	0.251	0.052	0.160	0.021	0.126	0.019			
DLS 88a-8	42.865	206.592	1458.677	0.106	1.336	2.450	0.341	1.406	0.277	0.066	0.301	0.048	0.283	0.059	0.169	0.022	0.131	0.020			
CCH-1 (Published values)	**284**	**54**	**1189**	**3.70**	**4.70**	**3.40**	**0.84**	**3.70**	**0.75**	**0.16**	**0.76**	**0.10**	**0.65**	**0.10**	**0.35**	**0.05**	**0.27**	**0.04**			
CCh-1-1	361.615	59.315	402.557	4.248	6.302	4.604	1.234	5.212	0.980	0.230	1.097	0.161	0.882	0.180	0.487	0.057	0.354	0.046			
CCh-1-2	297.381	48.697	692.677	4.727	4.695	3.326	0.867	3.838	0.698	0.190	0.923	0.145	0.822	0.166	0.458	0.057	0.347	0.050			
CCh-1-3	469.288	74.147	723.375	9.009	8.582	6.106	1.585	6.832	1.299	0.335	1.638	0.237	1.360	0.274	0.799	0.099	0.606	0.080			
CCh-1-4	267.257	42.000	246.940	2.575	4.048	2.934	0.814	3.333	0.621	0.147	0.697	0.110	0.564	0.110	0.311	0.039	0.228	0.032			
CCh-1-5	219.518	36.730	180.824	3.748	5.359	3.844	1.053	4.380	0.827	0.197	0.949	0.147	0.789	0.151	0.430	0.050	0.302	0.042			
CCh-1-6	299.973	43.491	242.728	3.186	4.693	3.425	0.940	3.908	0.747	0.171	0.821	0.120	0.654	0.136	0.361	0.046	0.262	0.041			
CCh-1-7	294.108	48.677	292.530	3.234	4.754	3.450	0.933	3.853	0.749	0.162	0.813	0.125	0.650	0.135	0.366	0.046	0.252	0.038			
CCh-1-8	318.536	49.182	280.550	3.082	4.586	3.355	0.901	3.711	0.686	0.173	0.767	0.120	0.664	0.127	0.374	0.047	0.261	0.036			

	Sr	Mn	Fe	U	La	Ce	Pr	Nd	Sm	Eu	Gd	Tb	Dy	Ho	Er	Tm	Yb	Lu	∑REEs	Ce/Ce*	$(La/Yb)_{SN}$
New Protocol																					
P-1: Water Washed (WW)																					
WW-1	551	459	777	0.16	1.27	2.48	0.23	0.97	0.18	0.05	0.24	0.04	0.23	0.06	0.16	0.03	0.16	0.03	6.13	0.98	0.58
WW-2	902	528	1417	0.10	1.10	1.78	0.21	0.94	0.19	0.05	0.25	0.04	0.25	0.06	0.17	0.03	0.15	0.03	5.26	0.78	0.54
WW-3	840	1982	3119	0.30	1.55	4.00	0.27	1.11	0.22	0.05	0.28	0.04	0.27	0.06	0.19	0.03	0.19	0.03	8.30	1.32	0.59
WW-4	946	876	1777	0.13	1.03	2.47	0.18	0.77	0.16	0.04	0.19	0.03	0.19	0.05	0.14	0.02	0.14	0.02	5.44	1.21	0.56
WW-5	1043	2073	2790	0.34	1.39	3.59	0.23	0.94	0.20	0.05	0.25	0.04	0.23	0.05	0.17	0.02	0.16	0.03	7.35	1.35	0.63
P-2: WW, Hydrogen Peroxide (H_2O_2)																					
WW, H_2O_2-1	1001	723	1036	0.10	1.71	2.67	0.34	1.50	0.31	0.08	0.38	0.06	0.36	0.08	0.24	0.03	0.21	0.03	8.01	0.75	0.60
WW, H_2O_2-2	1271	1305	1635	0.22	2.10	4.25	0.41	1.79	0.37	0.09	0.43	0.07	0.41	0.09	0.28	0.04	0.26	0.04	10.65	0.99	0.60
WW, H_2O_2-3	636	317	537	0.05	1.25	1.47	0.26	1.09	0.22	0.06	0.27	0.05	0.28	0.06	0.18	0.02	0.16	0.02	5.40	0.57	0.59
WW, H_2O_2-4	448	1053	978	0.13	1.58	1.77	0.30	1.25	0.26	0.06	0.32	0.06	0.34	0.07	0.22	0.03	0.20	0.03	6.48	0.56	0.58
P-3: WW, Physical Cleaning (PC)																					
WW, PC-1	542	103	171	0.02	0.32	0.39	0.06	0.30	0.06	0.01	0.07	0.01	0.08	0.02	0.06	0.01	0.06	0.01	1.45	0.58	0.41
WW, PC-2	437	169	323	0.02	0.32	0.54	0.06	0.26	0.05	0.01	0.07	0.01	0.07	0.02	0.06	0.01	0.06	0.01	1.55	0.83	0.41
WW, PC-3	637	113	783	0.03	0.28	0.38	0.05	0.23	0.04	0.01	0.06	0.01	0.06	0.01	0.05	0.01	0.05	0.01	1.25	0.67	0.44
WW, PC-4	443	183	980	0.03	0.29	0.50	0.06	0.23	0.07	0.01	0.06	0.01	0.07	0.02	0.05	0.01	0.05	0.01	1.43	0.87	0.43
P-4:WW, PC, Hydrochloric Acid (HCl)																					
WW, PC, HCl-1	838	71	126	0.03	0.83	0.26	0.17	0.72	0.15	0.04	0.19	0.03	0.20	0.05	0.14	0.02	0.13	0.02	2.94	0.15	0.48
WW, PC, HCl-2	428	20	46	0.00	0.12	0.05	0.03	0.11	0.02	0.01	0.03	0.01	0.02	0.01	0.02	0.00	0.02	0.00	0.43	0.22	0.56
WW, PC, HCl-3	850	55	144	0.02	0.64	0.24	0.13	0.59	0.13	0.03	0.15	0.03	0.16	0.04	0.11	0.02	0.10	0.02	2.37	0.18	0.46
WW, PC, HCl-4	562	59	106	0.01	0.31	0.17	0.06	0.27	0.05	0.01	0.07	0.01	0.07	0.02	0.06	0.01	0.05	0.01	1.18	0.26	0.45
P-5: WW, PC, H_2O_2, HCl																					
WW, PC, H_2O_2, HCl-1	386	5	14	N/A	0.04	0.01	0.01	0.04	0.01	0.00	0.01	0.00	0.01	0.00	0.01	0.00	0.01	0.00	0.16	0.13	0.56
WW, PC, H_2O_2, HCl-2	363	5	24	N/A	0.02	0.01	0.01	0.03	0.00	0.00	0.01		0.01	0.00	0.00	0.00	0.01	0.00	0.10	0.24	0.29
WW, PC, H_2O_2, HCl-3	379	7	26	N/A	0.02	0.01	0.00	0.03	0.01	0.00	0.00	0.00	0.01	0.00		0.00		0.00	0.09	0.22	N/A
WW, PC, H_2O_2, HCl-4	366	3	31	N/A	0.03	0.02	0.01	0.03	0.01	0.00	0.01	0.00	0.01	0.00	0.00	0.00	0.01		0.12	0.28	0.30
WW, PC, H_2O_2, HCl-5	672	24	124	0.01	0.22	0.08	0.05	0.22	0.05	0.01	0.06	0.01	0.07	0.01	0.04	0.01	0.04	0.01	0.87	0.17	0.37
WW, PC, H_2O_2, HCl-6	491	14	106	0.00	0.14	0.07	0.03	0.15	0.03	0.01	0.04	0.01	0.04	0.01	0.02	0.00	0.03	0.00	0.58	0.23	0.38
WW, PC, H_2O_2, HCl-7	664	25	520	0.01	0.14	0.07	0.03	0.14	0.04	0.01	0.03	0.01	0.04	0.01	0.03	0.00	0.03	0.00	0.59	0.24	0.36
WW, PC, H_2O_2, HCl-8	422	7	64	0.00	0.06	0.03	0.01	0.05	0.01	0.00	0.01	0.00	0.02	0.00	0.01	0.00	0.01	0.00	0.23	0.20	0.32
WW, PC, H_2O_2, HCl-9	374	2	51	N/A	0.03	0.01	0.01	0.04	0.00	0.00	0.01	0.00	0.01	0.00	0.01	0.00	0.00	0.00	0.12	0.18	0.47

B

	Sr	Mn	Fe	U	La	Ce	Pr	Nd	Sm	Eu	Gd	Tb	Dy	Ho	Er	Tm	Yb	Lu	∑REEs	Ce/Ce*	$(La/Yb)_{SN}$
Modern																					
Case Study 1 (Caribbean Sea)																					
Virgin Islands Basin (P-3)																					
VIB1[a]	N/A	N/A	N/A	N/A	0.20	0.53	0.04	0.23	0.05	0.01	0.07	0.01	0.07	0.01	0.04	0.01	0.04	0.00	1.32	1.18	0.34
VIB2	885	38	540	0.03	0.22	0.57	0.06	0.24		0.02	0.07	0.01	0.07	0.02	0.04	0.01	0.04	0.00	1.38	1.18	0.45
Venezuela Basin (P-5)																					
VB-St1-1[b]	880	9	414	0.09	0.03	0.03	0.00	0.02	0.00	0.00		0.00			0.00	0.00	0.01	0.00	0.10	0.46	0.21
VB-St1-2[b]	369	11	37	0.01	0.03	0.03	0.01	0.02			0.00	0.00	0.01	0.00	0.00		0.01		0.10	0.57	0.22
VB-St1-3[b]	361	23	61	0.00	0.06	0.07	0.01	0.06			0.02		0.02	0.01	0.02	0.00	0.01	0.00	0.28	0.54	0.37
VB-St2-1[b]	879	7	341	0.02	0.02	0.03	0.01			0.00	0.01	0.00			0.00	0.00	0.00	0.00	0.09		0.47
VB-St2-2[b]	393	24	50	0.00	0.06	0.07	0.01	0.05			0.01		0.02	0.00	0.01	0.00	0.01		0.26	0.53	0.44
VB-St2-3[b]	435	23	78	0.01	0.11	0.09	0.02	0.11	0.02	0.01	0.02	0.00	0.03	0.01	0.03	0.00	0.02	0.00	0.46	0.37	0.44
Case Study 2 (North Atlantic)																					
Irminger Basin (P-2)																					
IrB-D-1	854	22	26	0.01	0.03	0.07	0.01	0.04	0.01	0.00	0.01	0.00	0.01	0.00	0.00	0.00	0.00	0.00	0.18	0.87	0.72
IrB-D-2	861	20	29	0.01	0.03	0.08	0.01	0.04	0.01	0.00	0.01	0.00	0.01	0.00	0.00	0.00	0.00	0.00	0.21	1.10	1.04
Irminger Basin (P-5)																					
IrB-D-3	354	260	465	0.03	0.34	0.62	0.07	0.29	0.06	0.02	0.08	0.01	0.08	0.02	0.05	0.01	0.05	0.01	1.71	0.89	0.46
IrB-D-4	373	159	283	0.01	0.33	0.57	0.06	0.28	0.04	0.01	0.08	0.01	0.08	0.02	0.05	0.01	0.07	0.01	1.63	0.84	0.36
IrB-D-5	407	137	247	0.02	0.26	0.48	0.06	0.24	0.05	0.01	0.07	0.01	0.07	0.02	0.05	0.01	0.06	0.01	1.37	0.87	0.33
IrB-D-6	444	264	414	0.02	0.39	0.79	0.08	0.33	0.06	0.01	0.08	0.01	0.09	0.02	0.06	0.01	0.05	0.01	1.98	0.98	0.58
Iceland Basin (P-5)																					
IcB-D-1[b]	438	27	84	0.01	0.28	0.09	0.05	0.24	0.05	0.01	0.06	0.01	0.06	0.01	0.04	0.01	0.04	0.01	0.94	0.15	0.49
IcB-D-2[b]	465	23	60	0.00	0.18	0.06	0.04	0.15	0.03	0.01	0.05	0.01	0.05	0.01	0.03	0.01	0.03	0.00	0.66	0.16	0.43
IcB-D-3[b]	495	33	82	0.01	0.23	0.08	0.04	0.21	0.04	0.01	0.05	0.01	0.05	0.01	0.03	0.00	0.04	0.01	0.81	0.17	0.47

C

	Sr	Mn	Fe	U	La	Ce	Pr	Nd	Sm	Eu	Gd	Tb	Dy	Ho	Er	Tm	Yb	Lu	∑REEs	Ce/Ce*	$(La/Yb)_{SN}$
Case Study 3 (Paleozoic brachiopods and whole rock)																					
Uppermost Permian, Gyanyima Fm-Tibet																					
Brachiopods																					
Per. 1[c]	87	63	726	0.06	2.51	2.38	0.37	1.33	0.23	0.05	0.30	0.05	0.33	0.08	0.26	0.04	0.25	0.04	8.21	0.52	0.76
Per. 2[c]	194	41	91	0.06	3.13	1.67	0.47	1.89	0.33	0.08	0.43	0.07	0.40	0.09	0.26	0.03	0.21	0.03	9.10	0.29	1.09
Per. 3[c]	220	46	683	0.05	2.66	1.74	0.44	1.73	0.31	0.08	0.41	0.05	0.31	0.06	0.19	0.03	0.14	0.02	8.16	0.35	1.45
Per. 4[c]	184	82	628	0.02	2.31	1.69	0.36	1.33	0.23	0.06	0.27	0.04	0.27	0.06	0.18	0.02	0.12	0.02	6.97	0.40	1.39
Per. 5[c]	381	25	694	0.11	0.36	0.25	0.06	0.27	0.04	0.02	0.08	0.01	0.07	0.02	0.04	0.01	0.03	0.00	1.27	0.35	0.90
Per. 6[c]	208	36	93	0.06	3.81	2.15	0.63	2.61	0.49	0.11	0.62	0.10	0.53	0.12	0.33	0.04	0.25	0.04	11.84	0.29	1.10
Per. 7[c]	574	13	30	0.11	3.86	3.94	0.62	2.29	0.50	0.11	0.52	0.10	0.57	0.12	0.36	0.05	0.39	0.05	13.49	0.55	0.72
Per. 8[c]	576	4	19	0.03	0.23	0.14	0.03	0.12	0.02	0.00	0.02	0.00	0.02	0.00	0.01	0.00	0.01	0.00	0.61	0.33	2.59
Per. 9[c]	612	27	976	0.32	4.19	2.25	0.73	2.77	0.52	0.11	0.48	0.08	0.37	0.07	0.19	0.02	0.14	0.02	11.94	0.28	2.28
Per. 10[c]	518	27	659	0.06	2.26	1.08	0.34	1.43	0.25	0.05	0.30	0.04	0.22	0.05	0.14	0.01	0.09	0.01	6.28	0.25	1.83
Whole rock																					
Per. 1[c]	96	75	301	0.06	7.62	6.88	1.42	5.88	1.04	0.25	1.40	0.22	1.29	0.30	0.90	0.12	0.76	0.12	28.20	0.45	0.74
Per. 2[c]	99	69	91	0.06	3.98	2.95	0.63	2.60	0.45	0.11	0.56	0.08	0.48	0.11	0.31	0.04	0.24	0.03	12.55	0.39	1.24
Per. 3[c]	129	46	104	0.06	3.47	2.35	0.57	2.23	0.41	0.09	0.47	0.07	0.41	0.09	0.27	0.03	0.20	0.03	10.70	0.36	1.26
Per. 4[c]	96	61	98	0.06	4.31	2.23	0.62	2.44	0.41	0.10	0.51	0.07	0.40	0.08	0.24	0.03	0.18	0.02	11.63	0.28	1.80
Per. 5[c]	111	41	116	0.08	5.17	3.48	0.83	3.43	0.63	0.16	0.82	0.13	0.73	0.17	0.48	0.06	0.37	0.05	16.50	0.35	1.04
Per. 6[c]	128	45	98	0.10	7.32	4.05	1.23	4.92	0.93	0.23	1.08	0.17	0.94	0.20	0.56	0.07	0.41	0.06	22.15	0.29	1.32
Per. 7[c]	254	122	960	3.9*	8.11	6.20	1.36	5.40	0.97	0.21	1.12	0.18	0.96	0.22	0.66	0.09	0.56	0.08	26.13	0.40	1.08
Per. 8[c]	121	57	157	1.39	13.98	10.00	2.14	8.29	1.33	0.26	1.49	0.20	1.09	0.22	0.61	0.07	0.46	0.07	40.22	0.39	2.22
Per. 9[c]	277	52	819	2.68	4.40	2.28	0.61	2.58	0.48	0.10	0.58	0.08	0.50	0.11	0.31	0.04	0.21	0.03	12.30	0.28	1.57
Per. 10-1[c]	89	40	168	0.37	30.62	13.07	5.12	21.34	4.79	0.82	4.93	0.58	4.21	0.61	2.80	0.20	2.36	1.35	92.78	0.22	0.96
Per. 10-2[c]	82	38	146	0.38	33.49	14.49	5.81	23.17	4.15	0.94	4.52	0.66	3.37	0.69	1.90	0.23	1.33	0.18	94.94	0.22	1.87
Upper Desmoinsean Naco Formation, Arizona																					
Brachiopods																					
Penn. 2	397	51	346	0.42	4.44	4.51	0.65	2.03	0.31	0.07	0.30	0.04	0.24	0.06	0.22	0.05	0.36	0.06	13.34	0.58	0.92
Penn. 3-1	590	45	769	0.13	3.00	3.45	0.40	1.30	0.18	0.04	0.16	0.02	0.14	0.03	0.09	0.01	0.09	0.01	8.93	0.67	2.39
Penn. 3-2	509	84	913	0.24	5.51	6.71	0.81	2.76	0.38	0.08	0.43	0.06	0.30	0.07	0.22	0.03	0.24	0.03	17.64	0.68	1.71
Whole rock																					
Penn. 2	441	171	1434	1.17	7.24	10.86	1.51	5.67	1.04	0.19	1.01	0.15	0.80	0.15	0.43	0.05	0.34	0.05	29.47	0.75	1.59
Penn. 3	441	142	1490	0.97	5.18	7.62	1.08	4.04	0.72	0.14	0.75	0.11	0.61	0.12	0.34	0.05	0.27	0.04	21.08	0.74	1.39

	Sr	Mn	Fe	U	La	Ce	Pr	Nd	Sm	Eu	Gd	Tb	Dy	Ho	Er	Tm	Yb	Lu	∑REEs	Ce/Ce*	$(La/Yb)_{SN}$
Middle Desmoinsean, Boggy Formation, Oklahoma																					
Brachiopods																					
Penn. 1-1	449	54	369	0.35	0.91	1.10	0.14	0.53	0.11	0.03	0.13	0.02	0.12	0.03	0.07	0.01	0.06	0.01	3.27	0.65	1.08
Penn. 1-2	483	44	225	0.45	0.74	1.04	0.14	0.50	0.10	0.02	0.11	0.02	0.10	0.02	0.05	0.01	0.06	0.01	2.92	0.73	0.99
Penn. 1-3	765	93	794	0.05	0.22	0.24	0.03	0.12	0.009*	0.01	0.02	0.00	0.02	0.00	0.01	0.00	0.01	0.00	0.69	0.61	1.48
Whole rock																					
Penn. 1	1090	256	1682	0.93	5.03	7.92	1.00	3.95	0.69	0.17	0.76	0.12	0.58	0.12	0.33	0.04	0.27	0.04	21.03	0.79	1.38
Lower Silurian (Llandoverian), Anticosti Island, Canada																					
Brachiopods																					
Sil. 1-1[a]	1027	35	N/A	N/A	0.62	0.96	0.13	0.49	0.08	0.02	0.09	0.01	0.07	0.01	0.03	0.00	0.04	0.00	2.56	0.77	1.15
Sil. 1-2[a]	1027	35	N/A	N/A	0.61	1.00	0.13	0.51	0.09	0.02	0.09	0.01	0.06	0.01	0.04	0.00	0.03	0.00	2.61	0.81	1.64
Sil. 2-1[a]	1217	30	N/A	N/A	0.32	0.43	0.06	0.27	0.05	0.0029*	0.06	0.01	0.05	0.01	0.02	0.001*	0.02	0.00	1.32	0.66	1.14
Sil. 2-2[a]	1067	29	N/A	N/A	0.68	1.02	0.13	0.62	0.09	0.03	0.14	0.02	0.11	0.02	0.07	0.01	0.04	0.00	2.99	0.71	1.18
Sil. 2-3	929	25	450	0.03	1.13	1.54	0.22	0.88	0.17	0.04	0.20	0.03	0.17	0.03	0.09	0.01	0.07	0.01	4.58	0.68	1.16
Sil. 2-4	889	28	577	0.03	0.81	1.02	0.14	0.53	0.11	0.03	0.13	0.02	0.10	0.02	0.06	0.01	0.04	0.00	3.02	0.66	1.36
Sil. 3-1[a]	1309	22	N/A	N/A	0.53	0.51	0.10	0.41	0.06	0.02	0.09	0.01	0.06	0.02	0.03	0.00	0.01	0.00	1.87	0.49	2.65
Sil. 3-2	1060	76	806	0.06	0.84	0.92	0.17	0.71	0.15	0.04	0.18	0.02	0.14	0.03	0.08	0.01	0.05	0.01	3.34	0.53	1.15
Sil. 3-3	1101	69	451	0.06	1.59	1.59	0.29	1.27	0.27	0.06	0.30	0.05	0.25	0.05	0.13	0.02	0.09	0.01	5.97	0.50	1.32
Sil. 4-1[a]	1269	16	N/A	N/A	0.26	0.39	0.06	0.24	0.05	0.00	0.06	0.01	0.04	0.01	0.03	0.00	0.03	0.00	1.18	0.70	0.71
Sil. 4-2	1039	25	631	0.01	0.11	0.18	0.02	0.11	0.03	0.00	0.02	0.00	0.02	0.00	0.02	0.0003*	0.01	0.00	0.53	0.75	0.83
Sil. 4-3[a]	1275	23	N/A	N/A	0.35	0.54	0.08	0.30	0.08	0.02	0.07	0.01	0.07	0.01	0.03	0.00	0.02	0.00	1.58	0.74	1.11
Sil. 5[a]	N/A	N/A	N/A	N/A	0.18	0.26	0.04	0.16	0.03	0.01	0.03	0.00	0.03	0.01	0.01	0.00	0.02	0.00008*	0.79	0.70	0.70
Sil. 6	1129	18	631	0.02	0.17	0.27	0.03	0.13	0.03	0.01	0.03	0.00	0.02	0.00	0.01	0.00	0.01	0.00	0.72	0.78	0.97
Whole rock																					
Sil. 1	257	117	289	0.02	1.55	2.60	0.30	1.26	0.24	0.06	0.28	0.04	0.21	0.04	0.12	0.01	0.08	0.01	6.81	0.83	1.39
Sil. 2[a]	576	335	N/A	N/A	3.60	5.87	0.76	3.22	0.53	0.13	0.68	0.10	0.58	0.14	0.35	0.03	0.24	0.03	16.27	0.78	1.10
Sil. 3	875	633	20587.6*	0.65	20.40	28.62	4.79	19.78	3.96	1.00	4.15	0.61	3.19	0.60	1.57	0.19	1.13	0.16	90.14	0.65	1.33
Sil. 4	1050	203	2564	0.12	2.83	5.86	0.80	3.16	0.63	0.16	0.69	0.11	0.58	0.11	0.30	0.04	0.23	0.03	15.51	0.91	0.93
Sil. 5[a]	475	673	N/A	N/A	5.94	11.09	1.49	5.91	1.20	0.27	1.22	0.18	0.98	0.19	0.48	0.07	0.39	0.06	29.48	0.86	1.11
Sil. 6	784	48	838	0.10	1.01	1.95	0.26	1.01	0.21	0.05	0.22	0.03	0.17	0.04	0.10	0.01	0.07	0.01	5.15	0.89	1.02

Note: Concentations in ppm.
N/A: Value is not available due to the machine detection limit.
[a]: From Azmy et al. (2011).
[b]: From Zaky et al. (2015).
[c]: From Garbelli et al. (2015).
*: Anomalous concentrations, thus, ignored in the calculations.

Appendix 2-2. Traditional cleaning procedures of the different biogenic and abiogenic REE archives compiled from 53 published articles.

Source	Archive	Age	Cleaning
Biogenic apatite			
Hosler et al., 1991	Conodonts	Permian to Triassic	N/M
Grandjean-Lécuyer et al., 1993	"	Late Devonian	N/M
Armstrong et al., 2001	"	Devonian to Carboniferous	N/M
Sano and Terada 2001	"	Mississippian	N/M
Girard and Lécuyer 2002	"	Late Devonian	N/M
Bright et al., 2009	"	Pennsylvanian	Ultrasonically cleaned in deionized water
Chen et al., 2012	"	Ordovician	N/M
Song et al., 2012	"	Late Permian to Late Triassic	Water washed
Zhao et al., 2013	"	Permian	N/M
Wright et al., 1984	Conodonts & ichthyolith	Late Cambrian to Recent	Ultrasonically cleaned in absolute ethanol
Wright et al., 1987	Conodonts, inarticulated brachiopods & ichthyolith	Cambrian to Recent	Acetone washed; ultrasonically cleaned in absolute ethanol
Grandjean and Albarede, 1989	Conodonts & fish teeth	Devonian, Triassic & Eocene	N/M
Bertram et al., 1992	Conodont elements & fish material	Silurian	Sonicated in water and ammonium chloride
Felitsyn et al., 1998	Conodonts & organophosphatic brachiopods	Cambrian & Ordovician	N/M
Elderfield and Pagett, 1986	Ichthyolith	Modern	Water washed, ultrasonically cleaned; sonicated
Grandjean et al., 1987	Fish remains	Triassic to Recent	Ultrasonically cleaned
Grandjean et al., 1988	Fish debris	Late Cretaceous to Early Cenozoic	N/M
Lecuyer et al. , 2004	Fish teeth	Modern	Water washed; cleaned in nitric acid
Kocsis et al., 2007	Shark teeth	Miocene	N/M
Picard et al., 2002	Fish & reptile teeth	Jurassic	N/M
Lecuyer et al. , 1998	Phosphatic brachiopods	Cambrian, Ordovician & Modern	N/M
Kemp and Trueman 2003	Biogenic apatite (coprolite, bone & soft-tissue)	Jurassic	N/M
Lecuyer et al. , 2003	Vertebrate remains	Late Cretaceous	Sodium hypochlorite; acetic acid-acetate buffer
Grandstaff and Terry Jr., 2009	Vertebrates	Paleogene	Physically and ultrasonically cleaned
Kocsis et al., 2009	Vertebrates	Late Cretaceous	Ultrasonically cleaned in distilled water
Kocsis et al., 2010	Teeth & bones	Triassic & Cretaceous	Ultrasonically cleaned
Herwartz et al., 2013	Bones	Early Triassic to Recent	N/M
McArthur and Walsh, 1984	Phosphorites	Devonian to Recent	N/M
Ilyin, 1998	"	Early Cambrian	N/M
Shields and Stille 2001	"	Cambrian	Physically cleaned

Source	Archive	Age	Cleaning
Biogenic calcite			
Palmer, 1985	Foraminifera	N/A	Water washed
Palmer and Elderfield, 1986	"	Cenozoic	Water washed; sonicated with ultrapure water and methanol
Roberts et al., 2012	"	Modern	Water washed, and H_2O_2
Sholkovitz and Shen, 1995	Coral	Modern	Sonicated three times in pure water and HNO_3
Webb and Kamber, 2000	Reefal microbialites	Holocene	N/M
Kamber and Webb, 2001	Microbialites	Late Archaean	Physically cleaned
Nothdurft et al., 2004	Reefal carbonates	Late Devonian	Water washed
Olivier and Boyet, 2006	Coral- & sponge-microbialite reefs	Jurassic	Physically cleaned
Webb et al., 2009	Scleractinian coral skeletons	Pleistocene	Physically cleaned
Johannesson et al., 2014	Stromatolites	Modern	N/M
Azmy et al., 2011	Articulated brachiopods	Modern, Ordovician, Silurian, Eocene & Oligocene	Physically cleaned and HCL leached
Azmy et al., 2012	"	Late Devonian	Physically cleaned; ultrasonically cleaned
Brand et al., 2012a	"	Pennsylvanian	Physically cleaned and HCL leached
Brand et al., 2012b	"	Late Permian	Physically cleaned and HCL leached
Abiogenic calcite			
Zhou and Kyte, 1988	Whole rock	Permian to Triassic	N/M
Toyoda et al., 1990	Pelagic sediments	N/A	N/M
Dolenec et al., 2001	Whole rock	Late Permian to Early Triassic	Visually examined
Algeo et al., 2007	"	Late Permian to Early Triassic	Visually examined
Feng et al., 2008	Carbonates	Middle Devonian to Miocene	Physically cleaned
Komiya et al., 2008	Carbonate minerals in rocks	Neoproterozoic to Recent	N/M
Fio et al., 2010	Whole rock	Late Permian to Early Triassic	N/M
Azmy et al., 2011	"	Ordovician, Silurian, Eocene & Oligocene	Physically cleaned and HCL leached
Azmy et al., 2012	"	Late Devonian	Physically cleaned; ultrasonically cleaned
Brand et al., 2012a	"	Pennsylvanian	Physically cleaned and HCL leached
Brand et al., 2012b	"	Late Permian	Physically cleaned and HCL leached
Bodin et al., 2013	Micritic limestones	Cretaceous	Physically cleaned
Loope et al., 2013	Carbonates	Permian to Triassic	Physically cleaned

References

Algeo, T.J., Hannigan, R., Rowe, H., Brookfield, M., Baud, A., Krystyn, L., and Ellwood, B.B. (2007). Sequencing events across the Permian–Triassic boundary, Guryul Ravine (Kashmir, India). *Palaeogeography, Palaeoclimatology, Palaeoecology*, *252*(1), 328-346.

Armstrong, H.A., Pearson, D.G., and Griselin, M. (2001). Thermal effects on rare earth and strontium isotope chemistry in single conodont element. *Geochimica et Cosmochimica Acta, 65*, 435–441.

Azmy, K., Brand, U., Sylvester, P., Gleeson, S., Logan, A., and Bitner, M.A. (2011). Biogenic low–Mg calcite (brachiopods): proxy of seawater–REE composition, natural processes and diagenetic alteration. *Chemical Geology*, *280*, 180–190.

Azmy, K., Poty, E., and Mottequin, B. (2012). Biochemostratigraphy of the Upper Frasnian in the Namur–Dinant Basin, Belgium: Implications for a global Frasnian–Famennian pre–event, *Palaeogeography, Palaeoclimatology, Palaeoecology, 313–314*, 93–106.

Bertram, C.J., Elderfield, H., Aldridge, R.J., and Conway Morris, S. (1992). $^{87}Sr/^{86}Sr$, $^{143}Nd/^{144}Nd$ and REEs in Silurian phosphatic fossils. *Earth and Planetary Science Letters, 113*(1–2), 239–249.

Bodin, S., Godet, A., Westermann, S., and Föllmi, K.B. (2013). Secular change in northwestern Tethyan water-mass oxygenation during the late Hauterivian–early Aptian. *Earth and Planetary Science Letters*, *374*, 121-131.

Brand, U., Jiang, G., Azmy, K., Bishop, J., and Montañez, I.P. (2012a). Diagenetic evaluation of a Pennsylvanian carbonate succession (Bird Spring Formation, Arrow Canyon, Nevada, USA)—1: Brachiopod and whole rock comparison. *Chemical Geology, 308*, 26-39.

Brand, U., Posenato, R., Came, R., Affek, H., Angiolini, L., Azmy, K., and Farabegoli, E. (2012b). The end–Permian mass extinction: a rapid volcanic CO_2 and CH_4–climatic catastrophe. *Chemical Geology*, *322–323*, 121–144.

Bright, C.A., Cruse, A.M., Lyons, T.W., MacLeod, K.G., Glascock, M.D., and Ethington, R.L. (2009). Seawater rare–earth element patterns preserved in apatite of Pennsylvanian conodonts?, *Geochimica et Cosmochimica Acta*, *73*, 1609–1624.

Chen, X., Zhou, L., Wei, K., Wang, J., and Li, Z. (2012). The environmental index of the rare earth elements in conodonts: Evidence from the Ordovician conodonts of the Huanghuachang Section, Yichang area. *Chinese Science Bulletin*, *57*, 349–359.

Dolenec, T., Lojen, S., and Ramovš, A. (2001). The Permian–Triassic boundary in Western Slovenia (Idrijca Valley section): magnetostratigraphy, stable isotopes, and elemental variations. *Chemical Geology*, *175*(1), 175-190.

Elderfield, H., and Pagett, R. (1986). Rare earth elements in ichthyoliths: variations with redox conditions and depositional environment. *Science of the Total Environment*, *49*, 175–197.

Felitsyn, S., Sturesson, U., Popov, L., and Holmer, L. (1998). Nd isotope composition and rare earth element distribution in early Paleozoic biogenic apatite from Baltoscandia: a signature of Iapetus ocean water. *Geology*, *26*(12), 1083-1086.

Feng, D., Chen, D., and Peckmann, J. (2009). Rare earth elements in seep carbonates as tracers of variable redox conditions at ancient hydrocarbon seeps. *Terra Nova*, *21*(1), 49-56.

Fio, K., Spangenberg, J.E., Vlahović, I., Sremac, J., Velić, I., and Mrinjek, E. (2010). Stable isotope and trace element stratigraphy across the Permian–Triassic transition: A redefinition of the boundary in the Velebit Mountain, Croatia. *Chemical geology*, *278*(1), 38-57.

Girard, C., and Lécuyer, C. (2002). Variations in Ce anomalies of conodonts through the Frasnian/Famennian boundary of Poland (Kowala–Holy Cross Mountains): implications for the redox state of seawater and biodiversity. *Palaeogeography, Palaeoclimatology, Palaeoecology, 181*, 299–311.

Grandjean, P., Cappetta, H., Michard, A., and Albaréde, F. (1987). The assessment of REE patterns and $^{143}Nd/^{144}Nd$ ratios in fish remains. *Earth and Planetary Science Letters, 84*, 181–196.

Grandjean, P., Cappetta H., and Albaréde F. (1988). The REE and εNd of 40–70 Ma old fish debris from the west–African platform. *Geophysical Research Letters,* 15, 389–392.

Grandjean-Lécuyer, P., Feist, R., and Albaréde, F. (1993). Rare earth elements in old biogenic apatites. *Geochimica et Cosmochimica Acta*, *57*, 2507–2514.

Grandjean-Lécuyer, P., and Albaréde, F. (1989). Ion probe measurement of rare–earth elements in biogenic phosphates. *Geochimica et Cosmochimica Acta, 53*, 3179–3183.

Grandstaff, D.E., and Terry, D.O. (2009). Rare earth element composition of Paleogene vertebrate fossils from Toadstool Geologic Park, Nebraska, USA. *Applied Geochemistry*, *24*(4), 733–745.

Herwartz, D., Tütken, T., Jochum, K.P., and Sander, P.M. (2013). Rare earth element systematics of fossil bone revealed by LA-ICPMS analysis. *Geochimica et Cosmochimica Acta*, *103*, 161–183.

Holser, W.T., Schönlaub, H.P., Boeckelmann, K., Magaritz, M., and Orth, C.J. (1991). The Permian-Triassic of the Gartnerkofel-1 core (Carnic Alps, Austria): synthesis and conclusions. *Abhandlungen der Geologischen Bundesanstalt*,*45*, 213-232.

Ilyin, A.V. (1998). Rare–Earths Geochemistry of "Old" Phosphorites and Probability of Direct Synsedimentational Precipitation and Accumulation of Phosphate, *Chemical Geology*, *144*, 243–256.

Johannesson, K.H., Telfeyan, K., Chevis, D.A., Rosenheim, B.E., and Leybourne, M.I. (2014). Rare earth elements in stromatolites–1. Evidence that modern terrestrial stromatolites fractionate rare earth elements during incorporation from ambient waters. In *Evolution of Archean Crust and Early Life,* Springer Netherlands, 385–411.

Kamber, B.S., and Webb, G.E. (2001). The geochemistry of late Archaean microbial carbonate: implications for ocean chemistry and continental erosion history. *Geochimica et Cosmochimica Acta*, *65*(15), 2509-2525.

Kemp, R.A., and Trueman, C. (2003). Rare earth elements in Solnhofen biogenic apatite: geochemical clues to the paleoenvironment. *Sedimentary Geology*, *155*, 109–127.

Kocsis, L., Vennemann, T.W., and Fontignie, D. (2007). Migration of sharks into freshwater systems during the Miocene and implications for Alpine paleoelevation. *Geology*, *35*(5), 451–454.

Kocsis, L., Osi, A., Vennemann, T., Trueman, C.N., and Palmer, M.R. (2009). Geochemical study of vertebrate fossils from the Upper Cretaceous (Santonian) Csehbánya Formation (Hungary): Evidence for a freshwater habitat of mosasaurs and pycnodont fish. *Palaeogeography, Palaeoclimatology, Palaeoecology*, *280*(3), 532-542.

Kocsis, L., Trueman, C.N., and Palmer, M.R. (2010). Protracted diagenetic alteration of REE contents in fossil bioapatites: direct evidence from Lu–Hf isotope systematics. *Geochimica et Cosmochimica Acta*, *74*(21), 6077–6092.

Komiya, T., Hirata, T., Kitajima, K., Yamamoto, S., Shibuya, T., Sawaki, Y., Ishikawa, T., Shu, D., Li, Y., and Han, J. (2008). Evolution of the composition of seawater through geologic time, and its influence on the evolution of life. *Gondwana Research*, *14*(1), 159-174.

Lécuyer, C., Grandjean, P., Barrat, J.A., Emig, C.C., Nolvak, J., Paris, F., and Robardet, M. (1998). $\delta^{18}O$ and REE contents of phosphatic brachiopods: a comparison between modern and lower Paleozoic populations. *Geochimica et Cosmochimica Acta, 62*, 2429–2436.

Lécuyer, C., Bogey, C., Garcia, J.P., Grandjean, P., Barrat, J.A., Bardet, N., and Pereda-Superbiola, X. (2003). Stable isotope composition and rare earth element content of vertebrate remains from the late Cretaceous of northern Spain (Lano): did the environmental record survive?, *Palaeogeography, Palaeoclimatology, Palaeoecology*, *193*, 457–471.

Lécuyer, C., Reynard, B., and Grandjean, P. (2004). Rare earth element evolution of Phanerozoic seawater recorded in biogenic apatites. *Chemical Geology,* 204, 63–102.

Loope, G.R., Kump, L.R., and Arthur, M.A. (2013). Shallow water redox conditions from the Permian–Triassic boundary microbialite: The rare earth element and iodine geochemistry of carbonates from Turkey and South China. *Chemical Geology*, *351*, 195–208.

McArthur, J.M., and Walsh, J.N. (1984). Rare–earth geochemistry of phosphorites. *Chemical Geology, 47*, 91–220.

Nothdurft, L.D., Webb, G.E., and Kamber, B.S. (2004). Rare earth element geochemistry of Late Devonian reefal carbonates, Canning Basin, Western Australia: confirmation of a seawater REE proxy in ancient limestones. *Geochimica et Cosmochimica Acta*, *68*(2), 263–283.

Olivier, N., and Boyet, M. (2006). Rare earth and trace elements of microbialites in Upper Jurassic coral–and sponge–microbialite reefs. *Chemical Geology*, *230*(1), 105–123.

Palmer, M.R. (1985). Rare earth elements in foraminifera tests. *Earth and Planetary Science Letters, 73*, 285–298.

Palmer, M.R., and Elderfield, H. (1986). Rare earth elements and neodymium isotopes in ferromanganese oxide coatings of Cenozoic foraminifera from the Atlantic Ocean. *Geochimica et Cosmochimica Acta*, *50*(3), 409-417.

Picard, S., Lécuyer, C., Barrat, J.A., Garcia, J.P., Dromart, G., and Sheppard, S.M.F. (2002). Rare earth element contents of Jurassic fish and reptile teeth and their potential relation to seawater composition (Anglo–Paris Basin, France and England). *Chemical Geology*, *186*, 1–16.

Roberts, N.L., Piotrowski, A.M., Elderfield, H., Eglinton, T.I., and Lomas, M.W. (2012). Rare earth element association with foraminifera. *Geochimica et Cosmochimica Acta*, *94*, 57-71.

Sano, Y., and Terada, K. (2001). In situ ion microprobe U-Pb dating and REE abundances of a carboniferous conodont. *Geophysical research letters*, *28*(5), 831-834.

Shields, G., and Stille, P. (2001). Diagenetic constraints on the use of cerium anomalies as palaeoseawater redox proxies: an isotopic and REE study of Cambrian phosphorites. *Chemical Geology*, *175*(1), 29-48.

Sholkovitz, E.R., and Shen, G.T. (1995). The incorporation of rare–earth elements in modern coral. *Geochimica et Cosmochimica Acta*, *59*, 2749–2756.

Song, H., Wignall, P.B., Tong, J., Bond, D.P., Song, H., Lai, X., Zhang, K., Wang, H., and Chen, Y. (2012). Geochemical evidence from bio-apatite for multiple oceanic anoxic events during Permian–Triassic transition and the link with end-Permian extinction and recovery. *Earth and Planetary Science Letters*, *353*, 12-21.

Toyoda, K., Nakamura, Y., and Masuda, A. (1990). Rare earth elements of Pacific pelagic sediments. *Geochimica et Cosmochimica Acta*, *54*(4), 1093-1103.

Webb, G.E., and Kamber, B.S. (2000). Rare earth elements in Holocene reefal microbialites: a new shallow seawater proxy. *Geochimica et Cosmochimica Acta, 64*, 1557–1565.

Webb, G.E., Nothdurft, L.D., Kamber, B.S., Kloprogge, J.T., and Zhao, J.X. (2009). Rare earth element geochemistry of scleractinian coral skeleton during meteoric diagenesis: a sequence through neomorphism of aragonite to calcite. *Sedimentology*, *56*(5), 1433-1463.

Wright, J., Seymour, R.S., and Shaw, H.F. (1984). REE and Nd isotopes in conodont apatite: variations with geological age and depositional environment. *Geological Society of America Special Papers*, *196*, 325–340.

Wright, J., Schrader, H., and Holser, W.T. (1987). Paleoredox variations in ancient oceans recorded by rare earth elements in fossil apatite. *Geochimica et Cosmochimica Acta*, *51*(3), 631–644.

Zhao, L., Chen, Z.Q., Algeo, T.J., Chen, J., Chen, Y., Tong, J., Gao S., Zhou l., Hu Z., and Liu, Y. (2013). Rare–earth element patterns in conodont albid crowns: Evidence for massive inputs of volcanic ash during the latest Permian biocrisis?. *Global and Planetary Change*, *105*, 135–151.

Zhou, L., and Kyte, F.T. (1988). The Permian-Triassic boundary event: a geochemical study of three Chinese sections. *Earth and Planetary Science Letters*, *90*(4), 411-421.

Appendix 3-1. Geochemical data of the investigated modern deep-water (>500m) articulated brachiopods.

	La	Ce	Pr	Nd	Sm	Eu	Gd	Tb	Dy	Ho	Er	Tm	Yb	Lu	∑REEs (ppm	Ce/Ce*
Detection limit	0.000	0.000	0.000	0.001	0.001	0.000	0.001	0.000	0.001	0.000	0.000	0.000	0.001	0.000		
Bulk Samples																
blank-1	0.037	0.076	0.008	0.031	0.008	0.000	0.004	N/A	0.001	0.000	N/A	N/A	0.004	N/A		
blank-2	0.004	0.005	N/A	N/A	N/A	N/A	N/A	N/A	N/A	N/A	N/A	N/A	N/A	N/A		
blank-3	0.005	0.009	N/A	N/A	N/A	N/A	N/A	N/A	N/A	N/A	N/A	N/A	N/A	N/A		
blank-4	0.000	N/A	N/A	N/A	N/A	N/A	N/A	N/A	0.007	0.000	0.002	0.001	0.004	0.000		
blank-5	N/A	0.000	N/A	N/A	N/A	0.000	N/A	N/A	N/A	N/A	N/A	N/A	N/A	N/A		
blank-6	N/A	N/A	N/A	N/A	0.001	N/A	N/A	N/A	N/A	N/A	N/A	0.000	0.001	0.000		
blank-7	0.003	0.001	N/A	0.003	0.007	N/A	0.010	N/A	N/A	N/A	0.002	N/A	N/A	N/A		
blank-8	0.001	0.002	N/A	N/A	N/A	0.002	N/A	N/A	0.004	N/A	N/A	N/A	0.000	N/A		
Standards																
NBS 88a (Published values/underline are internal values)	1.422	2.561	0.357	1.464	0.298	0.068	0.322	0.050	0.287	0.059	0.173	0.023	0.138	0.019		
NBS 88a-1	1.580	2.875	0.395	1.617	0.321	0.068	0.358	0.056	0.323	0.067	0.194	0.024	0.154	0.022		
NBS 88a-2	1.626	2.918	0.393	1.698	0.362	0.096	0.426	0.068	0.375	0.087	0.241	0.030	0.190	0.028		
NBS 88a-3	1.608	2.914	0.406	1.711	0.345	0.079	0.413	0.064	0.360	0.072	0.210	0.026	0.172	0.022		
NBS 88a-4	1.040	1.808	0.253	1.043	0.210	0.051	0.238	0.036	0.210	0.045	0.116	0.015	0.105	0.015		
NBS 88a-5	1.406	2.481	0.343	1.423	0.288	0.063	0.306	0.049	0.281	0.062	0.168	0.021	0.127	0.017		
NBS 88a-6	1.311	2.343	0.328	1.348	0.263	0.063	0.305	0.048	0.262	0.058	0.164	0.022	0.129	0.018		
NBS 88a-7	1.307	2.314	0.327	1.300	0.275	0.065	0.285	0.044	0.251	0.052	0.160	0.021	0.126	0.019		
NBS 88a-8	1.336	2.450	0.341	1.406	0.277	0.066	0.301	0.048	0.283	0.059	0.169	0.022	0.131	0.020		
CCH-1 (Published values)	**4.700**	**3.400**	**0.840**	**3.700**	**0.750**	**0.160**	**0.760**	**0.100**	**0.650**	**0.100**	**0.350**	**0.050**	**0.270**	**0.040**		
CCh-1-1	6.302	4.604	1.234	5.212	0.980	0.230	1.097	0.161	0.882	0.180	0.487	0.057	0.354	0.046		
CCh-1-2	4.695	3.326	0.867	3.838	0.698	0.190	0.923	0.145	0.822	0.166	0.458	0.057	0.347	0.050		
CCh-1-3	8.582	6.106	1.585	6.832	1.299	0.335	1.638	0.237	1.360	0.274	0.799	0.099	0.606	0.080		
CCh-1-4	4.048	2.934	0.814	3.333	0.621	0.147	0.697	0.110	0.564	0.110	0.311	0.039	0.228	0.032		
CCh-1-5	5.359	3.844	1.053	4.380	0.827	0.197	0.949	0.147	0.789	0.151	0.430	0.050	0.302	0.042		
CCh-1-6	4.693	3.425	0.940	3.908	0.747	0.171	0.821	0.120	0.654	0.136	0.361	0.046	0.262	0.041		
CCh-1-7	4.754	3.450	0.933	3.853	0.749	0.162	0.813	0.125	0.650	0.135	0.366	0.046	0.252	0.038		
CCh-1-8	4.586	3.355	0.901	3.711	0.686	0.173	0.767	0.120	0.664	0.127	0.374	0.047	0.261	0.036		
RSD %																
First run	3.2	2.4	2.6	1.8	0.9	2.6	1.8	2.5	1.4	2.2	1.9	1.2	1.1	0.6		
Second run	2.1	2.5	3.0	3.6	3.7	0.5	4.5	3.6	5.4	5.2	5.1	1.9	1.4	2.6		
Third run	0.2	2.8	3.2	1.0	1.5	3.4	5.1	4.5	4.7	4.3	5.2	5.2	5.5	5.0		
Fourth run	1.7	1.5	1.6	2.3	2.2	1.0	1.2	1.4	2.7	2.5	2.0	1.8	1.7	0.7		
Fifth run	1.1	1.1	1.2	1.8	1.4	1.2	2.8	0.7	0.2	0.4	0.8	0.7	2.8	2.5		
Sixth run	1.2	1.7	1.9	2.0	1.9	1.9	1.9	1.4	1.5	1.0	0.7	1.1	0.7	0.4		
Seventh run	0.5	1.0	0.5	0.8	0.3	0.8	1.3	1.4	0.7	0.8	0.9	1.1	1.0	1.2		
Eighth run	0.7	1.0	0.7	1.9	2.1	2.4	2.5	2.8	2.7	2.1	2.6	1.1	1.3	0.2		
RSD Average	**1.3**	**1.8**	**1.8**	**1.9**	**1.7**	**1.7**	**2.6**	**2.3**	**2.4**	**2.3**	**2.4**	**1.8**	**1.9**	**1.6**		

	La	Ce	Pr	Nd	Sm	Eu	Gd	Tb	Dy	Ho	Er	Tm	Yb	Lu	∑REEs (ppm	Ce/Ce*
CARIBBEAN SEA																
Venezuela Basin																
VB-St1-1 (3986 m)	0.030	0.027	0.004	0.022	0.002	0.001	0.001	0.001	0.002	0.000	0.003	0.001	0.010	0.002	0.102	0.461
VB-St1-2 (3986 m)	0.027	0.029	0.005	0.017	#N/A	#N/A	0.004	0.001	0.005	0.001	0.004	#N/A	0.009	#N/A	0.102	0.568
VB-St1-3 (3986 m)	0.065	0.072	0.012	0.056	0.007	#N/A	0.016	0.001	0.017	0.005	0.015	0.002	0.013	0.002	0.275	0.536
VB-St2-1 (3998 m)	0.023	0.028	0.007	0.001	0.016	0.001	0.008	0.001	0.000	0.000	0.003	0.000	0.004	0.000	0.076	-
VB-St2-2 (3998 m)	0.059	0.066	0.011	0.051	0.017	0.001	0.012	0.001	0.017	0.003	0.012	0.002	0.010	0.001	0.242	0.535
VB-St2-3 (3998 m)	0.107	0.088	0.024	0.109	0.019	0.005	0.022	0.005	0.028	0.007	0.027	0.002	0.018	0.003	0.465	0.374
NORTH ATLANTIC OCEAN																
Denmark Strait																
DS-S-St1-1 (603.1-742.5 m)	0.305	0.222	0.069	0.299	0.058	0.019	0.075	0.015	0.077	0.017	0.046	0.005	0.041	0.004	1.252	0.338
DS-S-St2-1 (696.9-706.4 m)	0.155	0.091	0.034	0.157	0.032	0.010	0.042	0.007	0.041	0.007	0.024	0.000	0.029	0.003	0.631	0.268
Irminger Basin																
IrB-S-St1-1 (678.5-698.1 m)	0.353	0.252	0.075	0.347	0.078	0.021	0.093	0.016	0.087	0.018	0.054	0.005	0.040	0.006	1.447	0.331
IrB-S-St1-2 (678.5-698.1 m)	0.269	0.244	0.083	0.377	0.072	0.024	0.094	0.015	0.086	0.020	0.056	0.007	0.038	0.006	1.392	0.365
IrB-S-St1-3 (678.5-698.1 m)	0.113	0.155	0.026	0.101	0.027	0.005	0.027	0.004	0.027	0.006	0.014	0.001	0.015	0.000	0.519	0.659
IrB-S-St1-4 (678.5-698.1 m)	0.120	0.107	0.026	0.120	0.025	0.008	0.040	0.005	0.036	0.006	0.018	#N/A	0.018	0.001	0.529	0.408
IrB-S-St2-1 (704.9-724.4 m)	0.145	0.187	0.035	0.168	0.032	0.010	0.037	0.008	0.041	0.008	0.019	0.003	0.023	0.003	0.719	0.562
Iceland Basin																
IcB-D-1 (2567.7-2568.5 m)	0.276	0.085	0.052	0.236	0.050	0.012	0.057	0.010	0.062	0.014	0.036	0.006	0.042	0.006	0.944	0.151
IcB-D-2 (2567.7-2568.5 m)	0.185	0.060	0.038	0.154	0.033	0.011	0.047	0.006	0.047	0.009	0.028	0.005	0.032	0.004	0.660	0.158
IcB-D-3 (2567.7-2568.5 m)	0.226	0.080	0.045	0.214	0.037	0.010	0.049	0.009	0.053	0.012	0.032	0.003	0.035	0.006	0.812	0.167
SOUTH PACIFIC OCEAN																
Lau Arc																
LA-1 (589 m)	0.300	0.260	0.060	0.255	0.043	0.012	0.072	0.011	0.074	0.016	0.042	0.007	0.047	0.008	1.207	0.421
LA-2 (589 m)	0.207	0.287	0.044	0.169	0.034	0.010	0.041	0.008	0.044	0.011	0.036	0.004	0.028	0.003	0.928	0.682
LA-3 (589 m)	0.151	0.226	0.030	0.124	0.027	0.008	0.027	0.005	0.034	0.007	0.025	0.002	0.020	0.002	0.688	0.738
LA-4 (589 m)	0.197	0.296	0.041	0.170	0.032	0.010	0.048	0.007	0.045	0.010	0.022	0.005	0.029	0.003	0.916	0.728
Colville Arc																
CA-1 (660 m)	0.080	0.062	0.012	0.060	0.012	0.003	0.018	0.003	0.024	0.002	0.012	0.001	0.011	0.002	0.300	0.391
CA-2 (660 m)	0.264	0.135	0.054	0.232	0.049	0.013	0.076	0.012	0.074	0.018	0.062	0.007	0.056	0.008	1.060	0.246
Havre Trough																
HT-St1-1 (1115-1172 m)	0.041	0.012	0.008	0.039	0.008	0.002	0.011	0.003	0.009	0.003	0.011	0.002	0.005	0.001	0.155	0.132
HT-St1-2 (1115-1172 m)	0.025	0.013	0.006	0.026	0.005	0.001	0.005	0.000	0.006	0.002	0.004	0.000	0.006	0.001	0.100	0.237
HT-St1-3 (1115-1172 m)	0.022	0.011	0.004	0.028	0.011	0.001	0.004	0.001	0.006	0.002	0.002	0.001	0.000	0.000	0.091	0.216
HT-St1-4 (1115-1172 m)	0.030	0.019	0.005	0.031	0.007	0.001	0.007	0.001	0.008	0.002	0.004	0.001	0.007	0.000	0.123	0.282
HT-St1-5 (1115-1172 m)	0.218	0.078	0.049	0.216	0.045	0.011	0.061	0.010	0.066	0.015	0.041	0.006	0.043	0.006	0.866	0.166
HT-St1-6 (1115-1172 m)	0.142	0.073	0.032	0.150	0.030	0.007	0.036	0.007	0.039	0.008	0.023	0.004	0.028	0.003	0.582	0.233
HT-St1-7(1115-1172 m)	0.145	0.074	0.033	0.136	0.044	0.008	0.028	0.007	0.039	0.010	0.028	0.004	0.030	0.003	0.588	0.241
HT-St1-8 (1115-1172 m)	0.058	0.025	0.013	0.054	0.010	0.003	0.014	0.003	0.016	0.004	0.011	0.001	0.013	0.001	0.228	0.203
HT-St1-9 (1115-1172 m)	0.032	0.013	0.008	0.037	0.004	0.002	0.006	0.002	0.006	0.002	0.006	0.000	0.005	0.001	0.124	0.185
HT-St2-1 (1520 m)	0.175	0.055	0.034	0.149	0.033	0.011	0.037	0.007	0.043	0.010	0.023	0.003	0.027	0.004	0.613	0.152

M

	La	Ce	Pr	Nd	Sm	Eu	Gd	Tb	Dy	Ho	Er	Tm	Yb	Lu	∑REEs (ppm	Ce/Ce*
Kermadec Arc																
KA-St1-1 (1244 m)	0.545	0.258	0.110	0.491	0.108	0.027	0.121	0.020	0.126	0.028	0.076	0.013	0.069	0.010	2.003	0.226
KA-St2-1 (1460 m)	0.309	0.111	0.059	0.275	0.052	0.015	0.070	0.012	0.075	0.018	0.050	0.006	0.042	0.006	1.101	0.173
KA-St2-2 (1460 m)	0.319	0.121	0.073	0.283	0.066	0.016	0.073	0.013	0.097	0.020	0.067	0.009	0.054	0.008	1.219	0.183
KA-St3-1 (1583 m)	0.525	0.159	0.110	0.471	0.098	0.028	0.117	0.020	0.125	0.028	0.082	0.012	0.071	0.010	1.855	0.145
KA-St4-1 (1740 m)	0.311	0.096	0.062	0.263	0.054	0.014	0.065	0.012	0.078	0.017	0.051	0.007	0.045	0.006	1.082	0.150
Northland Plateau																
NP-St.1-1 (1293 m)	0.120	0.048	0.029	0.122	0.025	0.006	0.028	0.006	0.032	0.008	0.020	0.003	0.022	0.004	0.474	0.183
NP-St.1-2 (1293 m)	0.056	0.031	0.013	0.041	0.007	0.000	0.002	0.001	0.012	0.004	0.013	0.002	0.018	0.001	0.198	0.193
NP-St.1-3 (1293 m)	0.170	0.067	0.038	0.153	0.038	0.011	0.037	0.008	0.036	0.010	0.027	0.004	0.031	0.004	0.632	0.188
NP-St.2-1 (1583 m)	0.285	0.139	0.060	0.269	0.057	0.010	0.074	0.013	0.076	0.019	0.048	0.007	0.042	0.007	1.105	0.229
SOUTHERN OCEAN																
Ross Sea																
SO-S-1 (547 m)	0.072	0.07021	0.014	0.050	0.013	0.003	0.018	0.002	0.012	0.002	0.009	0.002	0.005	#N/A	0.272	0.506
SO-S-2 (547 m)	0.122	0.06722	0.023	0.082	0.041	0.000	0.024	0.002	0.025	0.002	0.024	0.003	0.014	0.000	0.384	0.287
SO-S-3 (547 m)	0.015	0.00747	0.002	0.012	#N/A	#N/A	0.005	0.000	0.001	#N/A	0.002	#N/A	#N/A	#N/A	0.043	0.253
SO-S-4 (547 m)	0.058	0.03368	0.014	0.055	0.014	0.001	0.018	0.002	0.005	0.003	0.009	0.002	0.004	#N/A	0.214	0.272
SO-S-5 (547 m)	0.052	0.02898	0.011	0.052	0.012	#N/A	0.013	0.002	0.009	0.002	0.003	0.002	0.003	0.001	0.188	0.256

Note: Concentations in ppm.

N

Appendix 3-2. Summary statistics of the investigated modern deep-water (>500m) articulated brachiopods.

	La	Ce	Pr	Nd	Sm	Eu	Gd	Tb	Dy	Ho	Er	Tm	Yb	Lu	∑REEs	Ce/Ce*
CARIBBEAN SEA																
Venezuela Basin (3986-3998 m)																
n	6	6	6	5	2	3	5	4	4	4	6	5	6	4	6	5
Average	**0.052**	**0.051**	**0.010**	**0.051**	**0.011**	**0.002**	**0.012**	**0.002**	**0.017**	**0.004**	**0.011**	**0.001**	**0.011**	**0.002**	**0.237**	**0.495**
Stdev	0.032	0.027	0.007	0.037	0.012	0.003	0.007	0.002	0.009	0.003	0.010	0.001	0.005	0.001	0.149	0.078
Median	0.045	0.047	0.009	0.051	0.011	0.001	0.012	0.001	0.017	0.004	0.008	0.002	0.010	0.002	0.172	0.535
Max	0.107	0.088	0.024	0.109	0.019	0.005	0.022	0.005	0.028	0.007	0.027	0.002	0.018	0.003	0.465	0.568
Min	0.023	0.027	0.004	0.017	0.002	0.001	0.004	0.001	0.005	0.001	0.003	0.000	0.004	0.000	0.076	0.374
NORTH ATLANTIC OCEAN																
Denmark Strait (603.1-742.5 m)																
n	2	2	2	2	2	2	2	2	2	2	2	1	2	2	2	2
Average	**0.230**	**0.157**	**0.051**	**0.228**	**0.045**	**0.014**	**0.059**	**0.011**	**0.059**	**0.012**	**0.035**	**0.005**	**0.035**	**0.004**	**0.944**	**0.303**
Stdev	0.105	0.093	0.025	0.101	0.018	0.007	0.023	0.006	0.025	0.007	0.016		0.008	0.001	0.439	0.050
Median	0.230	0.157	0.051	0.228	0.045	0.014	0.059	0.011	0.059	0.012	0.035	0.005	0.035	0.004	0.941	0.303
Max	0.305	0.222	0.069	0.299	0.058	0.019	0.075	0.015	0.077	0.017	0.046	0.005	0.041	0.004	1.252	0.338
Min	0.155	0.091	0.034	0.157	0.032	0.010	0.042	0.007	0.041	0.007	0.024	0.005	0.029	0.003	0.631	0.268
Irminger Basin (678.5-724.4 m)																
n	5	5	5	5	5	5	5	5	5	5	5	3	5	3	5	5
Average	**0.200**	**0.189**	**0.049**	**0.223**	**0.047**	**0.014**	**0.058**	**0.009**	**0.055**	**0.011**	**0.032**	**0.005**	**0.027**	**0.005**	**0.925**	**0.465**
Stdev	0.106	0.061	0.028	0.130	0.026	0.008	0.033	0.006	0.029	0.007	0.021	0.002	0.012	0.002	0.462	0.140
Median	0.145	0.187	0.035	0.168	0.032	0.010	0.040	0.008	0.041	0.008	0.019	0.005	0.023	0.006	0.719	0.408
Max	0.353	0.252	0.083	0.377	0.078	0.024	0.094	0.016	0.087	0.020	0.056	0.007	0.040	0.006	1.447	0.659
Min	0.113	0.107	0.026	0.101	0.025	0.005	0.027	0.004	0.027	0.006	0.014	0.003	0.015	0.003	0.519	0.331
Iceland Basin (2567.7-2568.5 m)																
n	3	3	3	3	3	3	3	3	3	3	3	3	3	3	3	3
Average	**0.229**	**0.075**	**0.045**	**0.202**	**0.040**	**0.011**	**0.051**	**0.008**	**0.054**	**0.012**	**0.032**	**0.005**	**0.036**	**0.005**	**0.804**	**0.169**
Stdev	0.045	0.014	0.007	0.042	0.008	0.001	0.005	0.002	0.008	0.003	0.004	0.001	0.005	0.001	0.142	0.008
Median	0.226	0.080	0.045	0.214	0.037	0.011	0.049	0.009	0.053	0.012	0.032	0.005	0.035	0.006	0.812	0.158
Max	0.276	0.085	0.052	0.236	0.050	0.012	0.057	0.010	0.062	0.014	0.036	0.006	0.042	0.006	0.944	0.167
Min	0.185	0.060	0.038	0.154	0.033	0.010	0.047	0.006	0.047	0.009	0.028	0.003	0.032	0.004	0.660	0.151

SOUTH PACIFIC OCEAN																
Lau Arc and Colville (589-660 m)																
n	6	6	6	6	6	6	6	6	6	6	6	6	6	6	6	6
Average	**0.200**	**0.211**	**0.040**	**0.168**	**0.033**	**0.009**	**0.047**	**0.008**	**0.049**	**0.011**	**0.033**	**0.004**	**0.032**	**0.004**	**0.850**	**0.534**
Stdev	0.079	0.093	0.017	0.071	0.013	0.004	0.024	0.003	0.021	0.006	0.018	0.003	0.017	0.003	0.320	0.208
Median	0.202	0.243	0.042	0.170	0.033	0.010	0.045	0.007	0.045	0.011	0.030	0.005	0.028	0.003	0.922	0.551
Max	0.300	0.296	0.060	0.255	0.049	0.013	0.076	0.012	0.074	0.018	0.062	0.007	0.056	0.008	1.207	0.738
Min	0.080	0.062	0.012	0.060	0.012	0.003	0.018	0.003	0.024	0.002	0.012	0.001	0.011	0.002	0.300	0.246
Havre Trough (1115-1172 m)																
n	10	10	10	10	10	10	10	9	10	10	9	10	9	9	10	10
Average	**0.089**	**0.037**	**0.019**	**0.087**	**0.020**	**0.005**	**0.021**	**0.004**	**0.024**	**0.006**	**0.017**	**0.002**	**0.018**	**0.002**	**0.351**	**0.205**
Stdev	0.074	0.029	0.016	0.069	0.017	0.004	0.019	0.003	0.021	0.005	0.013	0.002	0.014	0.002	0.285	0.046
Median	0.050	0.022	0.011	0.047	0.011	0.003	0.013	0.003	0.013	0.004	0.011	0.002	0.013	0.001	0.192	0.210
Max	0.218	0.078	0.049	0.216	0.045	0.011	0.061	0.010	0.066	0.015	0.041	0.006	0.043	0.006	0.866	0.282
Min	0.022	0.011	0.004	0.026	0.004	0.001	0.004	0.001	0.006	0.002	0.004	0.000	0.005	0.000	0.091	0.132
Kermadec Arc (1244-1760 m)																
n	5	5	5	5	5	5	5	5	5	5	5	5	5	5	5	5
Average	**0.402**	**0.149**	**0.083**	**0.357**	**0.076**	**0.020**	**0.089**	**0.016**	**0.101**	**0.022**	**0.065**	**0.009**	**0.056**	**0.008**	**1.452**	**0.175**
Stdev	0.122	0.065	0.026	0.114	0.026	0.007	0.027	0.004	0.025	0.005	0.014	0.003	0.013	0.002	0.442	0.032
Median	0.319	0.121	0.073	0.283	0.066	0.016	0.073	0.013	0.097	0.020	0.067	0.009	0.054	0.008	1.219	0.173
Max	0.545	0.258	0.110	0.491	0.108	0.028	0.121	0.020	0.126	0.028	0.082	0.013	0.071	0.010	2.003	0.226
Min	0.309	0.096	0.059	0.263	0.052	0.014	0.065	0.012	0.075	0.017	0.050	0.006	0.042	0.006	1.082	0.145
Northland Plateau (1293-1538 m)																
n	4	4	4	4	4	3	3	4	4	4	4	4	4	3	4	4
Average	**0.158**	**0.071**	**0.035**	**0.146**	**0.032**	**0.009**	**0.047**	**0.007**	**0.039**	**0.010**	**0.027**	**0.004**	**0.028**	**0.005**	**0.617**	**0.221**
Stdev	0.097	0.047	0.019	0.095	0.021	0.003	0.025	0.005	0.027	0.007	0.015	0.002	0.011	0.002	0.380	0.047
Median	0.145	0.057	0.033	0.137	0.031	0.010	0.037	0.007	0.034	0.009	0.024	0.003	0.026	0.004	0.553	0.208
Max	0.285	0.139	0.060	0.269	0.057	0.011	0.074	0.013	0.076	0.019	0.048	0.007	0.042	0.007	1.105	0.284
Min	0.056	0.031	0.013	0.041	0.007	0.006	0.028	0.001	0.012	0.004	0.013	0.002	0.018	0.004	0.198	0.183
SOUTHERN OCEAN																
Ross Sea (547 m)																
n	5	5	5	5	3	1	5	3	3	3	4	4	4	1	5	5
Average	**0.064**	**0.042**	**0.013**	**0.050**	**0.013**	**0.003**	**0.016**	**0.002**	**0.015**	**0.003**	**0.011**	**0.002**	**0.007**	**0.001**	**0.240**	**0.315**
Stdev	0.039	0.027	0.007	0.025	0.001		0.007	0.000	0.009	0.000	0.009	0.000	0.005		0.124	0.108
Median	0.058	0.034	0.014	0.052	0.013	0.003	0.018	0.002	0.012	0.002	0.009	0.002	0.004	0.001	0.214	0.272
Max	0.122	0.070	0.023	0.082	0.014	0.003	0.024	0.002	0.025	0.003	0.024	0.003	0.014	0.001	0.384	0.506
Min	0.015	0.007	0.002	0.012	0.012	0.003	0.005	0.002	0.009	0.002	0.002	0.002	0.003	0.001	0.043	0.253

Note: Concentations in ppm.

Appendix 3-3. Hydrographic setting

1- Caribbean Sea

Surface waters enter the Caribbean through the Lesser Antilles Passage (Osborne et al., 2014). The westward currents flowing towards the Gulf of Mexico include the Northern Equatorial Current that drives water of the tropical and subtropical Atlantic gyres into the Caribbean (Alvera-Azcarate et al., 2009). The origin of Caribbean deep-water is complicated (Fig. 2A) because the sills through which the water passes from the Atlantic are shallower than the abyssal depth of the Caribbean (Osborne et al., 2015). It is through the Anegada-Jungfern Passages (2800 m deep), the Upper North Atlantic Deep Water flows southward, filling the abyssal depths of the Virgin Islands, Venezuela and eastern Caribbean basins (Borenäs and Nikolopoulos, 2000).

2- North Atlantic Ocean

The Iceland Basin (southwest of Iceland) represents a separate oceanographic region in the northeast North Atlantic (Fig. 2B). The vertical distribution of the basin's main water mass consists of North Atlantic, Labrador Sea and Iceland-Scotland Overflow waters (Blindheim et al., 1996). The Irminger Basin (northwest of Iceland; Fig. 2B) represents a dynamic region of the North Atlantic where confluence, mixing, transformation and formation of water masses take place (Magaldi et al., 2012). The polar water of the East Greenland Current and salty North Atlantic water of the Irminger Current compose the uppermost water layer of the basin, whereas Labrador Sea water constitutes the intermediate water (Fig. 2B; Sutherland and Pickart, 2008). The Denmark Strait Overflow and Norwegian Sea Deep waters fill the basin's abyssal depth (Raddatz et al., 2014). The upper water mass of the Denmark Strait (Fig. 2B) is influenced by the same surface water as is the Irminger Basin, whereas its deep water consists of deep Arctic Ocean and Norwegian Sea waters (Hansen and Østerhus, 2000).

3- South Pacific Ocean

Surface water of the western South Pacific originates from the westward inflow of highly saline South Equatorial Current water and is formed in the dry center of the southeast Pacific gyre (Ridgway, 2007). The northern Tonga-Lau arc-back-arc system is awashed by the South Equatorial Current (Webb, 2000). The Subtropical Counter Current flows eastward passing over the Lau-Colville arc, Harve Trough-Lau Basin and Kermadec-Tonga arc (Ganachaud et al., 2008). The Tasman Front flows across the Tasman Sea as far north as New Zealand, and in the southern Kermadec-Havre-Colville arc-back-arc system as the East Auckland Current (Bowen et al., 2006). The renewal of deep water in the western basins, troughs and

ridges of the western South Pacific takes place through the inflow of North Pacific deep water (Fig. 2C), which enters through the Solomon Trough to the North (e.g., Wyrtki, 1961, Bostock et al., 2011).

4- Southern Ocean

In the Southern Ocean, the prevailing westerly wind drives water eastward creating the Antarctic Circumpolar Current (the West Wind Drift current: Rintoul, 2010). The Antarctic Coastal Current flows pole- and westward in a narrow continental zone parallel to the Antarctic coastline; it is driven mainly by easterly winds and partly by thermohaline effects (Fig. 2D; e.g., Keys and Fowler, 1989). Water of the Circumpolar Current consists of two layers, an oxygen minimum layer (the Upper Circumpolar Deep Water, at 200 to 1400 m) and a salinity maximum layer (the Lower Circumpolar Deep Water, at 1400 to 2600 m; Whitworth et al., 1998; Zhang et al., 2008).

References

Alvera-Azcárate, A., Barth, A., & Weisberg, R. H. (2009). The surface circulation of the Caribbean Sea and the Gulf of Mexico as inferred from satellite altimetry. *Journal of Physical Oceanography*, *39*(3), 640-657.

Blindheim, J., Buch, E., Fogelqvist, E., Tanhua, T., & Østerhus, S. (1996). The R/V Johan Hjort 1994 NORDIC WOCE cruise: on hydrography and tracers. ICES.

Borenäs, K., & Nikolopoulos, A. (2000). Theoretical calculations based on real topography of the maximum deep-water flow through the Jungfern Passage.*Journal of marine research*, *58*(5), 709-719.

Bostock, H. C., Hayward, B. W., Neil, H. L., Currie, K. I., & Dunbar, G. B. (2011). Deep-water carbonate concentrations in the southwest Pacific. *Deep Sea Research Part I: Oceanographic Research Papers*, *58*(1), 72-85.

Bowen, M. M., Sutton, P. J., & Roemmich, D. (2006). Wind-driven and steric fluctuations of sea surface height in the southwest Pacific. *Geophysical research letters*, *33*(14).

Ganachaud, P., Brassington, G., Kessler, W., Mechoso, C. R., Wijffels, S., Ridgway, K., Cai, W., Holbrook., N., Sutton, P., Bowen, M., Qiu, B., Timmermann, A., Roemmich, D., Sprintall, J., Neelin, D., Lintner, B., Lintner, H., Lintner, S., Gourdeau, L., Eastwood, P., & Aung., T. (2008). Southwest Pacific Ocean Circulation and Climate Experiment (SPICE): Part II. Implementation Plan.

Hansen, B., & Østerhus, S. (2000). North Atlantic–Nordic Seas exchanges.*Progress in Oceanography*, *45*(2), 109-208.

Keys, H., & Fowler, D. (1989). Sources and movement of icebergs in the south-west Ross Sea, Antarctica. *Annals of glaciology*, *12*, 85-88.

Magaldi, M. G., Haine, T. W. N., & Pickart, R. S. (2012). On the nature and variability of the East Greenland Spill Jet. A Case Study in Summer 2003*, Journal of Physical Oceanography, 41(12), 2307-2327.

Osborne, A. H., Haley, B. A., Hathorne, E. C., Flögel, S., & Frank, M. (2014). Neodymium isotopes and concentrations in Caribbean seawater: Tracing water mass mixing and continental input in a semi-enclosed ocean basin. *Earth and Planetary Science Letters*, *406*, 174-186.

Osborne, A. H., Haley, B. A., Hathorne, E. C., Plancherel, Y., & Frank, M. (2015). Rare earth element distribution in Caribbean seawater: Continental inputs versus lateral transport of distinct REE compositions in subsurface water masses. *Marine Chemistry*.

Raddatz, J., Rüggeberg, A., Liebetrau, V., Foubert, A., Hathorne, E. C., Fietzke, J., ... & Dullo, W. C. (2014). Environmental boundary conditions of cold-water coral mound growth over the last 3 million years in the

Porcupine Seabight, Northeast Atlantic. *Deep Sea Research Part II: Topical Studies in Oceanography*, *99*, 227-236.

Ridgway, K. R. (2007). Long-term trend and decadal variability of the southward penetration of the East Australian Current. *Geophysical Research Letters*,*34*(13).

Rintoul, S. R. (2010). Antarctic circumpolar current. *Ocean Currents: A Derivative of the Encyclopedia of Ocean Sciences*, 196.

Sutherland, D. A., & Pickart, R. S. (2008). The East Greenland coastal current: Structure, variability, and forcing. *Progress in Oceanography*, *78*(1), 58-77.

Webb, D. J. (2000). Evidence for shallow zonal jets in the South Equatorial Current region of the southwest Pacific. *Journal of Physical Oceanography*,*30*(4), 706-720.

Whitworth III, T., Orsi, A. H., Kim, S. J., Nowlin, W. D., & Locarnini, R. A. (1998). Water masses and mixing near the Antarctic Slope Front. *Ocean, ice, and atmosphere: interactions at the Antarctic continental margin*, 1-27.

Wyrtki, K. (1961). The flow of water into the deep sea basins of the western South Pacific Ocean. *Marine and Freshwater Research*, *12*(1), 1-16.

Zhang, Y., Lacan, F., & Jeandel, C. (2008). Dissolved rare earth elements tracing lithogenic inputs over the Kerguelen Plateau (Southern Ocean). *Deep Sea Research Part II: Topical Studies in Oceanography*, *55*(5), 638-652.

Appendix 3-4. Classification and distribution coefficient values of the investigated modern deep-water (>500m) articulated brachiopods.

	Classification				Distribution coefficient values													
	Order	Family	Genus	Species	La	Ce	Pr	Nd	Sm	Eu	Gd	Tb	Dy	Ho	Er	Tm	Yb	Lu
CARIBBEAN SEA																		
Venezuela Basin																		
VB-St1-1 (3986 m)	Terebratulida	Chlidonophoridae	Chlidonophora	*Chlidonophora incerta*	9.1	29.8	6.2	8.2	3.8	3.7	-	4.5	-	-	3.2	5.1	13.0	10.6
VB-St1-2 (3986 m)	"	"	"	"	8.1	31.3	9.0	6.3	-	-	4.8	6.3	5.7	3.5	4.8	-	11.1	-
VB-St1-3 (3986 m)	"	"	"	"	19.9	78.7	21.2	20.6	-	-	18.5	-	18.0	19.9	17.0	15.0	16.0	11.4
VB-St2-1 (3998 m)	"	"	"	"	7.2	31.2	12.5	-	-	3.9	9.7	7.8	-	-	3.4	2.8	4.5	2.1
VB-St2-2 (3998 m)	"	"	"	"	18.2	71.8	18.9	18.8	-	-	13.4	-	17.1	10.8	13.5	10.8	12.5	-
VB-St2-3 (3998 m)	"	"	"	"	32.8	96.0	41.0	40.1	32.8	31.6	25.5	36.9	28.8	28.8	30.4	14.4	22.5	19.5
NORTH ATLANTIC OCEAN																		
Denmark Strait																		
DS-S-St1-1 (603.1-742.5 m)	"	Dallinidae	Macandrevia	*Macandrevia cranium*	98.0	211.4	122.7	122.9	123.5	203.1	111.0	160.9	86.4	72.1	56.1	54.9	54.7	47.5
DS-S-St2-1 (696.9-706.4 m)	"	"	"	"	50.1	86.6	60.6	64.6	68.2	104.0	62.7	77.5	46.1	28.6	29.0	-	39.1	27.8
Irminger Basin																		
IrB-S-St1-1 (678.5-698.1 m)	"	"	"	"	113.5	239.9	134.5	142.8	166.4	228.0	137.0	169.1	98.0	76.0	66.6	56.6	54.1	63.3
IrB-S-St1-2 (678.5-698.1 m)	"	"	"	"	86.1	230.6	146.4	154.1	152.2	254.9	137.7	162.5	95.7	85.8	67.7	77.7	51.1	64.4
IrB-S-St1-3 (678.5-698.1 m)	"	"	"	"	36.3	148.0	46.9	41.8	58.1	52.6	39.5	41.1	30.1	24.2	17.0	-	20.4	-
IrB-S-St1-4 (678.5-698.1 m)	"	"	"	"	38.7	101.5	45.7	49.6	53.7	88.6	59.4	49.6	41.0	24.3	22.0	-	24.0	-
IrB-S-St2-1 (704.9-724.4 m)	"	"	"	"	46.8	178.0	62.7	69.1	69.3	107.7	54.9	81.9	45.9	33.9	23.3	34.2	31.4	30.1
Iceland Basin																		
IcB-D-1 (2567.7-2568.5 m)	"	"	"	"	87.6	86.6	100.4	102.5	105.4	131.0	80.8	109.1	69.6	76.9	48.5	60.3	55.2	58.7
IcB-D-2 (2567.7-2568.5 m)	"	"	"	"	58.7	60.6	73.2	67.0	70.9	112.8	66.7	68.0	53.0	50.0	36.8	53.9	42.5	45.5
IcB-D-3 (2567.7-2568.5 m)	"	"	"	"	71.7	81.5	87.0	93.2	78.9	110.1	69.0	91.1	59.1	64.1	43.2	35.7	47.2	60.7
SOUTH PACIFIC OCEAN																		
Lau Arc																		
LA-1 (589 m)	"	Terebratulidae		*Terebratulida* sp.	181.0	807.2	259.5	247.3	208.4	215.9	208.4	171.9	145.8	101.2	76.4	89.9	85.2	77.5
LA-2 (589 m)	"	"		"	125.0	891.0	191.2	164.2	166.1	187.6	119.3	124.6	87.5	71.0	64.4	52.6	50.1	32.2
LA-3 (589 m)	Rhynchonellida	Basiliolidae	Basiliola	*Basiliola beecheri*	90.9	702.7	127.7	120.1	129.6	145.5	77.0	85.2	67.6	44.7	44.9	23.7	36.5	22.6
LA-4 (589 m)	"	"	"	"	119.0	920.9	176.3	164.8	154.7	187.3	140.5	109.8	89.5	64.8	39.8	58.5	52.2	30.8
Colville Arc																		
CA-1 (660 m)	Terebratulida	Dallinidae	Dallina	*Dallina* sp.	48.5	193.5	54.3	58.8	59.1	49.6	51.6	44.5	47.2	12.1	21.7	7.6	20.3	17.6
CA-2 (660 m)	"	"	"	"	160.9	424.2	234.3	227.2	241.0	236.3	222.9	193.9	147.2	112.2	112.5	86.5	103.5	79.9

T

	Classification				Distribution coefficient values													
	Order	Family	Genus	Species	La	Ce	Pr	Nd	Sm	Eu	Gd	Tb	Dy	Ho	Er	Tm	Yb	Lu
Havre Trough																		
HT-St1-1 (1115-1172 m)	"	Terebratulidae	Liothyrella	*Liothyrella neozelanica*	15.0	47.9	24.9	24.5	26.3	23.8	21.8	29.3	11.3	14.8	12.8	13.3	6.0	7.5
HT-St1-2 (1115-1172 m)	"	"	"	"	9.0	53.4	17.8	16.1	16.0	15.8	10.0	-	7.8	7.6	4.3	3.0	7.0	8.0
HT-St1-3 (1115-1172 m)	"	"	"	"	8.0	46.5	12.5	17.3	36.7	11.5	7.0	11.4	8.1	7.5	-	6.5	-	2.8
HT-St1-4 (1115-1172 m)	"	"	"	"	11.1	77.3	15.1	19.4	22.5	9.0	13.1	13.1	9.9	10.4	4.2	7.8	8.3	-
HT-St1-5 (1115-1172 m)	"	"	"	"	80.5	326.0	146.6	135.1	146.1	131.6	121.6	101.0	86.6	63.5	48.7	44.1	48.1	35.6
HT-St1-6 (1115-1172 m)	"	"	"	"	52.4	304.2	96.5	93.6	96.4	75.9	71.9	71.0	50.9	34.0	27.0	28.4	30.8	18.7
HT-St1-7(1115-1172 m)	"	"	"	"	53.3	307.4	98.2	84.8	140.8	88.5	55.2	78.9	50.8	41.6	32.7	27.7	33.2	20.4
HT-St1-8 (1115-1172 m)	"	"	"	"	21.4	103.7	39.4	33.7	31.1	40.0	28.3	28.6	21.4	17.2	12.6	10.5	14.8	7.8
HT-St1-9 (1115-1172 m)	"	"	"	"	11.6	55.6	22.4	22.9	11.5	25.1	12.2	18.6	8.2	8.7	7.2	2.8	5.5	5.3
HT-St2-1 (1520 m)	"	Dyscolidae	Goniobrochus	*Goniobrochus ewingi*	64.4	226.9	102.2	93.0	107.7	128.4	73.1	74.4	55.5	44.5	27.6	24.1	30.2	22.2
Kermadec Arc																		
KA-St1-1 (1244 m)	"	Terebratulidae	Stenosarina	*Stenosarina crosnieri*	200.9	1068.7	329.7	306.0	349.0	308.9	239.1	216.6	164.5	118.6	89.8	102.1	76.8	62.5
KA-St2-1 (1460 m)	"	Dallinidae	Dallina	*Dallina triangularis*	113.7	460.7	175.9	171.3	166.2	172.8	139.2	127.8	98.3	77.5	59.5	48.8	46.7	35.6
KA-St2-2 (1460 m)	"	Terebratulidae	Stenosarina	*Stenosarina crosnieri*	117.9	506.1	219.1	177.3	214.2	185.5	144.8	143.5	127.6	86.2	79.2	66.7	60.2	45.2
KA-St3-1 (1583 m)	"	Dallinidae	Dallina	*Dallina triangularis*	193.1	658.3	329.8	293.9	316.8	322.9	230.8	206.8	163.4	119.3	96.3	87.6	78.7	59.5
KA-St4-1 (1740 m)	"	Dyscolidae	Goniobrochus	*Goniobrochus ewingi*	114.3	397.2	184.8	164.0	175.4	161.4	128.8	126.3	102.1	74.6	60.3	55.9	49.5	35.2
Northland Plateau																		
NB-St.1-1 (1293 m)	Rhynchonellida	Basiliolidae	Basiliola	*Basiliola pompholyx*	44.1	198.5	86.5	76.0	81.8	70.6	55.4	61.2	42.3	35.4	23.9	21.8	24.8	23.7
NB-St.1-2 (1293 m)	"	"	"	"	20.7	129.3	38.1	25.4	24.1	-	-	13.3	15.8	15.5	15.4	12.5	19.5	-
NB-St.1-3 (1293 m)	"	"	"	"	62.6	276.7	113.2	95.2	121.0	126.8	73.8	79.3	47.5	41.9	31.6	29.0	33.9	21.7
NB-St.2-1 (1583 m)	Terebratulida	Dyscolidae	Abyssothyris	*Abyssothyris wyvillei*	105.4	577.6	178.8	168.4	182.8	120.3	147.7	135.5	100.0	82.7	56.7	51.2	46.6	41.5
SOUTHERN OCEAN																		
Ross Sea																		
SO-S-1 (547 m)	"	Terebratulidae	Magellania	*Magellania fragilis*	20.6	75.2	28.9	23.2	32.1	28.7	29.0	20.2	14.2	10.4	10.8	15.3	4.7	-
SO-S-2 (547 m)	"	"	"	"	35.0	71.8	47.9	37.8	-	-	38.4	-	30.3	-	27.3	19.7	14.4	-
SO-S-3 (547 m)	"	"	"	"	4.2	8.0	4.4	5.5	-	-	7.9	-	-	-	2.7	-	-	-
SO-S-4 (547 m)	"	"	"	"	16.8	36.2	29.8	25.5	36.1	-	28.5	22.0	-	12.3	10.9	13.1	4.6	-
SO-S-5 (547 m)	"	"	"	"	15.0	31.1	24.0	24.1	31.2	-	20.7	18.4	10.5	9.5	-	13.0	3.3	3.6

Terebratulida		La	Ce	Pr	Nd	Sm	Eu	Gd	Tb	Dy	Ho	Er	Tm	Yb	Lu
	Average	61.4	223.5	91.9	88.9	106.3	116.7	74.7	83.1	59.5	45.9	36.1	35.7	33.7	32.9
	Stdev	55.1	254.1	88.5	81.2	86.9	91.2	67.4	64.2	47.5	35.8	29.4	29.3	25.6	23.8
	Median	47.6	98.8	57.5	64.6	74.9	107.7	55.2	74.4	49.0	33.9	27.4	27.7	30.5	30.1
	Max	200.9	1068.7	329.8	306.0	349.0	322.9	239.1	216.6	164.5	119.3	112.5	102.1	103.5	79.9
	Min	4.2	8.0	4.4	5.5	3.8	3.7	4.8	4.5	5.7	3.5	2.7	2.8	3.3	2.1
Rhynchonellida															
	Average	67.5	445.6	108.4	96.3	102.2	132.6	86.7	69.8	52.5	40.5	31.1	29.1	33.4	24.7
	Stdev	38.6	347.0	51.1	51.7	50.9	48.5	37.1	36.0	27.7	17.8	11.9	17.5	12.6	4.1
	Median	62.6	276.7	113.2	95.2	121.0	136.1	75.4	79.3	47.5	41.9	31.6	23.7	33.9	23.2
	Max	119.0	920.9	176.3	164.8	154.7	187.3	140.5	109.8	89.5	64.8	44.9	58.5	52.2	30.8
	Min	20.7	129.3	38.1	25.4	24.1	70.6	55.4	13.3	15.8	15.5	15.4	12.5	19.5	21.7

U

Appendix 4-1. Species, cleaning procedurea and geochemical data of the investigated modern shallow water (<500 m) brachiopods, their Ce/Ce* anomalies were calculated based on de Baar et al. (1988) equation. race element results were normalized to C and Mg value of 395,00 ppm (cf. Brand and Veizer, 1980).

Sample	Cleaning procedure	Ca (ppm)	Mg (ppm)	Mn (ppm)	Fe (ppm)	U (ppm)	La (ppm)	Ce	Pr	Nd	Sm	Eu	Gd	Tb	Dy	Ho	Er	Tm	Yb	Lu (ppm)	∑REEs (ppm)	Ce/Ce*
Detection limit		0.0545	0.1744	0.0000	0.0025	0.0002	0.0004	0.0002	0.0005	0.0007	0.0009	0.0003	0.0007	0.0003	0.0005	0.0001	0.0004	0.0002	0.0008	0.0002		
Bulk Samples																						
blank-1		11	0	0.0	-23.6	0.00	0.00	0.00	0.00	0.00	0.00	0.00	0.00	0.00	0.00	0.00	0.00	0.00	0.00	0.00		
blank-2		26	1	0.0	-2.0	0.00	0.00	0.00	0.00	0.00	0.00	0.00	0.00	0.00	0.00	0.00	0.00	0.00	0.00	0.00		
blank-3		21	1	0.0	54.2	0.00	0.00	0.00	0.00	0.00	0.00	0.00	0.00	0.00	0.00	0.00	0.00	0.00	0.00	0.00		
blank-4		184	7	13.8	666.6	0.02	0.02	0.02	0.00	0.00	-0.01	0.00	0.00	0.00	-0.01	0.00	0.00	0.00	0.00	0.00		
blank-5		386	5	7.9	398.9	0.00	0.01	0.01	0.00	-0.01	-0.01	0.00	0.00	0.00	-0.01	0.00	0.00	0.00	-0.01	0.00		
blank-6		34	17	0.1	12.6	0.00	0.00	0.00	0.00	-0.01	0.00	0.00	0.00	0.00	-0.01	0.00	0.00	0.00	-0.01	0.00		
blank-7		114	1	0.2	9.7	0.00	0.00	0.00	0.00	0.00	-0.01	0.00	-0.01	0.00	0.01	0.00	0.00	0.00	0.00	0.00		
blank-8		21	2	0.1	12.7	0.00	0.00	0.00	0.00	-0.01	0.00	0.00	0.00	0.00	0.00	0.00	0.00	0.00	0.01	0.00		
blank-9		129	1	0.1	18.9	0.00	0.00	0.00	0.00	0.00	0.00	0.00	0.00	0.00	0.00	0.00	0.00	0.00	0.00	0.00		
Standards																						
NBS 88a (Published values/underline are internal values)		**215123**	**128468**	**232.0**	**1958.0**	0.16	1.42	2.56	0.36	1.46	0.30	0.07	0.32	0.05	0.29	0.06	0.17	0.02	0.14	0.02		
NBS 88a-1		213432	109308	189.2	1464.9	0.09	1.38	2.49	0.35	1.48	0.30	0.07	0.34	0.05	0.29	0.06	0.17	0.02	0.14	0.02		
NBS 88a-2		211459	122998	190.0	1432.3	0.09	1.47	2.67	0.38	1.54	0.31	0.08	0.37	0.05	0.32	0.06	0.19	0.02	0.15	0.02		
NBS 88a-3		264407	138241	226.0	1406.6	0.12	1.70	2.99	0.42	1.73	0.33	0.08	0.39	0.06	0.32	0.07	0.21	0.03	0.17	0.03		
NBS 88a-4		208512	135917	201.0	1968.9	0.14	1.50	2.73	0.38	1.56	0.32	0.08	0.33	0.05	0.30	0.06	0.18	0.02	0.14	0.02		
NBS 88a-5		176113	61335	193.0	1557.7	0.17	1.61	2.91	0.41	1.71	0.35	0.08	0.41	0.06	0.36	0.07	0.21	0.03	0.17	0.02		
NBS 88a-6		209026	122169	176.8	1168.5	0.08	1.21	2.15	0.30	1.20	0.25	0.05	0.27	0.04	0.24	0.05	0.15	0.02	0.11	0.02		
NBS 88a-7		162656	96728	140.7	916.2	0.08	1.04	1.81	0.25	1.04	0.21	0.05	0.24	0.04	0.21	0.04	0.12	0.01	0.11	0.01		
NBS 88a-8		160614	106519	135.5	872.0	0.09	1.11	1.97	0.28	1.13	0.24	0.05	0.25	0.04	0.23	0.05	0.14	0.02	0.11	0.01		
NBS 88a-9		156818	62604	165.8	1069.0	0.09	1.41	2.48	0.34	1.42	0.29	0.06	0.31	0.05	0.28	0.06	0.17	0.02	0.13	0.02		
CCH-1 (Published values)		**372552**	**17551**	**54.0**	**1189.0**	**3.70**	**4.70**	**3.40**	**0.84**	**3.70**	**0.75**	**0.16**	**0.76**	**0.10**	**0.65**	**0.10**	**0.35**	**0.05**	**0.27**	**0.04**		
CCh-1-1		400821	17791	50.6	337.4	3.41	5.23	3.76	1.04	4.24	0.81	0.19	0.92	0.14	0.74	0.15	0.42	0.05	0.31	0.04		
CCh-1-2		452925	22380	57.0	386.7	4.34	6.42	4.63	1.24	5.06	1.01	0.24	1.12	0.17	0.88	0.18	0.53	0.06	0.37	0.05		
CCh-1-3		391932	15521	44.6	273.9	3.36	5.00	3.56	0.97	3.98	0.78	0.18	0.85	0.13	0.69	0.14	0.39	0.05	0.29	0.04		
CCh-1-4		318425	19727	56.6	877.8	3.68	5.13	3.74	1.00	4.15	0.82	0.19	0.89	0.13	0.70	0.14	0.40	0.05	0.29	0.04		
CCh-1-5		508109	14945	74.1	723.4	9.01	8.58	6.11	1.59	6.83	1.30	0.34	1.64	0.24	1.36	0.27	0.80	0.10	0.61	0.08		
CCh-1-6		363097	18020	38.6	208.7	2.44	3.91	2.82	0.78	3.20	0.61	0.14	0.68	0.10	0.54	0.11	0.30	0.04	0.22	0.03		
CCh-1-7		374500	23957	42.0	246.9	2.57	4.05	2.93	0.81	3.33	0.62	0.15	0.70	0.11	0.56	0.11	0.31	0.04	0.23	0.03		
CCh-1-8		369317	26582	43.6	254.4	3.01	4.65	3.35	0.92	3.77	0.74	0.18	0.81	0.12	0.67	0.13	0.37	0.04	0.28	0.04		
CCh-1-9		279059	7281	36.7	180.8	3.75	5.36	3.84	1.05	4.38	0.83	0.20	0.95	0.15	0.79	0.15	0.43	0.05	0.30	0.04		

Sample	Cleaning procedure	Ca (ppm)	Mg (ppm)	Mn (ppm)	Fe (ppm)	U (ppm)	La (ppm)	Ce	Pr	Nd	Sm	Eu	Gd	Tb	Dy	Ho	Er	Tm	Yb	Lu (ppm)	∑REEs (ppm)	Ce/Ce*
RSD																						
First run		0.15	0.17	0.14	0.25	0.04	0.03	0.03	0.03	0.03	0.03	0.03	0.03	0.03	0.03	0.04	0.04	0.04	0.04	0.04		
Second run		0.02	0.02	0.00	0.03	0.01	0.02	0.02	0.02	0.01	0.02	0.01	0.02	0.01	0.01	0.01	0.01	0.02	0.02	0.01		
Third run		0.01	0.02	0.02	0.01	0.00	0.01	0.00	0.02	0.00	0.00	0.00	0.00	0.00	0.00	0.00	0.00	0.00	0.00	0.00		
Fourth run		0.03	0.02	0.03	0.04	0.01	0.03	0.05	0.04	0.03	0.03	0.03	0.02	0.01	0.02	0.02	0.02	0.01	0.02	0.02		
Fifth run		0.03	0.01	0.02	0.01	0.03	0.00	0.03	0.03	0.01	0.02	0.03	0.05	0.04	0.05	0.04	0.05	0.05	0.06	0.05		
Sixth run		0.00	0.03	0.01	0.01	0.05	0.02	0.02	0.02	0.02	0.01	0.02	0.02	0.02	0.02	0.02	0.01	0.01	0.02	0.02		
Seventh run		0.01	0.05	0.01	0.01	0.00	0.02	0.02	0.02	0.02	0.02	0.01	0.01	0.01	0.03	0.02	0.02	0.02	0.02	0.01		
Eighth run		0.05	0.04	0.02	0.00	0.00	0.00	0.01	0.00	0.00	0.00	0.00	0.00	0.00	0.00	0.00	0.00	0.00	0.00	0.00		
Ninth run		0.03	0.03	0.00	0.03	0.03	0.01	0.01	0.01	0.02	0.01	0.01	0.03	0.01	0.00	0.00	0.01	0.01	0.03	0.02		
RSD Average		**0.04**	**0.04**	**0.03**	**0.04**	**0.02**	**0.01**	**0.02**	**0.02**	**0.02**	**0.02**	**0.02**	**0.02**	**0.02**	**0.02**	**0.02**	**0.02**	**0.02**	**0.02**	**0.02**		
Denmark Strait, Iceland																						
D.S.-1 (Pedicle)	P-5	414444	2344	11.3	26.2	0.01	0.03	0.04	0.01	0.04	0.01	0.00	0.00	0.00	0.01	0.00	0.00	0.00	0.00	0.00	0.14	0.60
D.S.-2 (Brachial)	P-5	628307	4539	25.4	646.8	0.02	0.06	0.08	0.01	0.06	0.01	-0.02	0.01	0.00	0.01	0.00	0.00	0.00	0.00	0.00	0.24	0.59
D.S.-3 (Brachial)	P-5	331663	1558	49.6	55.3	0.02	0.03	0.02	0.01	0.03	0.00	0.00	0.00	0.00	0.01	0.00	0.01	0.00	0.00	0.00	0.11	0.26
D.S.-4 (Pedicle)	P-5	317175	1259	40.2	54.7	0.02	0.04	0.01	0.01	0.03	0.01	0.00	0.01	0.00	0.01	0.00	0.00	0.00	0.00	0.00	0.13	0.19
Norwegian Sea, Iceland																						
N.S.-1 (Pedicle)	P-5	331161	2310	15.0	34.5	0.01	0.04	0.07	0.01	0.05	0.00	0.00	0.01	0.00	0.01	0.00	0.00	0.00	0.01	0.00	0.20	0.69
N.S.-2 (Pedicle)	P-5	367317	1576	58.6	58.9	0.02	0.02	0.01	0.00	0.02	0.00	0.00	0.00	0.00	0.00	0.00	0.01	0.00	0.00	0.00	0.08	0.30
N.S.-3 (Brachial)	P-5	334482	1599	43.0	51.3	0.02	0.03	0.02	0.01	0.02	0.00	0.00	0.01	0.00	0.01	0.00	0.01	0.00	0.00	0.00	0.10	0.28
N.S.-4 (Brachial)	P-5	433731	4069	37.4	39.8	0.01	0.08	0.10	0.02	0.09	0.02	0.00	0.02	0.00	0.02	0.00	0.01	0.00	0.01	0.00	0.37	0.57
Irminger Sea, Iceland																						
I. S.-1 (Brachial)	P-5	568457	2775	4.0	-8.3	0.01	0.01	0.01	0.00	0.00	0.00	0.00	0.00	0.00	0.00	0.00	0.00	0.00	0.00	0.00	0.02	
I. S.-2 (Pedicle)	P-5	259086	1537	5.6	1.4	0.01	0.01	0.01	0.00	0.01	0.00	0.00	0.00	0.00	0.00	0.00	0.00	0.00	0.00	0.00	0.05	0.58
I. S.-3 (Brachial)	P-5	355659	2310	8.0	-4.4	0.01	0.02	0.03	0.01	0.02	0.01	0.00	0.01	0.00	0.01	0.00	0.00	0.00	0.00	0.00	0.11	0.65
I. S.-4 (Brachial)	P-5	530005	3753	4.0	6.6	0.01	0.00	0.01	0.00	0.00	0.00	0.00	0.00	0.00	0.00	0.00	0.00	0.00	0.00	0.00	0.01	
I. S.-5 (Pedicle)	P-5	308394	2537	6.9	12.5	0.01	0.02	0.02	0.00	0.02	0.01	0.00	0.00	0.00	0.00	0.00	0.00	0.00	0.00	0.00	0.07	0.52
I. S.-6 (Brachial)	P-5	308393	2768	7.1	9.9	0.01	0.02	0.03	0.01	0.02	0.00	0.00	0.01	0.00	0.00	0.00	0.00	0.00	0.00	0.00	0.09	0.62
I. S.-7 (Pedicle)	P-5	335952	3504	48.1	31.1	0.02	0.08	0.09	0.02	0.11	0.02	0.01	0.03	0.00	0.02	0.00	0.01	0.00	0.01	0.00	0.40	0.44
I. S.-8 (Brachial)	P-5	334193	1920	10.0	-3.1	0.01	0.03	0.04	0.01	0.02	0.01	0.00	0.00	0.00	0.01	0.00	0.00	0.00	0.00	0.00	0.13	0.65
I. S.-9 (Pedicle)	P-5	357106	1926	13.1	3.4	0.01	0.04	0.06	0.01	0.05	0.01	0.00	0.01	0.00	0.01	0.00	0.01	0.00	0.00	0.00	0.20	0.61
I. S.-10 (Brachial)	P-5	290070	2375	9.1	9.7	0.01	0.03	0.05	0.01	0.03	0.00	0.00	0.01	0.00	0.01	0.00	0.00	0.00	0.00	0.00	0.13	0.74
I. S.-11 (Pedicle)	P-5	322682	2445	12.5	16.0	0.02	0.05	0.07	0.01	0.06	0.01	0.00	0.01	0.00	0.01	0.00	0.01	0.00	0.00	0.00	0.24	0.60
I. S.-12 (Pedicle)	P-5	303543	1703	13.6	25.4	0.01	0.04	0.06	0.01	0.05	0.01	0.00	0.00	0.00	0.01	0.00	0.01	0.00	0.01	0.00	0.22	0.65

W

Sample	Cleaning procedure	Ca (ppm)	Mg (ppm)	Mn (ppm)	Fe (ppm)	U (ppm)	La (ppm)	Ce	Pr	Nd	Sm	Eu	Gd	Tb	Dy	Ho	Er	Tm	Yb	Lu (ppm)	∑REEs (ppm)	Ce/Ce*
I. S.-12 (Pedicle)	P-5	303543	1703	13.6	25.4	0.01	0.04	0.06	0.01	0.05	0.01	0.00	0.00	0.00	0.01	0.00	0.01	0.00	0.01	0.00	0.22	0.65
I. S.-13	P-3	349136	2512	24.0	52.3	0.02	0.07	0.13	0.02	0.08	0.03	0.00	0.01	0.00	0.01	0.00	0.01	0.00	0.00	0.00	0.36	0.83
I. S.-14	P-3	310879	1666	13.3	29.5	0.01	0.05	0.08	0.01	0.04	0.00	0.00	0.01	0.00	0.01	0.00	0.00	0.00	0.00	0.00	0.21	0.86
I. S.-15	P-3	378741	2097	11.7	15.6	0.01	0.02	0.04	0.01	0.02	0.00	0.00	0.00	0.00	0.00	0.00	0.00	0.00	0.00	0.00	0.08	1.00
I. S.-16	P-3	402824	2532	20.5	40.6	0.02	0.06	0.12	0.01	0.06	0.01	0.00	0.00	0.00	0.01	0.00	0.00	0.00	0.00	0.00	0.27	0.93
I. S.-17	P-3	353708	2709	17.5	39.3	0.01	0.05	0.11	0.01	0.05	0.01	0.00	0.01	0.00	0.01	0.00	0.00	0.00	0.00	0.00	0.25	1.03
I. S.-18	P-3	330743	1796	17.8	27.0	0.01	0.03	0.07	0.01	0.04	0.01	0.00	0.01	0.00	0.01	0.00	0.01	0.00	0.00	0.00	0.19	0.83
I. S.-19	P-3	311984	2463	22.0	37.3	0.02	0.07	0.11	0.02	0.06	0.02	0.00	0.01	0.00	0.01	0.00	0.01	0.00	0.01	0.00	0.33	0.78
I. S.-20	P-3	287613	2307	17.0	38.2	0.02	0.06	0.15	0.02	0.07	0.01	0.00	0.01	0.00	0.01	0.00	0.00	0.00	0.01	0.00	0.35	1.10
I. S.-21	P-2	393816	3657	69.2	72.0	0.02	0.12	0.15	0.03	0.14	0.04	0.01	0.04	0.00	0.03	0.00	0.01	0.00	0.01	0.00	0.60	0.55
I. S.-22	P-2	405359	2621	17.9	394.2	0.01	0.03	0.04	0.01	0.02	0.01	0.00	0.01	0.00	0.01	0.00	0.00	0.00	0.00	0.00	0.13	0.80
I. S.-23	P-2	321489	1993	18.6	595.7	0.02	0.04	0.04	0.01	0.03	0.00	0.00	0.00	0.00	0.00	0.00	0.01	0.00	0.00	0.00	0.14	0.56
I. S.-24	P-2	367498	3199	69.4	2860.7	0.02	0.05	0.08	0.01	0.06	0.01	0.00	0.02	0.00	0.01	0.00	0.01	0.00	0.00	0.00	0.25	0.63
I. S.-25	P-1	444307	2895	25.7	430.3	0.02	0.07	0.15	0.01	0.06	0.02	0.00	0.02	0.00	0.01	0.00	0.01	0.00	0.01	0.00	0.35	1.08
I. S.-26	P-1	325172	2777	41.5	648.4	0.03	0.12	0.30	0.03	0.11	0.02	0.00	0.02	0.00	0.02	0.00	0.01	0.00	0.00	0.00	0.62	1.22
I. S.-27	P-1	308302	2372	35.6	624.2	0.03	0.13	0.26	0.03	0.12	0.02	0.00	0.02	0.00	0.02	0.00	0.01	0.00	0.01	0.00	0.62	0.97
I. S.-28	P-1	287932	2485	61.9	640.1	0.03	0.21	0.56	0.05	0.20	0.03	0.01	0.04	0.01	0.03	0.01	0.02	0.00	0.01	0.00	1.18	1.24
Bonne Bay, Newfoundland																						
B.B.-1 (Pedicle)	P-5	342352	2535	5.8	-5.7	0.01	0.03	0.03	0.01	0.02	0.01	0.00	0.00	0.00	0.00	0.00	0.00	0.00	0.00	0.00	0.09	0.50
B.B.-2 (Brachial)	P-5	350870	2551	5.6	-1.5	0.01	0.06	0.04	0.01	0.04	0.01	0.00	0.01	0.00	0.01	0.00	0.00	0.00	0.00	0.00	0.19	0.37
B.B.-3 (Pedicle)	P-5	321887	2432	5.5	5.4	0.01	0.02	0.02	0.01	0.02	0.00	0.00	0.00	0.00	0.00	0.00	0.00	0.00	0.00	0.00	0.09	0.43
B.B.-4 (Brachial)	P-5	315054	2370	5.3	9.9	0.01	0.05	0.04	0.01	0.04	0.00	0.00	0.01	0.00	0.00	0.00	0.00	0.00	0.00	0.00	0.16	0.38
B.B.-5 (Pedicle)	P-5	285179	2148	5.4	-5.1	0.01	0.08	0.07	0.02	0.07	0.01	0.00	0.01	0.00	0.01	0.00	0.00	0.00	0.00	0.00	0.29	0.38
B.B.-6 (Pedicle)	P-5	323681	2565	4.5	-5.3	0.01	0.01	0.02	0.00	0.01	0.00	0.00	0.00	0.00	0.00	0.00	0.00	0.00	0.00	0.00	0.05	0.49
B.B.-7 (Pedicle)	P-5	300395	1704	4.5	-9.3	0.01	0.01	0.01	0.00	0.01	0.00	0.00	0.00	0.00	0.00	0.00	0.00	0.00	0.00	0.00	0.04	0.62
B.B.-8 (Pedicle)	P-5	286990	2199	5.6	0.0	0.02	0.09	0.07	0.02	0.08	0.02	0.00	0.01	0.00	0.01	0.00	0.00	0.00	0.00	0.00	0.31	0.36
B.B.-9 (Pedicle)	P-5	277679	2175	4.0	-3.6	0.01	0.01	0.02	0.00	0.01	0.00	0.00	0.00	0.00	0.00	0.00	0.00	0.00	0.00	0.00	0.05	0.52
B.B.-10 (Pedicle)	P-5	308192	1743	4.8	-11.5	0.01	0.01	0.02	0.00	0.01	0.00	0.00	0.00	0.00	0.00	0.00	0.00	0.00	0.00	0.00	0.05	0.61
B.B.-11	P-1	303617	1885	8.9	394.7	0.01	0.02	0.02	0.00	0.01	0.00	0.00	0.00	0.00	0.00	0.00	0.00	0.00	0.00	0.00	0.05	0.58
B.B.-12	P-1	477093	1064	11.5	428.3	0.01	0.36	0.19	0.06	0.25	0.02	0.00	0.04	0.00	0.01	0.00	0.00	0.00	0.00	0.00	0.93	0.27
B.B.-13	P-1	313882	654	15.2	511.8	0.01	0.37	0.22	0.05	0.24	0.04	0.00	0.03	0.00	-0.01	0.00	0.01	0.00	0.00	0.00	0.97	0.32

X

Sample	Cleaning procedure	Ca (ppm)	Mg (ppm)	Mn (ppm)	Fe (ppm)	U (ppm)	La (ppm)	Ce	Pr	Nd	Sm	Eu	Gd	Tb	Dy	Ho	Er	Tm	Yb	Lu (ppm)	∑REEs (ppm)	Ce/Ce*
Friday Harbour, Washington																						
F.H.-1 (Umbo)	P-5	363688	1501	21.0	52.3	0.01	0.00	0.01	0.00	0.01	0.00	0.00	0.00	0.00	0.00	0.00	0.00	0.00	0.00	0.00	0.02	0.64
F.H.-2 (Pedicle)	P-5	365341	1252	35.1	54.5	0.02	0.02	0.02	0.00	0.02	0.00	0.00	0.00	0.00	0.00	0.00	0.00	0.00	0.00	0.00	0.08	0.40
F.H.-3 (Brachial)	P-5	371814	1718	44.5	54.2	0.02	0.02	0.01	0.00	0.01	0.00	0.00	0.00	0.00	0.00	0.00	0.00	0.00	0.00	0.00	0.06	0.37
F.H.-4 (Brachial)	P-5	379162	1678	44.0	51.9	0.01	0.03	0.01	0.00	0.02	0.00	0.00	0.01	0.00	0.00	0.00	0.00	0.00	0.00	0.00	0.08	0.27
F.H.-5 (Pedicle)	P-5	395067	1653	47.5	56.7	0.02	0.03	0.02	0.01	0.02	0.00	0.00	0.01	0.00	0.00	0.00	0.01	0.00	0.00	0.00	0.09	0.27
F.H.-6 (Pedicle)	P-5	344957	2507	15.6	20.1	0.02	0.05	0.06	0.01	0.04	0.00	0.00	0.01	0.00	0.01	0.00	0.00	0.00	0.00	0.00	0.19	0.61
Bay of Fundy, New Brunswick																						
B.F.-1	P-5	330359	2122	17.8	28.6	0.01	0.05	0.07	0.01	0.07	0.01	0.00	0.01	0.00	0.01	0.00	0.00	0.00	0.01	0.00	0.25	0.55
B.F.-2	P-5	364781	2754	4.8	-6.3	0.01	0.02	0.02	0.00	0.02	0.00	0.00	0.00	0.00	0.00	0.00	0.00	0.00	0.00	0.00	0.08	0.55
B.F.-3	P-5	296849	2257	4.2	-7.0	0.01	0.02	0.02	0.00	0.02	0.00	0.00	0.00	0.00	0.00	0.00	0.00	0.00	0.00	0.00	0.06	0.38
B.F.-4	P-5	354325	2840	5.8	-5.7	0.02	0.07	0.05	0.01	0.05	0.01	0.00	0.01	0.00	0.01	0.00	0.00	0.00	0.00	0.00	0.22	0.34
B.F.-5	P-5	300500	2449	5.1	1.9	0.02	0.06	0.04	0.01	0.04	0.01	0.00	0.01	0.00	0.01	0.00	0.00	0.00	0.00	0.00	0.19	0.36
B.F.-6	P-1	358583	2527	24.1	408.6	0.03	0.06	0.07	0.01	0.05	0.01	0.00	0.03	0.00	0.01	0.00	0.00	0.00	0.00	0.00	0.26	0.59
B.F.-7	P-1	394445	2511	38.8	375.3	0.02	0.04	0.05	0.01	0.02	0.00	0.00	0.00	0.00	0.01	0.00	0.00	0.00	0.00	0.00	0.14	0.77
B.F.-8	P-1	355958	2896	16.9	420.6	0.01	0.06	0.06	0.01	0.05	0.01	0.00	0.01	0.00	0.01	0.00	0.01	0.00	0.01	0.00	0.23	0.47
B.F.-9	P-1	458230	3788	23.8	498.5	0.04	0.15	0.17	0.03	0.14	0.04	0.00	0.03	0.01	0.02	0.00	0.02	0.00	0.01	0.00	0.62	0.54
B.F.-10	P-3	370305	2912	8.2	<34.19	0.01	0.04	0.02	0.01	0.01	<0.0016	<0.0004	0.04	<0.00015	0.02	<0.0005	0.00	0.00	0.00	0.00	0.13	
B.F.-11	P-3	373834	2556	17.3	<63	0.00	0.03	0.03	0.01	0.01	<0.0016	0.01	0.01	0.00	<0.0009	0.01	0.00	0.00	0.01	<0.0003	0.11	
B.F.-12	P-3	364553	2060	0.7	12.1	0.01	0.03	0.01	0.00	0.01	<0.0016	<0.0004	0.00	0.00	0.00	0.00	0.01	<0.0003	0.00	0.00	0.07	0.28
Philippine Sea, North Pacific Ocean																						
Pal.-1 (Pedicle)	P-5	281659	13674	3.0	47.9	0.02	0.00	0.00	0.00	0.00	0.00	0.00	0.00	0.00	0.00	0.00	0.00	0.00	0.00	0.00	0.01	
Pal.-2 (Pedicle)	P-5	313331	12832	1.4	53.7	0.01	0.00	0.00	0.00	0.00	0.00	0.00	0.00	0.00	0.00	0.00	0.00	0.00	0.00	0.00	0.01	0.58
Pal.-3 (Brachial)	P-5	266608	15637	1.8	49.8	0.03	0.00	0.00	0.00	0.00	0.00	0.00	0.00	0.00	0.00	0.00	0.00	0.00	0.00	0.00	0.01	
Pal.-4 (Umbo)	P-5	337809	19210	6.6	57.6	0.06	0.01	0.01	0.00	0.00	0.00	0.00	0.00	0.00	0.00	0.00	0.00	0.00	0.00	0.00	0.03	0.77
Ross Sea-1, Antarctica																						
R.S.-7	P-5	364198	2539	58.0	17.0	0.01	0.02	0.02	0.00	0.02	0.01	0.00	0.00	0.00	0.00	0.00	0.00	0.00	0.00	0.00	0.08	0.33
R.S.-8	P-5	393545	3085	289.7	15.7	0.02	0.02	0.01	0.00	0.02	0.00	0.00	0.01	0.00	0.00	0.00	0.00	0.00	0.00	0.00	0.07	0.30
R.S.-9	P-5	368131	963	15.5	13.9	0.00	0.02	0.02	0.00	0.01	0.00	0.00	0.01	0.00	0.00	0.00	0.00	0.00	0.00	0.00	0.07	0.57
R.S.-10	P-5	379983	2425	76.0	52.3	0.02	0.10	0.10	0.02	0.07	0.01	0.00	0.02	0.00	0.01	0.00	0.01	0.00	0.01	0.00	0.36	0.52
R.S.-11	P-5	323944	1527	6.5	30.6	0.01	0.15	0.09	0.03	0.12	0.02	0.00	0.04	0.00	0.02	0.00	0.01	0.00	0.01	0.00	0.50	0.31
R.S.-12	P-5	397772	2702	56.1	56.4	0.01	0.07	0.08	0.01	0.06	0.01	0.00	0.02	0.00	0.01	0.00	0.01	0.00	0.00	0.00	0.27	0.59
R.S.-13	P-5	352134	1385	48.2	23.8	0.00	0.03	0.03	0.01	0.02	0.00	0.00	0.01	0.00	0.01	0.00	0.00	0.00	0.00	0.00	0.11	0.54
R.S.-14	P-5	317104	370	5.8	10.5	0.00	0.03	0.02	0.01	0.03	0.00	0.00	0.01	0.00	0.00	0.00	0.00	0.00	0.00	0.00	0.11	0.20
R.S.-15	P-5	334325	304	2.0	8.7	0.00	0.03	0.01	0.00	0.02	0.00	0.00	0.00	0.00	0.00	0.00	0.00	0.00	0.00	0.01	0.06	0.15

Y

Sample	Cleaning procedure	Ca (ppm)	Mg (ppm)	Mn (ppm)	Fe (ppm)	U (ppm)	La (ppm)	Ce	Pr	Nd	Sm	Eu	Gd	Tb	Dy	Ho	Er	Tm	Yb	Lu (ppm)	∑REEs (ppm)	Ce/Ce*
Ross Sea-2, Antarctica																						
R.S.-1	P-5	300241	722	16.2	26.6	0.00	0.03	0.03	0.01	0.03	0.00	0.00	0.01	0.00	0.00	0.00	0.00	0.00	0.00	**0.00**	0.14	0.50
R.S.-2	P-5	300835	599	12.7	32.2	0.00	0.03	0.04	0.01	0.03	0.00	0.00	0.01	0.00	0.01	0.00	0.01	0.00	0.00	0.00	0.14	0.63
R.S.-3	P-5	404419	2444	173.4	47.9	0.05	0.15	0.23	0.03	0.11	0.02	**0.00**	0.03	0.00	0.02	**0.00**	0.01	0.00	0.01	0.00	0.62	0.79
R.S.-4	P-5	370771	3865	13.8	20.3	0.03	0.05	0.05	0.01	0.05	0.02	**0.00**	0.01	0.00	0.00	0.00	0.00	0.00	0.00	**0.00**	0.20	0.47
R.S.-5	P-5	363279	599	62.5	53.6	0.00	0.10	0.11	0.02	0.08	0.02	0.01	0.03	0.01	0.03	0.01	0.01	0.00	**0.00**	0.00	0.41	0.52
R.S.-6	P-5	435363	4122	67.7	42.3	0.01	0.05	0.09	0.02	0.07	0.01	0.00	0.02	0.00	0.01	0.00	0.01	**0.00**	0.01	0.00	0.31	0.70

Concentrations in red and bold font are either negative or below machine detection limit. Thus, were eliminated from the calculations

Concentrations in blue and bold font are anomalous (their shale normalized values are significantly depleted or enriched by at least a half order of magnitude relative to their neighbours). Thus, were ignored in the calculations

Z

Appendix 4-2. Summary statistics of the different cleaning procedures of the investigated modern articulated brachiopods.

Sample	Ca (ppm)	Mg (ppm)	Mn (ppm)	Fe (ppm)	U (ppm)	La (ppm)	Ce	Pr	Nd	Sm	Eu	Gd	Tb	Dy	Ho	Er	Tm	Yb	Lu	∑REEs (ppm)	Ce/Ce*
Denmark Strait, Iceland																					
P-5																					
Average	422897	2425	31.6	195.8	0.016	0.039	0.036	0.009	0.038	0.009	0.002	0.008	0.002	0.007	0.002	0.004	0.001	0.005	0.001	0.15	0.44
Stdev	143487	1482	16.8	301.0	0.006	0.015	0.028	0.003	0.012	0.004	0.001	0.005	0.001	0.001	0.001	0.002	0.000	0.000	0.000	0.06	0.22
Max	628307	4539	49.6	646.8	0.021	0.060	0.075	0.014	0.055	0.013	0.003	0.013	0.002	0.009	0.002	0.006	0.001	0.005	0.001	0.24	0.60
Min	317175	1259	11.3	26.2	0.007	0.027	0.014	0.007	0.027	0.005	0.001	0.004	0.001	0.006	0.001	0.002	0.000	0.005	0.000	0.11	0.19
Norwegian Sea, Iceland																					
P-5																					
Average	366673	2388	38.5	46.1	0.014	0.044	0.049	0.010	0.043	0.008	0.002	0.011	0.002	0.013	0.002	0.006	0.001	0.005	0.001	0.19	0.52
Stdev	47591	1171	18.0	11.0	0.006	0.025	0.042	0.007	0.032	0.010	0.002	0.009	0.000	0.006	0.000	0.001	0.001	0.002		0.13	0.20
Max	433731	4069	58.6	58.9	0.021	0.079	0.101	0.020	0.087	0.019	0.004	0.025	0.002	0.018	0.002	0.008	0.002	0.008	0.001	0.37	0.69
Min	331161	1576	15.0	34.5	0.007	0.024	0.014	0.005	0.019	0.002	0.000	0.004	0.001	0.007	0.001	0.005	0.001	0.003	0.001	0.08	0.28
Irminger Sea, Iceland																					
P-1																					
Average	341428	2632	41.2	585.8	0.026	0.130	0.318	0.030	0.122	0.020	0.004	0.026	0.003	0.019	0.003	0.011	0.001	0.008	0.001	0.69	1.15
Stdev	70255	245	15.3	104.1	0.007	0.061	0.174	0.015	0.059	0.006	0.003	0.012	0.002	0.011	0.002	0.005	0.000	0.003	0.000	0.35	0.13
Max	444307	2895	61.9	648.4	0.033	0.213	0.561	0.050	0.201	0.028	0.009	0.043	0.007	0.034	0.005	0.016	0.001	0.011	0.001	1.18	1.24
Min	287932	2372	25.7	430.3	0.017	0.066	0.149	0.014	0.059	0.016	0.002	0.016	0.002	0.008	0.001	0.006	0.000	0.006	0.001	0.35	0.97
P-2																					
Average	372041	2867	43.8	980.7	0.019	0.061	0.080	0.015	0.064	0.018	0.005	0.016	0.002	0.012	0.002	0.008	0.001	0.011	0.001	0.28	0.59
Stdev	37240	721	29.4	1,271.8	0.004	0.043	0.052	0.013	0.056	0.016	0.005	0.015	0.002	0.010	0.002	0.004	0.000		0.001	0.22	0.12
Max	405359	3657	69.4	2,860.7	0.022	0.123	0.155	0.033	0.145	0.037	0.010	0.037	0.004	0.027	0.004	0.014	0.001	0.011	0.001	0.60	0.80
Min	321489	1993	17.9	72.0	0.014	0.025	0.044	0.006	0.025	0.006	0.001	0.004	0.001	0.003	0.001	0.004	0.000	0.011	0.000	0.13	0.55
P-3																					
Average	340703	2260	18.0	35.0	0.015	0.050	0.101	0.012	0.053	0.013	0.002	0.009	0.001	0.010	0.001	0.005	0.001	0.005	0.000	0.25	0.91
Stdev	38132	374	4.2	10.9	0.007	0.017	0.036	0.004	0.020	0.009	0.001	0.004	0.001	0.002	0.001	0.003		0.004	0.000	0.10	0.11
Max	402824	2709	24.0	52.3	0.024	0.068	0.152	0.017	0.080	0.027	0.003	0.015	0.002	0.013	0.002	0.011	0.001	0.011	0.001	0.36	1.10
Min	287613	1666	11.7	15.6	0.006	0.018	0.037	0.005	0.016	0.004	0.000	0.003	0.000	0.007	0.000	0.002	0.001	0.002	0.000	0.08	0.78
P-5																					
Average	356128	2463	11.8	11.3	0.011	0.030	0.039	0.008	0.037	0.008	0.002	0.008	0.001	0.008	0.001	0.004	0.001	0.004	0.001	0.14	0.55
Stdev	94594	674	11.9	10.6	0.005	0.022	0.026	0.006	0.029	0.005	0.002	0.008	0.001	0.005	0.001	0.003	0.001	0.004	0.001	0.11	0.08
Max	568457	3753	48.1	31.1	0.024	0.082	0.088	0.023	0.108	0.019	0.006	0.030	0.003	0.019	0.005	0.011	0.002	0.010	0.001	0.40	0.74
Min	259086	1537	4.0	-3.1	0.006	0.005	0.006	0.001	0.010	0.004	0.000	0.001	0.000	0.001	0.000	0.001	0.000	0.001	0.000	0.01	0.44
Bonne Bay, Newfoundland																					
P-1																					
Average	364864	1201	11.9	444.9	0.008	0.249	0.142	0.040	0.164	0.018	0.002	0.025	0.002	0.006	0.002	0.004	0.001	0.002	0.000	0.65	0.39
Stdev	97329	627	3.2	60.3	0.003	0.202	0.110	0.031	0.136	0.017	0.000	0.018	0.002		0.001	0.005	0.000			0.52	0.16
Max	477093	1885	15.2	511.8	0.012	0.368	0.221	0.061	0.246	0.035	0.003	0.038	0.003	0.006	0.003	0.008	0.001	0.002	0.000	0.97	0.58
Min	303617	654	8.9	394.7	0.006	0.016	0.016	0.004	0.007	0.002	0.002	0.005	0.000	0.006	0.002	0.001	0.000	0.002	0.000	0.05	0.27
P-5																					
Average	311228	2242	5.1	5.1	0.012	0.038	0.032	0.009	0.032	0.007	0.002	0.007	0.001	0.004	0.001	0.002	0.001	0.002	0.001	0.13	0.41
Stdev	24362	315	0.6	4.9	0.003	0.030	0.020	0.007	0.025	0.006	0.001	0.005	0.000	0.004	0.001	0.002	0.000	0.001	0.000	0.10	0.10
Max	350870	2565	5.8	9.9	0.016	0.088	0.066	0.020	0.078	0.016	0.003	0.014	0.002	0.010	0.002	0.005	0.001	0.004	0.001	0.31	0.62
Min	277679	1704	4.0	0.0	0.008	0.009	0.014	0.002	0.011	0.001	0.001	0.001	0.000	0.001	0.001	0.001	0.000	0.001	0.000	0.04	0.36

Sample	Ca (ppm)	Mg (ppm)	Mn (ppm)	Fe (ppm)	U (ppm)	La (ppm)	Ce	Pr	Nd	Sm	Eu	Gd	Tb	Dy	Ho	Er	Tm	Yb	Lu	∑REEs (ppm)	Ce/Ce*
Friday Harbour, Washington																					
P-5																					
Average	371268	1762	37.3	47.5	0.017	0.028	0.024	0.006	0.023	0.005	0.001	0.006	0.001	0.004	0.001	0.004	0.000	0.001	0.000	0.10	0.42
Stdev	18415	457	13.0	15.4	0.002	0.012	0.021	0.003	0.011		0.000	0.002	0.000	0.002	0.000	0.001	0.000	0.000	0.000	0.05	0.14
Max	395067	2507	47.5	56.7	0.021	0.049	0.062	0.012	0.042	0.005	0.001	0.010	0.001	0.006	0.002	0.005	0.000	0.002	0.001	0.19	0.61
Min	344957	1252	15.6	20.1	0.014	0.016	0.012	0.003	0.014	0.005	0.001	0.004	0.001	0.002	0.001	0.002	0.000	0.001	0.000	0.06	0.27
Bay of Fundy, New Brunswick																					
P-1																					
Average	391804	2930	25.9	425.8	0.000	0.076	0.088	0.016	0.065	0.018	0.003	0.020	0.003	0.012	0.002	0.007	0.001	0.006	0.001	0.31	0.56
Stdev	47637	598	9.2	52.1	0.011	0.047	0.053	0.013	0.049	0.015	0.002	0.014	0.002	0.008	0.001	0.005		0.004	0.001	0.21	0.13
Max	458230	3788	38.8	498.5	0.037	0.145	0.167	0.035	0.136	0.036	0.005	0.033	0.005	0.024	0.002	0.015	0.001	0.011	0.002	0.62	0.77
Min	355958	2511	16.9	375.3	0.012	0.039	0.055	0.006	0.021	0.008	0.001	0.003	0.001	0.005	0.001	0.003	0.001	0.002	0.001	0.14	0.47
P-3																					
Average	369564	2509	8.8	12.1	0.006	0.032	0.021	0.008	0.008		0.012	0.022	0.001	0.011	0.004	0.007	0.001	0.008	0.001	0.10	0.42
Stdev	4685	428	8.3		0.003	0.007	0.009	0.004				0.019	0.001	0.009	0.004	0.005	0.000		0.001	0.03	
Max	373834	2912	17.3	12.1	0.009	0.039	0.031	0.011	0.008		0.012	0.036	0.002	0.017	0.007	0.011	0.001	0.008	0.002	0.13	0.28
Min	364553	2060	0.7	12.1	0.003	0.027	0.013	0.003	0.008		0.012	0.008	0.001	0.004	0.001	0.003	0.001	0.008	0.001	0.07	0.28
P-5																					
Average	329363	2484	7.5	15.2	0.013	0.045	0.039	0.010	0.038	0.007	0.001	0.007	0.001	0.006	0.001	0.004	0.001	0.003	0.000	0.16	0.42
Stdev	30695	310	5.8	18.9	0.004	0.024	0.021	0.005	0.021	0.003	0.001	0.005	0.001	0.004	0.001	0.000	0.000	0.002	0.000	0.09	0.11
Max	364781	2840	17.8	28.6	0.019	0.072	0.069	0.014	0.068	0.009	0.003	0.014	0.002	0.010	0.002	0.005	0.001	0.006	0.001	0.25	0.55
Min	296849	2122	4.2	1.9	0.010	0.020	0.016	0.003	0.017	0.002	0.000	0.002	0.000	0.001	0.000	0.004	0.000	0.001	0.000	0.06	0.34
Philippine Sea, North Pacific Ocean																					
P-5																					
Average	287199	14048	2.1	50.5	0.019	0.003	0.004	0.000	0.001	0.000	0.000	0.001	0.000	0.001	0.000	0.002	0.000		0.000	0.01	0.58
Stdev	23849	1439	0.8	2.9	0.006	0.000	0.001	0.000				0.001	0.000		0.000	0.000				0.00	
Max	313331	15637	3.0	53.7	0.025	0.003	0.005	0.001	0.001	0.000	0.000	0.002	0.000	0.001	0.000	0.002	0.000	0.000	0.000	0.01	0.58
Min	266608	12832	1.4	47.9	0.013	0.003	0.003	0.000	0.001	0.000	0.000	0.000	0.000	0.001	0.000	0.002	0.000	0.000	0.000	0.01	0.58
Ross Sea-1, Antarctica																					
P-5																					
Average	359015	1700	62.0	25.4	0.008	0.052	0.042	0.009	0.041	0.009	0.003	0.012	0.002	0.009	0.003	0.005	0.001	0.005	0.001	0.18	0.40
Stdev	29342	1033	89.6	17.7	0.009	0.046	0.038	0.010	0.035	0.006	0.002	0.010	0.001	0.006	0.002	0.003	0.001	0.000	0.001	0.16	0.16
Max	397772	3085	289.7	56.4	0.023	0.149	0.099	0.033	0.121	0.019	0.004	0.037	0.004	0.018	0.005	0.011	0.002	0.006	0.002	0.50	0.59
Min	317104	304	2.0	8.7	0.000	0.016	0.007	0.003	0.012	0.004	0.001	0.004	0.000	0.002	0.001	0.002	0.000	0.005	0.000	0.06	0.15
Ross Sea-2, Antarctica																					
P-5																					
Average	362485	2059	57.7	37.1	0.017	0.068	0.091	0.015	0.062	0.013	0.003	0.019	0.002	0.012	0.002	0.008	0.001	0.007	0.001	0.30	0.64
Stdev	54432	1656	61.9	12.9	0.020	0.046	0.072	0.010	0.030	0.008	0.001	0.010	0.002	0.010	0.002	0.004	0.000	0.006	0.000	0.19	0.13
Max	435363	4122	173.4	53.6	0.052	0.146	0.227	0.035	0.107	0.023	0.005	0.034	0.006	0.026	0.005	0.014	0.001	0.015	0.001	0.62	0.79
Min	300241	599	12.7	20.3	0.001	0.031	0.035	0.006	0.029	0.004	0.002	0.010	0.001	0.004	0.001	0.004	0.001	0.002	0.000	0.14	0.47

Note: Concentations in ppm.

Appendix 4-3. REE contents in the Paleozoic brachiopods and whole rock, their Ce anomalies (Ce*) calculated based on de Baar et al. (1988) equation.

	Species	La	Ce	Pr	Nd	Sm	Eu	Gd	Tb	Dy	Ho	Er	Tm	Yb	Lu	∑REEs	Ce/Ce*
Uppermost Permian, Gyanyima Fm, Tibet																	
Unit 9																	
Brachiopods																	
Per. 10[a]	*Marginalosa* sp.	2.26	1.08	0.34	1.43	0.25	0.05	0.30	0.04	0.22	0.05	0.14	0.01	0.09	0.01	6.28	0.25
Whole rock																	
Per. 10-2[a]		33.49	14.49	5.81	23.17	4.15	0.94	4.52	0.66	3.37	0.69	1.90	0.23	1.33	0.18	94.94	0.22
Per. 10-1[a]		30.62	13.07	5.12	21.34	4.79	0.82	4.93	0.58	4.21	0.61	2.80	0.20	2.36	1.35	92.78	0.22
Unit 8																	
Brachiopods																	
Per. 9[a]	*Costiferina indica*	4.19	2.25	0.73	2.77	0.52	0.11	0.48	0.08	0.37	0.07	0.19	0.02	0.14	0.02	11.94	0.28
Per. 8[a]	*Costiferina spiralis*	0.23	0.14	0.03	0.12	0.02	0.00	0.02	0.00	0.02	0.00	0.01	0.00	0.01	0.00	0.61	0.33
Whole rock																	
Per. 9[a]		4.40	2.28	0.61	2.58	0.48	0.10	0.58	0.08	0.50	0.11	0.31	0.04	0.21	0.03	12.30	0.28
Per. 8[a]		13.98	10.00	2.14	8.29	1.33	0.26	1.49	0.20	1.09	0.22	0.61	0.07	0.46	0.07	40.22	0.39
Unit 7																	
Brachiopods																	
Per. 7[a]	*Costiferina indica*	3.86	3.94	0.62	2.29	0.50	0.11	0.52	0.10	0.57	0.12	0.36	0.05	0.39	0.05	13.49	0.55
Per. 6[a]	*Martinia* sp.	3.81	2.15	0.63	2.61	0.49	0.11	0.62	0.10	0.53	0.12	0.33	0.04	0.25	0.04	11.84	0.29
Per. 5[a]	*Permophricodothyris* sp.	0.36	0.25	0.06	0.27	0.04	0.02	0.08	0.01	0.07	0.02	0.04	0.01	0.03	0.00	1.27	0.35
Whole rock																	
Per. 7[a]		8.11	6.20	1.36	5.40	0.97	0.21	1.12	0.18	0.96	0.22	0.66	0.09	0.56	0.08	26.13	0.40
Per. 6[a]		7.32	4.05	1.23	4.92	0.93	0.23	1.08	0.17	0.94	0.20	0.56	0.07	0.41	0.06	22.15	0.29
Per. 5[a]		5.17	3.48	0.83	3.43	0.63	0.16	0.82	0.13	0.73	0.17	0.48	0.06	0.37	0.05	16.50	0.35
Unit 6																	
Brachiopods																	
Per. 4[a]	*Permophricodothyris* sp.	2.31	1.69	0.36	1.33	0.23	0.06	0.27	0.04	0.27	0.06	0.18	0.02	0.12	0.02	6.97	0.40
Per. 3[a]	*Neospirifer* sp.	2.66	1.74	0.44	1.73	0.31	0.08	0.41	0.05	0.31	0.06	0.19	0.03	0.14	0.02	8.16	0.35
Per. 2[a]	*ichthofenia lawrenciana*	3.13	1.67	0.47	1.89	0.33	0.08	0.43	0.07	0.40	0.09	0.26	0.03	0.21	0.03	9.10	0.29
Per. 1[a]	*Dielasma* sp.	2.51	2.38	0.37	1.33	0.23	0.05	0.30	0.05	0.33	0.08	0.26	0.04	0.25	0.04	8.21	0.52
Whole rock																	
Per. 4[a]		4.31	2.23	0.62	2.44	0.41	0.10	0.51	0.07	0.40	0.08	0.24	0.03	0.18	0.02	11.63	0.28
Per. 3[a]		3.47	2.35	0.57	2.23	0.41	0.09	0.47	0.07	0.41	0.09	0.27	0.03	0.20	0.03	10.70	0.36
Per. 2[a]		3.98	2.95	0.63	2.60	0.45	0.11	0.56	0.08	0.48	0.11	0.31	0.04	0.24	0.03	12.55	0.39
Per. 1[a]		7.62	6.88	1.42	5.88	1.04	0.25	1.40	0.22	1.29	0.30	0.90	0.12	0.76	0.12	28.20	0.45

	Species	La	Ce	Pr	Nd	Sm	Eu	Gd	Tb	Dy	Ho	Er	Tm	Yb	Lu	∑REEs	Ce/Ce*
Upper Desmoinsean Naco Formation, Arizona																	
Brachiopods																	
Penn. 3-2[b]	*Composita subtilita*	5.51	6.71	0.81	2.76	0.38	0.08	0.43	0.06	0.30	0.07	0.22	0.03	0.24	0.03	17.64	0.68
Penn. 3-1[b]	*Composita subtilita*	3.00	3.45	0.40	1.30	0.18	0.04	0.16	0.02	0.14	0.03	0.09	0.01	0.09	0.01	8.93	0.67
Penn. 2[b]	*Composita subtilita*	4.44	4.51	0.65	2.03	0.31	0.07	0.30	0.04	0.24	0.06	0.22	0.05	0.36	0.06	13.34	0.58
Whole rock																	
Penn. 3[b]		5.18	7.62	1.08	4.04	0.72	0.14	0.75	0.11	0.61	0.12	0.34	0.05	0.27	0.04	21.08	0.74
Penn. 2[b]		7.24	10.86	1.51	5.67	1.04	0.19	1.01	0.15	0.80	0.15	0.43	0.05	0.34	0.05	29.47	0.75
Middle Desmoinsean, Boggy Formation, Oklahoma																	
Brachiopods																	
Penn. 1-3[b]	*Marginifera muricatina*	0.22	0.24	0.03	0.12	0.009*	0.01	0.02	0.00	0.02	0.00	0.01	0.00	0.01	0.00	0.69	0.61
Penn. 1-2[b]	*Marginifera muricatina*	0.74	1.04	0.14	0.50	0.10	0.02	0.11	0.02	0.10	0.02	0.05	0.01	0.06	0.01	2.92	0.73
Penn. 1-1[b]	*Marginifera muricatina*	0.91	1.10	0.14	0.53	0.11	0.03	0.13	0.02	0.12	0.03	0.07	0.01	0.06	0.01	3.27	0.65
Whole rock																	
Penn. 1[b]		5.03	7.92	1.00	3.95	0.69	0.17	0.76	0.12	0.58	0.12	0.33	0.04	0.27	0.04	21.03	0.79
Lower Silurian (Llandoverian), Chicotte Formation, Anticosti Island																	
Brachiopods																	
Sil. 1-2[c]	*Gotatrypa gibbosa*	0.61	1.00	0.13	0.51	0.09	0.02	0.09	0.01	0.06	0.01	0.04	0.00	0.03	0.00	2.61	0.81
Sil. 1-1[c]	*Gotatrypa gibbosa*	0.62	0.96	0.13	0.49	0.08	0.02	0.09	0.01	0.07	0.01	0.03	0.00	0.04	0.00	2.56	0.77
Whole rock																	
Sil. 1[b]		1.55	2.60	0.30	1.26	0.24	0.06	0.28	0.04	0.21	0.04	0.12	0.01	0.08	0.01	6.81	0.83
Lower Silurian (Llandoverian), Jupiter Formation, Anticosti Island																	
Brachiopods																	
Sil. 5[c]	*Gotatrypa* sp.	0.18	0.26	0.04	0.16	0.03	0.01	0.03	0.00	0.03	0.01	0.01	0.00	0.02	0.00008*	0.79	0.70
Sil. 4-3[a]	*Gotatrypa* sp.	0.35	0.54	0.08	0.30	0.08	0.02	0.07	0.01	0.07	0.01	0.03	0.00	0.02	0.00	1.58	0.74
Sil. 4-2[b]	*Gotatrypa* sp.	0.11	0.18	0.02	0.11	0.03	0.00	0.02	0.00	0.02	0.00	0.02	0.0003*	0.01	0.00	0.53	0.75
Sil. 4-1[c]	*Gotatrypa* sp.	0.26	0.39	0.06	0.24	0.05	0.00	0.06	0.01	0.04	0.01	0.03	0.00	0.03	0.00	1.18	0.70
Sil. 3-3[b]	*Gotatrypa* sp.	1.59	1.59	0.29	1.27	0.27	0.06	0.30	0.05	0.25	0.05	0.13	0.02	0.09	0.01	5.97	0.50
Sil. 3-2[b]	*Gotatrypa* sp.	0.84	0.92	0.17	0.71	0.15	0.04	0.18	0.02	0.14	0.03	0.08	0.01	0.05	0.01	3.34	0.53
Sil. 3-1[c]	*Gotatrypa* sp.	0.53	0.51	0.10	0.41	0.06	0.02	0.09	0.01	0.06	0.02	0.03	0.00	0.01	0.00	1.87	0.49
Sil. 2-4[b]	*Gotatrypa* sp.	0.81	1.02	0.14	0.53	0.11	0.03	0.13	0.02	0.10	0.02	0.06	0.01	0.04	0.00	3.02	0.66
Sil. 2-3[b]	*Gotatrypa* sp.	1.13	1.54	0.22	0.88	0.17	0.04	0.20	0.03	0.17	0.03	0.09	0.01	0.07	0.01	4.58	0.68
Sil. 2-2[c]	*Gotatrypa* sp.	0.68	1.02	0.13	0.62	0.09	0.03	0.14	0.02	0.11	0.02	0.07	0.01	0.04	0.00	2.99	0.71
Sil. 2-1[c]	*Gotatrypa* sp.	0.32	0.43	0.06	0.27	0.05	0.0029*	0.06	0.01	0.05	0.01	0.02	0.001*	0.02	0.00	1.32	0.66

DD

	Species	La	Ce	Pr	Nd	Sm	Eu	Gd	Tb	Dy	Ho	Er	Tm	Yb	Lu	∑REEs	Ce/Ce*
Whole rock																	
Sil. 5[c]		5.94	11.09	1.49	5.91	1.20	0.27	1.22	0.18	0.98	0.19	0.48	0.07	0.39	0.06	29.48	0.86
Sil. 4[b]		2.83	5.86	0.80	3.16	0.63	0.16	0.69	0.11	0.58	0.11	0.30	0.04	0.23	0.03	15.51	0.91
Sil. 3[b]		20.40	28.62	4.79	19.78	3.96	1.00	4.15	0.61	3.19	0.60	1.57	0.19	1.13	0.16	90.14	0.65
Sil. 2[c]		3.60	5.87	0.76	3.22	0.53	0.13	0.68	0.10	0.58	0.14	0.35	0.03	0.24	0.03	16.27	0.78
Lower Silurian (Llandoverian), Becscie Formation, Anticosti Island																	
Brachiopods																	
Sil. 6[b]	*Virgiana barrandii*	0.17	0.27	0.03	0.13	0.03	0.01	0.03	0.00	0.02	0.00	0.01	0.00	0.01	0.00	0.72	0.78
Whole rock																	
Sil. 6[b]		1.01	1.95	0.26	1.01	0.21	0.05	0.22	0.03	0.17	0.04	0.10	0.01	0.07	0.01	5.15	0.89

Note: Concentations in ppm.

[a]: From Garbelli et al. (2015)

[b]: From Zaky et al. (2015)

[c]: From Azmy et al. (2011)

*: Anomalous concentrations, thus, ignored in the calculations

Appendix 4-4: Classification and Log K_D values of REEs in the investigated modern shallow-water (<500m) articulated brachiopods

Sample	Order	Family	Genus	Species	La	Ce	Pr	Nd	Sm	Eu	Gd	Tb	Dy	Ho	Er	Tm	Yb	Lu
Denmark Strait, Iceland																		
D.S.-1 (Pedicle)	Terebratulida	Dallinidae	Macandrevia	*Macandrevia cranium*	8.179	33.632	11.497	13.853	26.390	26.858		22.458	6.831	11.150	2.554			2.895
D.S.-2 (Brachial)	Terebratulida	Dallinidae	Macandrevia	*Macandrevia cranium*	12.020	42.811	15.889	14.115	6.908		12.583	14.406	6.934		3.811		4.148	
D.S.-3 (Brachial)	Terebratulida	Dallinidae	Macandrevia	*Macandrevia cranium*	12.128	18.410	14.360	13.034		18.877	6.808	11.067	10.082	7.955	9.386	11.843		13.748
D.S.-4 (Pedicle)	Terebratulida	Dallinidae	Macandrevia	*Macandrevia cranium*	14.212	16.067	22.062	17.417	28.157		13.259	24.619	9.305	14.992	5.942	4.420	8.621	15.599
Norwegian Sea, Iceland																		
N.S.-1 (Pedicle)	Terebratulida	Dallinidae	Macandrevia	*Macandrevia cranium*	17.731	54.849	22.137	24.111		23.816	11.334	19.249	19.774	10.480		25.672	12.407	
N.S.-2 (Pedicle)	Terebratulida	Dallinidae	Macandrevia	*Macandrevia cranium*	9.102	10.923	10.410	9.003	7.800	2.650	5.894	14.079		8.005	8.478		5.262	
N.S.-3 (Brachial)	Terebratulida	Dallinidae	Macandrevia	*Macandrevia cranium*	11.879	12.941	13.751	10.687	4.480		15.809	12.198	9.247	7.115	8.239	6.295	5.625	
N.S.-4 (Brachial)	Terebratulida	Dallinidae	Macandrevia	*Macandrevia cranium*	25.013	64.564	35.672	34.780	37.931	27.558	33.754	17.053	19.592	9.854	9.108	5.474	10.327	5.004
Irminger Sea, Iceland																		
I. S.-1 (Brachial)	Terebratulida	Dallinidae	Macandrevia	*Macandrevia cranium*	1.146	3.923	1.370			3.203	0.964		1.303		0.760		1.591	
I. S.-2 (Pedicle)	Terebratulida	Dallinidae	Macandrevia	*Macandrevia cranium*	5.605	19.175	11.075	6.169		13.721	5.856	8.678	2.566	2.259	3.200	2.187	1.456	
I. S.-3 (Brachial)	Terebratulida	Dallinidae	Macandrevia	*Macandrevia cranium*	8.086	29.019	13.558	7.381	18.015	15.562	18.050	8.113	7.357	9.330	6.211			
I. S.-4 (Brachial)	Terebratulida	Dallinidae	Macandrevia	*Macandrevia cranium*	1.186	4.375	1.925					1.042						
I. S.-5 (Pedicle)	Terebratulida	Dallinidae	Macandrevia	*Macandrevia cranium*	6.540	22.918	9.780	10.315	14.311	6.872	4.219			2.228	2.176	4.750		2.645
I. S.-6 (Brachial)	Terebratulida	Dallinidae	Macandrevia	*Macandrevia cranium*	9.190	32.804	14.615	9.547	9.873	12.176	13.045	5.998	5.178	5.082	2.892		2.656	3.417
I. S.-7 (Pedicle)	Terebratulida	Dallinidae	Macandrevia	*Macandrevia cranium*	30.642	93.803	49.320	51.673	47.586	70.278	52.305	42.401	26.144	26.289	16.717		14.037	
I. S.-8 (Brachial)	Terebratulida	Dallinidae	Macandrevia	*Macandrevia cranium*	11.236	41.867	17.392	11.285	18.310	7.390	7.580	14.191	11.228	4.258	3.463		6.539	
I. S.-9 (Pedicle)	Terebratulida	Dallinidae	Macandrevia	*Macandrevia cranium*	15.200	58.828	22.242	20.752	16.052	29.387	16.440	24.079	15.393	10.532	8.012	8.237		
I. S.-10 (Brachial)	Terebratulida	Dallinidae	Macandrevia	*Macandrevia cranium*	12.953	56.466	21.034	14.316	12.316	9.668	15.069	11.514	9.541	7.504	4.007	3.975	1.786	3.440
I. S.-11 (Pedicle)	Terebratulida	Dallinidae	Macandrevia	*Macandrevia cranium*	19.540	76.052	25.970	28.422	37.201	26.828	25.132	18.710	9.079	5.629	9.664	8.647	4.378	5.051
I. S.-12 (Pedicle)	Terebratulida	Dallinidae	Macandrevia	*Macandrevia cranium*	17.743	74.463	25.130	25.853	19.875	39.562	9.272	30.301	18.866	11.261	11.531	32.827	18.394	19.865
I. S.-13	Terebratulida	Dallinidae	Macandrevia	*Macandrevia cranium*	24.070	131.658	31.638	36.656	66.842	29.427	25.083	21.742	17.522	9.102	9.054	6.070	2.935	2.282
I. S.-14	Terebratulida	Dallinidae	Macandrevia	*Macandrevia cranium*	18.785	95.022	26.491	20.798	9.665	36.300	18.302	7.792	14.176	12.185	4.219		4.270	
I. S.-15	Terebratulida	Dallinidae	Macandrevia	*Macandrevia cranium*	5.911	35.332	10.389	6.925				4.418		1.913				
I. S.-16	Terebratulida	Dallinidae	Macandrevia	*Macandrevia cranium*	17.844	104.596	23.554	24.113	12.416	4.608	4.590	3.589	7.697	4.018	3.132		3.104	
I. S.-17	Terebratulida	Dallinidae	Macandrevia	*Macandrevia cranium*	16.665	107.476	20.654	22.376	27.614	24.498	12.499	11.137	11.317	6.384	2.972		5.183	
I. S.-18	Terebratulida	Dallinidae	Macandrevia	*Macandrevia cranium*	13.128	73.592	20.995	20.863	22.181		11.763	9.648	13.634	5.136	9.115			
I. S.-19	Terebratulida	Dallinidae	Macandrevia	*Macandrevia cranium*	27.465	129.702	39.650	32.889	60.884	22.242	23.382	26.580	15.632	8.873	17.250		20.423	9.019
I. S.-20	Terebratulida	Dallinidae	Macandrevia	*Macandrevia cranium*	26.196	189.235	40.494	39.324	29.064	8.454	22.008	32.732	19.473	13.935	5.683		12.540	6.636
I. S.-21	Terebratulida	Dallinidae	Macandrevia	*Macandrevia cranium*	39.294	140.733	61.361	59.070	79.400	102.056	55.154	43.862	32.188	19.789	17.508	13.760	16.171	10.692
I. S.-22	Terebratulida	Dallinidae	Macandrevia	*Macandrevia cranium*	7.812	38.573	10.826	9.857	13.371	6.342	10.293	5.687	9.077	3.005	5.116	4.980		3.516
I. S.-23	Terebratulida	Dallinidae	Macandrevia	*Macandrevia cranium*	16.274	50.127	17.549	14.132			8.252	12.592	4.714		9.342			
I. S.-24	Terebratulida	Dallinidae	Macandrevia	*Macandrevia cranium*	18.839	73.815	23.610	24.638	27.483	46.213	25.717	18.531	14.284	3.582	8.179	6.359		15.818
I. S.-25	Terebratulida	Dallinidae	Macandrevia	*Macandrevia cranium*	18.658	120.277	22.724	21.450	31.128	18.527	20.856	18.815	8.719	3.739	6.645		7.636	5.147
I. S.-26	Terebratulida	Dallinidae	Macandrevia	*Macandrevia cranium*	44.824	326.693	63.204	52.084	41.989	32.341	37.836	37.040	21.951	15.628	19.497			13.978
I. S.-27	Terebratulida	Dallinidae	Macandrevia	*Macandrevia cranium*	51.752	305.820	65.771	63.201	55.374	28.256	43.884	30.680	27.176	16.736	12.780	5.813	11.952	18.048
I. S.-28	Terebratulida	Dallinidae	Macandrevia	*Macandrevia cranium*	93.402	698.621	124.531	111.860	83.331	126.157	88.177	95.632	54.534	35.558	27.464	10.522	22.053	16.726

FF

Sample	Order	Family	Genus	Species	La	Ce	Pr	Nd	Sm	Eu	Gd	Tb	Dy	Ho	Er	Tm	Yb	Lu
Bonne Bay, Newfoundland																		
B.B.-1 (Pedicle)	Terebratulida	Cancellothyrididae	Terebratulina	*Terebratulina septentrionalis*	5.967	7.300	8.003	4.794	8.461	13.549		2.713	2.570	2.584	1.596	4.595	1.721	
B.B.-2 (Brachial)	Terebratulida	Cancellothyrididae	Terebratulina	*Terebratulina septentrionalis*	12.678	11.655	12.046	10.441	11.737	4.484	11.869	9.952	6.672	8.184		6.481	2.424	
B.B.-3 (Pedicle)	Terebratulida	Cancellothyrididae	Terebratulina	*Terebratulina septentrionalis*	5.662	6.760	6.302	6.753	4.185		5.792		2.225	3.187	1.981			5.527
B.B.-4 (Brachial)	Terebratulida	Cancellothyrididae	Terebratulina	*Terebratulina septentrionalis*	12.572	12.013	12.719	10.960	7.468	5.166	8.780	6.512	5.233	4.097	2.557		2.432	
B.B.-5 (Pedicle)	Terebratulida	Cancellothyrididae	Terebratulina	*Terebratulina septentrionalis*	22.248	22.415	25.950	22.127	24.736	17.672	17.908	13.627	11.607	7.644	6.707	5.792	3.163	0.653
B.B.-6 (Pedicle)	Terebratulida	Cancellothyrididae	Terebratulina	*Terebratulina septentrionalis*	3.497	4.592	3.691	3.664	3.572	3.268			1.620		0.765	4.229	0.808	
B.B.-7 (Pedicle)	Terebratulida	Cancellothyrididae	Terebratulina	*Terebratulina septentrionalis*	2.392	4.383	2.980	3.365	1.912		3.232	4.220	1.819		1.481	8.348		
B.B.-8 (Pedicle)	Terebratulida	Cancellothyrididae	Terebratulina	*Terebratulina septentrionalis*	23.319	22.331	25.431	23.916	26.341	19.417	20.885	6.925	12.927	10.407	6.552	6.147	5.349	8.504
B.B.-9 (Pedicle)	Terebratulida	Cancellothyrididae	Terebratulina	*Terebratulina septentrionalis*	3.834	5.246	4.037	3.962			1.477		1.944					1.399
B.B.-10 (Pedicle)	Terebratulida	Cancellothyrididae	Terebratulina	*Terebratulina septentrionalis*	3.012	4.901	3.935	3.230			3.544				0.706			3.710
B.B.-11	Terebratulida	Cancellothyrididae	Terebratulina	*Terebratulina septentrionalis*	4.075	5.179	4.457	2.070	3.252		6.463	1.282			0.674	6.872		0.646
B.B.-12	Terebratulida	Cancellothyrididae	Terebratulina	*Terebratulina septentrionalis*	57.903	38.486	47.678	45.440	17.969	9.625	33.272	14.922	4.311	4.946				
B.B.-13	Terebratulida	Cancellothyrididae	Terebratulina	*Terebratulina septentrionalis*	89.462	68.326	64.944	67.472	53.893	17.063	42.857	21.985		11.774	9.989	5.276	2.183	
Friday Harbour, Washington																		
F.H.-1 (Umbo)	Terebratulida	Terebrataliidae	Terebratalia	*Terebratalia transversa*	1.220	3.059	1.278	2.490		4.300	4.564	2.932			2.027	6.491		
F.H.-2 (Pedicle)	Terebratulida	Terebrataliidae	Terebratalia	*Terebratalia transversa*	6.738	8.259	13.620	6.950	10.628		7.808	8.478	3.714	6.240	5.529	6.504	3.324	4.280
F.H.-3 (Brachial)	Terebratulida	Terebrataliidae	Terebratalia	*Terebratalia transversa*	4.777	5.738	9.741	5.910			5.670	14.169	2.990	4.789	6.261			
F.H.-4 (Brachial)	Terebratulida	Terebrataliidae	Terebratalia	*Terebratalia transversa*	7.781	6.403	13.078	7.860			9.885	9.229	5.795	4.373	3.447	1.827	1.884	5.273
F.H.-5 (Pedicle)	Terebratulida	Terebrataliidae	Terebratalia	*Terebratalia transversa*	7.809	6.971	16.815	9.765		5.751	8.485	16.850	4.310	3.659	7.948		3.005	1.688
F.H.-6 (Pedicle)	Terebratulida	Terebrataliidae	Terebratalia	*Terebratalia transversa*	15.488	30.751	39.318	18.933		8.385	16.634		9.121	11.449	6.862			
Bay of Fundy, New Brunswick																		
B.F.-1	Terebratulida	Cancellothyrididae	Terebratulina	*Terebratulina septentrionalis*	11.777	20.141	13.749	18.173	10.994	21.609	18.248	14.742	11.287	5.912	4.384		8.092	2.545
B.F.-2	Terebratulida	Cancellothyrididae	Terebratulina	*Terebratulina septentrionalis*	4.145	6.044	4.908	4.359		2.133	3.178	2.186	1.127	1.890			5.220	1.849
B.F.-3	Terebratulida	Cancellothyrididae	Terebratulina	*Terebratulina septentrionalis*	5.047	5.069	4.290	5.083	3.604	6.402	2.821			1.661			0.914	0.878
B.F.-4	Terebratulida	Cancellothyrididae	Terebratulina	*Terebratulina septentrionalis*	15.585	12.668	15.124	11.619	12.164	6.421	8.783	8.637	7.897	7.091	5.208	4.440	2.114	2.897
B.F.-5	Terebratulida	Cancellothyrididae	Terebratulina	*Terebratulina septentrionalis*	15.555	13.627	16.653	12.304	12.433	11.701	11.858	11.830	6.039	5.024	5.321	10.301	5.273	3.841
B.F.-6	Terebratulida	Cancellothyrididae	Terebratulina	*Terebratulina septentrionalis*	12.390	19.579	13.945	13.433	15.324	22.541	34.019	16.776	5.079	4.099	5.147	4.798	2.694	7.196
B.F.-7	Terebratulida	Cancellothyrididae	Terebratulina	*Terebratulina septentrionalis*	7.531	13.399	5.469	4.733		7.472	3.346	7.923	7.064		3.353		4.343	3.632
B.F.-8	Terebratulida	Cancellothyrididae	Terebratulina	*Terebratulina septentrionalis*	13.414	16.015	12.234	12.360	10.496		16.450	7.671	11.181		7.753		7.726	4.395
B.F.-9	Terebratulida	Cancellothyrididae	Terebratulina	*Terebratulina septentrionalis*	24.191	35.377	28.404	26.255	37.387	22.526	30.332	28.131	18.654	6.236	13.607		10.501	8.382
B.F.-10	Terebratulida	Cancellothyrididae	Terebratulina	*Terebratulina septentrionalis*	8.109	5.234	9.567				40.651		16.540		3.596	9.402		10.118
B.F.-11	Terebratulida	Cancellothyrididae	Terebratulina	*Terebratulina septentrionalis*	5.540	8.000	11.351			65.319	9.449	13.720		25.279		12.206	9.004	
B.F.-12	Terebratulida	Cancellothyrididae	Terebratulina	*Terebratulina septentrionalis*	5.854	3.340	2.992	1.904				5.021	4.185	3.528	12.102			5.776

GG

Sample	Order	Family	Genus	Species	La	Ce	Pr	Nd	Sm	Eu	Gd	Tb	Dy	Ho	Er	Tm	Yb	Lu
Philippine Sea, North Pacific Ocean																		
Pal.-1 (Pedicle)	Thecideida	Thecidellinidae	Thecidellina	*Thecidellina congregata*	9.185	14.758	6.590		1.734	1.304	3.202	2.495	4.348	3.324	11.588	10.709		
Pal.-2 (Pedicle)	Thecideida	Thecidellinidae	Thecidellina	*Thecidellina congregata*	8.095	9.760		3.397			15.965	4.971			12.913			5.454
Pal.-3 (Brachial)	Thecideida	Thecidellinidae	Thecidellina	*Thecidellina congregata*	8.216	9.877	4.474				7.535			8.872	10.960			
Pal.-4 (Umbo)	Thecideida	Thecidellinidae	Thecidellina	*Thecidellina congregata*	13.015	23.061	12.011	8.430				30.390	10.992		19.362		5.781	
Ross Sea-1, Antarctica																		
R.S.-7	Terebratulida	Dallinidae	Macandrevia	*Macandrevia sp.*	7.620	19.516	8.435	13.032	18.884		8.571		4.734		3.223	13.185		3.389
R.S.-8	Terebratulida	Dallinidae	Macandrevia	*Macandrevia sp.*	5.183	13.461	7.961	11.767		5.954	12.566		5.412		3.299	1.953		
R.S.-9	Terebratulida	Dallinidae	Macandrevia	*Macandrevia sp.*	6.142	23.615	6.387	6.973	15.605		21.660				6.338	8.308		
R.S.-10	Terebratulida	Dallinidae	Macandrevia	*Macandrevia sp.*	32.268	113.148	42.366	35.761	38.979	46.494	32.180	20.033	20.761	22.003	13.649	16.963	6.797	13.932
R.S.-11	Terebratulida	Dallinidae	Macandrevia	*Macandrevia sp.*	56.809	127.059	94.499	78.008	68.771	55.967	81.792	50.879	29.054	23.048	13.341	13.101	7.402	13.494
R.S.-12	Terebratulida	Dallinidae	Macandrevia	*Macandrevia sp.*	21.683	92.046	27.090	31.036	21.015		29.751	27.153	17.338	4.518	8.318	5.495		1.424
R.S.-13	Terebratulida	Dallinidae	Macandrevia	*Macandrevia sp.*	10.337	36.732	18.995	10.848		10.075	12.993		12.976	5.177	4.811	16.152		
R.S.-14	Terebratulida	Dallinidae	Macandrevia	*Macandrevia sp.*	13.567	21.164	15.029	22.514	15.744		20.586	3.573	2.544		2.907			
R.S.-15	Terebratulida	Dallinidae	Macandrevia	*Macandrevia sp.*	9.302	9.676	7.802	10.620			8.530	8.293			3.520	5.021		
Ross Sea-2, Antarctica																		
R.S.-1	Terebratulida	Terebratellidae	Magellania	*Magellania joubini*	13.604	39.403	19.672	22.661	18.147	34.359	27.229	20.517	7.471	8.652	8.036	11.916	5.901	
R.S.-2	Terebratulida	Terebratellidae	Magellania	*Magellania joubini*	12.980	46.536	23.997	20.451	15.446	31.134	32.105	12.789	9.333	10.533	10.685	10.224	3.433	3.134
R.S.-3	Terebratulida	Terebratellidae	Magellania	*Magellania joubini*	46.158	192.388	81.107	55.572	65.702		61.904	43.117	28.369		14.058	12.290	14.786	4.722
R.S.-4	Terebratulida	Terebratellidae	Magellania	*Magellania joubini*	16.502	46.612	31.944	29.011	48.607		20.457	8.647	5.533	8.647	4.875	7.303	5.587	
R.S.-5	Terebratulida	Terebratellidae	Magellania	*Magellania joubini*	35.660	99.919	42.988	46.139	62.522	59.981	57.079	72.615	39.843	28.080	20.432	10.558		11.222
R.S.-6	Terebratulida	Terebratellidae	Magellania	*Magellania joubini*	15.336	70.662	33.678	34.636	35.647	28.491	31.723	25.325	19.100	9.001	9.027		16.533	4.560